# Isolation and Characterization of Stem Cell Populations in the Periodontium


## Jimin Xiong

Master of Dentistry (Shandong University, China)

Bachelor of Medicine (Shandong University, China)

Colgate Australian Clinical Dental Research Centre

School of Dentistry, Faculty of Health Sciences

University of Adelaide

and

Mesenchymal Stem Cell Research Group

Bone and Cancer Research Laboratory, Division of Haematology

Hanson Institute, SA Pathology


A thesis submitted to the University of Adelaide

for the degree of Doctor of Philosophy

June 2012

***I dedicate this thesis to my dad. He will be greatly missed by all that had the privilege to know him.***

# Table of Contents

# Table of Figures

# Table of Tables

# Declaration

I certify that this work contains no material which has been accepted for the award of any other degree or diploma in any university or other tertiary institution and, to the best of my knowledge and belief, contains no material previously published or written by another person, except where due reference has been made in the text. In addition, I certify that no part of this work will, in the future, be used in a submission for any other degree or diploma in any university or other tertiary institution without the prior approval of the University of Adelaide and where applicable, any partner institution responsible for the joint-award of this degree.

I give consent to this copy of my thesis when deposited in the University Library, being made available for loan and photocopying, subject to the provisions of the Copyright Act 1968.

The author acknowledges that copyright of published works contained within this thesis (as listed below) resides with the copyright holder(s) of those works. I also give permission for the digital version of my thesis to be made available on the web, via the University's digital research repository, the Library catalogue, the Australasian Digital Theses Program (ADTP) and also through web search engines, unless permission has been granted by the University to restrict access for a period of time.

Signed Jimin Xiong

# List of Publications

Epithelial Cell Rests of Malassez contain unique stem cell populations capable of undergoing epithelial-mesenchymal transition. **Xiong J**, Mrozik K, Gronthos S and Bartold PM. *Stem Cells & Development.* In press.

Proteomic characterization of mesenchymal stem cell-like populations derived from various tissue types. Mrozik K*, **Xiong J***, Zilm PS, Gronthos S and Bartold PM. *Stem Cells and Cancer Stem Cells: Therapeutic Applications in Disease and Injury*. In press. (Mrozik K and Xiong J contributed equally)

Role of epithelial cell rests of Malassez in the development, maintenance and regeneration of periodontal ligament tissues. **Xiong J**, Gronthos S and Bartold PM. *Periodontology 2000*. In press.

# Acknowledgments

First and foremost I would like to thank both of my supervisors Professor Mark Bartold and Professor Stan Gronthos. I feel privileged to be guided by such intelligent and talented scientists. Thank you for being caring, sharing all your intelligence, believing in me and always finding time for me no matter how busy you are. In particular, thank you for your understanding of the challenges and difficulties for an international student without any science background. Thank you for giving me extra attention and support during my PhD, for your help in experimental design and all your encouragements in the first year, for your guidance in troubleshooting in the second year, and for your assistance in writing up in my third year. Also thank you for setting a great example of time management and keeping me on the right timeframe for my PhD. Thank you for guiding me get the “ticket” in science and helping me start building my career. I always feel that I am very lucky to have had you as my supervisors.

There are many people that deserve a big thank you! Dr Peter Zilm, thank you for teaching me proteomic techniques, for sharing your knowledge about proteins and for all your help in my project. Particularly, thank you for all your time and help with corrections for my thesis - I know how much effort you have put in. Professor Pishan Yang in Shandong University, thank you for being a great supervisor when I was in China and for all your support and suggestions during my PhD. Thank you for seeing me through all the achievements in the last three years. Professor Andrew Zannettino, thank you for being so nice, intelligent, willing to share all your brilliant ideas, and being full of energy all the time. I have learnt so much from you in our Tuesday lab meetings. Sandy McConachy, thank you for being caring and ready to help any time.

Krzysztof Mrozik, I cannot imagine having done my PhD without you. Thank you for teaching me almost all the techniques, being ready to help any time I had trouble, and telling me “it is not the end of the world” when I felt frustrated and “that happens” when I

did something wrong. DJ (Danijela Menicanin), I have so much to thank you for, you are so beautiful and such a sweetheart. Thank you for all your help, technically and emotionally. You helped me settle in and treated me like a sister when I arrived in Australia. Also thank you for sharing all your experience to help me survive throughout my PhD, understanding all my fears and being happy to help whenever I need you. Naohisa Wada, thank you for all your help and never minding staying after hours to help me. Thank you for setting an example of working hard and working smart. I had a good time working with you. Amy Li, thank you for sharing all your knowledge of keratinocyte culture and cell sorting. I also enjoyed all the chats, related or unrelated to research. Kiwi (Kim Hynes), thank you for your time looking at the hundreds of proteomic data, your help with everything including computer, writing…, and listening to all my problems. I had a great time sharing the same office with you. Catherine Offler, your time was greatly appreciated for figures in the paper, thesis formatting and many other things. Victor Marino, thank you for ovine tooth collection and decalcification, and animal ethics applications. Tracy Fitzsimmons, thank you for being there for me whenever I had some problems and wanted to talk. Jim Cakouros, thank you for your help with PCR. I would also like to thank all the lab members for helping the “Trouble” in the lab and answering my never ending questions. The discussions during the last three years have helped me develop novel ideas. Thank you for making me feel comfortable in the lab. Thank you for all the chats, for being so patient with my English and helping to improve it. They are: Agnes, Catherine, Jenny, Kate Vandyke, Kate Pilkington, Locky, Mary, Melissa, Peter, Romana, Sally, Sandra, Sara, Shaohua, Sharon, Shazzy, Steve, Thao and Tony. There are many people outside the lab that deserve thanks. I would like to thank Dr Yeesim Khew-Goodall and Assoc Prof Stuart Pitson for providing antibodies, Assoc Prof Peter Hoffman and Dr Megan Penno from Adelaide Proteomics Center for their technical assistance and Cathy and the staff from the department of Oral and Maxillofacial Surgery for human teeth

collection.

I would like to thank all my friends, Dongdong, Furong, Han Guoge, Jactty, Li Yun, Nihung, Rudy, Wu Yue, Yang Chengzhe, Zhang Yan and Zhu Wei. Thank you for being there for me and celebrating all my achievements. I would like to thank my friends who are dentists: Aaron Seet, Sushil Kaur, Teck Huah Tang and Tina Choo for discussions. Thank you also goes to my housemates, Annabel, Ji Yan, Lina and Nancy, for putting up with me. Also a big thank you to all the other wonderful people around. There are so many great people that let me enjoy my stay in Australia.

I would like to acknowledge the support I received from the China Scholarship Council-University of Adelaide Joint Postgraduate Scholarship, the Colgate Betty Fanning Postgraduate Scholarship, Australia Stem Cell Center (ASCC) International Travel Award and Postgraduate Travel Fellowship, University of Adelaide.

Finally, to my parents, thank you for the unconditional love and selfless support you have given me. Thank you for picking me up after every fall, getting me prepared for every phase in my life and always believing in me. Seeing Xiong Yikai (my nephew) growing up, I understand how much you have done for me since I was born. I feel sorry for keeping you worried about me in the last three years. Words are not enough in the world to express my gratitude to my parents. To my brother and his family (Jia Xiaoyu and Xiong Yikai: “Gugu, I miss you. When you coming back?”), thank you for supporting me enormously. Gege, you are the best brother in the world!!! I feel very lucky to be born in such a happy family where everyone loves and feel close to each other.

# List of Abbreviations

| | |
|---|---|
| α-MEM | Minimum essential medium, α modification |
| x g | Times gravity |
| µ | Microns |
| 2-DE | Two-dimensional electrophoresis |
| AAC | Acellular afibrillar cementum |
| ACN | Acetonitrile |
| AEFC | Acellular extrinsic fiber cementum |
| AIFC | Acellular intrinsic fiber cementum |
| ALP | Alkaline phosphatase |
| AMP | Adenosine 5’-monophosphate |
| ASC | Adult stem cells |
| bFGF | Basic fibroblast growth factor |
| bHLH | Basic helix-loop-helix |
| BMP | Bone morphogenic protein |
| BMSC | Bone marrow stem cells |
| BrdU | Bromodeoxyuridine |
| BSA | Bovine serum albumin |
| BSP | Bone sialoprotein |
| CAP | Cementum adhesion protein |
| cDNA | Complementary deoxyribonucleic acid |
| CFU-Epi | Colony Forming Unit-Epithelial cells |
| CFU-F | Colony Forming Unit-Fibroblast |
| CIFC | Cellular intrinsic fiber cementum |
| CK | Cytokeratin |
| CMFC | Cellular mixed stratified fiber cementum |
| $CO_2$ | Carbon dioxide |
| DAPI | 4',6-diamidino-2-phenylindole dihydrochloride |
| DEPC | Diethylpyrocarbonate |
| DF | Dental follicle |
| DFPC | Dental follicle progenitor cells |
| DIGE | Difference gel electrophoresis |
| Dlx-2 | Distal-less gene-2 |
| DMEM | Dulbecco’s modified eagle medium |
| DMSO | Dimethyl-sulfoxid |
| DNA | Deoxyribonucleic acid |
| DNCP | Dentin noncollagenous proteins |
| DP | Dental pulp |
| DPSC | Dental pulp stem cells |
| DTT | Dithiothreitol |
| ECM | Extracellular matrix |
| EDTA | Ethylenediaminetetra-acetic acid |
| EDX | Energy Dispersive X-ray Analysis |

| | |
|---|---|
| EGF | Epithelial growth factor |
| EMP | Enamel Matrix Proteins |
| EMP-1 | Epithelial membrane protein 1 |
| EMT | Epithelial to mesenchymal transition |
| EPMA | Electron Probe Micro-Analysis |
| ER | Endoplasmic reticulum |
| ERM | Epithelial Cell Rests of Malassez |
| ESC | Embryonic stem cells |
| FA | Formic acid |
| FACS | Fluorescence activated cell sorting |
| FCS | Foetal calf serum |
| FGF | Fibroblast growth factor |
| GAPDH | Glyceraldehyde 3-phosphate dehydrogenase |
| GF | Gingival fibroblasts |
| GFAP | Glial fibrillary acidic protein |
| GM-CSF | Granulocyte-macrophage colony stimulating factor |
| GMSC | Gingiva-derived mesenchymal stem cells |
| GoPro49 | Golgi protein 49kDa |
| GPI | Glycosyl phosphatidylinositol |
| GRAVY | Grand average of hydropathicity |
| H&E | Hematoxylin and eosin |
| $H_2O_2$ | Hydrogen peroxide |
| $H_2SO_4$ | Sulphuric acid |
| HA/TCP | Hydroxyapatite/tricalcium phosphate |
| HBSS | Hanks balanced salt solution |
| HCl | Hydrochloric acid |
| HEPES | 4-(2-hydroxyethyl)-1-piperazineethanesulfonic acid |
| HERS | Hertwig’s Epithelial Root Sheath |
| hnRNPC | Heterogeneous nuclear ribonucleoprotein C |
| HSC | Haematopoietic stem cell |
| HSP-90β | Heat shock protein-90β |
| IAA | Iodoacetamide |
| IBMX | 3-Isobutyl-1-methyl-xanthine |
| ICAT | Isotope coded affinity tag |
| ICC | Immunocytochemistry |
| IDO | Indoleamine 2,3-dioxygenase |
| IEF | Isoelectric focusing |
| Ig | Immunoglobulin |
| IHC | Immunohistochemistry |
| IPG | Immobilised pH gradient |
| iPSC | Induced pluripotent stem cells |
| ISCT | International Society for Cellular Therapy |
| ITSS | Insulin-transferrin-sodium-selenite supplement |

| | |
|---|---|
| KCl | Potassium chloride |
| kDa | Kilo Dalton |
| KSC | Keratinocyte stem cells |
| LC-ESI-IT | Liquid chromatography-electrospray ionisation ion-trap |
| M | Molar |
| mA | Milli amps |
| MACS | Magnetic activated cell sorting |
| ml/mm/mM | Millilitre/millimetre/millimolar |
| MMP | Matrix metalloproteinase |
| mRNA | Messenger ribonucleic acid |
| MS | Mass spectrometry |
| MSC | Mesenchymal stem cells |
| MSX | Muscle segment homeobox gene |
| NaCl | Sodium chloride |
| NaOH | Sodium hydroxide |
| NF | Nuclease free |
| NF-H | Neurofilament heavy chain |
| NFI-C | Nuclear factor I family member C |
| NGF | Nerve growth factor |
| $NH_4HCO_3$ | Ammonium bicarbonate buffer |
| NIH | National Institutes of Health |
| NOD/SCID mice | Non-obese diabetic–severe combined immunodeficient |
| NSC | Neural stem cells |
| OKGS | Oral keratinocyte growth supplement |
| OKM | Oral keratinocyte media |
| OPG | Osteoprotegerin |
| OPN | Osteopontin |
| P | Passage |
| P/S | Penicillin and streptomycin solution |
| PAGE | Poly-acrylamide gel electrophoresis |
| PBS | Phosphate buffered saline |
| PBS-T | Phosphate buffered saline + 0.1% Tween-20 |
| PBS-TX | Phosphate buffered saline + 0.3% triton-X 100 |
| PCR | Polymerase chain reaction |
| PDL | Periodontal ligament |
| PDLF | Periodontal ligament fibroblasts |
| PDLP | Periodontal ligament progenitor cells |
| PDLSC | Periodontal ligament stem cells |
| PE | Phycoerythrin |
| PFA | Paraformaldehyde |
| $PGE_2$ | Prostaglandin $E_2$ |
| PGP 9.5 | Protein gene product 9.5 |
| pI | Isoelectric point |
| PLAP-1 | Periodontal ligament associated protein-1 |

| | |
|---|---|
| PMD | Post-mitotic differentiating keratinocyte |
| PPAR | Perixosome proliferator-activated receptor |
| RA | Retinoic acid |
| RCDC | ReduCing agent and Detergent Compatible |
| RT | Room temperature |
| RT-PCR | Real time polymerase chain reaction |
| $Runx_2$ | Runt-related transcription factor-2 |
| S1P | Sphingosine-1-phosphate |
| SC | Stem cells |
| SCAP | Stem cells from root apical papilla |
| SD | Standard deviation |
| SDS | Sodium dodecyl sulphate |
| SEM | Standard error of the mean |
| SHED | Stem cells from human exfoliated deciduous teeth |
| SHH | Sonic hedgehog |
| SPARC | Secreted protein acidic and rich in cytokine |
| SPK | Sphingosine kinase |
| STRO-1 | Early mesenchymal stem cell marker |
| TA | Transit amplifying keratinocytes |
| TBP | Tributyl phosphine |
| TBS | Tris buffered saline |
| TEMED | N, N, N, N – tetramethyl - ethylenediamine |
| TGF | Transforming growth factor |
| Thy-1 | Thymocyte differentiation antigen-1 |
| TNSALP | Tissue nonspecific alkaline phosphatase |
| TUNEL | Terminal deoxynucleotidyl transferase dUTP nick end labeling |
| VSEL | Very small embryonic-like stem cells |
| w/v | Weight per volume |
| Zeb1 | Zinc finger E-box-binding homeobox |
| µg/µl/µM | Microgram/microlitre/micromolar |

# Abstract

Stem cells represent promising candidates for tissue engineering due to their capacity for self-renewal and their potential for differentiating into multiple cell lineages. The periodontal tissues are composed of various cell types, such as periodontal ligament fibroblasts, osteoblasts, cementoblasts, endothelial cells, the Epithelial Cell Rests of Malassez (ERM). Studies have previously identified periodontal ligament stem cells (PDLSC) within these tissues, which have the capacity to form periodontal ligament, cementum and bone. Another potential source of progenitor cells described in periodontal tissues are ERM, which are the only odontogenic epithelial cells in the adult periodontium. The present study identified that ERM contained a unique multipotential stem cell population with similar properties as described for PDLSC. Furthermore, the present proposal investigated the cell surface protein expression of PDLSC to identify unique markers for the isolation and purification of PDLSC.

The present study demonstrated that ovine Epithelial Cell Rests of Malassez contain a subpopulation of stem cells that could undergo epithelial-mesenchymal transition into mesenchymal stem-like cells with multi lineage potential. *Ex vivo*-expanded ERM expressed both epithelial (cytokeratin-8, E-cadherin and Epithelial Membrane Protein-1) and bone marrow stromal/stem cell markers (CD44, CD29, Heat Shock Protein-90β). Integrin $\alpha_6$/CD49f could be used for the enrichment of clonogenic cell clusters (colony-forming units-epithelial cells [CFU-Epi]) which was weakly expressed by PDLSC. Importantly, ERM demonstrated a capacity to differentiation into bone, fat, cartilage and neural cells *in vitro*, and form bone, cementum-like and Sharpey's fibre-like structures when transplanted into immunocompromised mice. Additionally, gene expression studies showed that osteogenic induction of ERM triggered an epithelial-mesenchymal transition.

The present study also examined the cell surface protein expression of human PDLSC

using CyDye cell surface labelling and two-dimensional electrophoresis coupled with liquid chromatography--electrospray-ionization tandem mass spectrometry. In addition to the expression of well known mesenchymal stem cell associated cell surface antigens such as CD73 (ecto-5'-nucleotidase) and CD90 (Thy-1), PDLSC were also found to express two novel cell surface proteins, Annexin A2 and sphingosine kinase 1. Interestingly, previous studies have implicated CD73, CD90, Annexin A2 and sphingosine kinase 1 expression in the maintenance of various stem cell populations. Comparative analyses investigated the expression of CD73, CD90, Annexin A2 and sphingosine kinase-1 in human gingival fibroblasts, human keratinocytes, ovine PDLSC and ovine ERM cells. Importantly, this study found that human skin epithelial cells lacked any cell surface expression for CD73, CD90 and Annexin A2.

In summary, ERM and PDLSC are both important stem cell sources that could play a pivotal role in periodontal homeostasis and regeneration following insult or disease. As periodontal regeneration is essentially a re-enactment of the periodontal tissue development process, it is plausible to suggest that the combination of ERM and PDLSC would hold greater potential for periodontal regeneration compared to established bone marrow-derived mesenchymal stem cells.

# Chapter 1. Introduction

## 1.1 Periodontal regeneration

The periodontal ligament (PDL) is a highly specialized cellular connective tissue that attaches the cementum of the tooth root to the alveolar bone to maintain teeth within the jaw and support tooth function [1]. Periodontal ligament has a high turnover rate with the ability to remodel to adjust to the mechanical loading or orthodontic movement. Periodontitis is an inflammatory disease that results in damage to the tooth-supporting tissues, potentially leading to tooth loss. Periodontal disease is one of the major public health problems worldwide. It has been documented that around 80% of the US population suffers from mild periodontitis with at least one site with clinical attachment loss of more than 2mm, where severe generalised periodontitis is found in 5-20% of any population worldwide [2]. The ultimate goal of periodontal therapy is to restore the damaged periodontal supporting tissues to their original form, structure and function. This procedure is known as periodontal regeneration, as opposed to periodontal repair, which involves the formation of long junctional epithelium without the restoration of the periodontal attachment apparatus. The regeneration of periodontal tissues is a complex process that involves the collaboration of four different tissues; two hard tissues (cementum and alveolar bone) and two soft tissues (gingiva and periodontal ligament). Among these tissues, gingiva is not an odontogenic tissue, but rather an adaptation of oral mucosa [3]. Current approaches for periodontal regeneration range from root surface conditioning, bone graft replacement, guided tissue regeneration to growth factor/enamel matrix protein application as well as combinations thereof [4]. However, no regenerative procedures to date provide predictable outcomes of regeneration. It is well accepted that periodontal regeneration is essentially a re-enactment of the periodontal development process including mimicking the microenvironment, recruiting stem/progenitor cells to the site, re-

establishing the extracellular matrix and growth factor production and directing resident stem/progenitor cells towards terminal differentiation [5]. Therefore, from a clinical perspective, to understand the rational basis of regenerative procedures a better understanding of the events associated with the formation of periodontal components will help establish reliable strategies for clinical practice. An important aspect of this is the role of Hertwig's Epithelial Root Sheath in periodontal development and that of its descendants, Epithelial Cell Rests of Malassez, in the maintenance of periodontium. Hertwig's Epithelial Root Sheath (HERS) is a double-layered, tube-like sleeve of epithelial cells during tooth root development that separates two cranial neural-crest-derived ectomesenchymal tissues: dental follicle (DF) and dental papilla (Figure 1.1). Upon the deposition of the first layer of mantle dentin, HERS fragments and gives rise to strands of epithelial cells named as Epithelial Cell Rests of Malassez (ERM), which are the only odontogenic epithelial cells in the adult periodontium.

## 1.2 HERS/ERM and the maintenance of periodontium

### 1.2.1 HERS and periodontium development

#### *1.2.1.1 Formation of HERS and the classical theory of periodontium development*

Periodontal ligament contains heterogeneous cell populations including an epithelial population (ERM) and various mesenchymal populations (fibroblasts, osteoblasts and cementoblasts). The reciprocal interactions between oral ectoderm-derived epithelial cells and neural-crest-derived mesenchymal cells play a pivotal role in tooth development. The formation of HERS commences at the end of the crown stage during tooth development. The ectoderm-derived inner and outer enamel epithelium of the enamel organ (devoid of stratum intermedium and stellate reticulum) proliferates and gives rise to a double-layered, tube-like sleeve of epithelial cells, named Hertwig's Epithelial Root Sheath (HERS). The formation of the periodontium, including cementum, periodontal ligament and alveolar bone, occurs in a spatially and temporally coordinated manner [6]. Initially, HERS

separates two ectomesenchymal tissues: dental follicle (DF) and dental papilla (Figure 1.1). On the tooth side, the inner epithelial cells of HERS stimulate dental papilla cells to differentiate into dentin-producing odontoblasts. Following dentin formation, HERS secretes a fine matrix of proteins termed the Hyaline layer of Hopewell Smith. Shortly after the deposition of the first layer of mantle dentin matrix the disintegration of HERS occurs, which results in strands of epithelial cells, the Epithelial Cell Rests of Malassez (ERM). This disintegration allows the DF cells to migrate and attach to the Hyaline layer of Hopewell Smith where they differentiate into cementum-producing cementoblasts. Dental follicle-derived periodontal ligament fibroblasts (PDLF) give rise to collagen fibers that are embedded in the cementum, termed Sharpey's fiber.



**Figure 1.1 Schematic representation of root development and fragmentation of epithelial root sheath**

Enamel (E), dentine (D), and dental papilla (DP) (reproduced, with permission from reference 21).

On the bone side, osteoblasts derived from DF cells deposit an alveolar bone layer up the tooth socket. Insertion of Sharpey's fiber into alveolar bone completes the development of periodontium.

Therefore, it appears that dental follicle cells have the capacity to differentiate into three cell types; cementoblasts, PDLF and osteoblasts that form cementum, Sharpey's fiber and alveolar bone, respectively. However, development of the periodontium is far more sophisticated than this. It is a complex process that involves a number of cascades and mechanisms [7, 8], with many fundamental questions remaining to be answered, such as whether HERS is an alternate cellular origin of cementoblasts, how HERS disintegration is initiated, how HERS withdraws from the root surface, and the fate of HERS after tooth root development [9].

#### *1.2.1.2 Root formation*

The establishment of HERS from the dental cervical loop is generally regarded as the commencement of tooth root formation [10, 11]. It is well accepted that HERS plays a significant role in establishing tooth support but the precise nature of this remains unclear [3]. The proposed roles of HERS in root formation range from structurally dividing dental ectomesenchymal tissues to dental follicle and dental papilla, inducers of mesenchymal stromal/stem cells (MSC) differentiation into odontoblasts and cementoblasts, cementoblast cell precursors to regulators of tooth root shape and numbers [12]. It is believed that HERS is the inducer and regulator of root formation determining the shape, size and number of roots, as the shape of HERS predicts the future shape of tooth roots [3, 13]. At the molecular level, the shape of HERS is determined by SHH (sonic hedgehog)/MSX2 (muscle segment homeobox gene) and insulin-like growth factor-1/BMP-4 (bone morphogenic protein-4) epithelio-mesenchymal interactions [14]. It has

been noted that teeth of some species such as rodent incisors and rabbit molars grow continuously throughout the lifetime of the animal [15]. These provide useful models for the study of tooth development. Most studies on root formation have been performed in rodents. However, species differences have been reported and thus caution needs to be exercised when extending the knowledge of other species to the human model [10, 11], where limited information for tooth root formation has come from direct observations of human teeth [1].

#### *1.2.1.2.1 Dentinogenesis*

The role of HERS in the initiation of dentinogenesis was first proposed as early as 1887 [16] and it has been well accepted that the inner epithelial cells of HERS induce dental papilla cells to differentiate into odontoblasts [3, 11, 14]. In this process, nuclear factor I family member C (NFI-C) is an essential transcription factor regulating odontoblast differentiation [17-21]. It has been noted that NFI-C deficient mice demonstrated prominent root abnormalities, including short root, aberrant odontoblast differentiation, defective dentin and no cementum, but no major changes were identified in molar crown formation [17, 21]. This indicates NFI-C is a transcription factor exclusively related to root development [17] and lends evidence that different inducing mechanisms might be involved in crown and tooth dentin formation. This abnormal root morphology in NFI-C deficient mice is mediated by the suppression of odontoblast proliferation and differentiation, as well as the promotion of odontoblast apoptosis [18]. A recent study investigated the role of Smad4 signalling, a central mediator for Transforming Growth Factor-beta/Bone Morphogenetic Protein (TGF-β/BMP) signalling pathway, on HERS in regulating root development [13]. In mice subjected to tissue specific inactivation of Smad4 in HERS, root formation is arrested as the cervical loop fails to form bilayered HERS and grow apically after crown development. This observation highlights the

essential role of HERS in the guidance of root formation. The authors also reported that in Smad4 deficient mice the ectopic expression of SHH (sonic hedgehog) could partially rescue the root defect and restore NFI-C expression and abnormal cellular dentin. However, the root defect in NFI-C$^{-/-}$ mice could not be corrected by the ectopic expression of SHH. Collectively, this study demonstrates that the Smad4-SHH-NIF-C signalling plays an important role in mediating epithelial-mesenchymal-interaction-initiated root development.

To better understand the mechanisms of root dentin formation, the process of dentinogenesis between tooth root and crown has been compared and two major similarities noted [11]. Firstly, for the formation of an interface and connection between the two different mineralised tissues (dentin and either enamel or cementum), a layer of unmineralised pre-dentin in both the crown and root forms which facilitates initial enamel or cementum deposition. Secondly, pre-odontoblasts arrange themselves along the basal lamina of epithelial cells in both the crown and root. However, many important differences in root and crown dentinogenesis have been noticed. For example, collagen fibrils in pre-dentin are less dense in the root than the crown, and the odontoblast processes retreat with their cell bodies from the basal lamina in the root, whereas they remain at the site in the crown. Morphologically, root odontoblasts are cuboidal while coronal odontoblasts are columnar. Furthermore, root and crown dentin have been shown to have different biochemical compositions. Taken together, these differences may be a reflection of alternate inductive mechanisms between root and crown dentin formation [11]. This theory is supported by subsequent studies [15, 21] showing that NFI-C specifically influences root formation but not crown formation [17, 21].

#### *1.2.1.2.2 Cementogenesis*

Cementum is a thin non-vascularised mineral tissue covering the root surface. The major function of cementum is to anchor the principle collagen ligamentous fibers (Sharpey's fibers) in the root surface. Additional functions of cementum include protecting dental pulp as a cover over the relatively porous dentin surface, adapting to occlusal force and repairing root defects from resorption or fracture [22, 23]. In contrast to periodontal ligament and bone, cementum does not undergo continuous turnover, but is capable of increasing in thickness. Histologically, cementum can be broadly classified into acellular and cellular cementum according to its cellular components. Acellular cementum covers the cervical two-thirds of the root surface while cellular cementum distributes in the apical third of the root surface and the furcation area in molars [24]. Cementum may also cover the enamel surface as coronal cementum in some species such as herbivora and some rodents [25]. The acellular cementum has been found to cover the cervical enamel in humans [24]. Additionally, cementum can be classified into 5 subgroups based on the origin of the collagenous matrix (extrinsic, intrinsic or mixed fiber): acellular afibrillar cementum (AAC), acellular extrinsic fiber cementum (AEFC), cellular intrinsic fiber cementum (CIFC), acellular intrinsic fiber cementum (AIFC), and cellular mixed (i.e. ex- and intrinsic) stratified fiber cementum (CMFC) [23, 26-29]. Intrinsic fibers are found to be arranged parallel to the root surface and are believed to be components of reparative tissues, whereas extrinsic fibers project at the right angles to the periodontal ligament space and thus are responsible for tooth anchorage. AAC is usually located at the cemento-enamel junction as small islands of cementum on the enamel surface [29]. This type of cementum contains homogenous matrix which lacks collagen fibers and embedded cells that can only be distinguished by electronic microscopic analysis. It is thought to have little functional value as it does not contribute to tooth anchorage [29]. AEFC, found in the cervical and middle third of the root surface [26], has densely twined fibers that are

perpendicular to the root surface projecting into the periodontal ligament space, and thus this type of cementum is closely involved in tooth anchorage [29]. The direction of extrinsic fibers might change according to the occlusal force. This type of cementum increases in thickness with age [29]. CIFC is usually located in the apical and furcation area of the tooth root [26]. It contains embedded cementocytes and lacks extrinsic fiber insertion with intrinsic collagen fibers arranged parallel to the root surface [28]. This type of cementum is usually found at root resorption lacunae and fracture sites as reparative cementum involved in repair and adaptation [29]. AIFC is a variant of CIFC during adaptive response with no cementocytes left behind. CMFC consists of AEFC and CIFC that deposit alternatively in an irregular way upon one another, with CIFC being the first layer of CMFC and growing faster than AEFC [29]. Located in the apical portion and furcation areas, this type of cementum contains a mixture of extrinsic and intrinsic collagen fibers involved in tooth anchorage and adaptation [29]. Among these five types of cementum, AEFC and CMFC are the most important types as they protrude extrinsic fibers projecting from the cementum to the periodontal ligament space. The classification of different types of cementum is important in a clinical perspective, as AEFC is the desired type of cementum following regenerative periodontal surgery, whereas CIFC (reparative cementum) frequently forms during periodontal repair.

The outcomes of periodontal regeneration depend largely on the new tissue attachment to the previously contaminated root surface. In this step, the predictability and quality of cementum regeneration plays an important role as Sharpey’s fibers cannot be inserted into the root dentin [23]. Although clinically successful periodontal regeneration has been reported [30-35], CIFC, rather than the desired AEFC, may form following periodontal treatment [23]. Cementum is the least understood mineralised tissue in the periodontal supporting tissues. Our lack of knowledge in cementum formation remains a major

drawback for clinical success in periodontal regeneration [23] thus further studies on cementum formation are warranted. Similar to the formation of other mineralised tissues, an unmineralised layer known as cementoid is initially formed by cementoblasts which then undergoes mineralization soon after its deposition [1]. Cementogenesis of rodent molars can be divided into two stages [11]. In pre-erupting and erupting teeth, acellular cementum (or primary cementum) is formed. The formation of acellular cementum coincides with the initial mineralisation of mantle dentin [36]. At this stage no cellular components are embedded, therefore primary cementum is also known as acellular cementum. HERS may play a role in regulating the amount of acellular cementum deposition, such that a normal periodontium is established without dento-alveolar ankylosis [11]. As the tooth reaches occlusion, cellular cementum (or secondary cementum) is formed where the proliferation of HERS dramatically reduces [11]. At this stage some HERS and dental sac cells are entrapped in the newly formed cementum as cementocytes and thus secondary cementum is also known as cellular cementum.

#### *1.2.1.2.2.1 Hyaline layer of Hopewell Smith and enamel matrix proteins*

The Hyaline layer of Hopewell Smith, also known as intermediate cementum, is a homogeneous mineralised matrix deposited by HERS [37, 38]. After the first root dentin (mantle dentin) forms, the innermost HERS cells secrete enamel-like proteins (as well as some dentin-associated proteins) into the space between the basement membrane of HERS and the newly formed dentin. Once these enamel-like proteins become mineralised, they form the Hyaline layer of Hopewell Smith [39]. It is found on the surface of root dentin from the cementoenamel junction to the apical third of the root where its identity is lost [8]. There has been debate on its composition; whether it is a variation of dentin or cementum [8]. After the disintegration of HERS and formation of ERM, DF cells migrate and differentiate into cementoblasts, which lay down cementum over Hyaline layer of

Hopewell Smith. In other words, the most likely function of this HERS secretary product is to facilitate “cementing” the primary acellular cementum to the root dentin [3]. Moreover, the initial fibers of the periodontal ligament get embedded into Hyaline layer of Hopewell Smith, thus it has been argued whether it should be considered as the fourth tooth supporting tissue [39].

The associations of enamel matrix proteins and the formation of cementum have been studied extensively. Enamel matrix proteins are a family of extracellular matrix secreted by ameloblasts during amelogenesis, including amelogenin, ameloblastin (also known as amelin or sheathlin), amelotin, tuftelin and enamelin [40]. Amelogenin represents around 90% of enamel matrix proteins [41] and is well conserved between species through the evolution, suggesting an important role of this protein [42]. The functions of enamel matrix proteins include being associated with amelogenesis, being involved in cell differentiation during the process of epithelial-mesenchymal interactions [40], and having a role in the differentiation of progenitor cells to cementoblasts to form cementum [42-44]. The application of porcine enamel matrix proteins have been shown to induce the formation of acellular cementum on a denuded monkey root surface [42]. Amelogenin and enamelin have been shown to be expressed during the formation of AEFC [45], whereas amelin and ameloblastin were found to be associated with the formation of the CIFC [46].

As the apical extension of the enamel organ, HERS retains some structural features and secretory functions of the enamel organ [9] [42] to produce enamel matrix proteins [45], as well as some cementum matrix proteins [47, 48]. As an initial step in cementum formation, Hyaline layer of Hopewell Smith is secreted by HERS prior to cementum formation [37, 38, 49]. Published evidence suggest that Hyaline layer of Hopewell Smith shares a similar origin with the innermost layer of prismless enamel, as they demonstrated similar patterns

of early mineralisation [49]. While root-derived Hyaline layer of Hopewell Smith proteins and crown-derived enamel proteins shared some similar epitopes as well as similar molecular weights and isoelectric points with one another, they demonstrated distinct forms of amino acid compositions, which distinguished Hyaline layer of Hopewell Smith proteins as a distinct class of enamel related proteins [45] [50]. The expression of enamel matrix proteins along the forming root surface has been shown to be associated with the formation of Hyaline layer of Hopewell Smith [37, 38, 49]. Studied showed that HERS is an active contributor of the formation and mineralisation of Hyaline layer of Hopewell Smith [38] both *in vivo* and *in vitro* along the forming root surface [45]. Moreover, the protein secreted by HERS in rodents does not appear to be amelogenin, in contrast to humans where this protein is believed to be amelogenin at the apical ends of developing tooth roots [42, 43]. The ERM in rat molars have the ability to produce amelogenin as a response to chronic inflammation [51]. A commercial product of enamel matrix derivative, Emdogain® (Biora AB, Malmo, Sweden), was shown to increase the proliferation, attachment and the osteopontin mRNA expression of ERM cells [52]. Although the association of enamel matrix proteins and the formation of AEFC has been challenged [9], there is mounting evidence that enamel matrix proteins are involved both in cementum formation and regeneration [42, 43].

#### *1.2.1.2.2.2 Cellular origin of cementoblasts*

Since cementum regeneration is one of the most important aspects of periodontal regeneration, it is imperative to determine the origin of cementoblasts [23]. In contrast to the origin of enamel- and dentin-forming cells, the origin of cementum-forming cells remains controversial. The widely accepted theory suggests that cementum is a dental follicle-derived tissue formed subsequent to HERS disintegration [3, 9]. However, evidence is available to suggest that dental follicle cells might not be the only cellular

origin of cementoblasts. It is worth noting that acellular cementum differs in many ways with cellular cementum [23]. While acellular cementum is a unique tissue, cellular cementum shares some similarities with bone and thus has been regarded as bone-like tissue [23, 53]. This discrepancy raises the possibility of different cellular origins for acellular-cementum-forming and cellular-cementum-forming cementoblasts [23]. This notion has been supported by studies reporting different immunophenotypic profile of cementoblasts associated with two types of cementum. A study based on the immunolabelling of osteoblast specific markers has suggested that cementoblasts of cellular cementum and osteoblasts share the same precursor cells, different from cementoblasts of acellular cementum [53]. In addition, cementoblasts of different origins have been distinguished by immunolabelling for epidermal growth factor [54]. During acellular cementum formation, the majority of cementoblasts show immunopositivity to Distal-less gene-2 (Dlx-2), while limited numbers of cellular-cementum-associated cementoblasts display this positivity [55]. Furthermore, different cytokeratin expression profiles in pre-erupting, erupting and erupted teeth also indicate different origins of cementoblasts [11, 56]. Two types of cementoblasts have been proposed: those derived from cranial neural crest cells (cellular and reparative cementum) and those derived from HERS (acellular cementum) [12, 55]. This seems a plausible explanation for different phenotype of cementoblasts and different properties of two types of cementum [23].

#### *1.2.1.2.2.3 HERS and cementogenesis*

The classical theory of cementogenesis supports that DF proper and perifollicular mesenchyme give rise to cementoblasts. This is based on the evidence from $^{3}$H-thymidine labelling studies [8, 10, 26]. However, the fact that HERS also incorporates $^{3}$H-thymidine [26] challenges the notion that DF cells are the only cellular origin of cementoblasts. There is also no general agreement about whether HERS or unmineralised root dentin is the

inducer of cementogenesis [11]. The recombination of dentin slices and DF cells has shown that an exposed dentin surface is not sufficient to induce the differentiation of cementoblasts [57]. Ever increasing evidence shows that HERS and it derivatives play important roles in cementum formation. Early studies produced conflicting data regarding HERS and cementogenesis. While some reports claim that the removal, rather than the presence of HERS, is a prerequisite for the onset of cementogenesis [58], most studies indicate that HERS are necessary for the production of cementum [59]. There is also a debate about whether HERS induces cementum formation or secretes cementum directly.

There is now support for the notion that HERS indirectly facilitates cementum formation. It has been accepted that epithelium and its products are able to induce bone formation in the surrounding mesenchyme, where a similar mechanism may occur during root formation [11]. It has also been reported that chemoattractant substances released from the hyaline layer or HERS cells induces pre-cementoblast differentiation and directs pre-cementoblast migration towards the root surface [60, 61]. The rationale for using a commercial derivative of Enamel Matrix Proteins, such as Emdogain®, in periodontal regeneration is based on the theory that Enamel Matrix Proteins, produced by HERS, are capable of inducing the differentiation of dental follicle cells to cementoblasts [43, 44]. One explanation for the inability of HERS to form cementum directly may be that HERS remains isolated through a basal lamina [62]. However, a possible inductive role of HERS in the initiation of cementogenesis is not excluded. A recent study on rat molar cementogenesis using keratin-vimentin and keratin-Runx2 (runt-related transcription factor 2) double immunolabelling reported that HERS cells were unable to transform to an intermediate phenotype from epithelial to mesenchymal cells to give rise to cementoblasts [63].

On the other hand, it has been proposed that HERS may have the capacity to produce cementum directly. One study reported that human HERS not only controls periodontal ligament stem cells differentiation, but also gives rise to cementoblasts through epithelial mesenchymal transition [64]. Furthermore, in addition to Enamel Matrix Proteins, HERS has been shown to secrete cementum-associated proteins [9, 26, 47] such as cementum attachment protein (CAP) [12], bone sialoprotein (BSP), osteopontin (OPN), fibrillar collagen [23] and amelogenin [9]. More importantly, HERS cells are able to be induced to form mineralized modules *in vitro* [12] through an epithelial mesenchymal transition [64]. These mineralised modules were shown to resemble physiological acellular cementum by transmission electron microscopic analysis [12]. To further characterise the mineralised matrix formed by HERS, studies were performed to analyse the protein expression of markers associated with enamel, dentin, bone and cementum [12]. The data suggests that the mineral deposited by HERS is similar to cementum or bone, rather than enamel or dentin [12]. The osteogenic capacity of HERS *in vitro* strongly supports the notion that HERS is capable of producing cementum directly. Secondly, electron microscopy and immunocytochemical analyses suggested that the HERS was a possible alternate cellular origin of the cementoblasts. Transmission electronic data revealed that dissipated HERS cells acquired the typical morphological features of cementoblasts during the very early stage of porcine root formation, which is possibly due to a phenotypic conversion of epithelial mesenchymal transition [9]. The bay-shaped indentations on the cell surface were filled with precementum collagen fibrils, as well as the expression of cytokeratin and the presence of desmosomes indicating an epithelial ancestry [9]. In addition, the expression of epithelial markers in a subpopulation of cementoblasts strongly indicates HERS as the origin of cementoblasts. Cytokeratin expression was observed in some cementoblasts in erupting and erupted teeth [11]. Both HERS and cementoblasts associated with acellular cementum are immunopositive for the cytokeratin pair 8 and 18 [56].

Expression of E-cadherin [65] and co-expression of cytokeratin and vimentin have been observed in some cementum-forming cells [56, 66]. Furthermore, it has also been proposed that HERS may be the progenitor cells for other mesenchymal cell populations within the PDL [23]. This is based on the observations of positive cytokeratin 19 expression [67] and the presence of simplified desmosomes [68] and desmosomal proteins [69] in a subpopulation of PDL fibroblasts. Taken together, current evidence suggests that HERS plays important roles in cementogenesis, with increasing evidence that HERS is capable of producing cementum directly.

In summary, there is increasing evidence from animal studies that HERS is not only a barrier between dental follicle and dental papilla cells but is also involved in the determination of the shape, size and number of roots, development of dentin and cementum or may act as a source of mesenchymal progenitor cells for cementoblasts in the periodontium. However, very little information on human tooth formation has been reported [1]. Species differences have been noted in tooth root formation [70, 71], thus caution needs to be taken when extending the findings in other species to humans [56].

### 1.2.2 The fate of HERS after tooth root development

During initial tooth root formation, HERS cells undergo an extensive period of proliferation. However, the proliferation rate of HERS at the later stages of tooth root development is not synchronised with the surrounding root-forming connective tissue cells, as space between HERS cells increases the number of HERS cells decreases on the maturing root surface. Different mechanisms have been put forward for the observed decrease of HERS cells [62]. One proposed mechanism is that some HERS cells migrate to the PDL away from the root surface and form Epithelial Cell Rests of Malassez (ERM). It is also suggested that HERS cells become incorporated into the advancing cementum front

[62] or differentiate into cementoblasts as described above [12, 64, 72]. Alternatively, some HERS cells undergo apoptosis [73-75]. However, a study using Terminal deoxynucleotidyl transferase dUTP nick end labeling (TUNEL) to assay late stage apoptosis, showed that only some of the HERS cells showed positive nuclei labelling. This indicates that while some HERS cells may undergo apoptosis, many of them remain viable and become part of adult PDL through other pathways. Moreover, HERS cells may undergo epithelial mesenchymal transition (EMT) and contribute to the mesenchymal cell populations in the PDL [11]. Ultrastructurally, HERS cells that remain on the root surface following fenestration display a mesenchymal morphology. This is also supported by the protein expression profile from immunohistochemical studies. By switching from media favouring epithelial cell growth to those favouring mesenchymal cell proliferation, HERS has been shown to demonstrate a more mesenchymal appearance concomitant with a switch from cytokeratin to vimentin expression [11].

### 1.2.3 The role of ERM in the maintenance of periodontal ligament function

After the fenestration of HERS, it forms strands or islands of epithelial cells known as ERM. Morphologically, these ectoderm-derived tissues are identified as islands of epithelial cells with a high nuclear cytoplasm ratio that can be easily distinguished histologically in most species [24]. Historically, our knowledge of ERM biology has been limited to the descriptive studies of their distribution and numbers using light and electron microscopy [3]. It is traditionally thought that the functional role of HERS ends after it breaks up into ERM [71], with ERM being regarded as a remnant of embryonic development based on ultrastructural observations. However, when stimulated in tissue culture or by inflammation in the PDL, ERM display biochemical and ultrastructural changes [3]. A remarkable characteristic of ERM cells is that they persist within a mesenchymal matrix during postnatal life, while epithelial cells in other tissues exist as a

layer separated from the underlying connective tissues by a basal lamina. The persistence of ERM in the adult periodontium suggests that they might represent more than a vestigial structure and play functional roles in tooth support [3]. In theory, the proposed roles of HERS in root formation need to be studied on ERM in adult periodontium to test whether ERM inherit some functional roles from HERS. Although there is no general agreement on the functions of ERM, accumulating evidence suggests that the putative roles of ERM in adult PDL include maintaining PDL homeostasis to prevent ankylosis and maintain PDL space, to prevent root resorption, to serve as a target during PDL innervation and to contribute to cementum repair.

#### *1.2.3.1 The maintenance of PDL homeostasis*

##### *1.2.3.1.1 The prevention of ankylosis and the maintenance of PDL space*

The periodontal ligament is the soft connective tissue that is incorporated between the tooth root and the inner wall of alveolar bone [1]. This “cushion”-like structure gives resilient support to tooth roots [1]. After the removal of PDL cells, ankylosis may occur and this non-resilient support leads to a loss of function and eventual resorption of the tooth root [1]. In ankylotic teeth, periodontal ligament space can be restored at the cost of the resorption of the cementum (or sometimes dentin) and of the alveolar bone. In other words, under certain conditions ankylosis can be reversed by bone and cementum being replaced by a functionally oriented PDL, however the underlying mechanism driving this process remains unclear [1]. Evidence that ERM play a role in the maintenance of PDL space is derived from observations that ERM are always found in the vital PDL areas of replanted teeth [76]. Additionally, the absence of ERM cells in regenerated PDL is associated with the narrowed PDL space [77]. The dento-alveolar ankylosis created from the denervation of the inferior alveolar nerve is thought to result in a reduced number of ERM cells [78]. Ten weeks post-denervation, the increased PDL space is associated with the regeneration of ERM [78]. This observation lends further support to the idea that ERM

could be involved, at least in part, in maintaining the PDL space and the prevention of dento-alveolar ankylosis [79]. This appears to be consistent with the theory that HERS might function as a regulator of acellular cementum deposition and thus prevent ankylosis as described above [11], although some studies report conflicting data sets which showed that the normal PDL space was restored with the absence of ERM during orthodontic tooth movement [80] and after the withdrawal of 1-hydroxyethylidene-1, 1-bisphosphonate (HEBP, a reagent used to reduce PDL space) [81]. One possible explanation of ERM mediating the maintenance of PDL space is that ERM cells might produce certain molecules to prevent alveolar bone from migrating to the cementum by modulating osteogenesis in the PDL space [78]. It has also been reported that the number of osteoclasts and odontoclasts increased with the disappearance of ERM cells during ankylosis, suggesting a potential inhibitory role of ERM cells on osteoclast and odontoclast function. Another possible explanation is that the maintenance of the PDL space and the prevention of ankylosis might be achieved by ERM producing collagenase and thus degrading collagen [82].

#### *1.2.3.1.2 The prevention of root resorption*

Using a re-implantation model in dogs, the absence of root resorption has been associated with the presence of ERM cells [83]. This might be linked to the role of ERM in the prevention of ankylosis, in that ERM produce certain molecules to modulate alveolar bone resorption, implying that root resorption is not essential to maintain the normal PDL space. In a human study, ERM were found in areas of orthodontic root resorption undergoing repair and were believed to be involved in cementum repair after migrating into the resorption bay [84]. Using double immunohistochemical analysis of ERM cells and blood vessels, physiological root resorption was related to loss of continuity of the ERM network and the incursion of blood vessels [85]. It was suggested that tooth resorption may be

derived from a loss of PDL homeostasis control possibly mediated by ERM. The proliferation of ERM cells and their increase in size during tooth movement indicate their response to mechanical stresses with a possible role in tooth remodelling activities [86]. Taken together, HERS/ERM may be “ultimate governor of the PDL, the regulator of its width and homeostasis and the shield against resorption and ankylosis” [62].

#### *1.2.3.2 A target during developmental PDL innervation*

A study of human ERM has reported a close apposition between Ruffini-like, free nerve endings and the basal lamina of ERM cells [87]. Additionally, some nerve fibers have been found to invest between ERM cells [88]. Moreover, a subpopulation of ERM cells has been shown to express a number of neuropeptides including parathyroid hormone-related protein [89], protein gene product (PGP) 9.5, calcitonin gene-related peptide, substance P, and vasoactive intestinal peptide [88, 90-92]. ERM cells also express protein for TrkA, a high-affinity receptor of nerve growth factor (NGF), where studies have shown that denervation of the inferior alveolar nerve resulted in a marked decrease in the distribution area and size of ERM cells. Therefore, sensory nerve innervation may have a regulatory role in the maintenance of ERM expressing TrkA [93]. The presence of neuroendocrine cells as a subpopulation of ERM cells strongly suggests the endocrine functions of ERM cells.

#### *1.2.3.3 Cementum repair*

Another role attributed to ERM cells is that they may contribute to cementum repair. This is compatible with the notion that HERS contributes to cementum formation during tooth root development. After experimentally induced root resorption, ERM cells expressed proteins for bone morphogenetic protein-2 (BMP-2), OPN and ameloblastin, while ERM cells in uninjured control sections did not express any of these proteins [94]. These findings suggest that although ERM cells appear quiescent by their ultrastructure, they may

be activated to secrete matrix proteins and participate in cementum repair. Furthermore, other researchers reported that ERM synthesized bone/cementum-related proteins such as OPN, BSP and osteoprotegerin [52, 94-97], as well as amelogenin and amelin [46], indicative of a potential role in periodontal regeneration. Among these, amelogenin, OPN and BSP are associated with acellular cementum formation [98, 99]. Emdogain®, an enamel matrix derivative from developing porcine teeth, enhanced the proliferation and attachment of ERM cells and their osteopontin mRNA expression [52]. In a human study, it was reported that ERM existed in areas of repairing orthodontic root resorption and are believed to be involved in cementum repair [84]. Considering the strategic position of ERM cells in healthy adult periodontium, together with their ability to secrete matrix proteins conducive to cementum repair, it is reasonable to propose that these cells are crucial for predictable and successful periodontal regeneration [82]. As for HERS, ERM may either induce PDL fibroblasts subpopulation to generate cementoblasts or directly give rise to cementoblasts by recapitulating epithelial mesenchymal transition [23].

In summary, the role of HERS in periodontal development and that of its descendants, ERM, in the maintenance of periodontium, remains an important aspect of our understanding of periodontal regeneration, which deserves further investigation.

## 1.3 Limited regenerative capacity of periodontal ligament tissues

Successful periodontal regeneration entails the reconstruction of gingival connective tissue, cementum, alveolar bone and periodontal ligament (PDL). The complex nature and the poor regenerative capacity of periodontal supporting tissues have impeded the development of reliable treatment procedures for periodontal disease. While the formation of new cementum, new bone and the reestablishment of periodontal ligament have been observed during orthodontic movement, this process is regarded more as a physiological

response, rather than true regeneration of pathologically diseased tissue [5]. Current approaches for the treatment of periodontal disease, ranging from root surface conditioning, bone graft replacement, guided tissue regeneration to growth factor/enamel matrix protein application or combinations thereof [4], show a limited potential for complete and reliable periodontal regeneration. In particular, the regeneration of cementum on the contaminated root surface and the insertion of functional collagen fibers thereafter are beyond the current technologies. Furthermore, the reestablishment of periodontal ligament is as important as the regeneration of hard tissues such as bone and cementum, in order to prevent the development of ankylosis [100]. To date, the application of acellular allogeneic bone grafts and growth factors falls short of regenerating periodontal ligament [101]. Collectively, periodontal ligament tissues have a poor regenerative capacity and the outcomes of current periodontal regenerative therapies are clinically unpredictable. Therefore, alternative strategies are being investigated to treat damaged tissues following insult or disease. Recently, periodontists have shown increasing interest in the putative stem cell populations present in the periodontal ligament which represent an important candidate for cell-based tissue engineering.

## 1.4 Stem cells

The term “stem cells” (SC) usually refers to uncommitted cells with the capacity to self renew, undergo extensive proliferation and reproducibly differentiate into numerous cell types *via* asymmetric cell division under appropriate conditions [102]. Self-renewal refers to the ability of SC to undergo self-renewal indefinitely while maintaining the undifferentiated state. The potency of a stem cell specifies its potential to differentiate into other cell types. The hierarchy of cell potency includes totipotency, pluripotency, multipotency, oligopotency and unipotency. To date, the different SC populations have been broadly categorized into embryonic stem cells (ESC), adult stem cells (ASC) and

more recently, through genetic manipulation, induced pluripotent stem cells (iPSC) (Table 1.1). ESC are the least restricted population of SC with robust developmental potential and as such have the ability to proliferate extensively and differentiate into any cell type that is ultimately derived from the three embryonic layers: endoderm, mesoderm and ectoderm [103-105]. Induced pluripotent stem cells (iPSC) are ESC-like cells, comparable to ESC in terms of their morphology, gene expression profiles, proliferation and differentiation capacities [106, 107], generated through reprogramming fibroblasts by ectopic expression of four transcription factors (Oct3/4, Sox2, Klf4, c-Myc), well known as Yamanaka factors [106, 107]. One of the advantages of iPS over ESC is that they are donor specific and thus have a reduced chance of immune rejection [108]. Despite the immense potential of ESC and iPSC in cell-based therapies, there are numerous challenges and limitations associated with their use, including ethical issues [109, 110], difficulty in controlling their differentiation and inhibition of growth, as well as the safety challenge in terms of tumour-forming properties which result in the formation of teratomas [111, 112]. As an alternative, adult, somatic or postnatal stem cells are found in specialised tissues and organs of human adult and are considered as a promising cell source for tissue engineering. They reside as subpopulations in various specialised tissues responding to environmental stimuli to proliferate, migrate and replenish cells that are lost during normal senescence or tissue injury [113]. Compared to ESC and iPS, ASC are more mature and much more limited in their differentiation potential thus have a lower tumorigenic potential. Whilst these cells exhibit limited proliferation and differentiation potential, they are easily accessible and not associated with ethical issues in relation to their use. Moreover, the immunomodulatory properties of ASC have encouraged the use of allogeneic MSC to treat various diseases [114, 115], another advantage of ASC over ESC. These studies showed that allogeneic ASC were not rejected by the host after transplantation as generally assumed, rather they are well-tolerated by the recipient body.

**Table 1.1 Derivation and properties of stem cell populations**

| | **Derivation** | **Differentiation capacities** | **Chance of immune rejection** | **Challenges in their use** |
|---|---|---|---|---|
| Embryonic stem cells | Inner cell mass of pre-implantation embryo | Robust differentiation potential to form any cell type from the 3 embryonic layers | High | (i) Ethical issues<br><br>(ii) Safety challenge (teratoma-generating potential)<br><br>(iii) Difficulty in controlling their differentiation and inhibition of growth |
| Induced pluripotent stem cells | Adult cells induced to an embryonic stem cell phenotype | Comparable to embryonic stem cells | They are donor specific thus less chance of immune rejection. | |
| Adult stem cells | Various adult specialised tissues | Limited differentiation potential | Immunomodulatory properties | Limited proliferation and differentiation potential |

### 1.4.1 Historical perspective and minimal criteria for defining multipotent mesenchymal stem cells

Mesenchymal stem cells (MSC) have been of interest long before the term "MSC" was introduced. Friedenstein and colleagues carried out a series of landmark studies characterizing stem cells derived from bone marrow that are clonogenic (colony-forming unit fibroblasts), plastic-adherent and capable of differentiating into osteoblasts, adipocytes and chondrocytes [116-118]. These cells were later named mesenchymal stromal cells by Owen in 1988 [119]. The term "mesenchymal stem cells" was first used in 1983 [120] and was popularized by Caplan in the early 1990s [121]. Thereafter the term MSC has become widely used in the literature.

To address the inconsistency in nomenclature and account for the biologic properties of multipotential, clonogenic, plastic adherent cells derived from various stromal tissues, it was proposed by the committee for the International Society for Cellular Therapy (ISCT) that fibroblast-like, plastic adherent cells be termed "multipotent mesenchymal stromal cells", regardless of their tissue of origin; while the term "mesenchymal stem cells" should be reserved for a subset of cells that demonstrate stem cell activity by clearly stated criteria. The acronym MSC may be used for both populations [122]. The ISCT has proposed a set of minimal standards for defining human MSC in 2006. These include firstly, adherence to plastic when maintained in standard culture conditions; secondly, specific surface antigen expression of MSC including the expression of CD105, CD73 and CD90, and lack of expression of CD45, CD34, CD14 or CD11b, CD79α or CD19 and HLA-DR surface molecules; thirdly, multipotency to differentiate to osteoblasts, adipocytes and chondroblasts under standard *in vitro* differentiating conditions [123]. This trilineage differentiation potential is recommended to be stained with Alizarin Red or von Kossa staining, Oil Red O staining and Alcian blue staining or immunohistochemical staining for collagen type II, respectively [123]. Whilst this minimal set of criteria helps to

standardize the field, the *in vitro* characterisation of MSC is an over simplified and relatively non-specific description of MSC that needs more rigorous assessment *in situ* and using *in vivo* serial transplantation methodologies to demonstrate self-renewal capacity and mutipotential [124, 125].

### 1.4.2 Adult MSC-like cells derived from dental tissues

Following tooth development, dental tissues exhibit limited regenerative or reparative capacity. As current therapeutic strategies for dental tissue regeneration have shown limited and unpredictable clinical outcomes, scientists hope to achieve better clinical outcomes using dental stem cell-based tissue engineering. Current studies support the hypothesis that stem cells can be isolated and identified from adult dental tissues that are capable of differentiation into functional, lineage specific cells [126]. According to their tissue origin and differentiation potential, dental stem/progenitor cells can be classified into six groups [100]: those associated with dental pulp including dental pulp stem cells (DPSC) [127], stem cells from apical papilla (SCAP) [128-130] and stem cells of human exfoliated deciduous teeth (SHED) [131]; those related with periodontium including periodontal ligament stem cells (PDLSC) [126] and dental follicle progenitor cells (DFPC) [132, 133]; and stem cells from gingival tissues termed as gingiva-derived mesenchymal stem cells (GMSC) [134]. Additionally, recent studies supported the existence of stem cells residing in inflamed dental pulp [135-137] and inflamed periodontium [138]. Recently, PDLSC have been isolated from the periodontium of other species such as sheep [139] and pig [129]. Bone marrow stromal/stem cells (BMSC) are used as the gold standard MSC-like population as they are the most characterized stem cell population [140]. Stem cells residing in dental tissues exhibit similar features to those described for BMSC, including a multipotent differentiation potential as well as the expression of MSC associated cell surface markers [126, 127, 131]. One common feature of dental MSC-like populations is

that they demonstrate potent capacities to differentiate into odontogenic lineages rather than osteogenic lineages [100], while they demonstrate weaker adipogenic and chondrogenic capacities than BMSC. Of note, dental MSC are derived from ectomesenchyme, where dental mesenchyme interacts with the neural crest, and therefore are thought to inherit some properties of neural crest cells [100]. For example, dental MSC, including DPSC [141], SHED, SCAP [128, 131] and PDLSC [142], illustrate a potent neurogenic capacity [100]. It is important to note that the origin of MSC may determine their fate and functional characteristics. Following subcutaneous transplantation into rodents, *ex vivo*-expanded MSC demonstrate the ability to develop into distinct tissues resembling the microenvironment from which they were derived *in vivo*. For example, PDLSC exhibit the capacity to form cementum/PDL-like tissues while DPSC and BMSC generate dentin/pulp-like and lamellar bone/marrow-like structures, respectively [126, 127]. A greater understanding of progenitor cells in the periodontal ligament is a prerequisite to manipulating stem cells in clinical applications.

#### *1.4.2.1 Stem cells associated with periodontal tissues*

Early studies by McCulloch *et al* reported a rare population of cells identified as “progenitor cells” that exhibited some of the classical cytological features of stem cells [143]. In order to identify putative stem cells in the periodontium, various techniques used to characterise BMSC or MSC and DPSC were employed. When plated under the same growth conditions as those described for BMSC and DPSC, PDLSC were found to possess the capacity to generate clonogenic adherent cell colonies, where the incidence of CFU-F was greater than that reported for BMSC and DPSC. Further characterisation found that PDLSC expressed the early BMSC associated cell surface molecules STRO-1 and CD146/MUC18, as well as high levels of scleraxis, a tendon-specific transcription factor [126]. The PDLSC niche was characterized by the combination of STRO-1/CD146/CD44

staining, located mainly in the perivascular regions as described for BMSC and DPSC [144]. While PDLSC demonstrated a greater incidence of CFU-F than BMSC and DPSC, DFPC showed limited number of plastic adherent cells, thus the colony forming efficiency could not be enumerated from freshly isolated dental follicle cells. The expression of Notch-1 and nestin in DFPC implies that they are in an undifferentiated state [132]. Functionally, PDLSC generated cementum/PDL-like structures showing connection of cementum-like structures and Sharpey's fiber-like tissues when transplanted into immunodeficient rodents [126]. In addition, PDLSC have been transplanted into the surgically created periodontal defects to assess their therapeutic capacity to contribute to periodontal tissue repair.

#### *1.4.2.2 The use of stem cells in periodontal tissue regeneration*

##### *1.4.2.2.1 The use of periodontal ligament progenitor cells in periodontal tissue regeneration*

The poor regenerative capacity of periodontal ligament tissues and unpredictable outcomes of current periodontal therapies have encouraged the investigation of alternative strategies to treat damaged tissues following insult or disease. As MSC hold great promise in clinical applications for tissue engineering, the discovery of PDLSC has offered a novel therapeutic avenue for the reconstruction of damaged periodontal tissues as they gave rise to cementum-PDL like structure *in vitro* [143, 145]. PDLSC-mediated regenerative therapy has been tested in large animal models to evaluate their potential in preclinical applications [129, 146, 147]. A recent study laid the foundation of stem cell therapy for periodontitis by transplanting autologous PDLSC in a miniature swine model of a periodontal defect by surgically removing alveolar bone and subsequent silk ligament suture around the cervical portion of the tooth [147]. Clinical and histological assessment indicated that PDLSC not only gave rise to the reestablishment of alveolar bone height, but also the regeneration of PDL [147]. The mixed stem cell sheet, composed of human PDLSC and osteoinductive

ceramic bovine bone powder, was shown to give rise to cememtum/PDL-like tissue regeneration with neovasularization [148]. Using a minipig model, extracted tooth roots were covered with *ex-vivo* expanded autologous periodontal ligament cells and implanted into bone defects. While the control group (without cells) showed resorption and ankylosis, the roots with periodontal ligament cells demonstrated orientated fiber bundles between bone and root within twelve weeks of implantation, resembling functional periodontal ligament [149]. Another study reported the biological effect of dentin noncollagenous proteins (DNCP) on human PDLSC *in vitro* and *in vivo* [150]. Attempts to improve the scaffolds in tissue engineering include the implantation of PDLSC with three dimensional methods [151, 152]. Collectively, the above-mentioned studies were conducted with autologous MSC and large variability in the design of the preclinical studies was noticed, including the type of carriers used, cell dose and types of defects. Recently, allogeneic MSC-based tissue engineering is emerging as a novel strategy, where PDLSC have been shown to posses similar immunomodulatory properties described for BMSC and DPSC [153]. Intriguingly, the implantation of allogeneic PDLSC sheets into miniature swine periodontal defects were well-tolerated by the recipient body with no major immunological rejections, which lends support to the potential of using allogeneic stem cells in preclinical studies [154].

To progress cell-based periodontal therapy further, the implantation of autologous periodontal ligament progenitor cells (PDLP) was performed in a pilot human clinical study. However, there was little characterisation of the cell properties of PDLP at the time of implantation, which were collected from explant cultures using crude isolation techniques, in contrast to the better characterised PDLSC which are isolated from single colony clusters. Autologous PDLP preparations were mixed with bone grafting material and implanted into intrabony defects in three patients. At 72 months follow-up, the PDLP

group demonstrated therapeutic improvements including a significant decrease in tooth movement and probing depth, increased gingival recession and importantly the improvement of attachment gain [155]. Retrospective comparison of PDLP and PDLSC indicated that PDLP might be more committed than PDLSC, with lower osteogenic and adipogenic potential *in vitro* and less cementum formation *in vivo* [155]. In addition, their expression of three early mesenchymal stem cell markers, STRO-1, CD146, and SSEA4, was lower than PDLSC [155]. However, these two populations demonstrated comparable capacities to form Sharpey's fibers in a mouse model, with a similar phenotype other than the expression of scelaxis [155]. Although human PDLP have demonstrated some potential for use in periodontal regeneration in a limited patient cohort, further clinical studies need to be conducted using large randomised patient groups with different periodontal defects such as furcation involvement, angular resorption and vertical resorption.

#### *1.4.2.2.2 Combination of periodontal ligament progenitor cells and other cell types in periodontal tissue regeneration*

As PDLSC exhibited lower osteogenic potential *in vitro* compared to BMSC, PDLSC were co-cultured with BMSC to enhance the formation of new alveolar bone. The co-culture of human PDLSC and BMSC *in vitro* significantly elevated the alkaline phosphatase activity, as well as the expression of collagen type I, osteocalcin and vascular endothelial growth factor [148]. In a recent study, the combination of Stem Cells from Apical Papilla (SCAP) and PDLSC has been shown to induce the formation of cementum and Sharpey's fibers anchored into the cementum. Additionally, when a combination of autologous SCAP/PDLSC was implanted into sockets in the minipig model with the artificial porcelain crown, a bio-root has been regenerated with root/periodontal structure and normal tooth function [130].

As the reciprocal interactions between HERS and the surrounding mesenchyme initiate

tooth root development [156], studies were carried out to demonstrate whether the combination of epithelial and mesenchymal cell populations would give rise to better tooth and periodontal regeneration. The successful tooth regeneration was achieved using the combination of tooth germ-derived epithelial and mesenchymal single cells. While epithelial or mesenchymal cells alone generated keratinized epithelium-like structures or bone, respectively, the combination of epithelial and mesenchymal cells generated reconstituted tooth germ *in vitro* [157, 158]. When transplanted into subrenal capsules or tooth cavity in mice, this tooth germ could generate incisors, in which tooth elements, such as odontoblasts, dentin, dental pulp and periodontal ligament, were arranged appropriately akin to a natural tooth [157, 158]. In another study, a bioengineered tooth unit comprising mature tooth, periodontal ligament and alveolar bone was generated in subrenal capsules in mice and transplanted into edentulous sites *in vivo*. This transplantation strategy not only restored tooth function but also helped regenerate the lost bone volume both vertically and horizontally [159]. These studies highlight that both epithelial and mesenchymal cell populations, as well as their interactions, are essential components for successful tooth reconstitution.

In adulthood, ERM cells are the only odontogenic epithelial population in the PDL. Although the use of periodontal ligament stem cells can result in significant periodontal regeneration [147], the combination of HERS/ERM and dental MSC populations gave rise to better outcomes in periodontal regeneration [160-162]. In combination with dental pulp cells, porcine ERM can differentiate into ameloblast-like cells and generate enamel-like tissues *in vivo* shown by positive amelogenin staining [162]. Co-culture of DF and HERS cells has significantly increased bone/cementum related gene expression as well as *in vitro* mineral nodule formation [160]. When transplanted into rat omenta, DF cells pre-exposed to HERS gave rise to cementum-like and PDL-like structures, while control cells only

produced fibrous tissues [160]. Collectively, the improved regenerative outcomes using the combination of HERS/ERM and dental MSC have highlighted the essential roles of HERS/ERM in the regenerative procedures.

#### *1.4.2.2.3 The use of non dental MSC in periodontal tissue regeneration*

Other than intraoral MSC, several extraoral MSC have been used for dental application. The potential of BMSC in dental applications has been investigated [163-166], including differentiation of BMSC into ameloblast like cells [167] and functional cementoblasts using enamel matrix proteins [168]. In a surgically created rat periodontal defect model, BMSC seem receptive to biological signals from the microenvironment and contribute to periodontal regeneration, with new bone formation and appropriately orientated periodontal ligament fibers [169]. The potential of BMSC and PDLSC in alveolar bone regeneration was compared in a canine peri-implant saddle-like defect model, where BMSC generated greater volumes of new bone than PDLSC, with both populations generating larger volumes of new bone than the corresponding control groups [170]. Furthermore, a clinical study reported that autologous BMSC in combination with platelet-rich plasma into periodontal angular defects resulted in a 4 mm reduction in probing depths and a 4 mm clinical attachment gain [171]. Other types of cells being used for dental regenerative studies include alveolar bone cells and adipose-derived stem cells. Alveolar bone cells have been demonstrated to facilitate regeneration in minipig periodontal defect models, with the formation of new cementum and alveolar bone and the establishment of a new attachment [172]. It has been reported that adipose-derived stem cells, which are mixed with platelet-rich plasma gel and placed into a rat periodontal defect, can promote the formation of a periodontal ligament-like structure *in vivo* [173]. However, no evidence has been provided that transplantation of adipose-derived stem cells alone was sufficient to facilitate periodontal regeneration.

Taken together, it remains to be determined which source of dental MSC will be the most suitable cell source for regenerative periodontal therapy [174]. Tooth germ cells display tremendous potential for tooth regeneration, however, the limited availability of tooth germ cells is one of the major problems encountered. Similarly, dental follicle cells appear to be a good source of progenitor cells but their application is constrained due to their limited availability [174]. Non dental MSC such as BMSC have been extensively studied but are required to be used following genetic manipulation or treatment with growth factors to enhance their odontogenic potential [174]. It is emerging that the progenitor cells in the adult periodontium, in combination with the epithelial components in the periodontium, offer a new avenue for periodontal tissue regeneration.

#### *1.4.2.2.4 The use of dental stem cells to treat extraoral disorders*

The potential of dental stem cells to treat disorders outside the oral cavity has also been reported. For example, dental MSC inherit some properties from neural crest cells following development [100], as demonstrated by their neurogenic capacity. Due to the difficulty of access to neuronal stem cells and the neural crest origin of dental pulp-associated tissues [141], SHED and DPSC hold great promise for treating Parkinson's disease [175] and other neurological disorders [141, 176]. In addition, gingival tissues, which can be easily obtained as discarded biological samples, show some therapeutic promise. Interestingly, wound healing in adult gingiva usually demonstrates fetal-like scarless healing. Potential therapeutic application of GMSC in inflammatory disorders has recently been reported where GMSC are thought to attenuate colitis and help restore normal digestive function by mediating immunological processes [134]. The ease of isolation, abundant tissue source and potent proliferation capacity make GMSC as an attracting candidate for treating chronic inflammatory disorders.

### *1.4.3 Surface markers of stem cell populations*

#### *1.4.3.1 Heterogeneity of stem cells*

Despite the encouraging outcomes for the therapeutic use of stem cells, their clinical application is still uncertain due to a lack of understanding of their properties and developmental status. Of these, the heterogeneity present within stem cell populations hinders the clinical progress within the stem cell and regenerative medicine fields. A growing body of evidence indicates that both embryonic and adult stem cells fall into two or more distinct subpopulations [177]. The heterogeneity, which has also been observed *in vivo* [177], includes morphological variability, inconsistency in levels of proliferation and differentiation potentials, as well as differences in patterns of gene and protein expression profiles [178]. Morphologically, stem cells exhibit different cell densities between colonies, and within the same colony, different cell morphologies and cell sizes [179]. The heterogeneity of morphology, proliferation and functions of stem cells indicates potential hierarchies of cellular differentiation [180], that is, different stages of cell immaturity [181], which is caused by the oscillatory expression of critical transcription factors [177]. In terms of the biological significance of the heterogeneity, it appears that the subpopulations with distinct phenotypes demonstrate different biological functions [177]. For example, the pluripotency-associated markers are heterogeneously expressed in embryonic stem cells [177]. Cell subsets with the positive expression of Nanog and Stella show a higher propensity for maintaining a self-renewal state, while cells that lack the expression of Nanog and Stella are more prone to differentiate [182, 183]. A recent study shed new light on the correlation of N-cadherin expression and hematopoietic stem cells function [184]. Whilst cells highly expressing N-cadherin are not stem cells, populations expressing N-cadherin at intermediate levels demonstrate poor repopulating potential, compared to those with low N-cadherin expression which have robust repopulating capacity [184]. Studies on skin keratinocytes correlated the expression of integrin subunits

with stem cell properties. Cells with high levels of integrin β1 (CD29) expression had a higher colony forming efficiency [185] and could generate an epithelium when grafted onto mice [186]. Basal keratinocytes expressing high levels of $\alpha_6$ integrin or CD49f have been shown to display stem cell attributes, while cells with low expression of $\alpha_6$ are post-mitotic differentiating keratinocytes [187-189]. In summary, various strategies allow the enrichment of stem cells to a high degree of purity from a heterogeneous population, utilising antibodies reactive against specific cell surface markers.

#### *1.4.3.2 Phenotypic profile of adult mesenchymal stem cells*

Since initial isolation techniques, based on plastic adherence, generate significant heterogeneity and possibly introduce contamination of other accessory cell types such as macrophage, other methods of isolation have been developed. In order to isolate a certain subset of stem cells to a high degree of purity, it is necessary to identify markers that allow the prospective isolation of that subset. Antibody based cell separation techniques such as fluorescence or magnetic activated cell sorting based on surface antigen expression, proved useful for enriching specific cell subsets from heterogeneous populations, particularly in the fields of immunology and haematology [123]. To investigate surface antigen expression, multicolor flow cytometric assay is often employed to demonstrate that individual cells co-express MSC markers and lack hematopoietic antigen [123].

As described above, the immunophenotype reported for BMSC includes positive expression of STRO-1, CD73 (ecto-5'-nucleotidase), CD90 (Thy-1), CD105 (endoglin), CD146 (MUC-18), Oct4, Nanog, CD29 (integrin β1) and a lack of expression of the haematopoietic associated markers CD14, CD34, CD45 and HLA-DR negativity [123, 190-193]. Among the above-mentioned cell surface markers, STRO-1 has been extensively studied. STRO-1, which is a murine IgM monoclonal antibody, has been generated to

identify a cell surface antigen on bone marrow stromal elements but not on committed progenitor cells [194]. Subsequent studies by Gronthos *et al* demonstrated that osteoprogenitors of bone marrow are present in the STRO-$1^+$ population [195]. Studies also showed that STRO-$1^+$ BMSC exhibited the potential to differentiate into multiple stromal cell lineages [191, 196, 197]. Of note, the STRO-1 antigen is associated with an immature phenotype, where its expression is down regulated in cells undergoing osteogenic differentiation [181, 198]. Another stem cell surface marker is CD146, a cell adhesion molecule expressed on smooth muscle cells. It is believed that clonogenic bone marrow cell population exhibited high levels of CD146 expression [125]. The combination of an antibody against CD146 and STRO-1 was used by Shi and Gronthos to purify putative stem cell populations within bone marrow and dental pulp tissues [193]. CD106/VCAM-1, a vascular cell adhesion molecule, has been used in combination with STRO-1 to isolate highly clonogenic BMSC population [191]. CD106 has also been used with other markers to purify BMSC [199]. STRO-3 is a novel monoclonal antibody developed by Gronthos *et al* that recognises an isoform of tissue nonspecific alkaline phosphatase (TNSALP), a cell-surface glycoprotein usually associated with cells of the osteoblast lineage [200]. More recently, STRO-4 has been generated as a monoclonal antibody that recognises heat shock protein 90β on the surface of ovine and human precursor cells [201]. Collectively, the surface expression of putative MSC markers allows the rapid and efficient isolation of bone marrow stromal precursor cells from a heterogeneous population consisting primarily of haematopoietic cell types.

In contrast, the periodontium is a fibrous tissue composed of various cell types including fibroblasts, endothelial cells, ERM cells, osteoblasts and cementoblasts. The presence of multiple cell types within the periodontium requires the use of specific markers for the proper characterisation of each population. Studies have shown that PDLSC share a similar

expression profile with BMSC such as CD29, CD44, CD90 and CD105. Importantly, PDLSC also express the early BMSC cell surface markers STRO-1 and CD146/MUC18 [126]. Due to the presence of STRO-1/CD146, PDLSC are thought to be derived from perivascular niches. In addition, a subset of PDLSC was shown to express antigens associated with perivascular tissues (alpha-smooth muscle actin and periocyte-associated antigen, 3G5) [5]. Taken together, these findings indicate a possible perivascular origin of PDLSC, in accord with the earlier findings by McCulloch and colleagues [143, 145]. However, comparative analyses showed that PDLSC exhibit higher expression levels of scleraxis (a tendon-specific transcription factor) [126] and periodontal ligament associated protein-1 (PLAP-1, which is a member of the class I small leucine-rich repeat proteoglycan family, also known as asporin) than the bone marrow and dental pulp counterparts [202]. Other studies have proposed a panel of markers to characterise PDLSC, such as alkaline phosphatase, type I collagen, periostin, runt-related transcription factor-2 (Runx2) and epithelial growth factor receptor, which are also expressed by BMSC [203]. In addition, it was reported recently that Golgi protein 49kDa (GoPro49) is a marker expressed by dental follicle but not by dental papilla cells, indicating that it can be used as a marker to distinguish between dental follicle and papilla cells in early tooth development [204]. The *in vitro* phenotypic features of dental stem cells have been summarized [100]. As cell surface markers such as CD29, CD44, CD90, CD73, CD105, CD146 and others are ubiquitously expressed by MSC-like populations derived from all dental tissues, specific cell surface markers have yet to be identified capable of distinguishing between individual dental stem cell population subsets [133]. In summary, our understanding of the cell surface phenotype of PDLSC falls short when considering the need to isolate and purify stem/progenitor cell subsets from the heterogeneous PDL populations. Further studies are necessary to fully characterise the cell surface phenotype of PDLSC in order to identify putative cell surface markers specific to this population.

### *1.4.3.3 Characterisation of epithelial stem cells*

Periodontal fibrous tissue contains the only odontogenic epithelial cell population in the periodontium, ERM cells. The investigation of ERM functions in adult periodontium calls for the selection and purification of ERM cells from a heterogeneous population. To date the isolation and purification of ERM using surface antigen expression has not been possible due to the lack of specific markers. In contrast, studies of the basal epidermal layer of skin have shown the presence of three epithelial subpopulations of cells [188]: keratinocyte stem cells (KSC) which are relatively quiescent and identified as $^{3}$H-Tdr label-retaining cells (1-10% of basal cells) (analogous to MSC in bone marrow); transit amplifying cells that are identified as rapidly cycling and short-lived (60% of basal cells) (analogous to committed progenitor cells in bone marrow) and post-mitotic differentiating keratinocyte (40% of basal cells). Keratinocyte stem cells were first isolated using β1 integrin as a cell surface marker using FACS [185]. Cells with high level of β1 integrin expression (designated as β1 integrin$^{high}$) had a higher colony forming efficiency [185] and could generate an epithelium when grafted onto mice [186]. However, it was subsequently found that this β1 integrin$^{high}$ population contained both KSC and transit amplifying cells [205]. The discovery of using the laminin receptor subunit, $\alpha_6$ integrin or CD49f, as a key surface marker for KSC was a further critical step for the purification of these epithelial progenitors [187]. Basal keratinocytes expressing high levels of $\alpha_6$ integrin or CD49f have been shown to display KSC attributes, while low expressing $\alpha_6$ cells are post-mitotic differentiating keratinocyte [187-189]. Subsequently, oral KSC have been isolated from oral mucosa using this selection strategy from keratinized oral mucosa [206]. Furthermore, oral KSC were physically isolated by their relative cell size and sorted cells were able to regenerate an oral mucosa graft [207]. Taken together, $\alpha_6$ integrin or CD49f can be used as a surface marker for skin and oral mucosa KSC and may be applied to different epithelial progenitor populations in other tissue sources.

## 1.5 Summary

Current strategies for periodontal regenerative therapy show limited and unpredictable clinical outcomes. Periodontal regeneration is believed to be a re-enactment of events in the developmental stage where the epithelial mesenchymal interactions play important roles. With this in mind, it is of great importance to investigate and characterize the descendants of critical cellular components during tooth root development, such as HERS (ERM) and dental follicle cells (PDLSC). As HERS plays a central role in tooth root development, it seems plausible to hypothesize that epithelial cell rests of Malassez, as the descendants of HERS, are more than “cell rests” in the adult periodontium. Furthermore, if ERM cells do express MSC-associated and bone-related markers, then it is also plausible to suggest that ERM cells may possess MSC-like properties and give rise to mineralised tissues. Although there is considerable interest in the roles of HERS cells in tooth root development, little is known of the exact roles of ERM cells in adult periodontium. To date, there have been very limited studies of ERM cells suggesting that these cells contain a subset of multi-potential cells.

It is emerging that the stem-cell-based approach for tissue engineering has shown great promise. PDLSC have already been explored for their potential in bone and periodontal regeneration/repair, therefore, the biological and functional properties of PDLSC deserve further characterisation before they are utilised in large-scale clinical studies. While the heterogeneity of stem cells has been widely accepted, the lack of specific cell surface markers for stem cells has hindered the progress of stem-cell-based tissue engineering. Knowledge of the phenotype and specific markers of PDLSC is vital in developing a stem-cell-based approach for tissue engineering.

## 1.6 Project aims

This PhD project characterised two cellular components in the periodontium: ERM cells and PDLSC. Based on the discussions above, we hypothesize that:

1. ERM cells represent a unique source of multi-potential stem cells within the periodontal tissue, with the capacity to undergo epithelial to mesenchymal transition.
2. PDLSC express specific cell surface markers that can be used to discriminate PDLSC from other populations within the periodontal tissue.

There are two broad aims for this study. The first aim examined methodologies to isolate ERM cells from ovine periodontium and investigated their MSC-like properties, utilising both *in vitro* and *in vivo* analyses. The second aim assessed the cell surface protein(s) expression for PDLSC to identify specific markers, utilising cell surface labelling and proteomic techniques coupled with mass spectrometry.

Specific Aims:

1. Characterise the cell surface marker profile of ovine ERM cells.
2. Investigate whether there is a subpopulation of stem/progenitor cells within ERM cells.
3. Determine whether ERM cells are capable of undergoing epithelial mesenchymal transition under osteogenic conditions.
4. Develop a novel method for investigating cell surface protein expression using cell surface labelling and proteomic techniques.
5. Investigate the cell surface protein profile of PDLSC using proteomic analyses.
6. Compare the expression of putative cell surface markers of PDLSC with different epithelial populations such as ERM cells and keratinocytes.

# Chapter 2. Materials and Methods

## 2.1 Materials

**Table 2.1 Cell Culture Media**

| Name | Content |
|---|---|
| Complete Media (MEM) | α-MEM (Sigma-Aldrich, St. Louis, MO, USA)<br>10% FCS (Thermo Electron, Melbourne, VIC, Australia)<br>50 U/ml, 50 µg/ml Penicillin, Streptomycin (Sigma-Aldrich, St. Louis, MO, USA)<br>1 mM Sodium Pyruvate (SAFC, Lenexa, KS, USA)<br>100 µM L-ascorbate-2-phosphate (Novachem, Melbourne, VIC, Australia)<br>2 mM L-Glutamine (SAFC, Lenexa, KS, USA) |
| Complete Oral Keratinocyte Media (OKM) | Oral Keratinocyte Medium (OKM, ScienCell Research Laboratories, Carlsbad, CA, USA, #2611)<br>oral keratinocyte growth supplement (OKGS, ScienCell Research Laboratories, #2652)<br>100 U/ml penicillin, 100 µg/ml streptomycin solution (P/S, ScienCell Research Laboratories, #0503). |
| Osteogenic Media | α-MEM (Sigma-Aldrich, St. Louis, MO, USA)<br>5% FCS (Thermo Electron, Melbourne, VIC, Australia)<br>50 U/ml, 50 µg/ml Penicillin, Streptomycin (Sigma-Aldrich, St. Louis, MO, USA)<br>1 mM Sodium Pyruvate (SAFC, Lenexa, KS, USA)<br>100 µM L-ascorbate-2-phosphate (Novachem, Melbourne, VIC, Australia)<br>2 mM L-Glutamine (SAFC, Lenexa, KS, USA)<br>$10^{-7}$ M dexamethasone phosphate (Hospira Australia)<br>2.64 mM inorganic phosphate, $KH_2PO4$, (BDH Chemicals, Poole, UK) |
| Adipogenic Media | α-MEM (Sigma-Aldrich, St. Louis, MO, USA)<br>5% FCS (Thermo Electron, Melbourne, 15-011-0500V)<br>50 U/ml, 50 µg/ml Penicillin, Streptomycin (Sigma-Aldrich, St. Louis, MO, USA)<br>1 mM Sodium Pyruvate (SAFC, Lenexa, KS, USA)<br>100 µM L-ascorbate-2-phosphate (Novachem, Melbourne, VIC, Australia)<br>2 mM L-Glutamine (SAFC, Lenexa, KS, USA)<br>0.5 µM hydrocortisone (Sigma-Aldrich, St. Louis, MO, USA)<br>60 µM indomethacin (Sigma-Aldrich, St. Louis, MO, USA)<br>0.5 mM IBMX (3-Isobutyl-1-methyl-xanthine) (Sigma-Aldrich, St. Louis, MO, USA) |
| Chondrogenic Media | DMEM (JRH Biosciences, Lenexa, KS, USA)<br>50U/ml, 50 µg/ml Penicillin, Streptomycin (Sigma-Aldrich, St. Louis, MO, USA)<br>1 mM Sodium Pyruvate (SAFC, Lenexa, KS, USA) |

| | |
|---|---|
| | 100 µM L-ascorbate-2-phosphate (Novachem, Melbourne, VIC, Australia)<br>2 mM L-Glutamine (SAFC, Lenexa, KS, USA)<br>rhTGFβ3 (PeproTech, Rocky Hill, NJ, USA) |
| Neurogenic Media A | Neurobasal A (Invitrogen, GIBCO BRL, Grand Island, NY)<br>x1 B27 supplement (Invitrogen, GIBCO BRL)<br>1% Penicillin/Streptomycin<br>20ng/ml EGF (PeproTech, #100-15)<br>40ng/ml bFGF (Prospec Tany Technogene, East Brunswick, NJ, USA, #CYT-218) |
| Neurogenic Media B | DMEM/F12<br>x1 ITSS<br>1% Penicillin/Streptomycin<br>40ng/ml bFGF |
| Neurogenic Media C | Neurogenic media B<br>0.5µM Retinoic Acid |

**Table 2.2 Buffers and Solutions**

| **Name** | **Content** |
|---|---|
| HBSS | Hanks balanced salt solution (JRH Biosciences, Lenexa, KS, USA) |
| 1xPBS | MilliQ water (Media production unit, IMVS)<br>10% PBS Phosphate Buffered Saline, calcium and magnesium free (Sigma-Aldrich, St. Louis, MO, USA) |
| HHF Buffer | HBSS<br>5% FCS (Thermo Electron, Melbourne, VIC, Australia)<br>50 U/ml, 50 µg/ml Penicillin, Streptomycin |
| Blocking solution (IHC) | 3% Normal goat serum in either PBS-T or PBS |
| Blocking solution (FACS) | 5% FCS<br>1% BSA (SAFC, Lenexa, KS, USA)<br>50 U/ml, 50 µg/ml Penicillin, Streptomycin<br>5% normal human serum (Red Cross, SA, Australia) |
| PUCK'S-EDTA | 5mM KCl, 130mM NaCl, 3mM $NaHCO_3$, 5mM D-glucose, 10mM HEPES (pH 7.3), 1mM EDTA in $ddH_2O$ |
| 4% PFA | 20g PFA powder (Sigma) in 500ml PBS |
| PBS-T | PBS, 0.1% Tween-20 |
| Tris-Glycine | 25mM Tris, 250mM glycine (pH 8.3), 0.1% SDS |

**Table 2.3 Equipment**

| Equipment | Company |
|---|---|
| ABI SDS 7000 light cycler –Real Time PCR | ABI prism SDS v1.1 (Applied Biosystems, California, USA |
| Centrifuges | cell culture - Eppendorf (5417R)<br>bench top - Eppendorf (5424)<br>FACS samples - DiaCent-12 DiaMed |
| ELISA plate reader | EL808 Ultra Microplate Reader, BIO-TEK INSTRUMENTS, INC |
| Fluorescent Activator Cell Sorter (FACS) | Sorter – FACS Star plus, BD<br>Analyser – EPICS (XL-MCL), Beckman Coulter, ADC |
| Incubators | cell culture – Sanyo (MCO-18A1C), distributed by Quantum Scientific |
| Microscopes | Inverted - Nikon (TE300)<br>Inverted – Olympus (CKX41)<br>Olympus (AX70) |
| Mini-gel (1.5mm) glass plates | Bio-Rad (165-3312) |
| Mini-gel (1.5mm) combs | Bio-Rad (165-3365) |
| Plate reader (Calcein) | Luminescence spectrometer (LS 55), Perkin Elmer Instruments |
| Spectrophotometer | Eppendorf, Hamburg, Germany |
| Thermocycler – PCR machine | MJ Research (PTC-200) |
| Typhoon | Typhoon 9410 Variable Mode Imager, Molecular Dynamics, part of Amersham Pharmacia Biotech, UK |

**Table 2.4 Antibodies**

| Name | Isotype | | Source | Dilution |
|---|---|---|---|---|
| 1B5 | $IgG_1$ | normal mouse $IgG_1$ | Prof. L.K Ashman (University of Newcastle, Australia) | 1:50 |
| 1D4.5 | $IgG_{2a}$ | normal mouse $IgG_{2a}$ | Prof. L.K Ashman (University of Newcastle, Australia) | 1:50 |
| integrin $\alpha_6$/CD49f | $IgG_{2a}$ | FITC rat anti-human CD49f | BD Pharminogen #555735 | 1:100 |
| control for CD49f | $IgG_{2a}$ | FITC rat | BD Pharminogen #555843 | 1:100 |
| cytokeratin 8 (CK-8) | $IgG_1$ | mouse monoclonal | AffinityBioReagents #MA1-19035 | 1:100 |
| E-cadherin | $IgG_{2a}$ | mouse anti-human | BD Transduction Laboratories #610181 | 1:800 |
| Epithelial membrane protein 1 (EMP-1) | IgG | Rabbit anti-human | Santa Cruz Biotechnology #sc-50467 | 1:50 |
| CD44 | $IgG_1$ | mouse anti-ovine | H9H11 supernatant | neat |
| CD29 | $IgG_1$ | mouse anti-ovine | Hybridoma B | neat |

| | | | | |
|---|---|---|---|---|
| HSP90β | $IgG_1$ | mouse anti-ovine | Hybridoma H/STRO-4 | neat |
| CD14 | $IgG_1$ | mouse anti-ovine | Serotec #MCA920 | 1:20 |
| CD45 | $IgG_1$ | mouse anti-ovine | Serotec #MCA2220 | 1:50 |
| CD31 | $IgG_{2a}$ | mouse anti-ovine | Serotec #MCA1097G | 1:20 |
| Collagen II | $IgG_1$ kappa | mouse anti-human | Millipore #MAB1330 | 1:100 |
| Nestin | $IgG_1$ | mouse anti-rat | BD Pharmingen #556309 | 1:4000 |
| Neurofilament-heavy chain (NF-H) | $IgG_1$ | mouse anti-human | Chemicon #MAB5446 | 1:5000 |
| Protein Gene Product 9.5 (PGP) 9.5 | Ig $G_1$ | mouse anti-human | CEDARLANE #CL31A3 | 1:1250 |
| Tau | | rabbit anti-human | DAKO #A0024 | 1:2500 |
| GFAP | | rabbit anti-cow | DAKO #Z0334 | 1:5000 |
| Osteocalcin | Ig G | rabbit anti-bovine | LF-126 | 1:750 |
| CD73 | Ig $G_1$ | mouse anti-human | BD Pharmingen #550256 | 1:25 |
| CD90 | Ig $G_1$ | biotin mouse anti-human | BD Pharmingen #555594 | 1:25 |
| Annexin A2 | Ig $G_1$ | mouse anti-human | Invitrogen #03-4400 | 1:12.5 |
| Sphingosine Kinase 1 | Ig G | rabbit anti-human | Cayman #10012201 | 1:20 |
| Secondary antibodies | | goat anti-mouse IgG biotin | SouthernBiotech #103008 | 1:200 |
| | | goat anti-mouse $IgG_1$ | Caltag #M32115 | 1:500 |
| | | goat anti-mouse $IgG_{2a}$ | Caltag #M32315 | 1:500 |
| | | rabbit anti-rat IgG biotin | Vector laboratories #BA-4001 | 1:250 |
| | | goat anti-rabbit IgG biotin | Vector laboratories #BA-1000 | 1:150 |
| | | horse anti-mouse IgG biotin | Vector laboratories #BA-2000 | 1:150 |
| | | goat anti-mouse IgG FITC | Caltag #M30101 | 1:50 |
| | | goat anti-rabbit FITC | Caltag #L42001 | 1:50 |
| | | sheep anti-rat IgG-conjugated magnetic beads M-450 | Dynal #110.07 | four beads per cell |
| | | donkey anti rabbit Cy3 | Jackson Immunoresearch #711-165-152 | 1:200 |

**Table 2.5 Primer Sequences for RT-PCR**

| Gene name | Accession Number | Forward (5'-3') reverse (5'-3') | Product size |
|---|---|---|---|
| β-actin | human NM_001101 | GATCATTGCTCCTCCTGAGC<br>GTCATAGTCCGCCTAGAAGCAT | 157bp |
| Runx-2 | bovine XM_002697262 | GACAGCCCCAACTTCCTGT<br>CGCCATGACAGTAACCACA | 106bp |
| Bone sialoprotein (BSP-II) | bovine S73144 | GCAATCACCGAAATGAAGAC<br>CCCCATTTTCTTCAGAATCC | 118bp |
| Osteopontin | ovine AF152416 | TAGCCAGGAACGAAGACAGG<br>CAGAGGAGCTGGCTGTCAAT | 116bp |
| PPARγ2 | ovine AY137204 | CGATGGTTGCAGATTATAAG<br>TGTACAGCTGAGTCTTTTCAG | 108bp |
| Leptin | ovine FR688118 | CAAGACGATTGTCACCAGG<br>ATGTCTGGTCCATCTTGGA | 131bp |
| Collagen II | ovine FJ378650 | GGCAACAGCAGGTTCACATA<br>CTATGTCCATGGGTGCAATG | 139bp |
| Collagen X | bovine X53556 | CCACTCCTCTTTCTCAGGAT<br>GCCTACCTCCATATGCATTT | 101bp |
| Aggrecan | ovine AF019758 | ATGACGCCATCTGCTACACA<br>CCAGGTCACCGTCTGGAT | 101bp |
| Sox-9 | bovine AF278703 | CAGCAAGACTCTGGGCAAG<br>CGTTCTTCACCGACTTCCTC | 149bp |
| Nestin | bovine AB257750 | GAGGTGGCCACATACAGGAC<br>TAGCTCCAGCTTAGGGTCCA | 108bp |
| B tubulin | bovine BC111295 | GGAGATCGTGCACATCCAG<br>CCAGCTGCAGGTCCGAGT | 128bp |
| Cytokeratin-8 (CK-8) | bovine X12877 | GAAGCTGAAGCTGGAaGtGG<br>CGGATCTCCTCTTCATAcAGtTG | 228 bp |
| E-cadherin | bovine NM_001002763 | ATGACAACAAGCCCcAgTTC<br>GATGACgCCTGTtTcCtTGT | 212 bp |
| Vimentin | ovine EF495195 | GGGACCTCTACGAGGAGGAG<br>gGATTCCACTTTaCGcTCcA | 239 bp |
| N-cadherin | bovine X53615 | TTCgCCCAACATGTTTACAA<br>GGATTGCCTTCCATGTCTGT | 126 bp |
| Fibronectin | ovine FJ234417 | TTGAGTGCTTCATGCCTTTg<br>GCTcGGAGAAGCTGTGAGTT | 210 bp |
| SNAI 1 | bovine NM_001112708 | cAAGGCCTTCAACTGCAAAT<br>CTTGACATCcGAGTGGGTCT | 250 bp |
| SNAI 2 | ovine NM 001126342 | GGACgCACACcTTACCTTGT<br>cGAGAAGGTTTTGGAGCAac | 218 bp |
| ZEB 1 | bovine NM_001206590 | GCAGTCTGGGgGTAATCGTA<br>TTGCAGTTTGGGCATTCATA | 126 bp |
| ZEB 2 | bovine BC120151 | CGGCTTCTTCATGCTTTTTC<br>ATTGGCTTGTTTGCGtCTCT | 188 bp |

| | | | |
|---|---|---|---|
| TWIST | human NM_000474 | TCTTACGAGGAGCTGCAGACGCA | 212 bp |
| | | ATCTTGGAGTCCAGCTCGTCGCT | |
| Cytokeratin-14 (CK-14) | bovine NM_001166575.1 | TGAGAAGGTGACCATGCAGA | 208 bp |
| | | ATTGT CCACA GTGGC TGTGA | |
| Vimentin | ovine EF495195 | GGGACCTCTACGAGGAGGAG | 239 bp |
| | | GGATTCCACTTTACGCTCCA | |

## 2.2 Cell culture

### 2.2.1 Cell culture conditions

All cell culture protocols were conducted in a Class II laminar flow hood (Top Safe 1.2, Bio Air, Siziano, Italy). *Ex vivo* expansion of cells was performed in MCO-18AIC Sanyo $CO_2$ incubators (Sanyo Oceania, North Ryde, NSW, Australia), at 37$^{o}$C, 5% $CO_2$ in a humidified environment. An Eppendorf 5810 centrifuge (Eppendorf South Pacific, North Ryde, NSW, Australia) was used for centrifugation of cell suspensions during expansion.

### 2.2.2 Isolation of human periodontal ligament stem cells and gingival fibroblasts

Ethical clearance was granted by the Human Research Ethics Committee of the University of Adelaide to collect freshly extracted human adult teeth at the Adelaide Dental Hospital following informed consent (Approval Number H-112-2008). These teeth are normally discarded as medical waste following routine dental care. The soft tissues of the extracted teeth (third molars or premolars) were used in this study to derive human adult periodontal ligament stem cells (PDLSC) and gingival fibroblasts (GF).

Human PDLSC and GF were isolated and cultured as previously described [126, 208]. Briefly, gingival and periodontal ligament tissues were collected from excised gingiva and middle third of the root, respectively. The tissues were then minced and digested in a solution of 1 ml Type I collagenase (3 mg/ml) and 1 ml dispase II (4 mg/ml) for 2 hours at 37$^{o}$C. An excess volume of HHF buffer was added to the digested tissues to neutralize

enzyme activity and the suspension was strained through a 70 µm Falcon cell strainer (Becton Dickinson Biosciences, San Jose, CA, USA) to remove undigested tissue from the liberated PDLSC and GF. The cell suspensions were pelleted by centrifugation at 400 g for 10 minutes at 4ºC, and resuspended in complete media. The PDLSC and GF were distributed evenly into a T75 flask in complete media and cultured at 37$^{o}$C, 5% $CO_2$ in a humidified environment. Cells were maintained with a twice-weekly medium change and any non-adherent cells were removed.

### 2.2.3 Culture of human PDLSC and GF

Cells were harvested and further expanded once upon reaching confluence. The cell monolayers were washed in HBSS, and treated with 0.05% trypsin/ 0.02% EDTA (SAFC, Lenexa, KS, USA) for 3 minutes. HHF was added to neutralise trypsin activity and cell suspensions were centrifuged at 800 *g* for 5 minutes at 4$^{o}$C. Cells were reseeded at 8x10$^{3}$ cells/cm$^{2}$ for further expansion. This process was repeated when cells reached 80% confluency until desired cell numbers were obtained.

### 2.2.4 Isolation of ovine ERM and PDLSC

Periodontal ligament cells were isolated from ovine incisor scavenges following approved guidelines set by the Institute of Medical and Veterinary Science (IMVS, South Australia, Australia) Animal Ethics Committee (#130/06). Periodontal ligament was removed from the middle third of the tooth root surface and enzymatically digested to generate single cell suspensions as previously described [126]. Selective enzymatic digestion [97, 209] was used to separate the trypsin sensitive periodontal fibroblasts from the adherent ERM cells using 0.05% trypsin/0.02% EDTA (SAFC, Sigma-Aldrich Biotechnology, Lenexa, KS, USA, #59418C). This technique is based on the fact that fibroblasts attach and detach at a faster rate than epithelial cells [210]. Briefly, following media removal, the flasks were washed with HBSS (JRH Biosciences, Lenexa, KS, USA) and digested with 0.05%

trypsin/0.02% EDTA solution to liberate the periodontal ligament fibroblasts. After 5 minutes treatment in trypsin, all detached cells were collected and the culture flasks were washed twice with HBSS before adding OKM with additives. Stringent multiple enzymatic digestion was repeated until no cells detached within 5 minutes and the cell cultures exhibited an epithelial morphology. Selective enzymatic digestion using trypsin was also performed in serial plating whenever cells became confluent. This process was repeated until desired cell numbers were obtained.

To isolate individual colonies, primary ERM cultures were plated into 10 cm culture dishes at cell low density ($5x10^3$ cells per $cm^2$) and incubated at 37°C, 5% $CO_2$ for 14 days. Individual colonies were isolated using colony rings and cultured in Oral Keratinocyte Medium (OKM, ScienCell Research Laboratories, Carlsbad, CA, USA, #2611) supplemented with oral keratinocyte growth supplement (OKGS, ScienCell Research Laboratories, #2652) and 100 U/ml penicillin, 100 µg/ml streptomycin solution (P/S, ScienCell Research Laboratories, #0503) for further expansion in individual vessels as previously described [211, 212].

### 2.2.5 Culture of ovine ERM and PDLSC

Ovine ERM cells were cultured at $8x10^3$-$12x10^3$ cells per $cm^2$ in complete OKM. Ovine PDLSC were cultured at $2x10^3$-$4x10^3$cells per $cm^2$ in complete media. Unless mentioned otherwise, the experiments were repeated for three donors.

### 2.2.6 Cell counting and viability testing

Washed cells were resuspended in the appropriate volume of appropriate media. Ten µl was taken from this cell suspension for counting. Depending on the estimated cell number (assessed by light microscopic analysis), a dilution factor between two and ten was used for counting. Cells were counted using trypan blue dye exclusion, by diluting cells in 0.4%

(w/v) trypan blue (Sigma-Aldrich, St. Louis, MO, USA) to detect living cells. To obtain an accurate cell number at least 100 cells were counted per sample using a haemocytometer.

### 2.2.7 Cryopreservation of cells

Cells were cryopreserved in FCS containing 10% (v/v) of dimethyl sulfoxide (DMSO, BDH AnalaR® Merck, Kilsynth, Victoria, Australia). Immediately prior to freezing, 1 ml of pre-prepared, cold 20% FCS DMSO solution was added drop wise to ~4 x $10^6$ cells in 1 ml of FCS on ice. One ml of the cell suspensions (~2 x $10^6$ cells) were then pipetted into 2 ml cryoampoules (Greiner Bio-One, Frickenhousen, Germany) and transferred into cryopreservation containers (C1562 Freezing Container, Nalgene, USA) before being placed into a -80$^o$C freezer for at least 4 hours. The freezing container ensured the cells were cooled at the appropriate rate of 1$^o$C per minute. After 4 hours cryoampoules were then transferred to liquid nitrogen vapour phase for extended storage at -150°C.

### 2.2.8 Thawing of cryopreserved cells

Cells were removed from liquid nitrogen (-196$^o$C) and immediately thawed at 37$^o$C in a water bath. Once thawed, the cell suspensions were immediately transferred to a 14 ml spin tube containing 11 ml of appropriate growth media. This preparation was centrifuged at 800 *g* for 7 minutes at 4$^o$C. Cell pellets were then resuspended in 10 ml of appropriate growth media and plated at an appropriate density.

## 2.3 Cell sorting

### 2.3.1 Immunomagnetic selection

Dynabead cell sorting was performed on single cell suspensions of periodontal ligament cells as previously described [193]. Freshly collected single-cell suspensions were obtained by enzymatic digestion at 37°C for 2 hours and passed through a 70 µm cell strainer (Falcon, BD Biosciences, Erembodegem, Belgium). Another 12 ml HHF was used to flush

the old tube and the strainer. Following centrifugation at 400 g for 5 minutes in 14 ml round bottom tubes, approximately 5.0 $x10^5$ cells were blocked for 30 minutes on ice with HBSS supplemented with 5% FCS, 1% BSA, 50 U/ml penicillin, 50 µg/ml streptomycin and 5% normal human serum. During this incubation, 20 µl of cell suspension was used for cell counting. After centrifugation, cells were incubated with an anti-integrin $\alpha_6$/CD49f antibody (Table 2.4) at 1 in 50 dilution for 1 hour on ice with shaking every 15 minutes.

During primary antibody incubation, secondary sheep anti-rat IgG-conjugated magnetic Dynabeads (Dynal Biotech, Oslo, Norway) (Table 2.4) were washed twice to remove unbound immunoglobulins. The volume of secondary antibody containing beads for magnetic selection was based on a concentration of 4 beads per cell, allowing for 20% loss of cells. Using the cell count mentioned in section 2.2.6, beads were resuspended well before adding required volume to 3 ml HHF and resting the tube in a MPC-1 magnetic particle concentrator (Dynal Biotech) at an angle for 2 minutes. The supernatant was aspirated carefully with a sterile transfer pipette without disturbing the beads. The beads were resuspended in 500 µl cold HHF and put on ice until required.

Following primary antibody incubation, cells were washed twice with HHF and then incubated with sheep anti-rat IgG-conjugated magnetic Dynabeads at 4 beads per cell for 1 hour on a rotary mixer at 4°C. Integrin $\alpha_6$/CD49f-positive cells were collected using a MPC-1 magnetic particle concentrator according to the manufacturer's recommendations.

### 2.3.2 Colony forming assay

To assess colony-forming efficiency, integrin $\alpha_6$ positive, negative and unfractionated cells were seeded in six well plates in α-MEM supplemented with 20 % FCS, 50 U/ml penicillin and 50 µg/ml streptomycin (Sigma-Aldrich, St. Louis, MO, USA), 1 mM Sodium pyruvate

(SAFC), 100 µM L-ascorbate-2-phosphate (Novachem, Melbourne, VIC, Australia) and 2 mM L-Glutamine (SAFC). Cells were seeded at 3,450 cells/well for integrin $\alpha_6$-positive fraction and at $1x10^4$ cells/well for integrin $\alpha_6$-negative and unfractionated cells. Day 14 cultures were fixed and stained with 0.1% toluidine blue O (Sigma-Aldrich, #198161) in 2.5% formaldehyde in PBS for 2.5 hours. Clusters with more than 50 cells were counted as colonies [193].

### 2.3.3 Fluorescence-activated cell sorting

*Ex vivo*-expanded ERM cells were liberated from the culture plates using 0.05% trypsin/0.02% EDTA and filtered through a 40 µm cell strainer (BD Biosciences, Erembodegem, Belgium). Single cell suspensions of $9x10^6$ cells were blocked for 45 minutes in HBSS supplemented with 5% FCS, 1% BSA, 50 U/ml penicillin, 50 µg/ml streptomycin and 5% normal human serum and then incubated with an anti-integrin $\alpha_6$ antibody or an isotype control antibody (Table 2.4) for 45 minutes at 4°C on a rotary mixer [187, 189]. Cells were washed twice with HBSS supplemented with 2% FCS at 4°C and then resuspended at $3x10^6$ cells per ml with cold sorting buffer consisting of HBSS supplemented with 2% FCS, 25 mM HEPES buffer (Sigma-Aldrich, #0887), 5mM EDTA (Merck, Kilsyth, VIC, Australia) and 10 U/ml DNase I (Sigma-Aldrich, #D5025). Cells were then sorted using an Epics Altra HyPer Sort FACS machine (Beckman Coulter). The high expressing integrin $\alpha_6$/CD49f positive cell fraction from these cultures (brightest 30%) was selected using Expo 32 Multi-comp software (Software version 1.2B). Selected cells were collected in 2 ml of OKM with additives and then centrifuged at 800 *g* for 5 minutes at $4^oC$, resuspended in fresh OKM with additives and plated at $1x10^4$ cells per $cm^2$.

## 2.4 Protein analysis

### 2.4.1 Immunohistochemistry

Chamber slides (Nalge-Nunc Lab-Tek, Rochester, NY, USA, #177445) were seeded with $8x10^3$ ERM cells per $cm^2$ in OKM with additives for 2 days. The slides were fixed with 4% paraformaldehyde (PFA) for 20 minutes at room temperature. After washing in PBS (Sigma-Aldrich), endogenous peroxidase activity was inhibited using 0.5% $H_2O_2$ in methanol at room temperature for 30 minutes. The sections were then washed in PBS and blocked for non-specific antibody binding using 3% goat serum in Tween PBS for 3 hours before incubating with primary antibodies or isotype control antibodies (Table 2.4) overnight at 4°C. After washing, the slides were incubated with appropriate secondary antibodies (Table 2.4) for 1 hour at room temperature. Following washing, slides were incubated with Vectastain ABC reagents (Vector Laboratories, Burlingame, CA, USA) according to the manufacturer's recommendations or horseradish-peroxidase-labelled streptavidin at 1 in 1000 dilution (Promega, Madison, WI, USA) and then developed with diaminobenzidine (Dako, Campbellfield, VIC, Australia) for 5-10 minutes. The slides were then washed and counterstained briefly with haematoxylin (ProSciTech, Turingowa Central, QLD, Australia) and mounted in DePex mounting media (BDH Chemicals, Poole, UK).

### 2.4.2 Flow cytometric analysis

To characterise the immunophenotype of *ex vivo*-expanded cells, flow cytometric analysis was used to analyse the expression of various surface proteins. Adherent *ex vivo*-expanded cells were washed once with HBSS and prepared as single cell suspension with 0.05% trypsin/0.02% EDTA. The single cell suspension was then washed twice in HHF buffer. Cell count and assessment of viability was performed as described in section 2.2.6. Cells were blocked with HBSS supplemented with 5% FCS, 1% bovine serum albumin (BSA, SAFC), 50 U/ml penicillin, 50 µg/ml streptomycin and 5% normal human serum (Red

Cross, SA, Australia) on ice for approximately 30 minutes to reduce the possibility of Fc receptor-mediated binding of antibodies. Individual FACS tubes containing approximately $2x10^5$ cells were incubated with primary antibodies specific for cell surface markers or isotype control antibodies (Table 2.4) at a concentration of 20 µg/ml for 1 hour on ice. After washing twice with HHF, cells were incubated with either fluorescein isothiocyanate (Green: FITC) or phycoerythrin (Red: PE) conjugated secondary detection reagent (Table 2.4) for 1 hour on ice. Samples were washed in 1 ml of HHF twice and fixed in 500 µl FACS Fix (PBS with 0.1% formalin, 20 mg/ml glucose and 0.02% sodium azide). Analysis was performed on a fluorescence-activated cell sorter fitted with a 250 MW argon laser (Beckman Coulter Cytomics FC500, using CXP Cytometry List Mode Data Acquisition and Analysis Software version 2.2 (Beckman Coulter, Miami, FL, USA)). In a dot plot of the data displaying forward scatter versus side scatter, a gate was placed around desired cell populations, eliminating dead cells, unnucleated cell debris and cell aggregates during data analysis. Positive reactivity for each antibody was defined as the level of fluorescence greater than 99% of the isotype matched control antibodies.

### 2.4.3 Preparation of protein lysates for western immunoblotting analysis

Whole cell lysates were prepared on ice from one confluent 10 cm dish (approximately 2 x $10^6$ cells). Cells were washed once with 10 ml of ice-cold PBS before 400 µl of lysis buffer was added and cells were scraped off the dish using a cell scraper. The constituents of lysis buffer included 20 mM Tris-HCl pH 7.4, 2 mM EDTA, 150 mM NaCl, 1% Triton-X100, 2 mM Sodium Vanadate, 2 mM Sodium Fluoride, 0.1% SDS, 2 mM PMSF, 10 mM Sodium Pyrophosphate and 10% Glycerol in RO water at their final concentrations. Cells were then transferred to an eppendorf tube and vortexed. This preparation mixture was incubated on ice for approximately 30 minutes and sonicated for 10 seconds on setting 3 of a Microson ultrasonic cell disruptor (XL2007, Misonix Inc., Farmingdale, NY, USA). Cell lysate was

then centrifuged for 30 minutes at 16,000 *g* at 4$^{o}$C. This centrifugation was enough to separate out the nuclear proteins and other cellular debris which formed a pellet at the bottom of the tube. The supernatant was transferred to a fresh tube and stored at –80$^{o}$C for future use.

### 2.4.4 ReduCing agent and Detergent Compatible (RCDC) protein assay

The protein concentration of all cell extracts was determined using the RCDC Protein Assay Kit (BioRad, Hercules, CA, USA) according to the manufacturer's instructions. Serial dilutions of BSA (Bovine Serum Albumin, 2 mg/ml, JRH Bioscience) at 1.5 mg/ml, 1 mg/ml, 0.75 mg/ml, 0.5 mg/ml and 0.2 mg/ml were used to create a standard curve. After protein quantitation, samples were allocated to appropriate amount for future use into multiple tubes to avoid multiple freeze/thaw cycles, which can lead to significant protein degradation. These preparations were left in liquid nitrogen overnight and then transferred to -80$^{o}$C for extended storage.

### 2.4.5 Western immunoblotting

Prior to loading onto gels for poly acrylamide gel electrophoresis (PAGE), protein lysate samples were boiled at 100$^{o}$C for 5 minutes to denature the protein secondary structures and then centrifuged at maximum speed for 5 minutes at 4$^{o}$C.

The stacking layer gel was made by mixing 5.6 ml of Milli Q water (Millipore, Billerica, MA), 8.0 ml of 30% Bis-acrylamide (BioRad, Gladesville, NSW, Australia), 5.0 ml of 1.5 M Tris (Sigma-Aldrich, St. Louis, MO, USA), 200 µl 10% SDS (Merck, Kilsyth, VIC, Australia), 200 µl 10% of APS (BioRad, Gladesville, NSW, Australia) and 20 µl of TEMED. The separating layer gel was made by mixing 5.061 ml of Milli Q water, 1.5 ml of 30% Bis-acrylamide (BioRad, Gladesville, NSW, Australia), 2.25 ml of 0.5 M Tris (Sigma-Aldrich, St. Louis, MO, USA), 90 µl 10% SDS (Merck, Kilsyth, VIC, Australia),

90 µl 10% of APS (BioRad, Gladesville, NSW, Australia) and 9 µl of TEMED. A general rule is that 20 to 50 µg were loaded per lane if the protein of interest is abundant and 100 µg for low abundant ones. In the present study, 30 µg of protein per lane was loaded to a 10% PAGE gel. Samples were run in SDS running buffer (0.3% (w/v) Tris-HCl, 1.44% (w/v) Glycine, 0.1% (w/v) SDS in water) at 20 mA per gel for the stacking layer and 30 mA per gel for the separating layer.

The gels were then transferred to a Hybond-P 0.45 µm PVDF membrane (Amersham Bioscience UK Limited, Little Chalfont, UK) using the SEMI-PHOR$^{TM}$ Hoefer Semi Dry blotter (Hoefer Scientific Instruments, San Francisco, CA, USA). The membranes were washed three times with TBS-T (Tris buffered saline/0.1% Tween 20) (Sigma-Aldrich, St Louis, MO, USA) and blocked overnight at 4$^{o}$C with 50 ml blocking buffer made up of 5% Amersham block (Amersham Biosciences UK Limited, Little Chalfont, UK) in TBS-T. After blocking, the membranes were washed three times using TBS-T to remove any residual blocking buffer solids.

The membrane was then ready to be probed with primary antibodies. Primary antibodies include rat anti-mouse α-tubulin (1 in 4000 dilution into 5% BSA/TBS-T), mouse anti-human β-actin (Sigma, A5441, 1 in 5000 dilution), mouse anti-human integrin β1/CD29 (1 in 400 dilution) and mouse anti-human CD44 (use as neat). The membrane was incubated with primary antibodies overnight at 4$^{o}$C on a rocker and then washed three times in TBS-T. Following the final wash, the membrane was probed with a secondary antibody (goat anti-mouse IgG affinity isolated alkaline phosphotase conjugated, AP326A/AP308A or goat anti-rat IgG affinity isolated alkaline phosphotase conjugated, AP136A) (Chemicon, Melbourne, VIC, Australia) diluted 1 in 2000 into 5% BSA/TBS-T. The membrane was incubated with secondary antibody for 1 hour at room temperature on a rocker. The

membrane was then washed three times with TBS-T and rinsed three times with TBS. Antibody binding was visualised by enhanced chemiluminescence using 1 ml ECF substrate (GE Healthcare, Europa Bio Products, RPN5785) using a Typhoon 9410 (Amersham, UK) with 488 nm excitation.

## 2.5 Proteomics analysis

All equipment and reagents were purchased from Bio-Rad Laboratories (Hercules, CA, USA) unless stated otherwise. CyDye DIGE Fluor minimal dye was purchased from GE Healthcare Life Sciences (Buckinghamshire, UK). The flow chart for cell surface labelling and subsequent proteomic preparation is outlined in Figure 2.1.

### 2.5.1 Cell surface labelling using CyDye DIGE Fluor minimal dye

CyDye fluorescent cell surface protein labelling was performed as previously reported [213]. Briefly, approximately 20 million sub-confluent human periodontal ligament stem cells (PDLSC) or gingival fibroblasts (GF) were washed with PBS and detached with either 1 mM PUCK's EDTA or 3 mg/ml Type I collagenase. Cells were counted as mentioned in section 2.2.6 and divided into aliquots of ~5 million cells per tube based on the volume. Cells were washed twice with ice cold HBSS (pH 7.4) before washing with ice cold HBSS (pH 8.5) and centrifuged at 800 *g* for 2 minutes. The cell pellet was resuspended in 200 µl labelling buffer containing HBSS (pH 8.5) and 1 M urea. Cells were then labelled with 600 pmol CyDye DIGE Fluor minimal dyes (Cy2, Cy3 or Cy5) on ice in the dark for 20 minutes. Staining was quenched by adding 20 µl lysine (10 mM) for 10 minutes. Surface-labelled cells were pelleted by centrifugation and washed twice with HBSS (pH 7.4) and then resuspended in 202 µl HBSS (pH 7.4). A 2 µl aliquot of cell suspension was taken prior to and after labelling to check the labelling efficiency using flow cytometry (section 2.4.2).

### 2.5.2 Preparation of cell lysates and membrane protein enrichment

Proteins were isolated and fractionated using a phase separation kit (Mem-PER Eukaryotic Membrane Protein Extraction Kit, PIERCE, #89826, Rockford, IL, USA) according to the manufacturer's instructions. Briefly, 150 µl Reagent A containing 1 µl protease inhibitor (Sigma, #8340) was added to the cell pellets (PDLSC or GF) and the preparation was incubated for 10 minutes at room temperature with occasional mixing. 450 µl mixture of Reagent B and C (150 µl Reagent B with 300 µl Reagent C) was then added to cell lysates and tubes were kept on ice for 30 minutes with mixing every five minutes. The preparation was cleared by centrifugation at 10,000 x *g* for 3 minutes at 4$^{o}$C. The supernatant was then transferred to a new tube and incubated at 37$^{o}$C in a water bath for 20 minutes. Following centrifugation at 10,000 x *g*, the top layer (hydrophilic proteins) were carefully removed from the bottom layer containing hydrophobic proteins and stored in a new tube. The hydrophobic samples were either purified immediately using ReadyPrep 2-D Cleanup Kit (section 2.5.4) or stored at -80$^{o}$C.

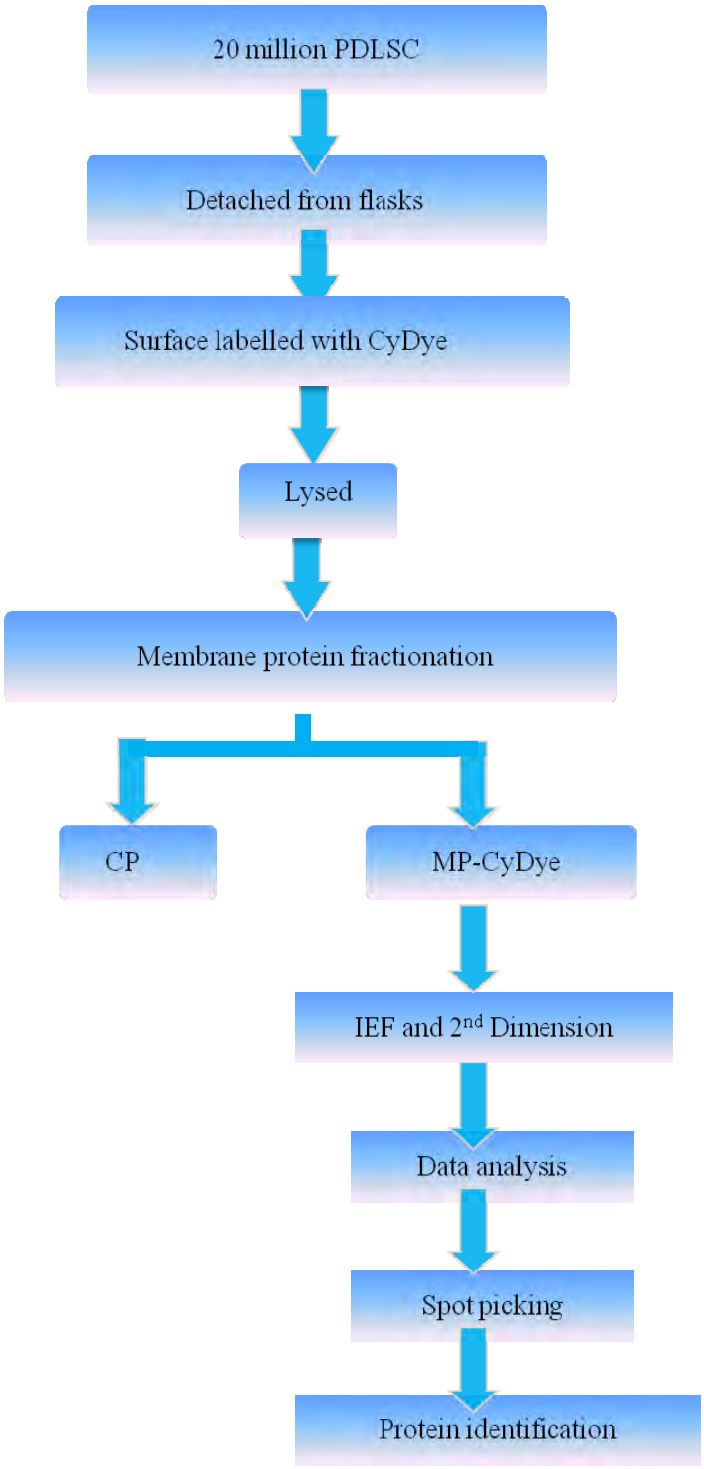


**Figure 2.1 Flow chart of cell surface labelling and subsequent proteomic preparation**

Approximately 20 millions subconfluent Periodontal Ligament Stem Cells (PDLSC) were detached and surfaced labelled with CyDye. Then cells were lysed and fractionated into Membrane Proteins (MP) and Cytosolic Proteins (CP). The MP preparation was separated through isoelectric focusing (IEF) and subsequently second dimension. The images were analysed before the spots were picked and identified using mass spectrometry.

### 2.5.3 Multiple membrane fractionations

To test whether multiple membrane protein enrichment steps improved the representation of membrane proteins in samples, cells were surface-labelled as mentioned in section 2.5.1 and subjected to up to three membrane fractionation steps. The flow chart for multiple fractionations is outlined in Figure 2.2. Membrane proteins were separated on 2-dimensional gel electrophoresis (2-DE) (section 2.5.5) and both membrane and cytosolic proteins were run on western immunoblotting to antibodies outlined in Table 2.4.

### 2.5.4 Sample preparation for proteomic analysis

Substances which might interfere with 2-DE were removed from the membrane protein fractions using ReadyPrep 2-D Cleanup Kit according to the manufacturer's instructions. Membrane proteins were then solubilised with ReadyPrep Reagent 3 buffer (Bio-Rad Laboratories) containing 5 M urea, 2 M thiourea, 2% (w/v) CHAPS, 2% (w/v) detergent sulfobetaine (SB) 3-10, 40 mM Tris, 0.2% Bio-lyte 3/10 and 2 mM tributyl phosphine (TBP). Samples were left for 1 hour at room temperature before being passed carefully (to avoid foaming) through a fine-gauge needle several times to solubilise the protein, as previously described [214]. After solubilisation the protein concentration was determined using RCDC Protein Assay Kit according to the manufacturer's instructions (section 2.4.4).

### 2.5.5 Protein separation by two-dimensional gel electrophoresis (2-DE)

#### *2.5.5.1 First dimension protein separation: Isoelectric focusing (IEF)*

Proteins were separated in the first dimension based on their isoelectric point (pI). Eleven cm immobilised pH gradient (IPG) strips (pH 3–10) were passively rehydrated for 24 hours in 330 µl rehydration/extraction buffer #3, containing 0.2% (w/v) pH 3-10 ampholytes, and 1.2% (v/v) De-Streak Reagent (GE Healthcare, Buckinghamshire, UK). IEF was performed using a Protean IEF cell (Bio-Rad Laboratories). Briefly, membrane

protein preparations containing 150 µg proteins were cup-loaded on the anode end of IPG strips (pH 3-10). The IEF cycle consisted of 8 steps outlined in Table 2.6, with a 50 µA/strip current limit, and the temperature was maintained at 20°C. Duplicate IPG strips were run concurrently.

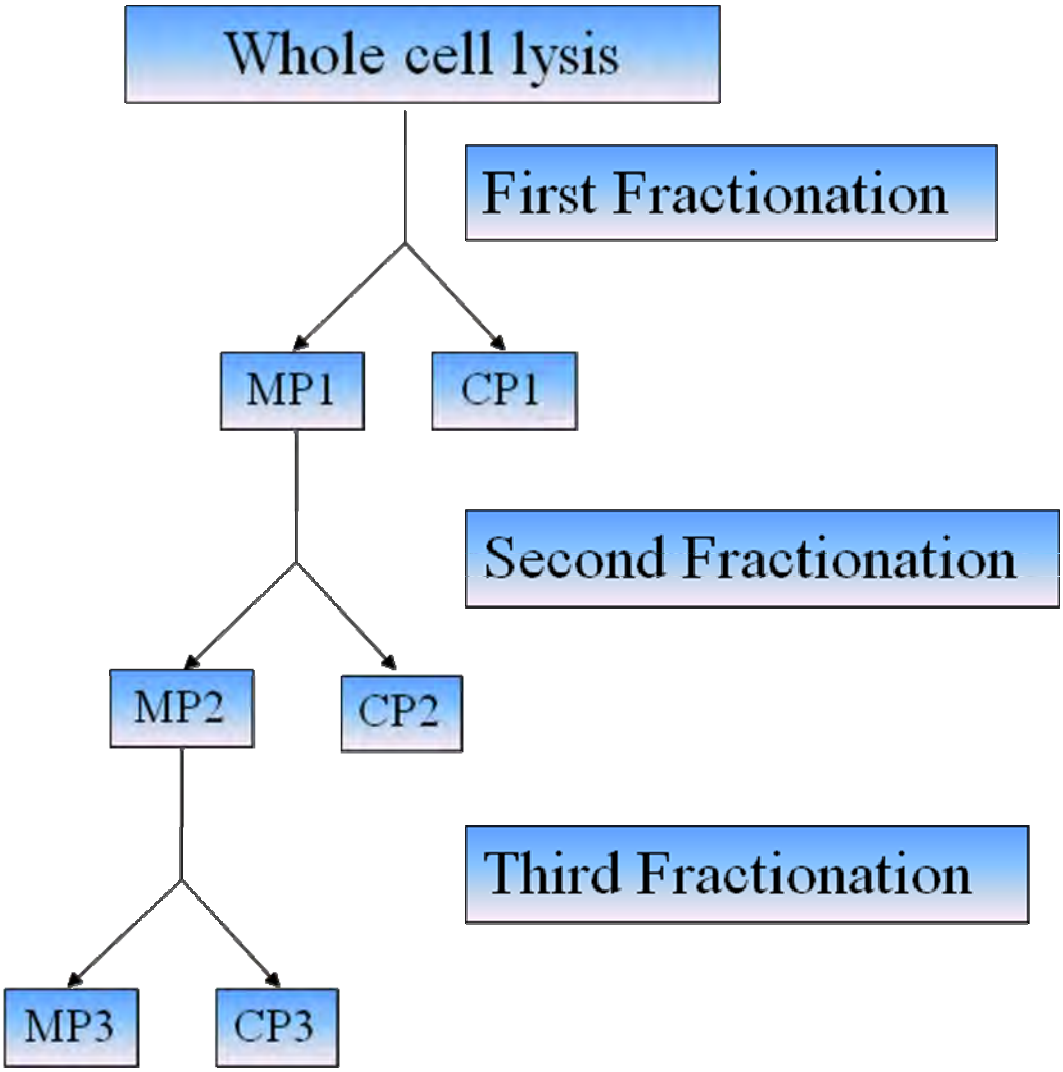


**Figure 2.2 Flow chart of multiple membrane fractionation**

Surface labelled cells were subjected to one, two or three membrane fractionations. Membrane protein and cytosolic protein fractionation after the first membrane fractionation are abbreviated as MP1 and CP1, respectively. MP1 was then subjected to the second fractionation and accordingly resulted in MP2 and CP2. Likewise, MP2 gave rise to MP3 and CP3 after the third fractionation.

**Table 2.6 Focusing conditions for 11 cm IPG strips (3–10)**

| Step number | Voltage | Voltage ramping mode | Time or Volt-hours (V-hr) |
|---|---|---|---|
| Step 1 | 150 V | Linear | 1 hour |
| Step 2 | 300 V | Linear | 2:30 hours |
| Step 3 | 600 V | Linear | 1:50 hours |
| Step 4 | 1200 V | Linear | 1:50 hours |
| Step 5 | 4000 V | Slow | 1:50 hours |
| Step 6 | 8000 V | Slow | 1h |
| Step 7 | 8000 V | Linear | 30000 V-hr |
| Step 8 | 500 V | Slow | 0:15 hours |

#### *2.5.5.2 Second dimension electrophoresis--SDS PAGE*

After IEF, the IPG strips were equilibrated as previously described [215]. Briefly, to reduce disulphide bonds, IPG strips were incubated in 2% (w/v) dithiothreitol (DTT) in equilibration buffer (6 M urea, 2% (w/v) SDS, 0.05 M Tris/HCl buffer (pH 8.8) and 20% (v/v) glycerol). IPG strips were then incubated in a second equilibration buffer containing 2.5% (w/v) iodoacetamide (IAA) to alkylate sulfhydryl groups. Either 10% (10% T, 3.3% C, 0.1% SDS and 375 mM Tris/HCl pH 8.8; for developmental stage) or 8% (8% T, 3.3% C, 0.1% SDS and 375 mM Tris/HCl pH 8.8; for experimental stage) large format (18 x 18 cm) polyacrylamide gels were cast without stacking gels using a Protean II XL casting chamber (Bio-Rad Laboratories). Molten agarose (1% w/v) was used to seal the IPG strips onto the top of the gels. The agarose contained 1% (w/v) bromophenol blue as a tracking dye. Proteins were separated in the second dimension using a Protean II XL Multi-cell (Bio-Rad Laboratories) in tris-glycine tank buffer (25 mM Tris, 192 mM glycine, 0.1% (w/v) SDS). Proteins were resolved at 7 mA/gel and the current was maintained until the dye front reached the bottom of the gel.

### 2.5.6 Gel visualisation

After 2-DE gels were removed from the glass plates and washed three times in Milli-Q water. Gels were scanned using a Typhoon Trio Variable Mode Imager (Molecular

Dynamics Inc., Sunnyvale, CA) with a pixel resolution of 100 µm. The excitation and emission wavelengths used for all three CyDye are listed in Table 2.7. Image analysis was performed using PD-Quest software (version 8.0, Bio-Rad Laboratories). Replicate groups each containing four gels were used for analysis. Proteins spots were automatically detected and manually edited. Gel staining was normalized using the total density in gels.

**Table 2.7 Detection of fluorescence of CyDye DIGE Fluor Minimal Dyes: Laser Excitation Source and Emission Filters [216]**



### 2.5.7 Flamingo fluorescent staining

To visualise all proteins on each gel, gels were fixed in 40% ethanol (v/v)/10% acetic acid (v/v) in Milli-Q water and stained with Flamingo Fluorescent Stain (Bio-Rad) according to manufacturer's instructions. Gels were de-stained in 0.1% (v/v) Tween 20 in Milli-Q water for 10 minutes before being washed twice in Milli-Q water prior to imaging. Gels were scanned using a Typhoon Trio Variable Mode Imager using a Green Laser (532 nm) excitation source and 610 ± 30 nm band pass emission filter.

### 2.5.8 Automated spot picking

Automated spot picking was performed at the Adelaide Proteomics Centre, University of Adelaide. Proteins were separated using 2-DE using the same method mentioned in section 2.5.5, with the exception that polyacrylamide gels were cast between low-fluorescence glass plates containing two reference marker disks. The gel images scanned using a Typhoon Trio Variable Mode Imager were imported into DeCyder software (version 6.5,

GE Healthcare) and spots were detected using the automated method. Spots of interest were selected to generate a pick-list. The pick-list was exported from DeCyder and imported into Spot Picker software (version 1.2, GE Healthcare). Spots were excised using the Ettan Spot Cutting Robot (GE Healthcare) according to the manufacturer's instructions. Gel plugs were washed twice with 0.1 M ammonium bicarbonate buffer ($NH_4HCO_3$), followed by Milli-Q water then dehydrated in acetonitrile (ACN) and dried.

### 2.5.9 Protein identification by liquid chromatography-electrospray ionisation ion-trap (LC-ESI-IT) mass spectrometry (MS)

This component of the study was performed at the Adelaide Proteomics Centre, University of Adelaide. Each gel plug was digested with 10 µl of 5 mM ammonium bicarbonate with 10% ACN containing 100 ng trypsin (Promega) for 16 hours at 37°C. Peptides were extracted sequentially with 1% formic acid (FA), 50% ACN/0.1% FA, and ACN, and the combined extracts were concentrated by centrifugal evaporation and diluted in 6 µl 3% ACN/0.1% FA. Vacuum concentrated samples were resuspended with 0.1% FA in 2% ACN to a total volume of ~8 µl. LC-ESI-IT MS/MS was performed using an online 1100 series HPLC system (Agilent Technologies) and HCT Ultra 3D-Ion-Trap mass spectrometer (Bruker Daltonics). The LC system was interfaced to the MS using an Agilent Technologies Chip Cube operating with a ProtID-Chip-150 (II), which integrates the enrichment column (Zorbax 300SB-C18, 4 mm, 40 nL), analytical column (Zorbax 300 SB-C18, 150 mm x 75 µm), and nanospray emitter. Five µl samples were loaded onto the enrichment column set at a flow rate of 4 µl/min in Mobile Phase A (0.1% FA in 2% v/v ACN) and resolved with 1-30% gradient of Mobile Phase B (0.1% FA in 98% w/v ACN) over 32 minutes at 300 nl/min. Ionizable species ($300 < m/z < 3{,}000$) were trapped and the two most intense ions eluting at the time were fragmented by collision-induced dissociation. Active exclusion was used to exclude a precursor ion for 30 seconds following the acquisition of two spectra.

### 2.5.10 Protein characterisation using web-based bioinformatics tools

Database searching and protein identification were performed at the Adelaide Proteomics Centre, University of Adelaide. MS and MS/MS spectra were subjected to peak detection and de-convolution using DataAnalysis (Version 3.4, Bruker Daltonics). Compound lists were exported into BioTools (Version 3.1, Bruker Daltonics) then submitted to Mascot (Version 2.2) using the following parameters; fixed modification = carbamidomethyl (C), variable modification = oxidation (M), MS mass tolerance = 1.5 Da, MS/MS mass tolerance = 0.8Da, peptide charge = 1+, 2+, or 3+, missed cleavages = 3. Data were matched to the SwissProt protein database.

## 2.6 Gene expression profiling

### 2.6.1 Preparation of total RNA

The collection and preparation of total cellular RNA was conducted using TRIzol (Life Technologies, Carlsbad, Canada). Up to 1 million cells were lysed in 1 ml of TRIzol, directly in wells or, if grown in a flask, removed from the flask using 0.05% trypsin/0.02% EDTA digestion prior to being lysed in TRIzol. Chloroform (200 µl per ml TRIzol) (Ajax Finechem, Taren Point, NSW, Australia) was added to this solution and tubes were shaken vigorously for 15 seconds followed by 3 minute incubation at room temperature. Centrifugation of this suspension at 12,000 *g* for 15 minutes at 4$^{o}$C, resulted in phase separation. The upper aqueous phase was transferred to a fresh tube and total RNA was precipitated out of the solution using isopropanol (500 µl per ml TRIzol) and glycogen (1µl per ml TRIzol) (Sigma-Aldrich, St. Louis, MO, USA). This preparation was incubated for 1 hour on ice to ensure maximum RNA precipitation. To pellet RNA, cells were centrifuged at 12,000 *g* at 4$^{o}$C for 10 minutes. After the supernatant removal, the pellets were washed in 1 ml of ice cold 75% ethanol before being centrifuged at 7,500 *g* at 4$^{o}$C for 5 minutes. Once most of the ethanol was removed, RNA was air dried for approximately

10 minutes. The dried RNA was then dissolved in RNAse free water (Promega, Madison, WI, USA) at 55$^{o}$C for 10 minutes before being analysed using a NanoDrop Mass spectrometer (NanoDrop ND-1000 Spectrophotometer, Biolab Group, Clayton, VIC, Australia).

### 2.6.2 Quantification and purity analysis of RNA

The NanoDrop Mass spectrometer was used for the quantification and purity analysis of RNA samples. Two µl of the sample was added to the stage of the NanoDrop. Subsequently, the absorbance was measured at 260 nm to determine the quantity of RNA and the purity was measured by the ratio of $A_{260}$:$A_{280}$. Samples with values between 1.85 and 1.95 were considered to be of high purity and were either used immediately to generate cDNA or stored at -20$^{o}$C for future use.

### 2.6.3 Complementary DNA (cDNA) synthesis

Complementary DNA was generated using the SuperScript III Reverse Transcriptase kit (Invitrogen, Carlsbad, Canada). Briefly, a mixture containing 1 µl of oligo (dT) (50 µM, Invitrogen, Carlsbad, Canada), 2 µl of dNTP mix (5 mM dideoxynucleotide triphopshates, Fisher Biotec, Wembley, WA, Australia), 1 µl of random primers (100 ng/µl), 1 µg of total RNA and RNAse free water was added to get a total volume of 13 µl. This mixture was heated to 65$^{o}$C for 5 minutes to denature the RNA secondary structures and then incubated on ice for at least 1 minute to allow the primer anneal to the RNA. The tubes were then briefly centrifuged before adding 4 µl of 5 x first-strand buffer (250 mM Tris-HCl, 375 mM KCl, 15 mM $MgCl_2$) (Invitrogen, Carlsbad, Canada), 2 µl of 0.1 M DTT (Dithiothreitol, Invitrogen, Carlsbad, Canada) and 1 µl of SuperScript III RT (200 units/µl) (Invitrogen, Carlsbad, Canada) with gentle pippetting and incubated at 25$^{o}$C for 10 minutes and at 50$^{o}$C for 1 hour to allow for primer extension and first strand synthesis. The reactions were stopped by incubating at 70$^{o}$C for 15 minutes, which leads to the

deactivation of the reverse transcriptase enzyme. The cDNA was diluted 1:5 in RNAse free water and stored at -20$^{o}$C for future use.

### 2.6.4 Real-time PCR

Using cDNA generated by the method described in section 2.6.3, PCR was performed to assess the levels of mRNA expression. Beta-actin (β-actin) was used as a housekeeping control gene against which samples were normalized. The primer pairs used in this thesis are outlined in Table 2.5. A reaction mixture containing 2 µl of sample cDNA, 7.5 µl SYBR Green (RT$^{2}$ RealTime$^{TM}$ SYBR Grren/Rox PCR master mix, SA Biosciences, MD, USA), 0.75 µl (10 µM) mixed primer pairs (Geneworks, SA, Australia) and 4.75 µl DEPC water was added to get a total volume of 15 µl for each tube of a 72 tube rotor of a Rotor Gene RG-6000 Realtime PCR machine (Corbett Research, Sydney, NSW, Australia). Cycling parameters include the following steps; for activation, hold 2 minutes at 50$^{o}$C and 15 minutes at 95$^{o}$C; for cycling (40 cycles), 15 seconds at 95$^{o}$C, 26 seconds at 58$^{o}$C, 10 seconds at 72$^{o}$C; for final extension, hold 30 seconds at 72$^{o}$C; and melt Curve for 90 seconds pre melt, 5 second steps, 1 degree per step, 72$^{o}$C to 99$^{o}$C. All mRNA quantification data represent the mean ± standard error of the mean (SEM) of triplicate experiments normalized to the house-keeping gene β-actin. Statistical differences (*) of $p<0.05$ were determined using the unpaired t-test.

### 2.6.5 Gene expression of epithelial-mesenchymal transition markers by real-time PCR

To examine whether ERM cells undergo epithelial-mesenchymal transition under osteogenic conditions, the levels of gene expression associated with epithelial-mesenchymal transition were examined by real-time PCR. ERM cells were cultured in osteogenic conditions as described in Table 2.1 and the total cellular RNA was collected after 1, 2, 3 and 4 weeks. Real-time PCR was performed as described in section 2.6.4 with

primers outlined in Table 2.5.

## 2.7 Differentiation assays

### 2.7.1 Assessment of osteogenic differentiation potential

Mineralisation assays were performed as previously described [191]. Briefly, ERM cells and PDLSC from three donors at passage 2 were seeded in 96-well plates at $1x10^4$ cells and $5x10^3$ per $cm^2$, respectively, in osteogenic media (Table 2.1) for 28 days with media changes twice weekly. At day 28 the wells were washed in 1xPBS and fixed with 10% Neutral Buffered Formalin (Fronine Laboratory Supplies, Lomb Scientific, Taren Point, NSW, Australia) for 1 hour. Mineral deposits were identified by Alizarin Red staining using 2% Alizarin Red S (Sigma-Aldrich Inc., St. Louis, MO, USA) in RO water.

For quantitative assessment, replicate plate was set up as described above and cells were cultured in mineralisation induction media as described above. At day 28 the wells were washed three times with 1xPBS before the mineralised matrix was dissolved in 100 µl of 0.6 M HCl (Merck, Kilsyth, VIC, Australia) for 1 hour at room temperature. The dissolved mineral solution was then transferred to 96-well microtitre plates where calcium levels were quantitated by the Cresolphthalein Complexone assay (Thermo Electron Corporation, Melbourne, VIC, Australia) according to the manufacturer's instructions. Briefly, 5 µl of supernatants were transferred to individual wells of a fresh microtitre plate in triplicate. A calcium chloride (calcium/phosphorous combined standard (Sigma Aldrich, St. Louis, MO, USA)) standard curve was established in triplicate. Equal volumes of reagent A (cresolphthalein complexone 0.10 mmol/L, 8-hydroxyquinoline 5.2 mmol/L, polyvinylpyrrolidine 0.07 mmol/L) and reagent B (2-amino-1-methylpropanol 260 mmol/L) were mixed and 200 µl were added per well. The plates were incubated at room temperature for 2 minutes and the absorbance was read at 540 nm on a microplate reader

(EL808 Ultra, BIO-TEK Instruments, Winooski, VT, US). Following dissolution of the mineral with HCl, the wells were washed with 1xPBS and the cells were digested with 100 µl of proteinase K (100 µg/ml) (Invitrogen, Carlsbad, Canada) for 2 hours at room temperature or overnight at 4°C. The cells were then triturated thoroughly to ensure complete disruption of the cells and a volume of 50 µl was transferred to a white 96-well microtitre plate (Costar, Corning, New York, NY, USA). DNA content per well was then determined using the Hoescht assay.

DNA content was measured using Hoescht 33258 dye as a surrogate marker of cell number. Diluted Hoescht 33258 solution was made by mixing equal volumes of 4 M sodium chloride (Sigma-Aldrich, St. Louis, MO, USA) and 0.1 M sodium phosphate (Sigma-Aldrich, St. Louis, MO, USA), and Hoescht 33258 dye (Sigma-Aldrich, St. Louis, MO, USA) at 2 µg/ml. Salmon sperm DNA (Sigma-Aldrich, St. Louis, MO, USA) was diluted in RO water to a 1 mg/ml stock solution. The stock DNA solution was diluted in sodium chloride/sodium phosphate solution to final concentrations of 50 µg/ml, 25 µg/ml, 12.5 µg/ml, 6.25 µg/ml, 3.12 µg/ml and 1.56 µg/ml and these were used to establish the standard curve for the assays. 150 µl of diluted Hoescht 33258 solution was added to the samples and DNA standards in white microtitre plates. The plates were gently agitated and fluorescence was then measured using a fluorescence spectrometer (LS 55, Perkin Elmer Instruments, Boston, MA, USA) with an excitation wavelength of 350 nm, an emission wavelength of 450 nm and a slit width of 2.5 nm.

ERM cells were also plated in 6-well plates as described above and RNA was isolated with TRIzol (Invitrogen, Carlsbad, CA) at day 14 of culture following osteogenic induction. RNA extraction and cDNA synthesis were performed as described in section 2.6.1 and section 2.6.3, respectively. Real-time PCR analysis was conducted as described in section

2.6.4 to assess the levels of expression of osteogenic-associated markers, Runx2, osteopontin (OPN) and bone sialoprotein (BSP-II).

### 2.7.2 Assessment of adipogenic differentiation potential

Adipogenesis was induced as previously described [102, 191, 217]. ERM cells and PDLSC from three donors at passage 2 were seeded at $1x10^4$ cells and $5x10^3$ per $cm^2$, respectively, in 96 well plates and were cultured for 28 days in the presence of adipogenic media (Table 2.1) with media changes twice weekly. At day 28 the wells were washed three times with 1xPBS and cells were fixed in 10% Neutral Buffered Formalin for 1 hour at room temperature. Formation of lipid deposits was determined by Oil Red O staining for 2 hours at room temperature. Oil Red O staining solution was made by dissolving 0.5 g of Oil Red O stain (MP Biomedicals, Solon, OH) in 100 ml of isopropanol (Ajax Finechem, Taren Point, NSW, Australia) and further diluted 1.5:1 in RO water.

For quantitative assessment, replicate plates were set up as described above. Cells were cultured in adipogenic media for 28 days with media changes twice weekly. At day 28 cells were washed three times with 1xPBS and then fixed in 10% Neutral Buffered Formalin for 1 hour at room temperature and stained with Oil Red O for 2 hours at room temperature. Oil Red O was quantified following the treatment of 100% isopropanol as previously described [102, 191]. The plates were allowed to dry before adding 100 µl of 100% isopropanol to each well. Following 10 minute incubation at room temperature, the extracted dye was quantified with the absorbance measured at 490 nm using a plate reader.
ERM cells were also plated in 6-well plates as described above and RNA was isolated with TRIzol (Invitrogen, Carlsbad, CA) at day 14 of culture following adipogenic induction. RNA extraction and cDNA synthesis were performed as described in section 2.6.1 and section 2.6.3, respectively. Real-time PCR analysis was employed as described in section

2.6.4 to assess the levels of expression of adipogenic-associated markers, peroxisome proliferator activated receptor-γ2 (PPARγ2) and leptin.

### 2.7.3 Assessment of chondrogenic differentiation potential

Chondrogenesis was performed as previously reported for human bone marrow-derived mesenchymal stem cells [218]. Cell pellets from $2x10^6$ ERM cells and PDLSC at passage 2 were centrifuged at 600 *g* and cultured in polypropylene tubes in chondrogenic media (Table 2.1) with media changes twice a week for 28 days. At day 28, pellet cultures designated for histological assessment were fixed in 10% Neutral Buffered Formalin overnight at $4^oC$, embedded and sectioned at 5 µm in the histology laboratory of the department of Neuroscience, Hanson Institute, Adelaide, SA, Australia. The sections were used for hematoxylin and eosin (H&E) staining, toluidine blue staining and immunohistochemical staining with mouse anti-human collagen type II monoclonal antibody (Table 2.4) (MAB1330, Chemicon International, Temecula, CA). Sections were de-paraffinised through two changes of xylene (Ajax Finechem, Taren Point, NSW, Australia), three changes of absolute ethanol (Merck, Kilsyth, VIC, Australia) and a final wash in RO water. To neutralise endogenous peroxidase activity, sections were incubated in 0.5% $H_2O_2$ (Ajax Finechem, Taren Point, NSW, Australia) (v/v) in methanol (Chem Supply, Gillman, SA, Australia) for 30 minutes and non-specific binding was blocked by incubating sections with 3% (v/v) normal goat serum in 1xPBS for 1 hour at room temperature. Immunohistochemical analysis was performed in section 2.4.1. The anti-collagen type II monoclonal antibody or an isotype-matched, non-binding control monoclonal antibody (1B5) and corresponding secondary antibody are outline in Table 2.4. Washing buffer was made by adding 50 mM Tris-HCl (Sigma-Aldrich, St. Louis, MO, USA) and 0.1% Tween-20 (Sigma-Aldrich, St. Louis, MO, USA) in RO water.

At day 28, pellet cultures designated for real-time PCR analysis were washed 3 times in 1xPBS and digested with collagenase type I (3 mg/ml; Worthington Biochemical, Lakewood, NJ) and dispase II (4 mg/ml; Roche Diagnostics, Indianapolis, IN) at 37°C for 1 hour and the total RNA was isolated with TRIzol (Invitrogen). RNA extraction and cDNA synthesis were performed as described in section 2.6.1 and section 2.6.3, respectively. Real-time PCR analysis was employed as described in section 2.6.4 to assess the levels of expression of chondrogenesis-associated markers type II collagen, aggrecan, Sox9 and type X collagen.

### 2.7.4 Assessment of neurogenic differentiation potential

For neuronal differentiation, a method based on a protocol for neurogenesis of human dental pulp stem cells was used [141]. In brief, ERM cells were seeded at $1x10^4$ cells per $cm^2$ onto polyornithine (10 µg/ml, Sigma-Aldrich, #P3655) and laminin (5 µg/ml, Invitrogen, #23017-015) pre-coated plates. Tissue culture flasks or wells were coated with polyornithine overnight at room temperature. Flasks and wells were washed twice with water and then coated with laminin overnight at 37°C in a humid incubator, followed by two washes with PBS. Neurobasal A Medium (Invitrogen, #10888-022) was used for the first 7 days, supplemented with B27 serum free supplement (Invitrogen, #17504-044), 50 µg/ml streptomycin, 50 U/ml penicillin, 2 mM L-glutamine, 15 mM HEPES buffer, 20 ng/ml Epidermal Growth Factor (PeproTech, #100-15) and 40 ng/ml basic fibroblast growth factor (bFGF) (Prospec Tany Technogene, East Brunswick, NJ, USA, #CYT-218). This was followed by a change in media for 7 days consisting of DMEM/F12 (Gibco BRL, Grand Island, NY, #11320) supplemented with 50 µg/ml streptomycin, 50 U/ml penicillin, 15 mM HEPES buffer, insulin-transferrin-sodium-selenite supplement (ITSS) (1:100) (Roche Diagnostics, Mannheim, Germany, #11074547001) and 40 ng/ml bFGF. The media for the final 7 days consisted of DMEM/F12 supplemented with 50 µg/ml streptomycin, 50

U/ml penicillin, 15 mM HEPES buffer, ITSS (1:100), 40 ng/ml bFGF and 0.5 µM retinoic acid (Sigma-Aldrich, #R2625). For immunofluorescence analysis, flasks were set up as described above and cells were liberated with 0.05% trypsin/0.02% EDTA post 3-week induction and seeded at $6x10^3$ cells per $cm^2$ in polyornithine and laminin pre-coated chamber slides. These chamber slides were fixed with 4% PFA for 30 minutes at room temperature following overnight adhesion and then washed with PBS. The staining protocol was used as following for all the neuron-associated antibodies, with the exception of anti-Glial fibrillary acidic protein (GFAP) antibody. Cultures were blocked with 3% normal horse serum for 2 hours at room temperature and then incubated with primary antibodies or isotype-matched control (Table 2.4) overnight at 4°C. After washing, sections were incubated with secondary antibodies (Table 2.4) for 30 minutes at room temperature. Following washing the slides were incubated with streptavidin Alexa Fluor 488 (Invitrogen, #S32354) for 1 hour at room temperature in the dark. Finally, cultures were washed and co-stained with Prolong gold anti-fade reagent with DAPI (4',6-diamidino-2-phenylindole) (Invitrogen, #P36931) for 10 minutes at room temperature, washed and then coverslipped with fluorescence mounting medium (DAKO, #S3023). Sections for anti-GFAP antibody were blocked and incubated in anti-GFAP antibody or isotype-matched control (Table 2.4) as described above. After washing, sections were incubated with donkey anti-rabbit Cy3 (orange-red) (Jackson Immunoresearch, West Grove, PA, USA, #711-165-152) for 1 hour at room temperature and then washed, co-stained with DAPI and cover-slipped as described above.

ERM cells were also plated in 6-well plates as described above and RNA was isolated with TRIzol (Invitrogen, Carlsbad, CA) at day 14 of culture following neurogenic induction. RNA extraction and cDNA synthesis were performed as described in section 2.6.1 and section 2.6.3, respectively. Real-time PCR analysis was employed as described in section

2.6.4 to assess the levels of expression of neurogenic-associated markers, β-III tubulin and nestin.

## 2.8 *In vivo* transplantation of ERM cells

### 2.8.1 Preparation of transplants

Integrin $\alpha_6$/CD49f-positive ERM cells were sorted as described in the section of Fluorescence-activated cell sorting (section 2.3.3). Following this, ERM cells (integrin $\alpha_6$/CD49f-positive) were expanded and trypsinized at passage 4, washed with HHF and resuspended in 1 ml OKM with additives. Hydroxyapatite tricalcium phosphate (HA-TCP) ceramic powder (Zimmer, Warsaw, IN) was washed in 1.5 ml HHF at 37$^{o}$C on a rotatory mixer for 1 hour before the HHF was aspirated. Approximately 5x10$^{6}$ of ERM cells (integrin $\alpha_6$/CD49f-positive) were mixed with 40 mg HA-TCP ceramic powder and then incubated at 37$^{o}$C on a rotary mixer for 1 hour. Following cells being centrifuged at 1000 rpm for 5 minutes and media being aspirated, 20 µl of mouse fibronogen (Sigma-Aldrich, #F-4385, 30 mg/ml in PBS) and 20 µl of thrombin (Sigma-Aldrich #T-8397, 100 U/ml in 2% $CaCl_2$ ) were added to the ceramic particles and mixed gently. The tubes were left for 3 minutes at room temperature to allow the mixture to polymerize.

### 2.8.2 Transplantation surgery

The mixtures of cells and HA/TCP particles were transplanted subcutaneously into the dorsal surface of 10-week-old immunocompromised NOD/SCID mice (IMVS animal facility, South Australia, Australia) as described [191], according to a protocol with animal ethics approval (University of Adelaide, South Australia, Australia, Animal Ethics Committee # M-2011-182). The mice were anaesthetised and a longitudinal incision of 1 cm in length was made along the skin. The skin on the lateral side of the opening was then teased away from the underlying tissue using blunt scissors to form two pockets behind each shoulder. Following this, the cell mixtures were inserted into each of the

subcutaneous pockets. The opening in the skin was closed by applying 2 to 3 sterile wound clips.

### 2.8.3 Histological analysis

The transplants were recovered at 8 weeks post-transplantation, fixed with 4% formalin, decalcified with buffered 10% EDTA (pH 8.0), and then embedded in paraffin. Sections (5 µm) were deparaffinized and stained with hematoxylin and eosin (H&E). Immunohistochemical staining using mouse anti-ovine CD44 antibody (H9H11 supernatants), which does not cross-react with murine tissues or murine mesenchymal stem cell populations, was performed to identify the origin of the bone tissue formed in the transplants. Moreover, staining of anti-osteocalcin and anti-CD44 was performed in serial sections. Furthermore, anti-CK-8 antibody was used to trace the fate of ERM cells in the transplants. For immunohistochemical analysis of anti-CD44, anti-osteocalcin and anti-CK-8 antibodies (Table 2.4), sections were pre-treated with 10 mM sodium citrate (pH 6.0) and then blocked with 3% normal goat serum. Immunohistochemistry was performed as described in section 2.4.1. Sections were imaged by NanoZoomer Digital Pathology (Hamamatsu, Hamamatsu City, Shizuoka, Japan).

## 2.9 Ovine tooth preparation

Fresh ovine incisors were collected from scavenges under the animal ethics approval (University of Adelaide, South Australia, Australia, Animal Ethics Committee) and fixed in 10% buffered formalin for 7 days. The tissues were then decalcified at room temperature in 10% EDTA solution (pH 7.4) where decalcification was determined by radiography. The tissues were then embedded in paraffin and cut into 5 µm sections. Haematoxylin and eosin (H&E) staining was performed every five sections to check for the presence of ERM cells prior to immunohistochemistry staining. Immunohistochemistry staining was

performed as described in section 2.4.1, with the exception that pre-treatment with 0.1% trypsin (Sigma-Aldrich, #T9201) for 20 minutes at 37°C was performed for anti-integrin α6/CD49f antibody.

## 2.10 Imaging

The bright field images of cell cultures were acquired using an Olympus CKX41 microscope with attached Olympus U-RFLT50 UV light and DP20 camera (Olympus, Tokyo, Japan). Cells were placed on microscope stage and microscope was manually or automatically adjusted to correct focal point. The *in vitro* neuronal differentiation stained images were acquired using the Olympus AX70 microscope fitted with a cooled CCD camera and V++ v.4 software. Sections of *in vivo* transplantation were imaged by NanoZoomer Digital Pathology (Hamamatsu, Hamamatsu City, Shizuoka, Japan).

## 2.11 Statistical analysis

Data analysis was carried out using Microsoft Excel 2007 (software version 12.0.4518.1014, Microsoft, Redmond, WA, USA). Data points are reported as the mean ± standard deviation (SD) or mean ± standard error of the mean (SEM). Statistical significance of (*) $p \leq 0.05$ was determined using the unpaired Student t-test. Statistical analysis was performed as described using three biological replicates unless otherwise stated in the Figure Legends.

# Chapter 3. Characterization and purification of ovine ERM cells *in vitro*

## 3.1 Introduction

The periodontium consists of various cell types including periodontal ligament fibroblasts (PDLF) (which are the dominant population in the periodontium), cementoblasts, osteoblasts, endothelial cells, macrophages and ERM. *Ex-vivo* expansion of porcine ERM cells was first described in 1976 [219]. Subsequent ERM cell cultures were reported in a number of studies in porcine [52, 97, 162, 220-232] and rodent models [12, 160, 233]. The existence of ERM cells from human periodontal ligament culture was first reported in 1981 [234] followed by other reports describing successful human ERM cell culture [64, 95, 235-240]. One of the most significant limitations in the characterization of Hertwig's Epithelial Root Sheath (HERS)/ERM is their limited expansion potential *ex vivo*. To help address this problem, an immortal HERS-derived cell line in rodents was established in order to examine the characteristics and properties of this cell population [12]. Furthermore, a novel technique of maintaining ERM cell expansion using feeder layers was established, which allowed the expansion of porcine ERM cells to achieve sufficient numbers for biomedical characterization and manipulation [162]. However, these advances have proved to be limited due to the lack of surface markers specific to ERM cells for the enrichment of this cell population.

In the present study, initial attempts to isolate ERM cells from human periodontal tissues for *ex vivo* expansion and characterisation were found to be technically challenging, due to the minimal cell numbers obtained from the available tissue sources and poor growth rate of human ERM, which was consistent with other reports [241]. Previous studies in our laboratory showed that both ovine PDLSC and ERM cells were present in higher cell numbers and at a higher growth rate in culture compared to human counterparts

(unpublished data). With the discovery that ovine PDLSC and DPSC exhibit similar properties to their human counterparts [139, 201], these ovine stem cell populations have become attractive candidates for periodontal and dentine matrix regeneration based on large animal models [139]. Therefore, the isolation and characterisation of putative stem cell populations from other species such as sheep are of particular significance for studying dental related conditions in preclinical large animal models [201]. With this in mind, we characterised ERM cells from ovine periodontal tissues in the present study, due to the easy availability of healthy tissue and the high growth potential of ERM from ovine periodontium, and as a potential source of stem cells for future large animal pre-clinical periodontal regeneration studies.

### 3.1.1 Methods for epithelial cell isolation from the periodontium

Conventional protocols involve the collection of periodontal ligament cells, after the upper and lower third of periodontal tissue is scraped off and discarded to avoid any cell contamination from gingiva or dental pulp tissues. However, the primary culture of periodontal ligament cells gives rise to ERM cells as well as contaminating PDLF. Selective enzymatic digestion using trypsin is currently used as a means to separate the trypsin sensitive PDLF cell fraction from the adherent ERM cells [209]. This technique is based on the fact that fibroblasts attach and detach at a faster rate than epithelial cells [210]. This is a crude method for isolating partially purified epithelial cells from a heterogeneous population, often requiring stringent multiple enzymatic digestion steps, which has the potential to introduce DNA damage to cells [242]. Alternatively, serum-free keratinocyte medium favouring epithelial over mesenchymal cell growth following successive cell passage has been widely used [64, 243, 244]. In serum-free culture system, it is essential to provide the cells with necessary growth factors, either from the commercial additives, conditioned medium or the use of feeder layer cells [12]. In the

present study, we used oral keratinocyte medium with additives to support ERM growth.

### 3.1.2 Prospective isolation of keratinocyte stem cells

Since ERM co-habitat with other PDL cell populations in the periodontium, the ability to select and enrich for ERM cells represents an important prerequisite for their further characterization. In contrast to the use of either cloning rings, mechanical disruption, serial plating or selective media to culture epithelial cells [210], sorting of stem/progenitor cells based on unique surface antigen expression has generated great interest over the last two decades which has led to the rapid identification and purification of specific cell populations in the fields of immunology and haematology [123]. Clearly, the availability of specific cell surface markers would greatly facilitate the isolation and characterization of ERM cells. Considering the lack of specific surface markers for ERM cells and that they share similar cellular and molecular properties with epithelial cells in other tissues, we hypothesized that cell surface markers of the well characterized skin keratinocyte stem cells (KSC) may be useful for the enrichment of ERM cells.

The basal epidermal layer of skin contains three subpopulations [188]: keratinocyte stem cells (KSC) which are relatively quiescent and identified as $^{3}$H-Tdr label-retaining cells (1-10% of basal cells) (analogous to MSC in the bone marrow); transit amplifying cells that are identified as rapidly cycling and short-lived (60% of basal cells) (analogous to committed progenitor cells in the bone marrow); and post-mitotic differentiating (PMD) keratinocyte (40% of basal cells). Previous studies have identified unique expression patterns of certain cell adhesion molecules such as integrins that have been used to select for KSC [185-187, 189, 205].

Integrins are cell surface glycoproteins responsible for regulating cell adhesion and

attachment. Structurally, integrins are heterodimers made up of alpha and beta subunits (Figure 3.1). The lamina receptor, integrin subunit $\alpha_6$ or CD49f, can bind to either β1 or β4 subunit, where $\alpha_6\beta4$ is believed to be an epithelial-specific integrin [245-247]. Two integrin subunits, β1 and $\alpha_6$ have been reported as surface markers for skin KSC. Skin KSC were first isolated using β1 integrin, or CD29, using Fluorescence Activated Cell Sorting (FACS) [185]. Cells with high levels of β1 integrin expression (designated as β1 integrin$^{high}$) exhibited a higher colony forming efficiency and could generate an epithelium when grafted onto mice [185, 186]. However, it was subsequently found that the β1 integrin$^{high}$ population contained both KSC and transit amplifying (TA) cells [205]. The discovery of using the laminin receptor subunit, $\alpha_6$ integrin, or CD49f, as a key surface marker for KSC was a critical step for the purification of these epithelial progenitors [187]. Basal keratinocytes expressing high levels of $\alpha_6$ integrin and low levels of CD71 (designated as $\alpha_6^{bri}CD71^{dim}$) displayed KSC attributes demonstrating greatest regenerative capacity, while $\alpha_6^{bri}CD71^{bri}$ cells and $\alpha_6^{dim}$ cells were more comparable to TA cells and PMD keratinocytes, respectively [187-189]. Subsequently, oral KSC have been isolated from oral mucosa using $\alpha_6\beta4$ integrin and CD71 from keratinized oral mucosa [206]. In view of the similar cellular and molecular properties of ERM cells with other epithelial cell populations from other tissues, we hypothesized that integrin $\alpha_6$ may provide a suitable cell surface marker for the purification of ERM cells.

In the present study, the immunophenotypic profile of ERM cells was assessed using immunocytochemical and flow cytometric techniques. Experiments were carried out to investigate the immunophenotypic profile of ERM cells and PDLF, as well as the immunophenotype of ERM cells in ovine incisor sections. To optimize the selection protocol for ERM cells, we identified the distinctive surface antigen expression profile for ERM cells in comparison to PDLF. Experiments were conducted to identify integrin

$\alpha_6$/CD49f as a cell surface marker for the enrichment of ERM cells from a heterogeneous population.

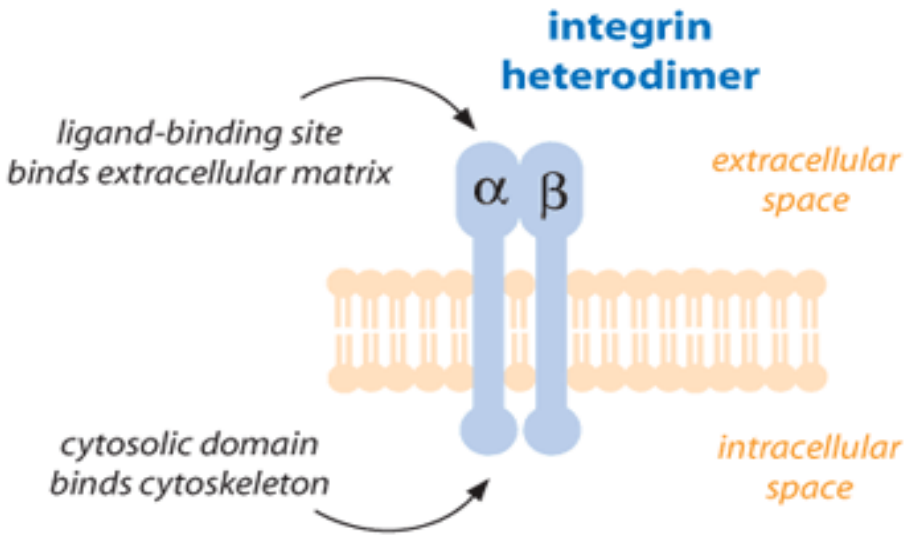


**Figure 3.1 The basic structure of integrin [44]**

Integrins are cell surface glycoproteins composed of two subunits, one alpha chain and one beta chain, which expand across the plasma membrane connecting the inside of the cell to the extracellular space.

## 3.2 Results

### 3.2.1 ERM and PDLF exhibited differential growth pattern

One week after seeding primary single cell suspension of ovine periodontal ligament cells, all flasks were monitored for cell growth and returned to the incubator to maintain culture for another week. Following this, mixed cultures of periodontal ligament cells were observed composed of two morphological types, epithelial-like and fibroblast-like (Figure 3.2A). Epithelial cells were easily distinguished by their characteristic cobblestone, pavement like or polygonal appearance. They were packed tightly together with almost zero or very little intercellular space between the cell bodies (Figure 3.2B). Fibroblastic cells exhibited an elongated, spindle shape (Figure 3.2C) and constituted roughly 90% of the cell population cultured from periodontal ligament tissue. Multiple selective enzymatic digestion, which takes advantage of the differential sensitivity to trypsin detachment

between ERM and PDLF, resulted in all cells in the cultures displaying an epithelial morphology. ERM cells tended to grow as colonies or clusters in subculture, while PDLF grew as individual cells.

### 3.2.2 Differential immunophenotypic profiles of ERM cells and PDLF

#### *3.2.2.1 ERM cells expressed both epithelial and mesenchymal markers*

To characterize the immunophenotype of ERM cells, immunocytochemical studies were performed using a panel of antibodies associated with epithelial or mesenchymal cell populations. *Ex vivo*-expanded ERM cells were found to express epithelial cell markers including cytokeratin-8 (CK-8), E-cadherin and epithelial membrane protein-1 (EMP-1) (Figure 3.3), confirming the epithelial nature of ERM cells. Interestingly, ERM cells also showed positive expression of mesenchymal stem cell associated markers CD44, CD29 and heat shock protein 90β (HSP90β) (Figure 3.3). These results suggested that ERM cells have characteristics of both epithelial and mesenchymal cells. Further immunochemical analysis demonstrated that haematopoietic cell markers CD14 and CD45 were not expressed by ERM cells (Figure 3.3). Confirmatory studies using flow cytometric analysis demonstrated that ERM cells exhibited cell surface expression of CD44, CD29 and HSP90β while lacking expression of CD14 and CD45 (Figure 3.4). However, the epithelial cell markers failed to be analysed by flow cytometry due to the intracellular expression of CK-8 and the availability of antibodies for ovine cells that are only reactive with the intracellular domain of E-cadherin and EMP-1.

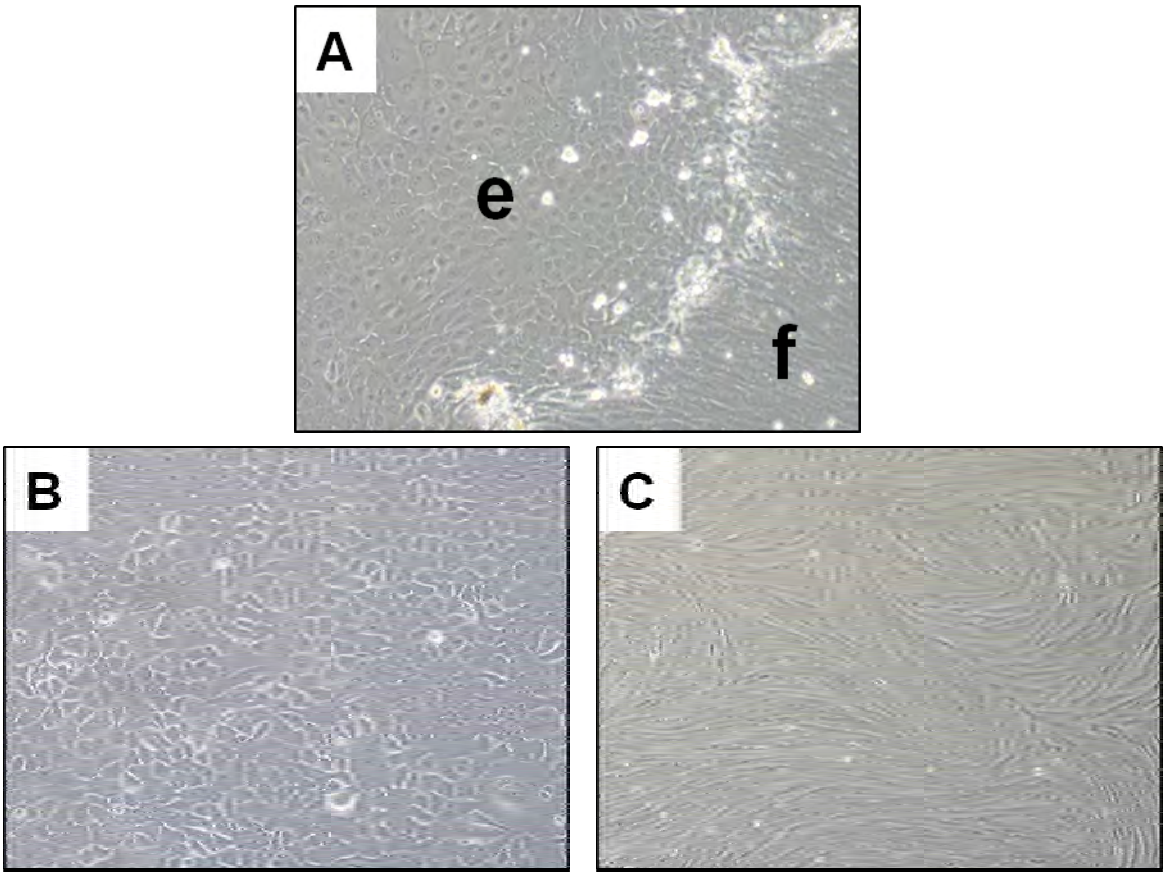


**Figure 3.2 Representative phase contrast images of ovine periodontal ligament cells**

(A) Mixed cell culture from ovine periodontal ligament displaying both epithelial cells (e) and fibroblasts (f) morphology. (B) Epithelial cell Rests of Malassez (ERM) demonstrated the characteristic cobblestone morphology in culture. (C) Periodontal Ligament Fibroblasts (PDLF) showed the typical spindle shape.

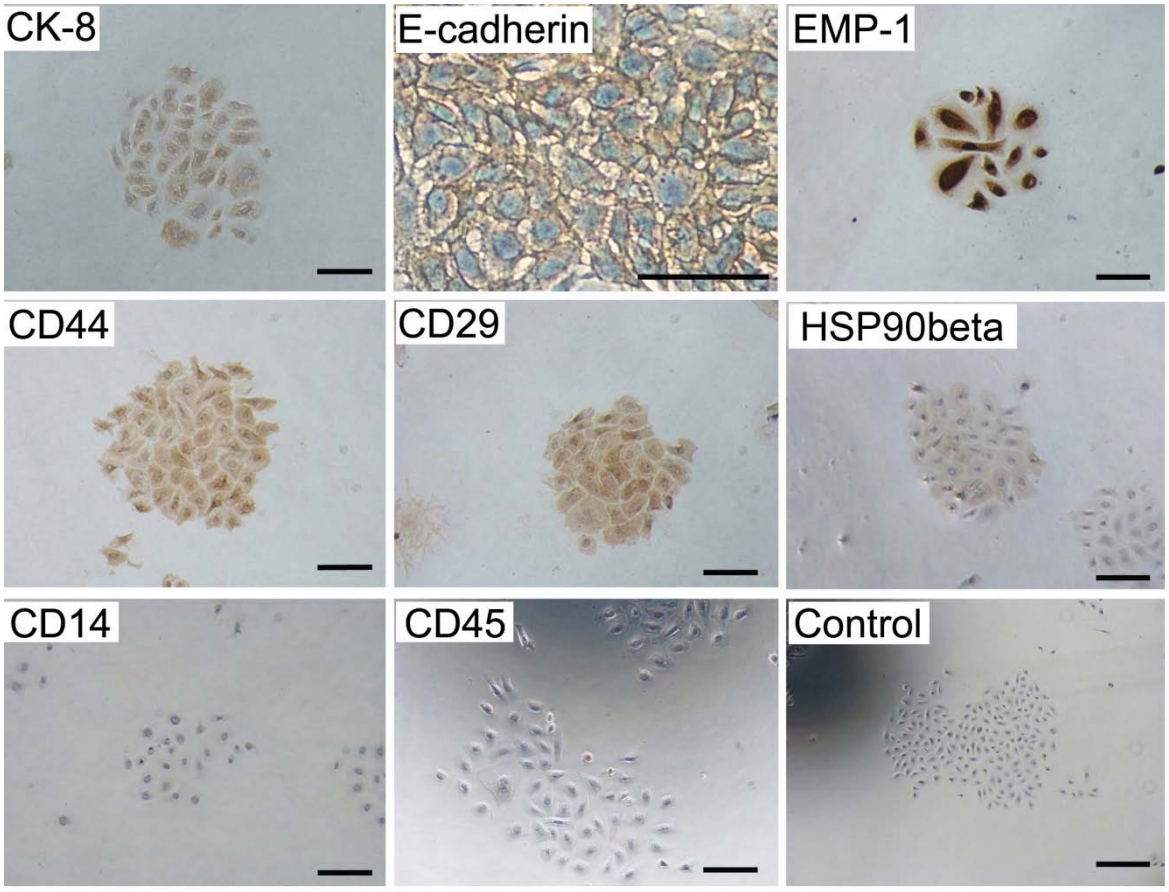


**Figure 3.3 Representative images of the protein expression profile of Epithelial cell Rests of Malassez (ERM) shown by immunocytochemistry**

ERM cells were positive for epithelial cell markers: cytokeratin 8 (CK-8), E-cadherin and epithelial membrane protein-1 (EMP-1) but they also expressed some mesenchymal cell associated markers: CD44, CD29 and Heat Shock Protein 90β (HSP90β), and lacked the hematopoietic cell markers: CD14 and CD45. Scale bar=50 μm.

### *3.2.2.2 ERM cells expressed epithelial markers in vivo*

Localisation of ERM cells in decalcified ovine teeth was demonstrated by histological analysis (Figure 3.5A). ERM cells were easily identified as small cell clusters of epithelial cells in proximity to radicular cementum surface (Figure 3.5A). Immunohistochemical staining showed that ERM cells were positive for CK-8 (Figure 3.5B) and integrin α6/CD49f (Figure 3.5C). No nonspecific staining was identified in the isotype-matched control (Figure 3.5D). This indicated that ERM cells express similar proteins *in situ* as they do *in vitro*.

### *3.2.2.3 Cell surface expression profiles of PDLF in vitro*

In parallel experiments, the immunophenotype of PDLF was investigated using the above-mentioned antibodies. PDLF exhibited the positive expression of EMP-1, CD44, CD29 and HSP90β while lacking the expression of CK-8, E-cadherin, CD14 and CD45 (Figure 3.6).

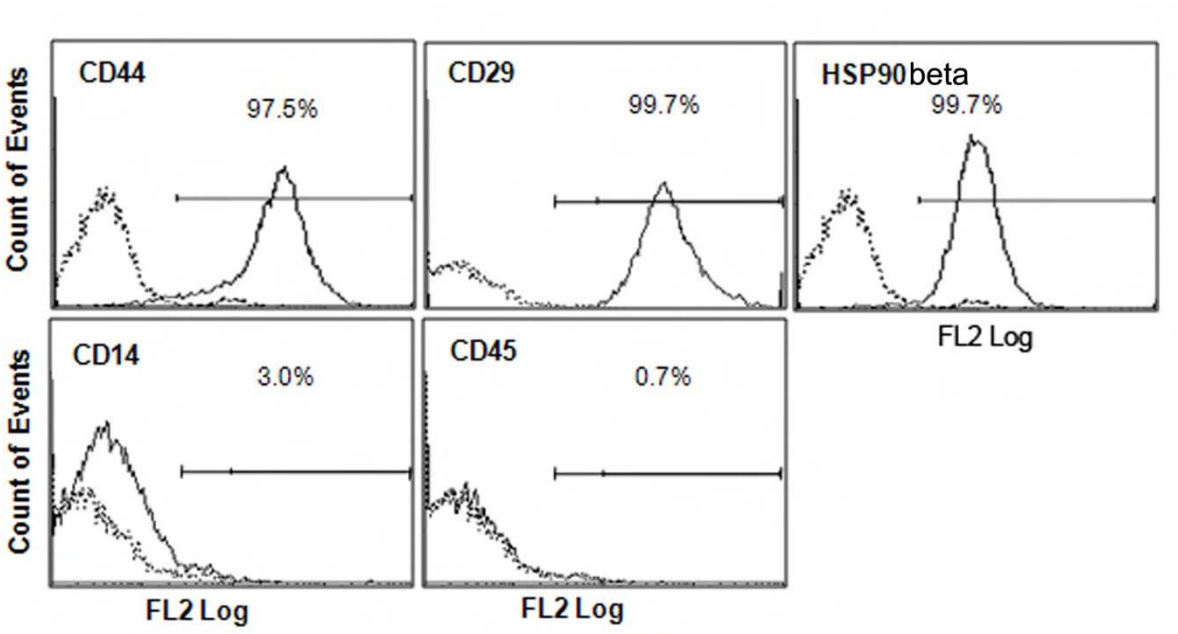


**Figure 3.4 Protein expression was confirmed by flow cytometric analysis**

Epithelial cell Rests of Malassez (ERM) were positive for CD44, CD29, Heat Shock Protein 90β (HSP90β) and negative for CD14 and CD45.

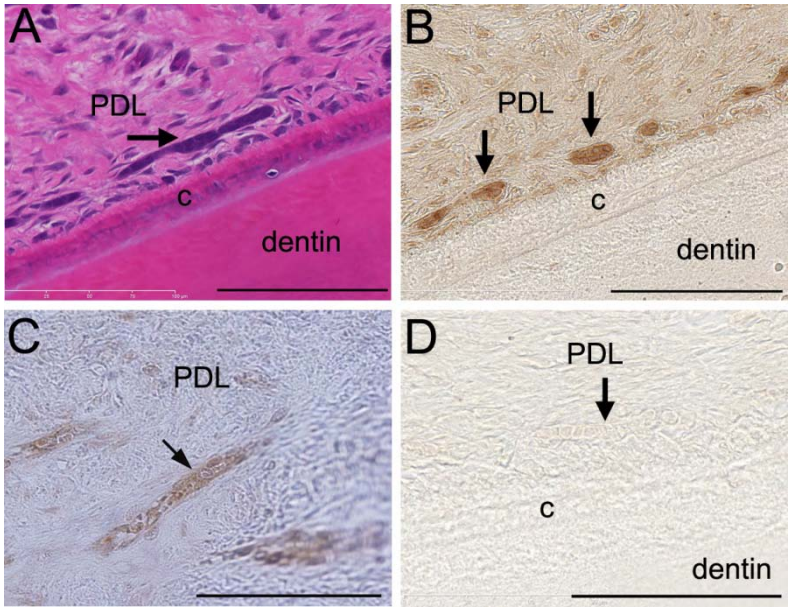


**Figure 3.5 Epithelial cell rests of Malassez (ERM) expressed epithelial cell markers *in vivo***

(A) Localisation of ERM cells (arrow) in decalcified ovine teeth was demonstrated by H&E staining. Immunohistochemical staining showed that ERM cells (arrows) were positive to cytokeratin-8 (B) and integrin α6/CD49f (C) antibodies. (D) Isotype matched control was used to determine the level of non-specific antibody binding. Scale bar=100 µm. c, cementum; PDL, periodontal ligament.

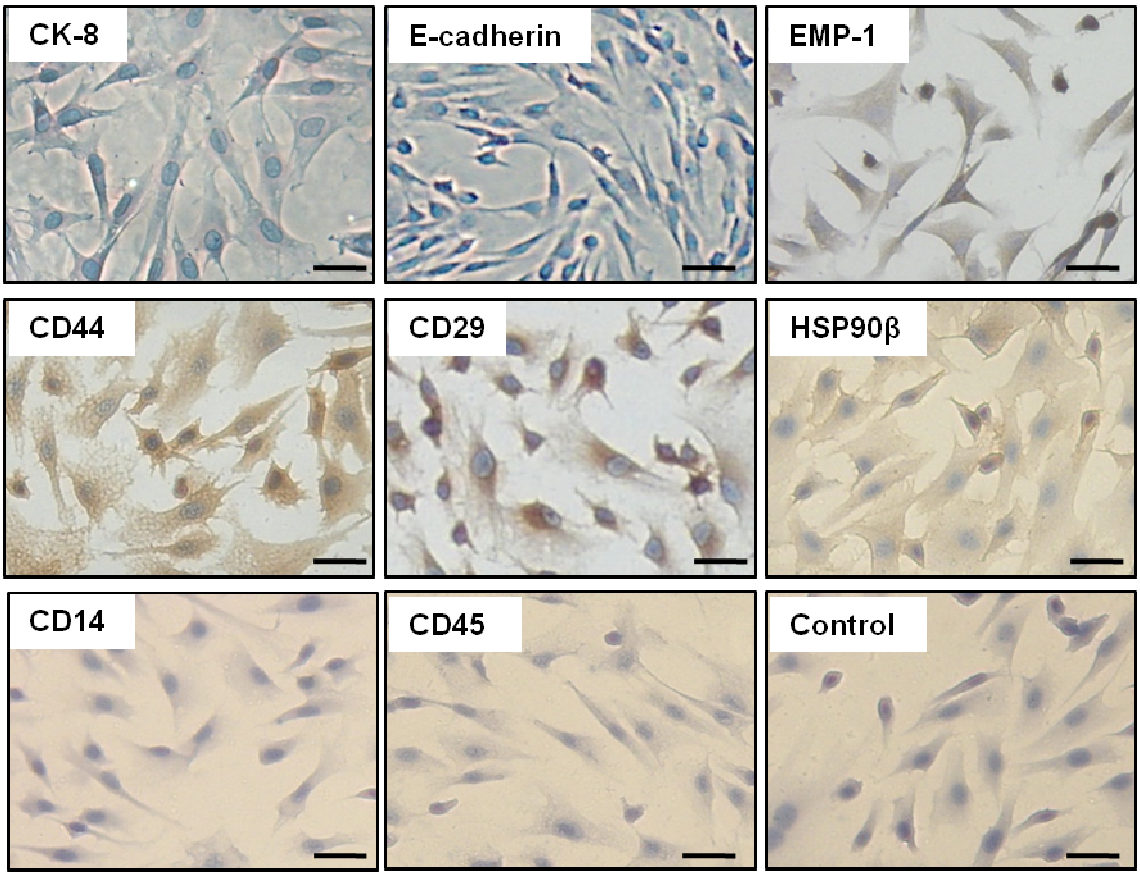


**Figure 3.6 Representative images of the protein expression profile of Periodontal Ligament Fibroblasts (PDLF) shown by immunocytochemistry**

PDLF were negative for cytokeratin 8 (CK-8) and E-cadherin. They expressed epithelial membrane protein-1 (EMP-1) and mesenchymal cell associated markers: CD44, CD29 and Heat Shock Protein 90β (HSP90β), and lacked the hematopoietic cell markers: CD14 and CD45. Scale bar=50 μm.

### 3.2.3 PDLF were unable to undergo mesenchymal epithelial transition when grown under keratinocyte culture conditions

Minimal numbers of PDLF were capable of surviving in oral keratinocyte medium with additives, which appeared to lose the capacity to proliferate. Morphologically, the PDLF maintained a spindle fibroblastic shape (Figure 3.7). Phenotypically, the sporadic PDLF identified in these cultures stained negative for cytokeratin-8 and integrin α6/CD49f, and positive for mesenchymal markers, CD44, CD29 and HSP90β in OKM (oral keratinocyte medium with additives) and MEM (minimum essential medium, α modification with additives) (Figure 3.7). These studies indicated that PDLF were unable to undergo

mesenchymal epithelial transition when grown under keratinocyte culture conditions.

### 3.2.4 Integrin α6/CD49f can serve as a surface marker to purify ERM cells

Previous studies have reported that human keratinocytes expressing high levels of integrin $\alpha_6$ subunit (laminin ligand) and low levels of CD71 (transferrin receptor) possess many of the features of stem cells including small cell size, quiescence and skin regenerative capacity [187]. Given that ERM cells appear to display a cell surface expression profile overlapping with PDLF, we examined whether the surface expression of integrin $\alpha_6$/CD49f could be used as a potential selective marker of epithelial cells within a heterogeneous periodontal ligament cell population.

*Ex vivo*-expanded ERM cells were found to be positive for integrin $\alpha_6$/CD49f while PDLF were largely negative or $\alpha_6$/CD49f low expressing (Figure 3.8A). Immunomagnetic bead selection was used to determine the efficiency of enrichment for ERM cells from digested periodontal ligament tissues based on their expression of integrin $\alpha_6$/CD49f. The integrin α6/CD49f-positive fraction represented approximately 2% of the total freshly isolated periodontal ligament cell population (data not shown). The presence of clonogenic cell populations was demonstrated in ERM cells and PDLF. Cells within epithelial clones were characterized by typical cobblestone morphology (Figure 3.8A), while PDLF clones showed a typical spindle-shaped fibroblastic morphology (Figure 3.8A). The colony-forming capacity of integrin $\alpha_6$/CD49f-positive selected epithelial cells (colony-forming unit epithelial cells (CFU-Epi)) at day 14 of culture showed a significant high level of enrichment of over 50- and 7-fold (173.91±40.99 per $10^5$ cells plated) greater than the integrin $\alpha_6$/CD49f-negative cells (3.33±5.77 per $10^5$ cells plated) and unfractionated cells (26.67±11.55 per $10^5$ cells plated), respectively (Figure 3.8B). Taken together, these results demonstrated that integrin $\alpha_6$/CD49f could be used as a surface marker to enrich and purify

clonogenic ERM cells from a heterogeneous periodontal ligament cell population.

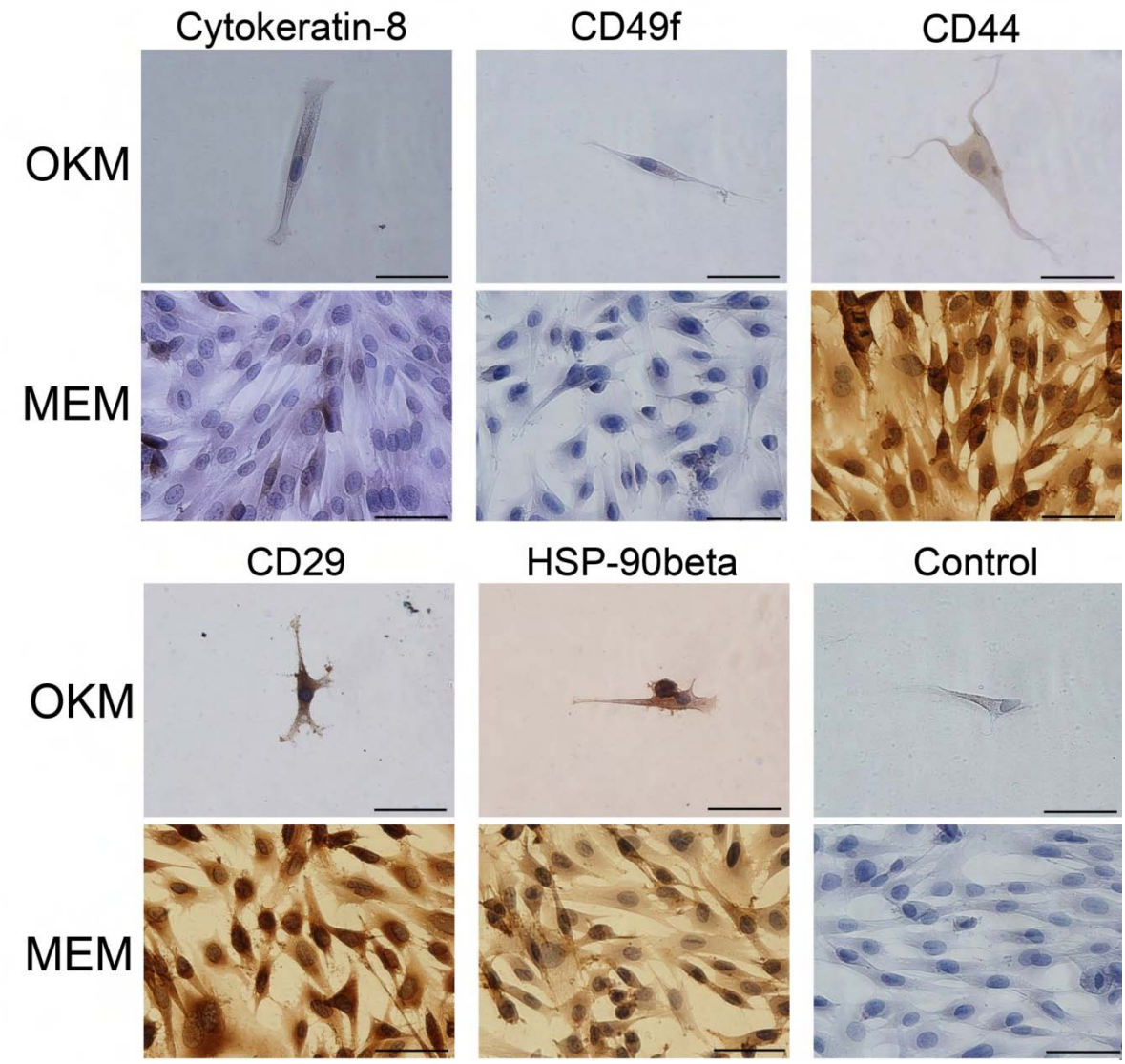


**Figure 3.7 Periodontal ligament stem cells did not under mesenchymal epithelial transition in keratinocyte culture system**

Minimal number of periodontal ligament stem cells could survive in OKM with additives. Morphologically, they showed spindle shape of fibroblasts. They stained negative for cytokeratin-8 and integrin α6/CD49f, and positive for mesenchymal markers, CD44, CD29 and HSP-90β in OKM and MEM. Isotype matched control was used to determine the level of non-specific antibody binding. Scale bar=50 μm. OKM, oral keratinocyte media with additives; MEM, Minimum essential medium, α modification with additives.

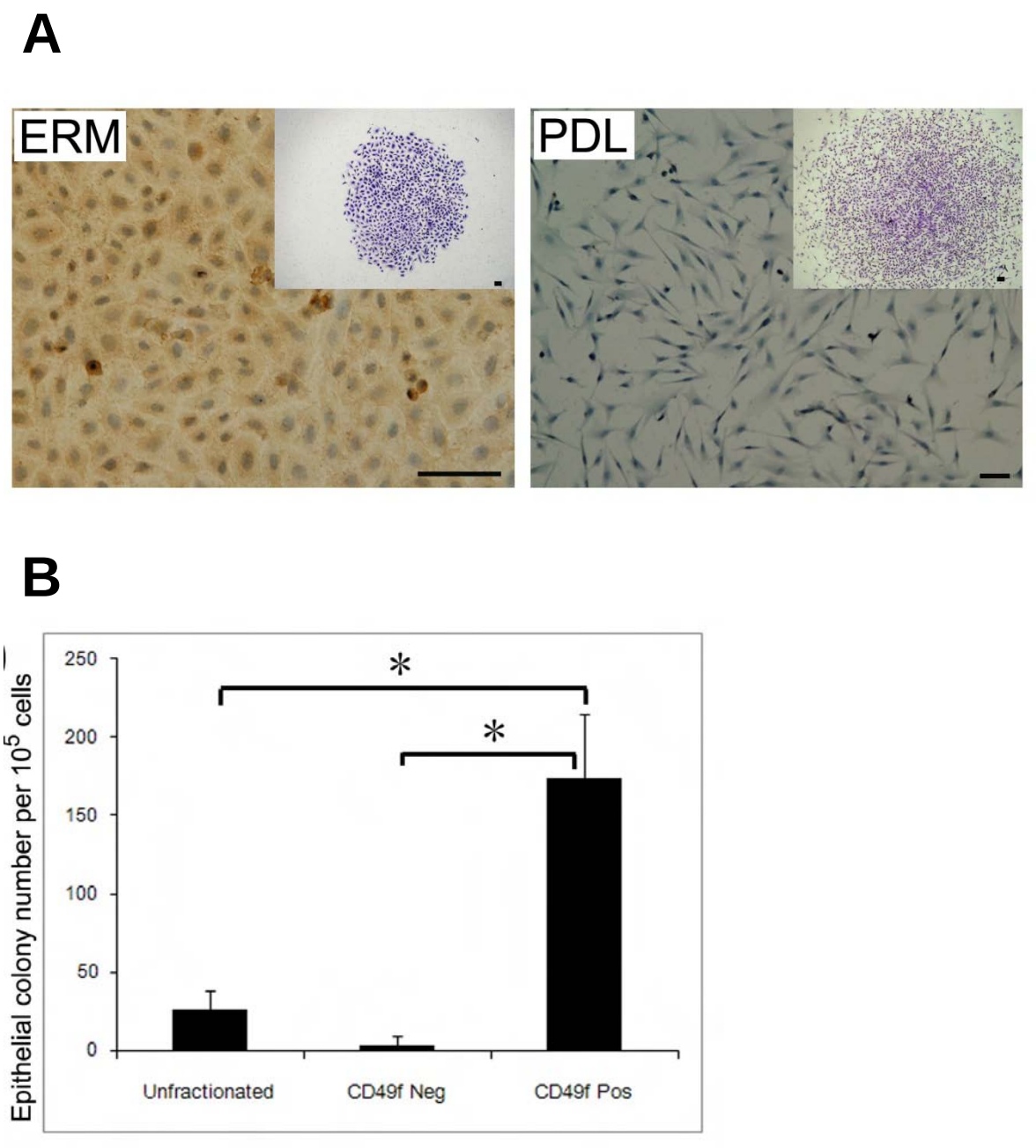


**Figure 3.8 Integrin α6/CD49f can serve as a surface marker to purify Epithelial cell Rests of Malassez (ERM)**

(A) Immunocytochemistry showed that ERM cells expressed integrin α6/CD49f while periodontal ligament fibroblasts (PDL) lacked its expression. Scale bar=50 μm (B) Integrin α6/CD49f was used for the enrichment of colony forming units-epithelial cells (CFU-Epi) with characteristic cobblestone morphology by immunomagnetic bead selection. The colony forming capacity of integrin α6/CD49f $^{+}$ selected CFU-Epi at day 14 showed a high level of enrichment of over 50 and 7 fold (173.91±40.99 per $10^5$ cells plated) greater than the integrin α6/CD49f $^{-}$ cells (3.33±5.77 per $10^5$ cells plated) and unfractionated cells (26.67±11.55 per $10^5$ cells plated), respectively. Statistical differences (*) of $p<0.05$ was determined using the unpaired *t*-test.

Subsequently, we used integrin $\alpha_6$/CD49f as a surface marker for the enrichment of ERM cells from three donors (Figure 3.9). ERM cells showed approximately 95% of integrin $\alpha_6$/CD49f positivity after selective enzymatic digestion using trypsin, indicating that this technique allows for the partial purification of ERM cells. Moreover, the high expressing integrin $\alpha_6$/CD49f positive cell fraction from these cultures (brightest 30%) was selected using fluorescent-activated cell sorting for the functional experiments in Chapter 4.

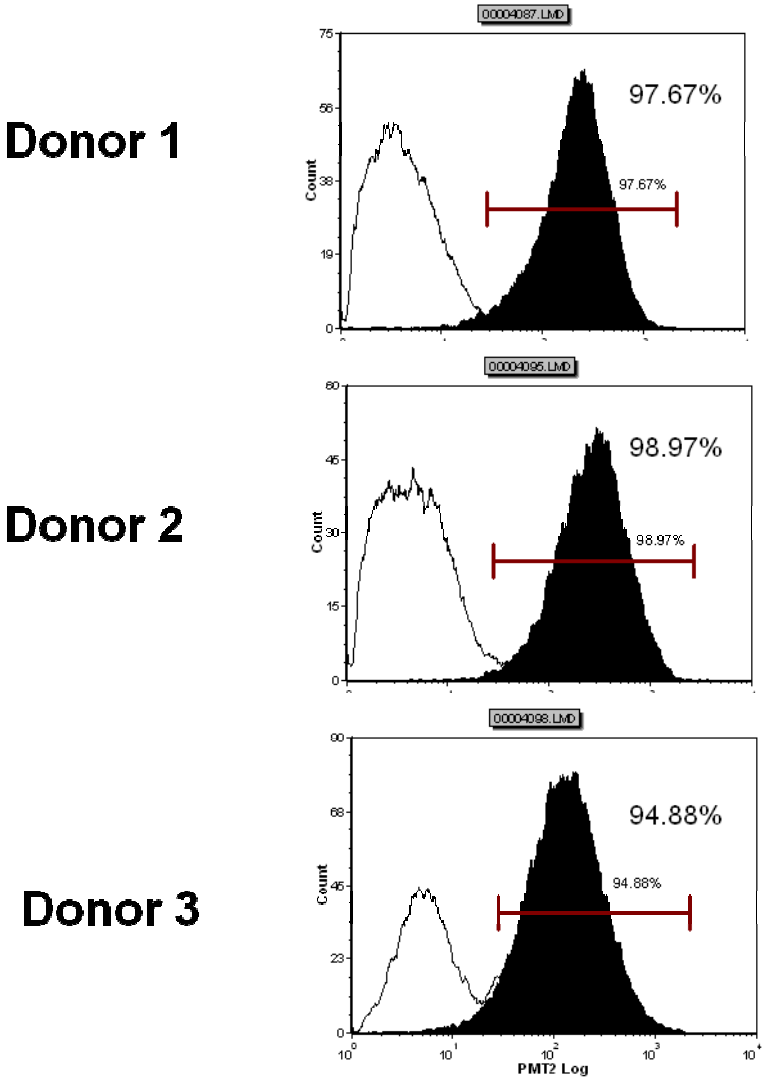


**Figure 3.9 Integrin α6/CD49f was used as a surface marker for the enrichment of Epithelial cell Rests of Malassez (ERM) from three donors**

FACS was used to select the brightest 30% of cells in the integrin $\alpha_6$/CD49f-positive fraction of ERM cultures from three donors prior to subcutaneous transplantation. The white and black histograms illustrated the isotype matched control and anti-CD49f antibody, respectively.

## 3.3 Discussion

The epithelial tissue acts as a barrier to protect the underlying tissues from toxins and physical trauma. This tissue is known collectively as the epithelium or endothelium if it occurs on surfaces of the cavities. Epithelial tissue is distinguished by several important features. Firstly, cells in epithelial tissues are extremely tightly packed and form continuous sheets by tight junctions and desmosomes, with minimal intercellular spaces between them. Furthermore, the epithelial tissue, regardless of the type, is usually separated from the underlying tissue by a basal laminin which provides structural support for the epithelium and binding to neighbouring structures. A remarkable characteristic of ERM cells is that they persist within a mesenchymal matrix during postnatal life, while epithelial cells in other tissues exist as a layer separated from the underlying connective tissues by a basal lamina. Studies are needed to explore factors that allow ERM to survive in the connective tissues during postnatal life. Understanding these factors is paramount to elucidating the roles of ERM in adult periodontium.

It should be noted that different seeding densities of ERM cells were used to establish primary cultures in the present study, because ERM cells were found to adhere less efficiently and proliferate much slower than PDLF. Single cell suspensions from freshly enzymatic digested ovine periodontal tissues were seeded at a low density to allow the expansion of ERM colonies by avoiding the overgrowth of contaminating PDLF in primary ERM cultures. Selective enzymatic digestion in established primary cultures was then used to eliminate the majority of PDLF, which allowed the growth of ERM cells at a higher cell seeding density ($8x10^3$-$12x10^3$ cells per $cm^2$) in subsequent subcultures. This finding is consistent with the reported findings that porcine ERM cells grew poorly when subcultured at a seeding density less than $2x10^4$ per ml (equivalent to $3.2x10^3$ cells per $cm^2$ in a T75 flask) [248].

Immunocytochemical techniques were utilized to confirm that ERM cells exhibited similar characteristics to other epithelial cell populations. Cytokeratins are routinely used to discriminate epithelial cells from mesenchymal cells both *in vitro* and *in situ* as they are not expressed by mesenchymal cells. The expression of CK-8 on ovine ERM cells in the present study is in agreement with previous studies [249-251]. In a previous study using human and non-human primate cells, ERM displayed a comparable cytokeratin expression pattern to that of the junctional epithelium [251]. E-cadherin, also known as cadherin 1, CDH 1, CAM 120/80, epithelial cadherin, uvomorulin or CD324, is a calcium-dependent cell-cell adhesion glycoprotein expressed predominantly in epithelial tissues. It is a transmembrane protein composed of five extracellular cadherin repeats, a transmembrane region and a highly conserved cytoplasmic tail. E-cadherin has been shown to have a central role in the maintenance of epithelial polarity and architecture [252-254]. Inactivation of E-cadherin is thought to contribute to cancer progression by increasing proliferation, invasion and/or metastasis [255]. Epithelial membrane protein-1 (EMP-1), also known as CL-20, tumour-associated membrane protein (TMP), B4B and PAP, is a tetraspan transmembrane protein of 160 amino acids with two extracellular loops [256]. Its expression has been reported to be associated with a liver stem cell line based on cDNA microarray analysis [257]. In addition, evidence is emerging that its expression level might be correlated with tumour prognosis, as the down regulation of EMP-1 was shown to be associated with lymph node metastasis of oral squamous cell carcinoma [258]. As the expression of EMP-1 has been shown to be associated with the acquisition of gefitinib clinical resistance in lung cancer, it has been suggested that EMP-1 can be used as a potential biomarker of gefitinib resistance [259]. In the present study, EMP-1 was shown to be expressed in ovine ERM cells as well as PDLF despite this marker being associated with epithelial cells.

Interestingly, in addition to epithelial cell markers, we have shown that ERM cells demonstrate the protein expression of several MSC associated markers: CD29, CD44 and HSP90β. This is consistent with the previous report that Hertwig's Epithelial Root Sheath, as ancestors of ERM, expresses multiple types of cell markers associated with epithelial cells (amelogenin, cytokeratin and E-cadherin), cementoblasts/osteoblasts (bone sialoprotein and osteocalcin), mesenchymal cells (vimentin), and epithelial-mesenchymal transition-associated molecules (β-catenin and N-cadherin) [64].

CD29, also known as integrin β1, glycoprotein IIa, fibronectin receptor β polypeptide, very late activation protein β, has been reported to be the major adhesion receptor subfamily for human osteoblast-like cells to bind to a variety of extracellular matrix such as collagen, fibronectin and laminin [260]. A recent study has reported that the recruitment of human MSC to injured liver tissues occurred in a CD29 and CD44 manner [261]. The expression of CD29 (integrin β1) and fibronectin has been reported at a significant level in porcine ERM cells [231].

CD44 (the hyaluronic acid receptor), also known as hermes antigen, In (Lu)-related p80 glycoprotein, is a single-pass transmembrane protein identified as a lymphocyte homing receptor and a member of the cartilage link protein family [262], with different isoforms expressed in a cell-specific manner [263]. More than 30 isoforms of CD44 have been characterised, including the smallest, standard or hematopoietic form (CD44s or CD44H) [264], a variant form (CD44v), an epithelial cell form (CD44E) [263]. CD44 has been extensively studied owing to its essential functions in cell-cell, cell-matrix interactions, as well as in diseases [263] such as tumour metastasis [265] and chronic inflammatory diseases [266]. The isoforms containing exon v6 are believed to be highly correlated with tumour metastasis [267]. Recently, CD44 has been recognised as the common marker for

cancer initiating cells [262, 268, 269]. Moreover, CD44 also accounts for the homing and settlement of adult stem cells [262]. The *in situ* CD44 expression has been demonstrated in ERM cells of periapical lesions [270].

HSP90 is most studied among heat shock proteins, which are chaperone proteins involved in the folding and unfolding of other proteins. Recently, the utilization of HSP inhibitors led to the suppression of cellular signalling in several oncogenic pathways and thus HSP inhibitors have become promising candidates for anti-cancer therapies [271-274]. A recent study by Gronthos *et al* generated a novel monoclonal antibody, STRO-4, which recognises the cell surface protein HSP90β, as a prospective selection agent of ovine and human mesenchymal precursor cells with extensive proliferative potential and tri-potential differentiation capacity [201]. To the best of our knowledge, the present study is the first report of HSP90β expression on ERM cells.

A recent study reported the differentially expressed genes in porcine ERM and gingival epithelial cells using cDNA microarray analyses [225]. Of the significantly regulated genes, tissue factor/CD142 and FAT cadherin were also up-regulated at the protein level in ERM cells and were thus proposed as potential markers to distinguish ERM cells from gingival epithelial cells *in vitro*. Since the mesenchymal and epithelial populations are the two major components during tooth regeneration, the improvement of isolation and purification of ERM cells is a matter of considerable interest in order to understand the role of this subpopulation in tissue homeostasis. The ability to isolate ERM cells represents an important prerequisite for their further characterization. To optimize the selection techniques for ERM cells, the present proposal examined the potential cell surface makers specific for ERM cells which are not expressed in other PDL populations, such as PDLF. During this work the identification of specific surface markers to ovine ERM cells was

found to be difficult and challenging for two main reasons. Firstly, ERM cells were found to display a cell surface expression profile overlapping with PDLF despite their distinctive nature and origin. Of the panel of eight antigens discussed above, the expression of six markers was found to be commonly expressed between ERM and PDLF, with the exception of CK-8 and E-cadherin. Moreover, species differences are a challenge for antibody selection due to the availability of ovine antibodies. As most available antibodies are manufactured to be reactive against mouse or human antigens, the reactivity relies on whether the antibodies identify a conservative portion of the antigen. Other antibodies we have investigated include DJ18 (an antibody generated against Collagen type VI) [275] and EpCAM/CD326 (DAKO #M0804) which lacked any positivity to ovine cells or tissue, possibly due to the species difference as they are both mouse monoclonal anti-human antibodies. Other considerations involve the loss of surface antigens due to their sensitivity to trypsin digestion for flow cytometric analysis, where alternative dissociation reagents affect cell viability. Moreover, antigens that are not expressed on the cell surface membrane such as CK-8, or antibodies that are not manufactured based on the extracellular domain of the antigen, such as EMP-1, cannot be used for the isolation of living ERM cells using either fluorescence or magnetic activated cell sorting. In addition, cell surface protein expression profiles of different cell types undergo constant changes responding to the environment such as changes in culture conditions and different cell densities. For example, E-cadherin is a calcium-dependent glycoprotein. However, most serum-free medium for keratinocyte expansion is calcium-free or contains low calcium, which makes E-cadherin impractical to be used for FACS sorting.

A number of integrin subunits have been used for FACS sorting of various stem cell populations [185, 187, 189]. Integrins are integral cell-surface proteins composed of an alpha chain and a beta chain. There are 24 known integrin heterodimers comprising of one

of 18 alpha subunits with one of 8 beta subunits [276]. The binding ligands of each integrin subunit have been summarised [276]. Some integrins, such as integrin α6β1 and α6β4, bind to only one extracellular matrix, laminin, while others, such as integrin αvβ3, bind to multiple ligands such as collagen, fibronectin, laminin, vibronectin. [260]. Each subunit has a large extracellular domain and a short cytosolic domain, forming type I transmembrane glycoprotein [277]. Some integrin subunits, such as integrin β1, are expressed extensively in most tissues, while others are expressed in specific tissues. Integrins play important roles in the communication between the cytoplasm and the extracellular space, as well as cell adhesion and cell-surface mediated signalling [276]. The knockout model allows the examination of the specific role of integrin subunits. The absence of ubiquitously expressed subunits, such as integrin β1, leads to inner cell mass deficiencies and failure to implant [278]. The deletion of integrin subunits specific to certain tissue types, such as α6, results in the dysfunction of the corresponding tissues.

The alpha 6 integrin subunit, also known as CD49f or VLA-6, may either combine in the heterodimer with beta 4 subunit to form tumour-associated antigen (TSP) 180 (in epithelial cells), or with beta 1 as VLA-6 (in many cell types). The capability of alpha 6 to associate with multiple beta subunits is unusual because most of the known integrin alpha subunits only associate with one type of beta subunit, except alpha 6, alpha 4 and alpha V [279, 280]. Integrin α6β4 is expressed predominantly on the basal surface of most epithelia [245], with its involvement in hemidesmosome organization well-documented [281, 282]. Knockdown studies have shown that integrin α6β4 is critical in maintaining epidermis integrity and resistance to mechanical stress [281], with no other integrins compensating for the loss of this heterodimer [282]. Damaged barrier functions of epidermis due to lack of integrin α6β4 normally lead to death shortly post-birth with extensive detachment of the epidermis [281], which underscores the significance of integrin α6β4 in the maintenance of

epithelia integrity [245]. In addition to the findings mentioned above, it has also been reported that integrin α6β4 plays a critical role in the migration of epithelia [283, 284] and carcinoma cells [285, 286]. This highlights its important roles in would healing and carcinoma invasion [245]. Moreover, another study highlighted the essential role of integrin-laminin interactions in the proper development of the nervous system [287]. As integrins α6β1 and α6β4 are major laminin receptors and laminin is one of the extracellular matrix proteins expressed in neural tissues, the knockout of laminin receptor α6 leads to abnormalities in the laminar organization of the developing cerebral cortex and retina [287].

The integrin expression profiles in human ESC, MSC, haematopoietic stem cells (HSC) and neural stem cells (NSC) have been summarised [276]. Integrin α6 expression was reported in undifferentiated human ESC [288] and HSC (or $CD34^+$ haematopoietic progenitors) [289]. α6 expression has also been reported to be either present or absent in MSC in different publications [290], as variation of integrin expression has been reported for MSC-like populations originating from different tissues [276]. The cell surface expression of integrin α6 on NSC has been demonstrated to be involved in the migration of NSC on laminin (possibly *via* α6β1) [291]. The majority of the colony-forming-unit (CFU) population from normal bone marrow aspirates were shown to express integrin α6β1 [292]. The combination of the functional blocking antibodies of anti-α1β1, -α2β1 and -α6β1 led to the significant reduction of the number of CFU on laminin pre-coated plates [292]. Interestingly, integrin α6β1 was expressed by stromal progenitor cells but not expressed by osteoblast-like cells, suggesting a correlation of integrin α6β1 expression and the immature state of precursor cells [260, 293, 294]. Furthermore, the altered integrin α6 subunit expression has been reported in stem cells undergoing differentiation. For example, the expression of α6 was down-regulated upon the differentiation of human ESC toward

endoderm [295] and cardiomyocyte [296]. This suggests that it may be essential to alter the extracellular matrix constitution to differentiate stem cells to the desirable cell lineages [276].

Based on the differential expression of integrin $\alpha_6$/CD49f in ERM and PDLF, immunomagnetic bead selection was used in the present study to determine the efficiency for the enrichment of ERM cells according to their expression of integrin α6/CD49f, as previously performed for the isolation of DPSC [193]. Our data clearly demonstrated that the integrin α6/CD49f selection resulted in a considerable enrichment of ERM cells compared with the integrin $\alpha_6$/CD49f-negative and unfractionated cell fractions (greater than 50- or 7-fold colony forming efficiency, respectively), using freshly isolated single periodontal ligament cell suspensions. Immunoprecipitation experiments in future studies would help elucidate the binding subunit of α6 in ERM cells (either β1 or β4) to identify different potential binding ligands. This could help optimize future *in vitro* culture conditions by pre-coating the culture flasks with the corresponding ligand for selective attachment of ERM cell populations.

It should be noted that, other than the enrichment of ERM cells using the cell surface expression of integrin $\alpha_6$/CD49f, other cell sorting strategies based on cell size [297-299] or cytokine profiling [121, 300-303] deserve future investigation. For example, MSC distributed in low forward scatter and low side scatter in FACS analysis exhibited 90% clonogenicity that could be differentiated into osteoblasts or adipocyte [297-299]. This physical separation based on cell size is a practical way to manipulate stem cells for clinical therapeutic applications.

As ERM cells co-habitate with periodontal ligament stem cells, it is critical to remove any

possible contamination of periodontal ligament stem cells. Firstly, stringent selective enzymatic digestion using trypsin was performed for the isolation of ERM cells. Secondly, serum-free keratinocyte medium (OKM) favouring epithelial over mesenchymal cell growth was used, whereas previous studies have shown that mesenchymal cells struggle to survive in the presence of keratinocyte medium [64, 243, 244]. We found that few periodontal ligament stem cells were capable of surviving in OKM, which subsequently appeared to lose the capacity to proliferate. Phenotypically, the sporadic periodontal ligament stem cells identified in these cultures expressed mesenchymal markers, CD44, CD29 and HSP-90β but lacked the expression of epithelial markers cytokeratin-8 and integrin α6/CD49f. These studies indicated that periodontal ligament stem cells were unable to undergo mesenchymal epithelial transition when grown under keratinocyte culture conditions. Thirdly, any possible contamination of periodontal ligament stem cells has been minimized by using fluorescence activated cell sorting to isolate integrin α6/CD49f high expressing epithelial cells following *ex vivo* expansion.

In this chapter, ERM cells were isolated from ovine periodontal ligament tissue and their immunophenotype was investigated. The ability to isolate ERM cells represents an important prerequisite for their further characterization. Importantly, integrin α6/CD49f could be used for the enrichment of clonogenic epithelial cell clusters (colony-forming units-epithelial cells [CFU-Epi]). Interestingly, e*x vivo*-expanded ERM expressed both epithelial and mesenchymal stromal/stem cell-associated markers. These observations led us to examine whether ERM cells exhibit mesenchymal stromal/stem cell-like properties under specific conditions. This study provides the basis for further characterization of ovine ERM cells in Chapter 4.

# Chapter 4. Multilineage differentiation potential of ERM cells *in vitro* and *in vivo*

## 4.1 Introduction

### *4.1.1 Mineral-forming capacities of ERM cells in vitro and in vivo*

While Hertwig's Epithelial Root Sheath (HERS) plays a pivotal role in tooth root development, the role of ERM cells in the adult periodontium remains unknown. A growing body of evidence has demonstrated that ERM cells express some bone/cementum-related markers despite their epithelial nature. Notably, ERM cells have been reported to express a significant amount of osteopontin (OPN) mRNA in several studies [95-97, 238]. Furthermore, ERM express transcripts for bone-related proteins and enamel matrix proteins including alkaline phosphatase (ALP) [96, 238], osteonectin/secreted protein, acidic and rich in cysteine (SPARC), osteoprotegerin (OPG), bone morphogenetic protein (BMP)-2, BMP-4 [95], amelogenin [238] and tuftelin [95]. The expression of osteocalcin and bone sialoprotein was not detected in human [238] and porcine ERM cells [97].

Considering the expression of bone-related markers by ERM cells, it is not surprising that they form mineral nodules when subjected to osteogenic inductive culture conditions. Human HERS cells have been reported to form mineralized matrix when cultured for 28 days under osteogenic inductive conditions containing L-ascorbate-2-phosphate, dexamethasone and inorganic phosphate [64], although in a separate study no Von Kossa positive mineral nodules were formed by porcine ERM cells cultured in osteogenic inductive conditions for 14 days in a dexamethasone and β-glycerophosphate-based mineralization conditions [97]. The discrepancy of these two studies might be due to the different formulations of mineralization media and different culture periods (28 days versus 14 days). The osteogenic potential of ERM cells has also been reported using an *in vivo* experimental root resorption model, where ERM cells were identified adjacent to root

resorption lacunae and found to be immunoreactive to bone-related markers such as BMP-2, OPN and ameloblastin [94]. Hence, it has been proposed that ERM cells may be involved in early cementum repair [94]. In a recent study that focused on the mineralization capacities of human HERS cells in the presence of TGF-β (an epithelial mesenchymal transition inducer), HERS cells treated with TGF-β generated cementum-like tissues when transplanted into non-obese diabetic-severe combined immunodeficient (NOD/SCID) mice [64]. While this study demonstrated the effect of TGF-β on human HERS in a mouse transplantation model [64], to our knowledge, there has been no report on the *in vivo* mineralization potential of HERS/ERM cells alone.

### 4.1.2 Epithelial-mesenchymal-interactions during tooth development and regeneration

A number of studies have highlighted the important role of epithelial-mesenchymal-interactions during tooth development. The combination of tooth germ-derived epithelial and mesenchymal single cells give rise to successfully reconstituted tooth germ *in vitro*, while epithelial or mesenchymal cells alone generated keratinized oral epithelium-like structures or bone, respectively. When transplanted into subrenal capsules or tooth cavity, this tooth germ could generate incisors with tooth elements arranged appropriately akin to a natural tooth [157, 158]. More recently, a bioengineered tooth unit comprising mature tooth, periodontal ligament and alveolar bone was generated in subrenal capsules and transplanted into edentulous sites *in vivo*. This transplantation not only restored tooth function but also re-established the lost bone volume both vertically and horizontally [159]. These studies highlight that both epithelial and mesenchymal populations are essential components involved in tooth development.

It has been proposed that periodontal regeneration is a re-enactment of periodontal development [82]. As the interactions of epithelial and mesenchymal cells play pivotal roles during tooth development, the combination of HERS/ERM with dental MSC has

been used for periodontal regeneration [160, 162, 236]. In combination with dental pulp cells, porcine ERM can differentiate into ameloblast-like cells and generate enamel-like tissues *in vivo*, where positive amelogenin staining was observed [162]. Co-culture of dental follicle (DF) and HERS cells has been shown to increase bone/cementum related gene expression as well as *in vitro* mineral nodule formation compared to DF cells alone. Moreover, when transplanted into rat omenta, DF cells pre-exposed to HERS gave rise to cementum-like and PDL-like structures, while DF cells alone only produced fibrous tissues [160]. Collectively, these data suggest that the introduction of HERS/ERM cells may improve the outcomes of periodontal regeneration.

### 4.1.3 Epithelial mesenchymal transition

Epithelial mesenchymal transition (EMT) is the process by which epithelial cells lose their epithelial traits and acquire mesenchymal cell properties. EMT happens as early as the gastrulation stage and in late developmental stages such as the formation of neural crest tissue [304]. During development, EMT occurs transiently followed by its reversal, mesenchymal epithelial transition, to give rise to structures such as kidney, gut, lung and skin [305]. In addition, EMT plays a central role in epithelial plasticity [306] and contributes to disease states such as fibrosis and tumour progression/metastasis [304, 305, 307-311] [312].

During EMT, a cascade of events occurs at the cellular and molecular levels, induced by a variety of signals including the exposure to certain cytokines and chemokines, such as TGF-β1, that induce the expression of transcription factors, such as the Twist or Snail family members [307]. At the cellular level, EMT causes significant changes in cell behaviour and physiology, including the disruption of cell junctions, changes in cell shape and polarity, the expression of new adhesion molecules and migration of cells through

basal lamina [311]. At the molecular level, EMT typically involves the switch in cell membrane cadherin from E-cadherin to N-cadherin, which is associated with the up-regulation of Snail [313]. Snail 1 and Snail 2 (Slug) are strong repressors of E-cadherin transcription, where the well-known EMT inducer, TGF-β1, has been reported to partially act through Snail [314]. Using a function-perturbing antibody, the role of E-cadherin during mouse gastrulation was investigated [315]. The data showed that the disruption of E-cadherin allowed epiblast cells to adopt a mesenchymal morphology with mesoderm cell-like properties including the expression of vimentin, the loss of cell-cell contact and increased migration [315], indicating that the blocking of E-cadherin was sufficient to induce EMT. In addition, the EMT induced by the loss of E-cadherin was found to be irreversible [315]. Other molecular changes during EMT include the elevation of the transcriptional regulators, Zinc finger E-box-binding homeobox (Zeb1), Zeb 2 and Twist [304, 316]. Of note, Twist is a conserved basic helix-loop-helix (bHLH) containing transcription factor which is known to be critical in mesodermal development, where many of the Twist functions are regulated by Snail 1 [311].

Two recent studies provide evidence that HERS, from which ERM cells are derived, exhibits the capacity to undergo EMT in the presence of TGF-β1 [64, 233]. A human study has reported that HERS not only controls periodontal ligament stem cell differentiation but also gives rise to cementum-like tissues *in vitro* and *in vivo* through EMT following TGF-β1 treatment [64]. It has been proposed that HERS cells may undergo EMT following tooth development and potentially contribute to the mesenchymal cell populations in the periodontium [11]. For example, HERS cells that remain on the root surface assume the morphology of cementoblasts, which can be explained by a phenotypic conversion of EMT [9]. Collectively, these studies lend support to the idea that HERS may directly give rise to cementoblasts through EMT [23].

### *4.1.4 Multilineage differentiation potential of ERM cells in vitro and in vivo*

Data from the initial characterization of ovine ERM cells in Chapter 3 demonstrated that *ex vivo*-expanded ERM cells expressed epithelial (CK-8, E-cadherin and EMP-1) and MSC associated markers (CD44, CD29 and HSP90β). This led us to investigate whether ERM cells exhibited MSC-like properties under specific inductive conditions. It has recently been reported that human ERM cells derived from HERS express embryonic stem cell associated markers such as Oct-4, Nanog and SSEA-4, providing circumstantial evidence for the stem cell nature of ERM cells [237]. Previous studies have focused on the roles of HERS/ERM cells on the induction and differentiation of dental derived MSC-like populations, however, to our knowledge there have been no studies to date examining the multi-lineage differentiation potential of ERM cells both *in vitro* and *in vivo*. Determining the capacity of ERM cells to undergo EMT and differentiate into multiple periodontal tissues would greatly enhance our understanding of the role of ERM cells in adult periodontium, in particular whether ERM cells contribute to periodontal regeneration and repair.

The present study examined the *in vitro* differentiation capacity of ERM cells into three lineages of mesoderm origin: osteocytes/cementocytes, adipocytes and chondrocytes, as well as neuron-like cells, a lineage of ectoderm origin. In parallel experiments, the osteogenic, adipogenic and chondrogenic differentiation potential of PDLF was investigated as a positive control. The *in vivo* potential of ERM cells to form periodontal tissues was determined by transplanting ERM cells subcutaneously into immunodeficient NOD/SCID mice seeded into an osteoconductive carrier material. Furthermore, experiments were conducted to determine whether the osteogenic induction of ERM cells induced an EMT by assessing the gene expression levels of EMT-associated markers using

RT-PCR. Unless mentioned otherwise, three independent donors were examined in these experiments.

## 4.2 Results

### *4.2.1 Multilineage differentiation potential of ERM cells in vitro*

#### *4.2.1.1 Mineralization differentiation potential of ERM cells*

The potential of ovine ERM cells and control PDLF from the same donor animals to undergo mineralization differentiation *in vitro* was examined in the presence of media supplemented with dexamethasone, ascorbate and inorganic phosphate [139]. After four weeks of osteogenic induction, cells from all three ERM donors examined produced Alizarin Red stained mineralized nodules akin to PDLF cultures (Figure 4.1A). The differentiation capacity of ERM cells from three donors following culture in osteogenic condition was confirmed by quantitative analysis of extracellular matrix calcium concentration compared to non-induced control cultures ($n$=3) (Figure 4.1B). The data represent the mean values ± standard deviations of triplicate experiments normalized to the DNA content. Statistical significance of (*) of $p<0.05$ was determined by the unpaired $t$-test.

These results were confirmed using RT-PCR to investigate the mRNA expression of various mineral-related markers. As extensive collagen matrix was deposited under the osteogenic conditions, it was very hard to harvest single cells for RNA collection. To circumvent this, the combination of collagenase and dispase was used to break up the extracellular matrix and scraping was applied before and after trypsin treatment, respectively. When ERM cells were cultured under osteogenic inductive conditions, a significant increase in mRNA expression levels was observed for markers associated with cemento/osteogenesis, including Runx2, OPN and bone sialoprotein (BSP-II) compared to non-induced control cultures ($n$=3) (Figure 4.1C). The data represent the mean values ±

standard error of the mean (SEM) of triplicate experiments normalized to the house keeping β-actin gene. Statistical significance of (*) of $p<0.05$ was determined by the unpaired *t*-test.

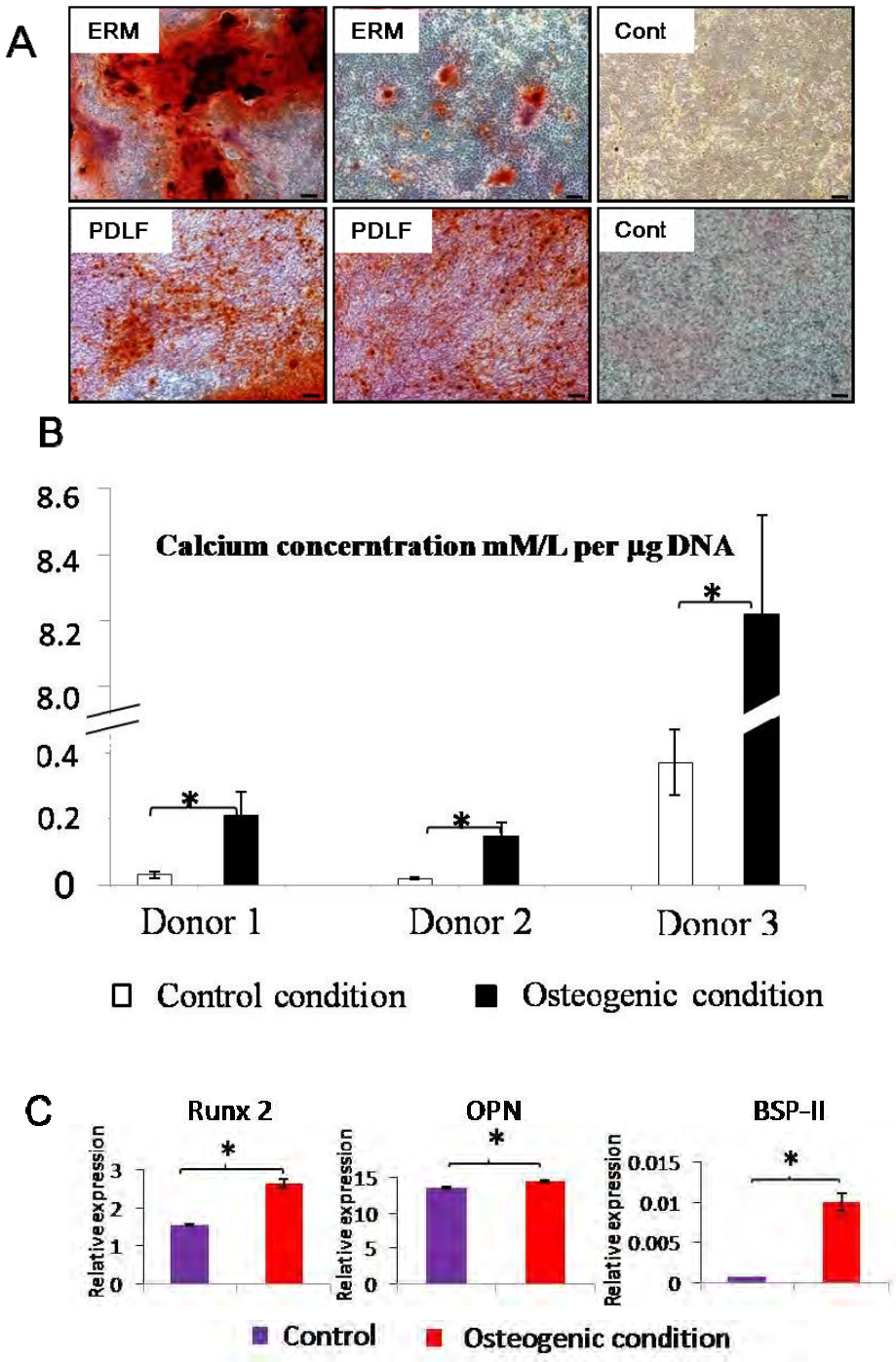


**Figure 4.1 Osteogenic differentiation potential of ERM cells *in vitro***

(A) Alizarin Red Staining of mineralized deposits formed by ERM cells (ERM) and periodontal ligament fibroblasts (PDLF) in osteogenic media and in control media (Cont). Scale bar=50 µm. (B) Quantitative analysis of extracellular matrix calcium concentration following ERM culture in osteogenic condition compared to non-induced control cultures ($n$=3). The data represent the mean values ± standard deviations of triplicate experiments normalized to the DNA content. Statistical significance of $p \leq 0.05$ (*) was determined using an unpaired Student $t$-test.. (C) Real time PCR analysis for markers of osteogenesis, including Runx2, OPN and bone sialoprotein (BSP-II) in ERM cells cultured in osteogenic and control condition. The data represent the mean values ± standard error of the mean (SEM) of triplicate experiments normalized to the house keeping β-actin gene. Statistical significance of $p \leq 0.05$ (*) was determined using an unpaired Student $t$-test.

#### *4.2.1.2 Adipogenic differentiation potential of ERM cells*

Similar studies were conducted to examine the adipogenic potential of ERM cells and corresponding control PDLF populations. After four weeks of adipogenic induction supplemented with hydrocortisone, indomethacin and IBMX, ERM cells developed into Oil Red O positive lipid-containing adipocytes, similar to that observed for PDLF (Figure 4.2A). Confirmatory quantitative analysis demonstrated increased levels of triglyceride present in ERM cells under adipogenic conditions in comparison to those in non-induced control cultures ($n$=3) (Figure 4.2B). The data represent the mean values ± standard deviations of triplicate experiments normalized to the DNA content. Statistical significance of (*) of $p<0.05$ was determined by the unpaired $t$-test.

Adipogenic differentiation potential of ERM cells was further confirmed by elevated levels of mRNA expression of adipogenic-associated markers, leptin and perixosome proliferator-activated receptor gamma 2 (PPARγ2), a key transcription factor involved in the regulation of adipogenesis, under adipogenic inductive conditions compared to non-induced control cultures ($n$=3) (Figure 4.2C). The data represent the mean values ± standard error of the mean (SEM) of triplicate experiments normalized to the house keeping β-actin gene. Statistical significance of (*) of $p<0.05$ was determined by the unpaired $t$-test.

#### *4.2.1.3 Chondrogenic differentiation potential of ERM cells*

The chondrogenic potential of ERM cells and control PDLF was studied following culture in three-dimensional cell aggregates in the presence of TGF-β3, bovine serum albumin, dexamethasone and ITS+Premix. Whilst PDLF formed one tightly compact pellet, the chondrocyte pellets of ERM cells were less compact and formed a number of smaller aggregates (data not shown). Sections of chondrocyte pellets were stained with H&E (Figure 4.3A) and toluidine blue (Figure 4.3B). Immunohistochemical staining showed that

chondrocyte pellets were comprised of type II collagen (Figure 4.3C). Isotype matched controls were used to demonstrate levels of non-specific antibody binding (Figure 4.3D).

These findings were associated with an elevated mRNA expression of chondrocyte-associated markers, type II collagen, aggrecan, type X collagen and the master chondrogenic transcriptional regulator Sox9 (Figure 4.3E) ($n$=3) at week three of chondrogenic cultures in comparison to non-induced control cultures, shown by real time RT-PCR. The data represent the mean values ± standard error of the mean (SEM) of triplicate experiments normalized to the house keeping β-actin gene. Statistical significance of (*) of $p<0.05$ was determined by the unpaired $t$-test.

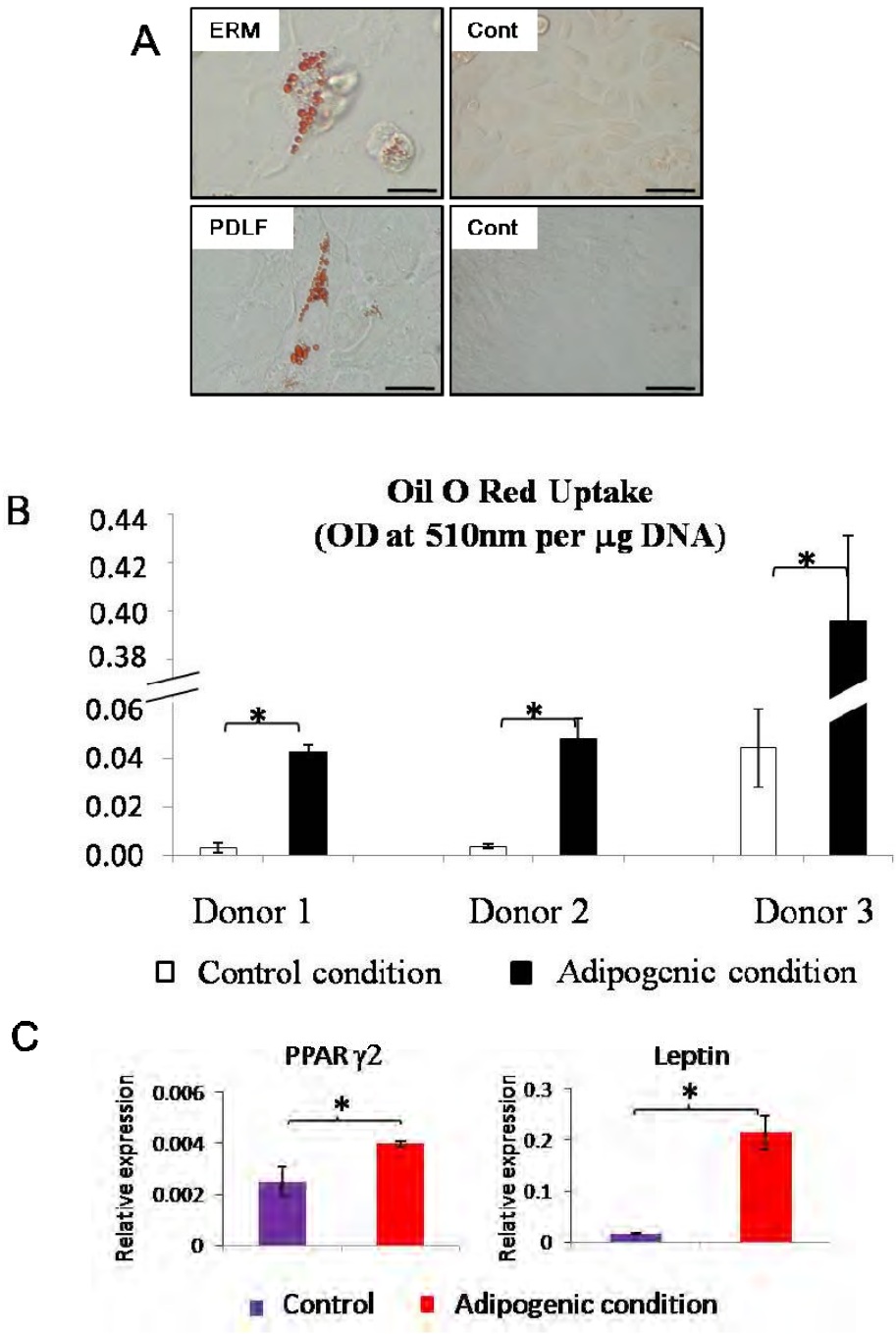


**Figure 4.2 Adipogenic differentiation potential of ERM cells *in vitro***

(A) Oil Red O Staining for lipid formation by ERM cells (ERM) and periodontal ligament fibroblasts (PDLF) in adipogenic media and in control media (Cont). Scale bar=50 µm. (B) Increased levels of triglyceride present in ERM cells under adipogenic conditions in comparison to those in non-induced control cultures ($n$=3). The data represent the mean values ± standard deviations of triplicate experiments normalized to the DNA content. Statistical significance of $p \leq 0.05$ (*) was determined using an unpaired Student $t$-test.. (C) Real time PCR analysis for markers of adipogenesis, including peroxisome proliferator activated receptor-γ2 (PPARγ2) and leptin in ERM cells cultured in adipogenic and control condition. The data represent the mean values ± standard error of the mean (SEM) of triplicate experiments normalized to the house keeping β-actin gene. Statistical significance of $p \leq 0.05$ (*) was determined using an unpaired Student $t$-test.

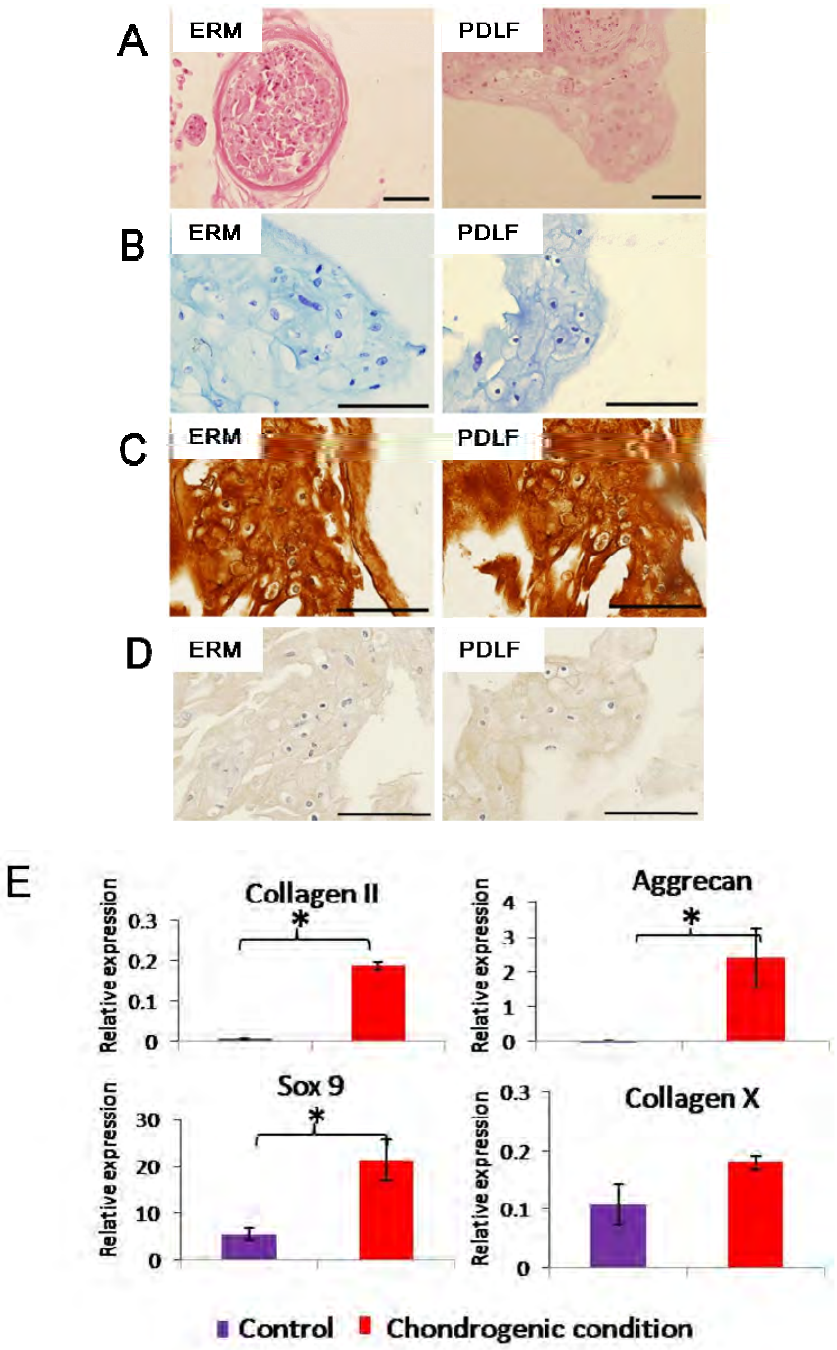


**Figure 4.3 Chondrogenic differentiation potential of ERM cells *in vitro***

Chondrogenic differentiation of ERM cells (ERM) and periodontal ligament fibroblasts (PDLF) (A) hematoxylin and eosin (H&E) staining, (B) toluidine blue staining and (C) immunohistochemical staining with anti-collagen type II antibody. (D) Isotype matched controls demonstrated levels of non-specific antibody binding. (E) Real time PCR analysis for expression of chondrocyte markers: type II collagen, aggrecan, Sox9 and type X collagen in ERM cells cultured in chondrogenic and control condition. The data represent the mean values ± standard error of the mean (SEM) of triplicate experiments normalized to the house keeping β-actin gene. Statistical significance of $p \leq 0.05$ (*) was determined using an unpaired Student *t*-test. Scale bar=50 µm

#### *4.2.1.4 Multilineage differentiation potential of clonal ERM cell populations in vitro*

To verify the stem cell-like properties of ERM cells, multi-lineage differentiation assays were performed at the clonal level. Individual colonies were isolated using cloning rings, expanded and subjected to multi-differentiation analyses. All of the clones assessed (7/7) produced Alizarin Red stained mineralized nodules and chondrocyte pellets showing positivity to anti-collagen type II antibody, while 43% of the clones (3/7) exhibited adipogenic differentiation potential, illustrated by the formation of Oil Red O positive lipid (Table 4.1). The tri-differentiation potential of three clones is shown in Figure 4.4. Taken together, these findings indicated that a subpopulation of ERM cells have the potential to differentiate into three major mesodermal lineages, mineral, fat and cartilage.

**Table 4.1 Multilineage differentiation potential of ERM cells at the clonal level**

| The number of clones studied | The number of clones formed mineral nodules | The number of clones formed adipocytes | The number of clones formed chondrocytes |
|---|---|---|---|
| 7 | 7 | 3 | 7 |

#### *4.2.1.5 Neuronal differentiation potential of ERM cells by exogenous growth factors*

Studies were performed to determine whether ERM cells could give rise to ectoderm derived neural cells under neurogenic inductive conditions previously described for dental pulp stem cells (DPSC) [141] and PDLSC [317]. The major components of the neuroinductive conditions included EGF, FGF and retinoic acid (RA) in either Neurobasal A media or DMEM/F12 media. In the first week, while DPSC displayed growth arrest in Neurobasal A media (data not shown), ERM cells proliferated extensively and formed multi-layer in some cultures (Figure 4.5A). Some cells gained morphological changes three days post neurogenic induction, becoming long and thin with some processes (Figure 4.5B), in contrast to the typical cobblestone shape of ERM cells in control conditions (Figure 4.5F). Network of neuritis developed on top of basal cells (Figure 4.5C). After three weeks of neuronal induction, a subpopulation of ERM cells developed to neuron-like

cells (Figure 4.5D,E), compared to the typical cobblestone morphology of non-induced cells (Figure 4.5F).

After three weeks of neurogenic induction, ERM cells were enzymatically digested and replated for immunocytochemistry where they exhibited a neuron-like morphology (Figure 4.6Ai-iii). Immunocytochemical analysis demonstrated that ERM cells cultured in neurogenic conditions expressed various neural-associated markers including neuronal markers, Nestin (Figure 4.6Bi), Neurofilament protein-heavy chain (NF-H) (Figure 4.6Bii), Neuronal marker protein gene product 9.5 (PGP 9.5) (Figure 4.6Biii), Tau (Figure 4.6Biv), and Glial and Schwann cell marker, Glial Fibrillary Acidic Protein (GFAP) (Figure 4.6Bv). Isotype matched controls were used to demonstrate levels of non-specific antibody binding (Figure 4.6 Bvi).

Real-time RT-PCR analysis demonstrated an up-regulation of the intermediate neural marker, β-III tubulin, which correlated to the down-regulation of the neuronal stem cell marker, nestin in comparison to those in non-induced control cultures ($n$=3) (Figure 4.6C). The data represent the mean values ± standard error of the mean (SEM) of triplicate experiments normalized to the house keeping β-actin gene. Statistical significance of (*) of $p<0.05$ was determined by the unpaired $t$-test. Collectively, these findings indicated that neurogenic induction of ERM cells resulted in a neuronal-like morphology and the expression of neuron-specific proteins as well as the regulation of neuron-associated mRNA expression.

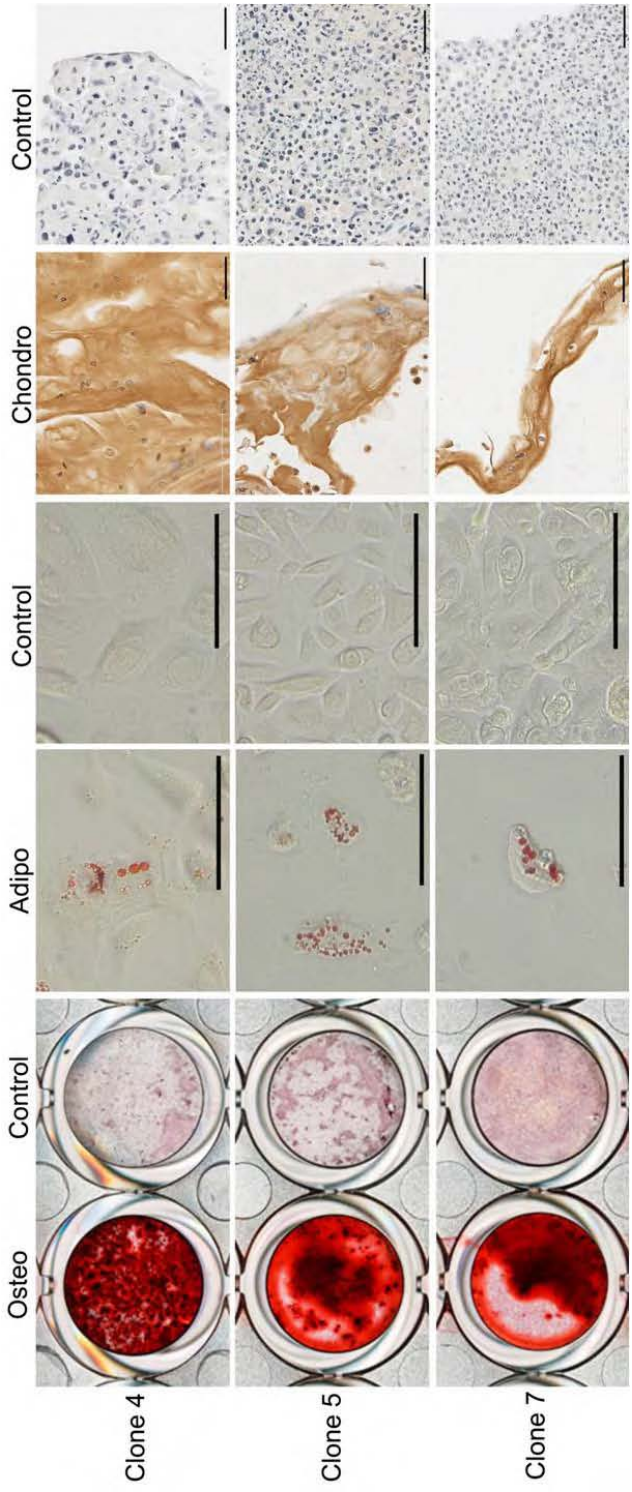


**Figure 4.4 Multilineage differentiation potential of ERM cells at the clonal level.**

All of the ERM clones (7/7) tested showed the potential to form mineral and cartilage, and 3 out of 7 ERM clones exhibited the capacity to form fat lipid. Alizarin Red and Oil Red O Staining of 3 tri-potential clones cultured under osteogenic (Osteo), adipogenic (Adipo) and control conditions identified the presence of mineral nodules and fat lipid, respectively. Chondrogenic (Chondro) differentiation potential of 3 tri-potential clones was assessed by immunohistochemical staining with anti-collagen type II antibody. Isotype matched control was used to determine the level of non-specific antibody binding. Scale bar=50 μm

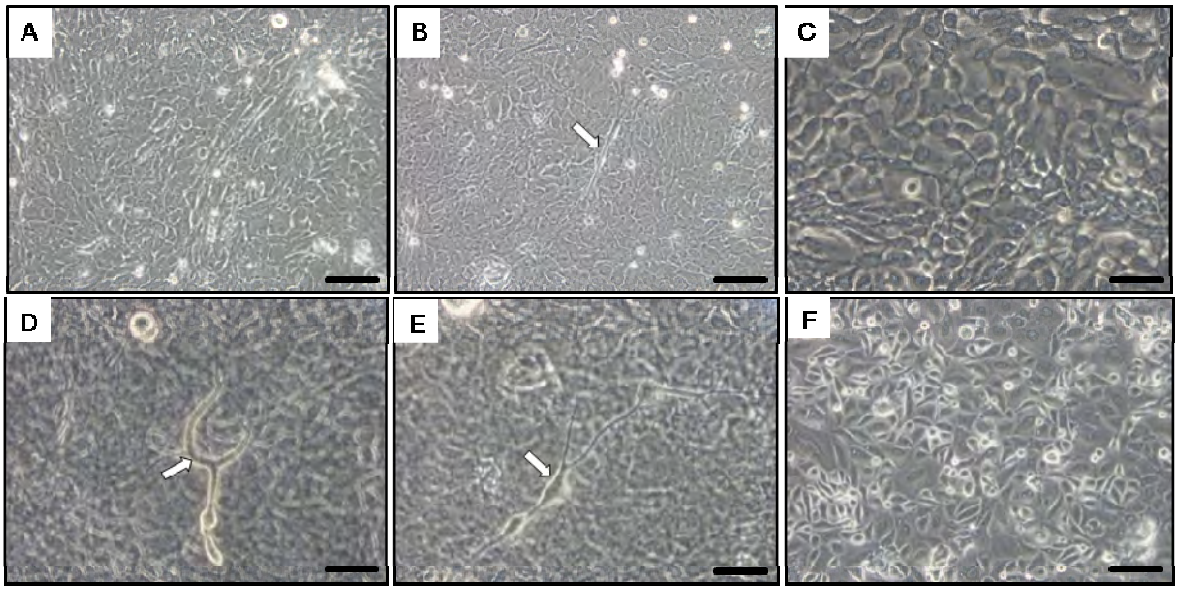


**Figure 4.5 Morphologically ERM cells became neuron-like cells in neurogenic conditions**

In the first week, ERM cells proliferated extensively and formed multi-layer in some cultures (A). Some cells gained morphological changes 3 days post neurogenic induction, becoming long and thin with some processes (B, arrow), in contrast to the typical cobblestone shape of ERM cells in control conditions (F). In the second week, network of neuritis developed on top of basal cells (C). After 3 weeks of neuronal induction, a subpopulation of ERM cells developed to neuron-like cells (D,E, arrows), compared to the typical cobblestone morphology of non-induced cells (F). Scale bar=50 µm

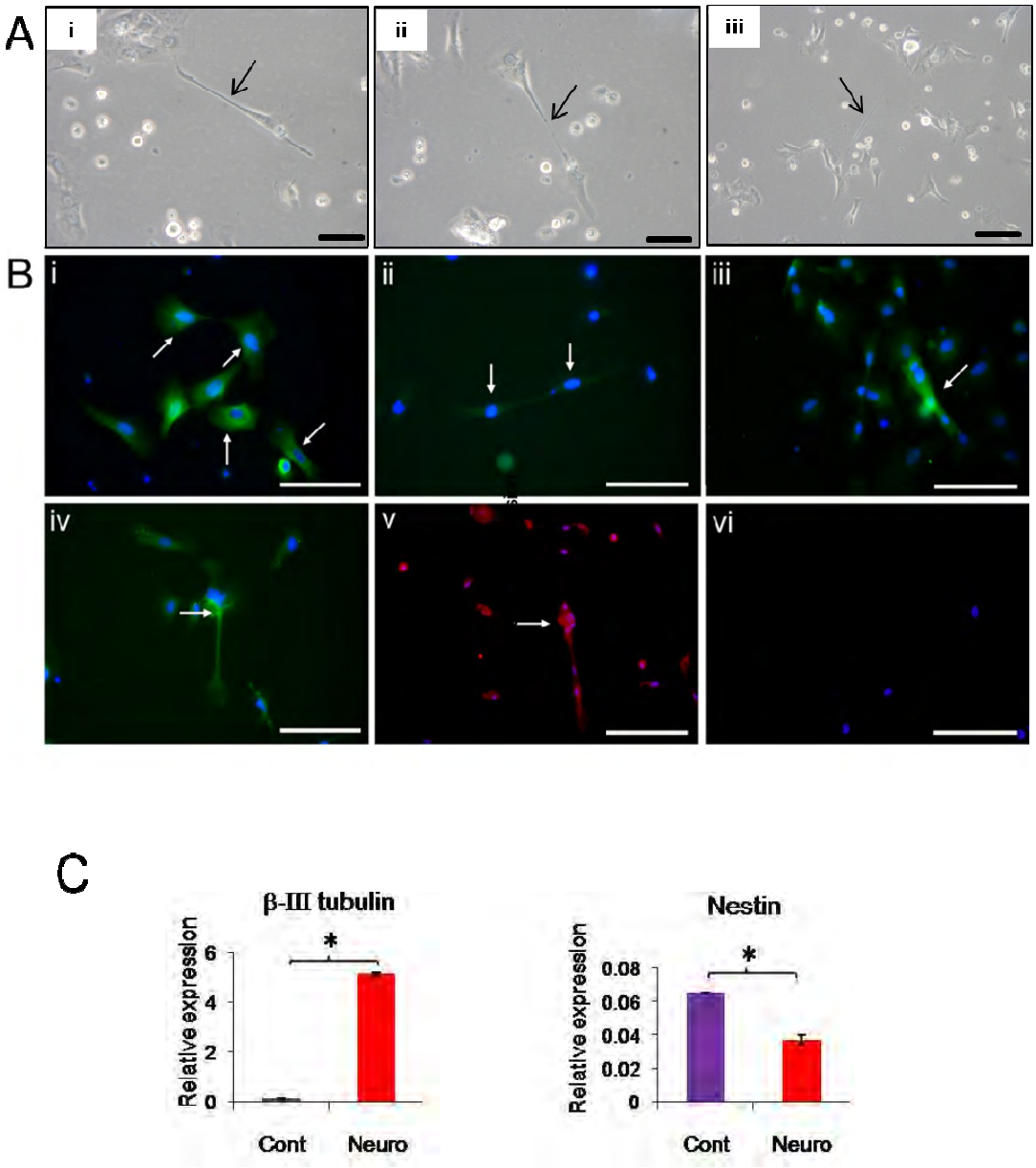


**Figure 4.6 Neurogenic potential of ERM cells *in vitro***

(A) To get monolayer for immunocytochemistry, ERM cells were trypsinized and replated post 3-week neurogenic induction. Attached cells exhibited neuron-like morphology (i-iii, arrows).
(B) Immunocytochemical identification of neuron-associated markers for ERM cells in neurogenic conditions: neuronal markers [Nestin (i, arrows), Neurofilament protein-heavy chain (NF-H) (ii, arrows), Neuronal marker protein gene product 9.5 (PGP 9.5) (iii, arrow) and Tau (iv, arrow)] and Glial and Schwann cell marker, Glial Fibrillary Acidic Protein (GFAP) (v, arrow). Isotype matched controls were used to determine the level of non-specific antibody binding (vi).
(C) Real-time RT-PCR analysis for the intermediate neural marker, β-III tubulin and Nestin in ERM cells cultured in neurogenic (Neuro) and control (Cont) conditions. The data represent the mean values ± standard error of the mean (SEM) of triplicate experiments normalized to the house keeping β-actin gene. Statistical significance of $p \leq 0.05$ (*) was determined using an unpaired Student *t*-test. Scale bar=50 µm

### *4.2.2 Ex vivo-expanded ERM cells can generate bone, cementum-like tissue and Sharpey's fibre-like structures in vivo*

The high expressing integrin $\alpha_6$/CD49f positive cell fraction from ERM cultures of three donors (brightest 30%) was selected using fluorescence activated cell sorting (Figure 4.7). To examine the osteo/cementogenic potential of ERM cells *in vivo*, $5x10^6$ integrin $\alpha_6$/CD49f-positive ERM cells (*n*=5 donors) were transplanted subcutaneously with HA/TCP particles into the dorsal surface of NOD/SCID mice. After eight weeks, ERM cells generated mineralized bone structures which contained encapsulated osteocytes and lined with osteoblast-like cells at the surface of the HA/TCP particles in all 5 transplants (Figure 4.8A,B). In addition to the mineralized bone structures, another type of mineral was generated (Figure 4.8C,D). Sharpey's fibre-like structures were observed in 2 of 5 transplants (Figure 4.8E,F). Furthermore, thin layers of cementum-like structures formed in 3 of 5 transplants (Figure 4.8G,H).

An anti-CD44 ovine antibody, which does not react with murine tissue, was used to investigate whether the mineral formation was derived from ERM cells or endogenous murine osteoprogenitor cells. Immunohistochemical staining showed that ERM cells which had differentiated into osteocytes and osteoblasts were stained positive for ovine anti-CD44 antibody (Figure 4.9A,B). These CD44 positive ERM cells were also identified around blood vessels (Figure 4.9C,D), indicating that ERM cells were able to home to the perivascular stem cell niche as previously described for BMSSC, DPSC and PDLSC [144, 193]. Furthermore, an anti-cytokeratin-8 (CK-8) antibody was used to determine whether ERM cells maintained epithelial features during the mineral forming process. Interestingly, ERM cells that had differentiated into osteoblasts remained positive for CK-8, while those that had differentiated into osteocytes lacked CK-8 expression (Figure 4.9E,F). The co-localization of CD44 and osteocalcin antigens in osteocytes and bone-lining cells was demonstrated on the same area in serial sections (Figure 4.9G,H). Isotype matched controls

were used to demonstrate levels of non-specific antibody binding (Figure 4.9I)

### 4.2.3 ERM undergo epithelial-mesenchymal transition during osteogenic induction

To examine whether ERM cells were capable of undergoing EMT, various epithelial, mesenchymal and EMT markers were measured by real-time RT-PCR following osteogenic induction after 1, 2, 3 and 4 weeks. ERM cells showed a decline of the expression of epithelial markers, cytokeratin-8, cytokeratin-14 and E-cadherin over the time course (Figure 4.10A), which correlated to an up-regulation in gene expression of mesenchymal-associated markers, fibronectin and N-cadherin (Figure 4.10B). However, the expression level of a major cytoskeletal component of mesenchymal cells, vimentin, was down-regulated during osteogenic induction (Figure 4.10B). Moreover, ERM cells expressed high levels of various transcription factors known to regulate EMT during embryogenesis and in different cancers, such as Twist, Zinc finger E-box-binding homeobox 1 (ZEB 1), ZEB 2 and SNAI 1 (Figure 4.10C). The data represent the mean values ± standard error of the mean (SEM) of triplicate experiments normalized to the house keeping β-actin gene. Statistical significance of (*) of $p<0.05$ was determined by the unpaired *t*-test.

### 4.2.4 Survival of PDLSC in oral keratinocyte media (OKM) and subsequent mesenchymal epithelial transition

As PDLSC co-habitate with ERM cells, it is important to demonstrate that there is no contamination of PDLSC in the ERM bulk cultures. Few PDLSC were capable of surviving in the epithelial growth medium, OKM, where the remaining cells appeared to lose their capacity to proliferate (Figure 4.11). Phenotypically, the sporadic PDLSC identified in these cultures expressed mesenchymal markers, CD44, CD29 and HSP90β but lacked the expression of epithelial markers cytokeratin-8 and integrin α6/CD49f (Figure 4.11). These phenotypes are akin to that of PDLSC in Minimal Essential Media (MEM)-

based complete media (Figure 4.11), indicating that PDLSC are unable to readily undergo mesenchymal epithelial transition when grown under keratinocyte culture conditions.

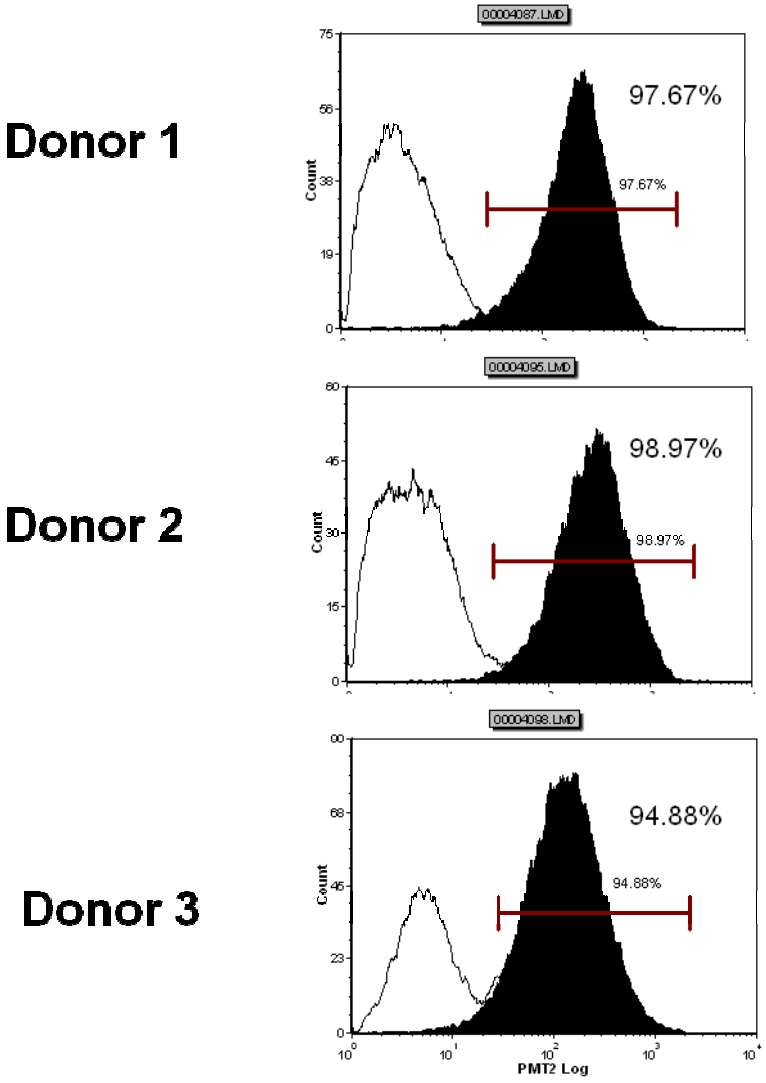


**Figure 4.7 Selection of integrin $\alpha_6$/CD49f-high fraction of ERM cultures by Fluorescence activated cell sorting (FACS)**

FACS was used to select the brightest 30% of cells in the integrin $\alpha_6$/CD49f-positive fraction of ERM cultures from three donors prior to subcutaneous transplantation. The white and black histograms illustrated the isotype matched control and anti-CD49f antibody, respectively.

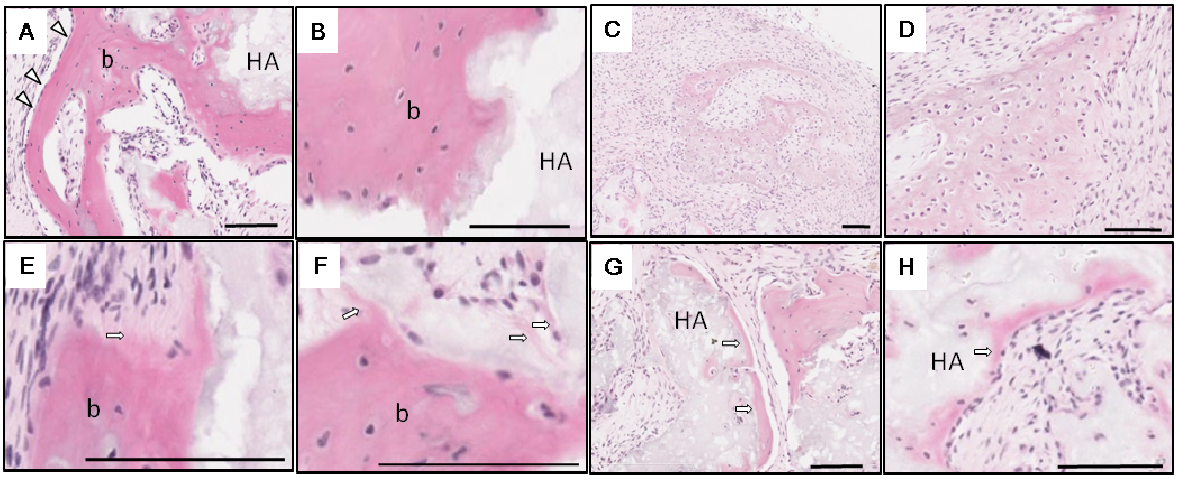


**Figure 4.8 Generation of bone, cementum-like and Sharpey's fibre-like structures *in vivo* by ERM cells**

(A, B) After 8 weeks of transplantation, ERM cells differentiated into osteoblast-like cells (triangles) that formed bone (b) on the surface of hydroxyapatite/tricalcium phosphate (HA) particles.
(C, D) In addition to the mineralized bone structures, another type of mineral was generated.
(E, F) Sharpey's fibre-like structures (arrows) were observed on the surface of bone (b).
(G, H) Thin mineralized, cementum-like structures (arrows) on the surface of the HA particles.
Scale bar=100 µm; A-H were stained with H&E.

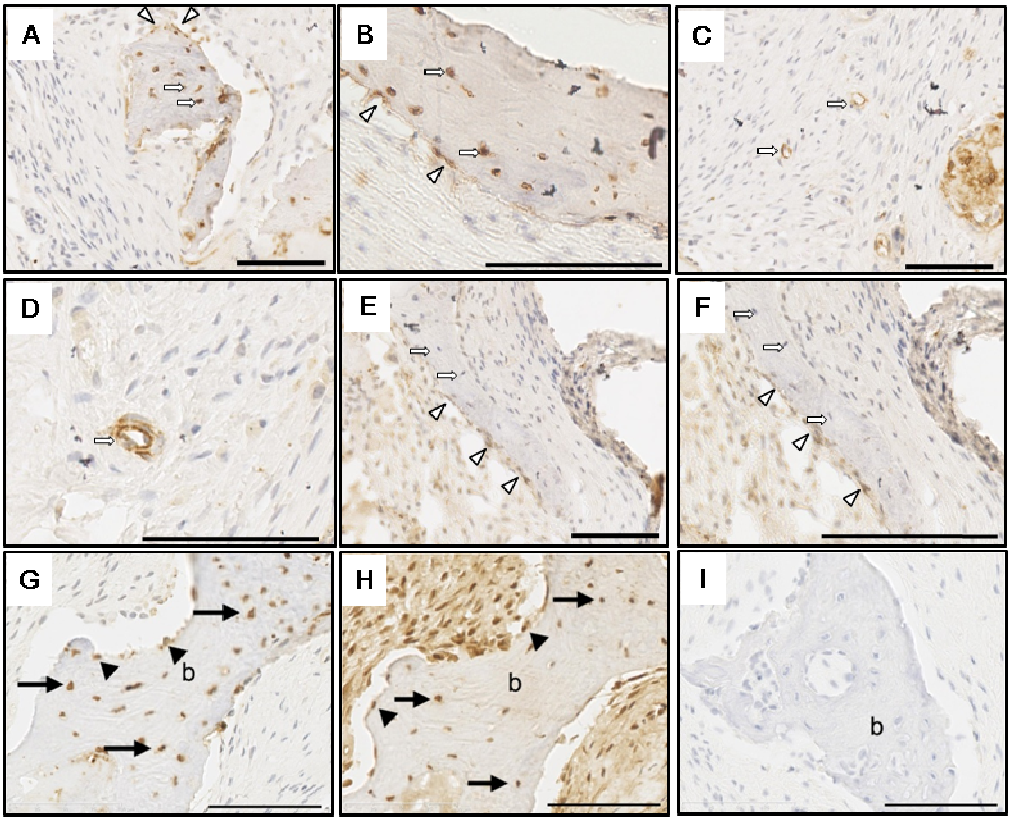


**Figure 4.9 ERM cells gave rise to the mineral formation in subcutaneous transplantation**

(A, B) Immunohistochemical staining with anti-ovine CD44 antibody showed that ERM cells had differentiated into osteocytes (arrows) and bone-lining cells (triangles).
(C, D) CD44 positive cells were also identified around blood vessels (arrows).
(E, F) ERM cells that differentiated into bone lining cells (triangles) were positive for anti cytokeratin-8 (CK-8) antibody while those differentiated into osteocytes (arrows) lacked CK-8 expression.
(G, H) Serial sections showed the co-localization of CD44 and osteocalcin in osteocytes (arrows) and bone-lining cells (triangles).
(I) Isotype matched controls for CD44 and osteocalcin antibodies were used to determine the level of non-specific antibody binding. Scale bar=100 μm

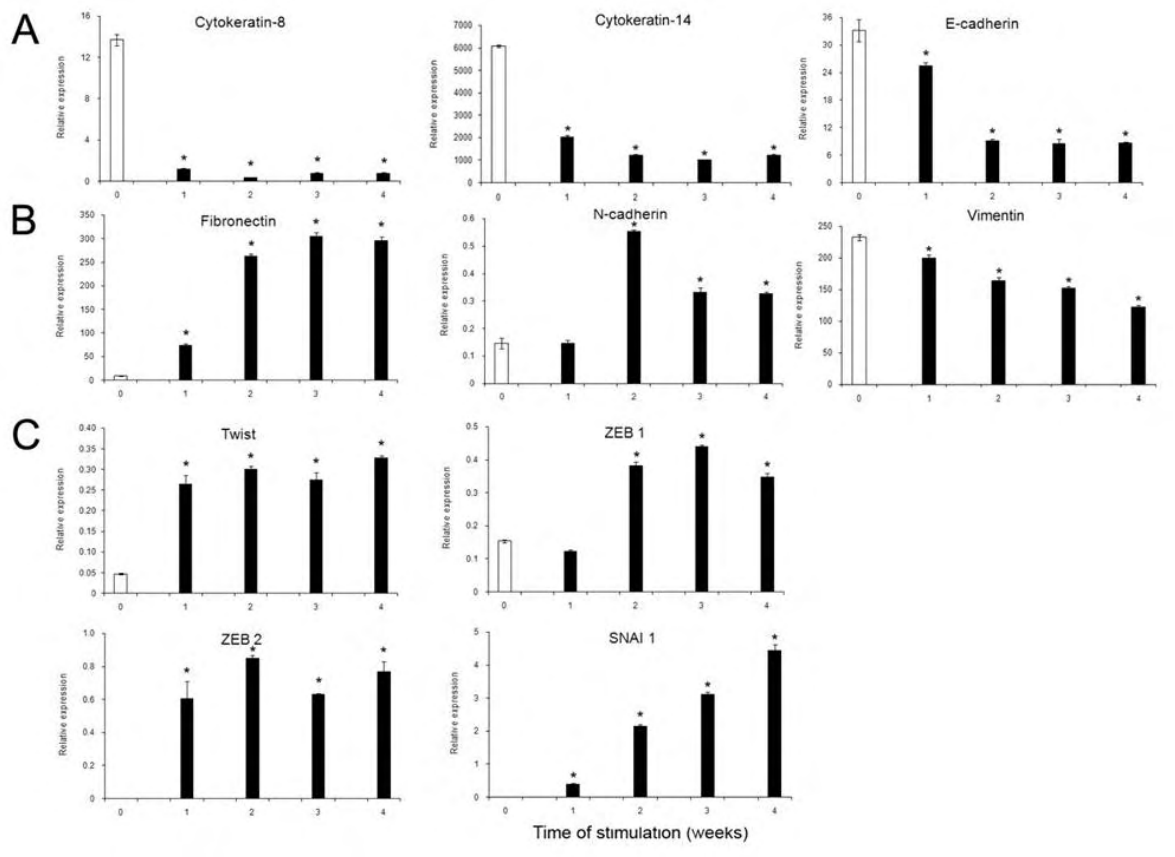


**Figure 4.10 ERM cells are capable of undergoing epithelial-mesenchymal transition under osteogenic conditions**

Real time-PCR analysis following osteogenic induction of ERM cells after 1, 2, 3 and 4 weeks for the expression of:
(A) Epithelial markers cytokeratin-8, cytokeratin-14 and E-cadherin
(B) Mesenchymal-associated genes fibronectin, N-cadherin and vimentin
(C) Epithelial-mesenchymal transition-regulating transcription factors, Twist, Zinc finger E-box-binding homeobox 1 (ZEB 1), ZEB 2 and SNAI 1.
The data represent the mean values ± standard error of the mean (SEM) of triplicate experiments normalized to the house keeping β-actin gene. Statistical significance of $p \leq 0.05$ (*) was determined using an unpaired Student *t*-test.

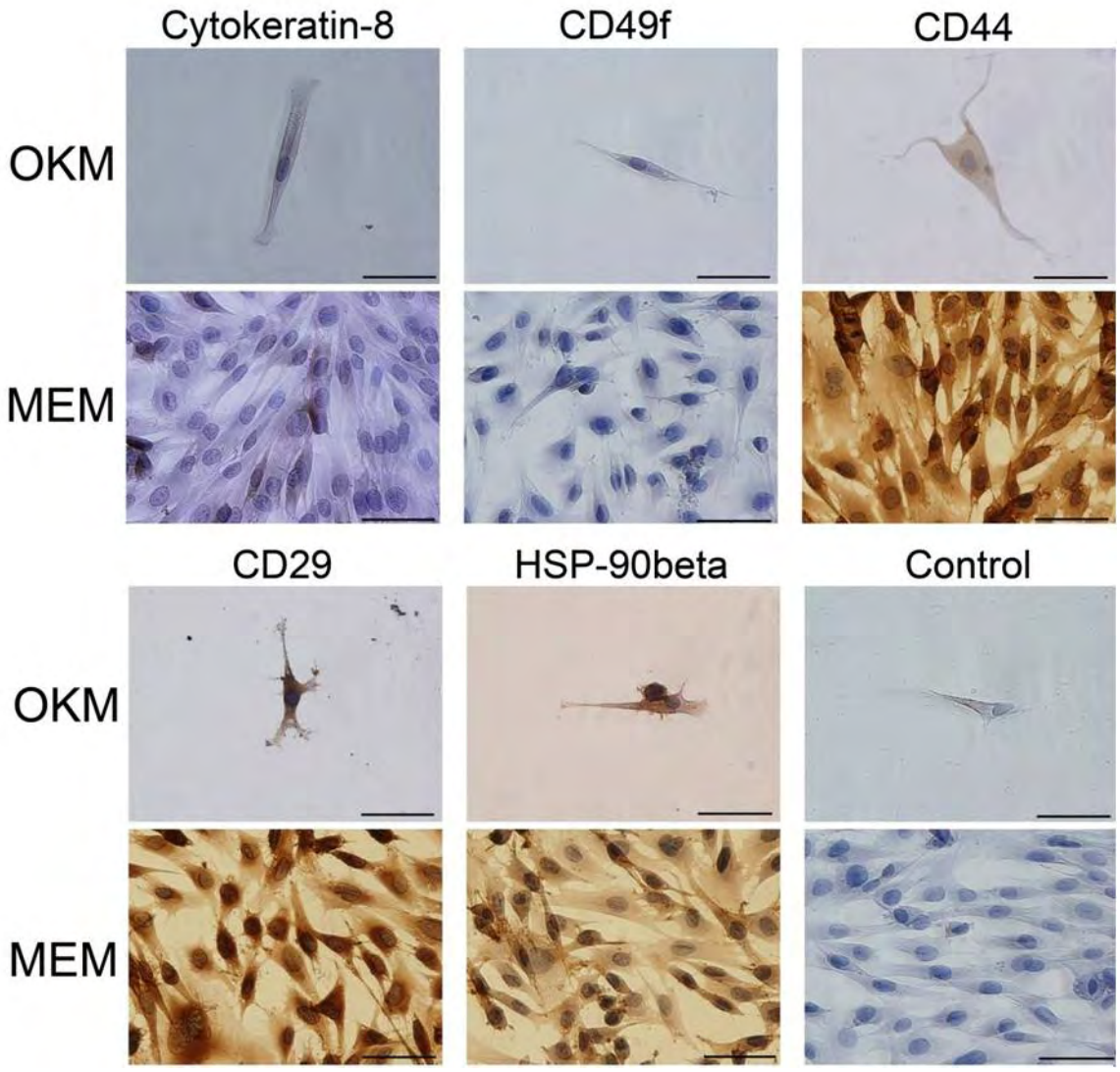


**Figure 4.11 Periodontal ligament stem cells did not undergo mesenchymal epithelial transition in keratinocyte culture system**

Minimal number of periodontal ligament stem cells could survive in OKM with additives. Morphologically, they showed spindle shape of fibroblasts. Phenotypically, they stained negative for cytokeratin-8 and integrin α6/CD49f, and positive for mesenchymal markers, CD44, CD29, and HSP90β in OKM and MEM. Isotype-matched control was used to determine the level of nonspecific antibody binding. Scale bar = 50 μm. OKM, oral keratinocyte media with additives, α modification with additives; MEM, minimum essential medium.

## 4.3 Discussion

Initial characterization of ovine ERM cells in Chapter 3 demonstrated that *ex vivo*-expanded ERM express various MSC associated markers, which formed the basis for further studies in Chapter 4 examining their potential MSC-like properties under specific inductive conditions. By culturing ERM cells in differentiation conditions previously

reported for dental MSC-like populations such as DPSC, SHED and PDLSC [126, 127, 131, 141], we showed that ectoderm-derived ERM cells share similar phenotypic and functional attributes with MSC, as judged by their capacity to differentiate into three major mesodermal lineages (bone, fat and cartilage) and one ectodermal lineage (neuron-like cells) *in vitro*. The neurogenic potential of ERM cells suggests a possible role for ERM cells in periodontium innervation. Furthermore, ERM cells displayed the potential to generate three tissues of periodontium, including bone, cementum-like and Sharpey's fibre-like structures in a xenogeneic ectopic transplantation model. Whilst ERM cells are thought to be cell "rests" in postnatal life, our data indicate that ERM contain a subpopulation of stem cells that are capable of undergoing EMT. This lends support to a recent report that human ERM cells express embryonic stem cell markers such as Oct-4, Nanog and SSEA-4, providing circumstantial evidence for the stem cell nature of ERM cells [237]. Therefore, ERM cells in postnatal tissues may function as a source of progenitor cells in periodontal ligament similar to that described for PDLSC [126] with the capacity for stem cell plasticity in terms of cross germ layer differentiation.

Stem cells are uncommitted cells capable of self-renewal and multi-lineage differentiation, where postnatal stem cells reside as subpopulations in various tissues responding to environmental stimuli to proliferate, migrate and regenerate damaged tissues. While adult stem cells were initially thought to be restricted to regenerating the tissues in which they reside, ever increasing evidence has shown that adult stem cells exhibit a broader differentiation capacity to form cell types outside of the germ layer from which they were originally derived [318, 319]. In the very early embryo there are three primary germ cell layers, mesoderm, endoderm and ectoderm. Mesoderm gives rise to bone, muscle, connective tissue and the middle layer of the skin. Endoderm differentiates first to the embryonic gut and then to the linings of respiratory and digestive tracts, the liver and

pancreas. Ectoderm-derived tissues include the epidermis, the teeth, the lens of the eye, parts of the inner ear, the nervous system (spine, peripheral nerves and brain) and spinal cord. A growing body of evidence has suggested that adult stem cells can differentiate across germinal boundaries *in vitro*. For example, mesoderm-derived BMSC injected into the central nervous systems of newborn mice were able to migrate throughout the brain and differentiate into astrocytes and neurons morphologically and phenotypically [320]. Bone marrow derived MSC have also been shown to differentiate into endothelial-like cells both phenotypically and functionally in the presence of vascular endothelial growth factor [321]. Another study established an *in vitro* model of pre-angioblast-to-endothelium differentiation from BMSC to generate endothelial cells, which could contribute to neo-angiogenesis when engrafted in models of wound healing and tumorgenesis [322]. Furthermore, adipose tissue-derived adult stem cells can be differentiated into epithelial cells in the presence of all-trans retinoic acid [323]. These studies highlighted that adult stem cells from various tissues exhibited broad differentiation potential to cross germ layer boundaries.

Studies on the properties of adult stem cells have discovered that some of these populations, such as adult neural stem cells, exhibited pluripotency to give rise to cell types of all germ layers [324]. Similarly, pluripotency has been identified in adult BMSC, termed very small embryonic-like stem cells [325]. In addition, single BMSC have been shown to differentiate into epithelial cells which were traditionally thought to be exclusively of endoderm or ectoderm origin [326]. Collectively, these studies indicate that adult stem cells demonstrate broader plasticity than initially anticipated. However, it is still an open question under which circumstances adult stem cells demonstrate plasticity. Several alternative explanations are emerging, including the well accepted process of cell fusion and epigenetic modifications when cells are exposed to extrinsic stimuli [325]. Equally

important has been the discovery of factors responsible for regulating stem cell plasticity [108, 327, 328]. The establishment of induced pluripotent stem cells has helped us understand the mechanisms for cell fate determination. A recent study highlighted the crucial roles of mesenchymal epithelial transition in inducing pluripotency [306, 327], where factors such as E-cadherin may help mediate the process of cellular reprogramming [327]. Mesenchymal epithelial transition is an early event during reprogramming by Yamanaka factors (Sox2, KLF4, Oct4 and c-Myc), through transforming fibroblasts into tightly packed cell clusters and converting fibroblasts into an intermediate epithelial cell stage [327]. This is consistent with the previous observations that morphologically embryonic stem cells resemble epithelial-like cells more than mesenchymal-like cells, and human keratinocytes can be reprogrammed 100-fold more efficient and two fold faster than human fibroblasts [306, 327, 329]. Our findings are in agreement with these previous studies that epithelial mesenchymal transition, the reversal of mesenchymal epithelial transition, endows ERM cells the potential to differentiate into multiple lineages.

As ERM cells co-habitate with PDLSC, it is important to demonstrate that the cultures used in this study had no contamination from PDLSC. Firstly, stringent selective enzymatic digestion was performed for the isolation of ERM cells. Secondly, serum-free keratinocyte medium (OKM) favouring epithelial over mesenchymal cell growth, was used as previous studies have shown that mesenchymal cells do not survive in keratinocyte medium [64, 243, 244]. We found that few PDLSC were capable of surviving under keratinocyte culture conditions, which appeared to lose the capacity to proliferate. Phenotypically, the sparse PDLSC identified in these cultures expressed mesenchymal markers, CD44, CD29 and HSP90β but lacked the expression of epithelial markers cytokeratin-8 and integrin α6/CD49f. Thirdly, any possible contamination of PDLSC was minimised by using fluorescence activated cell sorting to isolate integrin α6/CD49f high

expressing epithelial cells. Additionally, to verify the stem cell properties of ERM cells, multi-lineage differentiation assays were performed at the clonal level. Individual epithelial colonies were isolated in low density cultures using colony rings. Every subculture was expanded from one single epithelial colony, minimising the contamination of other cell types. These data from single cell derived epithelial colonies support the notion that different somatic stem cells are a heterogeneous population of multi-potent stem cells and bi-potential progenitors similar to that described for the haematopoietic and mesenchymal cellular systems. Collectively, these studies indicate that PDLSC were unable to undergo mesenchymal epithelial transition when grown under keratinocyte culture conditions.

Recent published data have supported the mineral-forming potential of ERM cells which was summarised in the introduction to this chapter. In the present study, the osteogenic potential of ERM cells was further examined using an *in vivo* ectopic mineralization assay, as the reliance of the *in vitro* differentiation assays has been challenged [330]. The mineral forming capacities of ERM cells were demonstrated in the NOD/SCID xenogenic transplantation model, which is the "gold standard" for assessing stem cell characteristics [331] [125, 211]. Using ovine specific antibodies, ovine ERM cells were demonstrated to be incorporated into the newly formed bone as osteocytes and bone-lining cells. This indicated that ovine ERM cells, rather than endogenous mouse cells, were responsible for the bone formation. Intriguingly, transplanted ERM cells that had differentiated into bone lining cells showed immunoreactivity for CK-8, demonstrating the maintenance of some epithelial characteristics, while those ERM cells which had terminally differentiated into osteocytes lacked expression of CK-8. It would be of interest to further investigate the underlining mechanisms regulating the loss of epithelial nature of ERM cells, and whether they were mediated by the process of epithelial mesenchymal transition. In terms of

mineral formation, morphologically two kinds of mineral were generated from ERM cells; one was the typical mineralized bone structures and the other one appeared to have more cellular components. Further characterization is required to identify their elemental composition, using Electron Probe Micro-Analysis (EPMA) or Energy Dispersive X-ray Analysis (EDX) with undecalcified specially treated transplant samples [332-335]. Morphologically, three periodontium elements, bone, Sharpey's fibre-like and cementum-like structures were generated by the transplanted ERM cells. However, they were not organised in a manner akin to physiological periodontium. One possible explanation is that this *in vivo* ectopic mineralization model which utilizes an osteoconductive biomaterial may not provide the microenvironmental and external signals required for functional periodontium regeneration. Alternatively, ERM cells might need to be combined with PDLSC to form properly arranged periodontium. While the present study indicates that ERM cells harbour mineral forming capacity *in vitro* and *in vivo*, it does not yet demonstrate their role in periodontal regeneration. Consequently, a more direct demonstration of this point will depend on transplantation of these cells into a rodent or ovine periodontal defect model. Collectively, the current study lends further support to the idea that ERM cells contribute, at least partially, to the production of bone/cementum-like mineral deposits and periodontal ligament-like structures or Sharpey's fibres.

It is of particular interest to note that ERM cells expressed both epithelial and MSC associated markers. This observation is consistent with previous studies demonstrating the expression of not only epithelial but also mesenchymal molecules [72, 233]. We next explored the question whether this is an innate feature of these cells or the consequence of the EMT. Two recent studies provide evidence that HERS, from which ERM cells are derived, can undergo EMT in the presence of TGF-β [64, 233]. Hertwig's Epithelial Root Sheath is able to regulate PDLSC differentiation and give rise to cementum-like tissues

after being treated with TGF-β through EMT [64]. The present study demonstrated that ERM cells, which are derived from HERS, underwent EMT when exposed to osteoinductive signals over time. Interestingly, the expression level of vimentin, as a major cytoskeletal component of mesenchymal cells, was down-regulated during osteogenic differentiation, in contrast with other mesenchymal markers such as fibronectin and N-cadherin. However, this is consistent with the previous report showing that vimentin inhibits osteocalcin transcription and osteoblast differentiation, thus a down-regulation of vimentin expression may be essential for osteogenesis to proceed during bone cell maturation [336]. EMT involves a phenotypic shift from epithelial cells to mesenchymal cells that allows epithelial cells to migrate to other locations of the body [307]. Moreover, EMT is believed to be involved in regulating cellular plasticity in normal adult tissues and in tumours [312]. This multipotency endowed by EMT [337] allows cells to migrate to injured sites and contribute to tissue repair or tumour progression, depending on their nature. The present study gives further support to previous studies by showing that EMT plays a central role to induce ERM plasticity, which allows them to participate in mineral formation and periodontal regeneration.

A direct link between experimentally induced EMT and the generation of cancer stem cells has been demonstrated in a recent study [309], which highlights that EMT is sufficient to generate cancer stem cells. The same group also reported that, by ectopic expression of Twist or Snail, epithelial cells not only share antigenic profile typical of mesenchymal stromal/stem cells but also behave functionally similar with MSC including the capacity to differentiate into bone, fat and cartilage and to invade and migrate toward tumour cells and wound sites [337]. Of note, these characteristics were not observed in the untreated epithelial cell fraction. However, in the present study, we have shown that without being forced to overexpress any EMT-associated genes, ERM cells exhibit mesenchymal

stromal/stem cell-like multipotency. It therefore appears that ERM cells are more capable of adapting to the foreign environment than epithelial cells from other tissues. This higher plasticity of ERM cells may be correlated to the fact that these cells exist as epithelial islands within mesenchymal surroundings during postnatal life, while most epithelial cells in other tissues, if not all of them, are separated from adjacent tissues by a basal lamina [304]. The present study demonstrated an inverse correlation of epithelial and mesenchymal gene expression patterns during osteogenic differentiation, which are generally used as markers of EMT during embryonic development and cancer metastasis [304, 307, 310, 312]. Future studies will explore the underlying mechanisms which maintain ERM cells residing in the mesenchymal surroundings and whether these molecular signals are changed during times of tissue regeneration.

In conclusion, this study demonstrated that adult derived ovine ERM cells harbour clonogenic epithelial stem cell populations that demonstrate similar properties to mesenchymal stromal/stem cells both functionally and phenotypically. This highlights that ERM cells, rather than being “cell rests” as indicated by their name in the literature, are an alternate stem cell source that may play a pivotal role in periodontal regeneration. In addition, ERM cells may be a useful model to address some fundamental questions in the stem cell field, such as stem cell plasticity and EMT.

# Chapter 5. Development of a protocol for fluorescent cell surface labelling and 2-dimensional gel electrophoresis

## 5.1 Introduction

The success of stem cell based therapies for treating diseases relies on the ability to isolate and manipulate primary progenitor cells for therapeutic applications [338], based largely on the cell surface marker expression profiles of immature stem/progenitor cell subsets. The official National Institutes of Health (NIH, USA) definition of a biological marker (biomarker) is “a characteristic that is objectively measured and evaluated as an indicator of normal biologic processes, pathogenic processes, or pharmacologic responses to a therapeutic intervention” [339]. Cell surface markers can be any epitopes present on proteins, lipids and carbohydrates [338], which can be targeted by specific reagents such as monoclonal antibodies. Sorting of stem/progenitor cells based on their unique surface antigen expression profiles has generated great interest over the last two decades in the disciplines of immunology and haematology. This has led to the rapid identification and purification of specific cell populations [123], where changes in the abundance of surface proteins also plays an important role in the classification of certain cell types [338]. In addition to their great potential for use in the purification of putative stem/progenitor cells, cell surface markers often play important roles in regulating cell adhesion, migration and attachment, as well as tumour progression. Furthermore, the altered expression of surface molecules is often closely related to the onset of disease, with membrane proteins representing two thirds of commercially available drug targets [340]. Collectively, these studies highlight the increasing interest in the characterization of cell membrane proteins and specifically those that are exposed on the cell surface.

As no specific singular marker is sufficient to define an authentic stem cell, a panel of defined cell surface protein markers is often utilised to characterise specific

stem/progenitor cell populations [338]. One of the minimal defining criteria for multipotent mesenchymal stromal/stem cells (MSC) proposed by the International Society for Cellular Therapy includes the positive expression of CD105, CD73 and CD90, and the negative expression of CD45, CD34, CD14 or CD11b, CD79α or CD19 and HLA class II [123]. While various other MSC associated surface markers have also been described, such as the positive expression of STRO-1, -3 and -4, CD44, CD146 and CD166 [123, 127, 195, 200, 201], the identification and isolation of purified MSC populations for experimental purposes are difficult due to the lack of surface antigens specific to MSC, which has driven the use of technologies investigating global gene (micro-array) or protein expression (proteomics).

In contrast to hypothesis-driven technologies, systematic 'data-mining' 'omics' approaches such as genomics, transcriptomics, proteomics, and metabolomics, are frequently used to identify the global gene, transcript, protein expression profiles and chemical processes involving metabolites, respectively, in stem cells [212, 341-348]. It is believed that the combination of gene expression signatures and mapping of the cell surface proteome is necessary for the discovery of putative stem cell surface markers [338]. Although molecular technology such as gene microarray has generated extensive data sets and valuable information on molecular regulation, one of the drawbacks of genomic studies is that the transcript levels do not always correlate with translated protein expression at the functional level [349]. In addition, post-transcriptional modifications including gene splicing and post-translational protein modifications, such as phosphorylation and glycosylation, are not detected by transcript-based analyses. A more accurate approach to global expression profile, proteomics, which depicts the entire protein complement, or proteome, has generated extensive databases comparing tissue specific stem cells and stem cells with their differentiated progeny [341-344, 346-348]. As proteins are functional

molecules, the expression of proteins will provide valuable direct information for different cellular functions [350]. A cell's proteome is considered to be dynamic in nature, with alterations in protein expression, activation and modification occurring in response to signals in the microenvironment [351]. While current antibody-based techniques, such as flow cytometry and antibody arrays provide invaluable information on the surface protein expression profile, whether these markers are suitable for isolating defined population largely relies on the antibody availability and accessibility [338]. In contrast with these knowledge-driven techniques, proteomic approaches offer a new avenue of investigation towards information on undetectable cell surface proteins in a discovery-driven manner [338].

Over the past decade, the majority of proteomic studies performed on MSC populations have utilized a two-dimensional electrophoresis (2-DE) approach coupled with mass spectrometry (MS) analysis. Considered the central technique of proteomics, 2-DE separates proteins based on their isoelectric point (the pH at which a protein has a net zero charge in an electric field) followed by separation according to molecular weight using a modified version of SDS-PAGE [215]. Fluorescent dyes such as CyDye Fluors (Cy2, Cy3 and Cy5) have been used in two dimensional-difference in gel electrophoresis (2D-DIGE, GE Healthcare) to circumvent the poor sensitivity of traditional dyes such as silver or Coomassie™ brilliant blue stains. Three charge- and size-matched CyDye fluorophores are used to label cysteine residues on protein samples derived from up to three individual cell populations. Additionally, they are designed to have different wavelengths to allow multiple experimental samples to be run on the same 2-DE, thus the ability to compare protein expression quantitatively across multiple samples and minimising gel-to-gel variation. Recently, a novel strategy was reported by Mayrhofer *et al* to selectively label cell surface proteins prior to lysis, using impermeable fluorescent CyDyes without the need

for prior subset fractionation to reduce sample complexity [213]. As such, this technique allows the detection of only cell surface proteins and does not rely on resolving these proteins from highly abundant cytosolic proteins. Briefly, after being detached non-enzymatically, intact cells were labelled with CyDye fluorophores. After quenching of the CyDye label, cells were lysed and proteins were separated using 2-DE followed by mass spectrometry (MS) analysis. Subsequent studies have been reported using this technique to investigate the monocyte plasma membrane proteome [352] and the BMSC membrane proteome during adipogenic differentiation [353]. A combination of CyDye and biotin cell surface labelling has been used on embryonic stem cells [354].

Periodontal Ligament Stem Cells (PDLSC) are believed to be good candidates to restore damaged periodontal tissues both architecturally and functionally following tissue damage [5]. A significant challenge for further characterisation of PDLSC is the lack of specific markers for this cell population [5]. In this chapter, a modified proteomic approach described by Mayrhofer *et al* [213] was used to determine the efficacy of identifying CyDye fluorophore labelled cell surface proteins following separation using 2-DE in combination with MS analysis.

## 5.2 Results

### 5.2.1 Confirmation of cell surface CyDye labelling of human gingival fibroblasts using flow cytometry

Pilot studies used human gingival fibroblasts (GF) as a generic adherent cell population to optimise the fluorescence labelling and 2-DE protocols because of the easy accessibility of gingival tissues and the high growth potential of GF *in vitro* which have a similar immunophenotype to cultured PDLSC [153]. To assess the cell surface labelling efficiency prior to cell lysis, CyDye-labelled GF were fixed and analysed by flow cytometry. Data revealed that 84.47% of the GF population were positive for phycoerythrin (Red: PE)

(Figure 5.1), indicating that the majority of GF had been labelled with Cy3.

### 5.2.2 Comparative 2-DE profiles of CyDye-labelled proteins and total proteins in hydrophobic and hydrophilic protein fractions

After CyDye-labelling and prior to 2-DE, hydrophobic and hydrophilic proteins in GF were separated in the detergent and aqueous phase respectively, using a detergent-based phase separation kit. Hydrophobic and hydrophilic protein preparations were then separated by 2-DE after which the gels were scanned at the excitation wavelength for the CyDye used to label each preparation. The same gels were then stained with flamingo fluorescent dye (Biorad Laboratories, Hercules, CA USA) to detect all proteins in the gel.

According to the manufacture's protocol, CyDye labelling should selectively label the surface exposed proteins, while the same proteins and other non-surface exposed proteins would only be labelled with flamingo fluorescent dye. Figure 5.2 shows, in the same gel, the 2-DE pattern of CyDye-labelled (A) and flamingo fluorescent dye-stained (B) proteins in GF. As expected, all CyDye-labelled proteins were also stained with flamingo fluorescent dye although a difference in spot densities was noticed in some spots using the two detection systems. Spots stained only with flamingo fluorescent dye but not by CyDye labelling were expected to be non-surface exposed hydrophobic proteins, which could include other compartmental membrane proteins, and hydrophobic cytosolic proteins separated in the detergent phase.

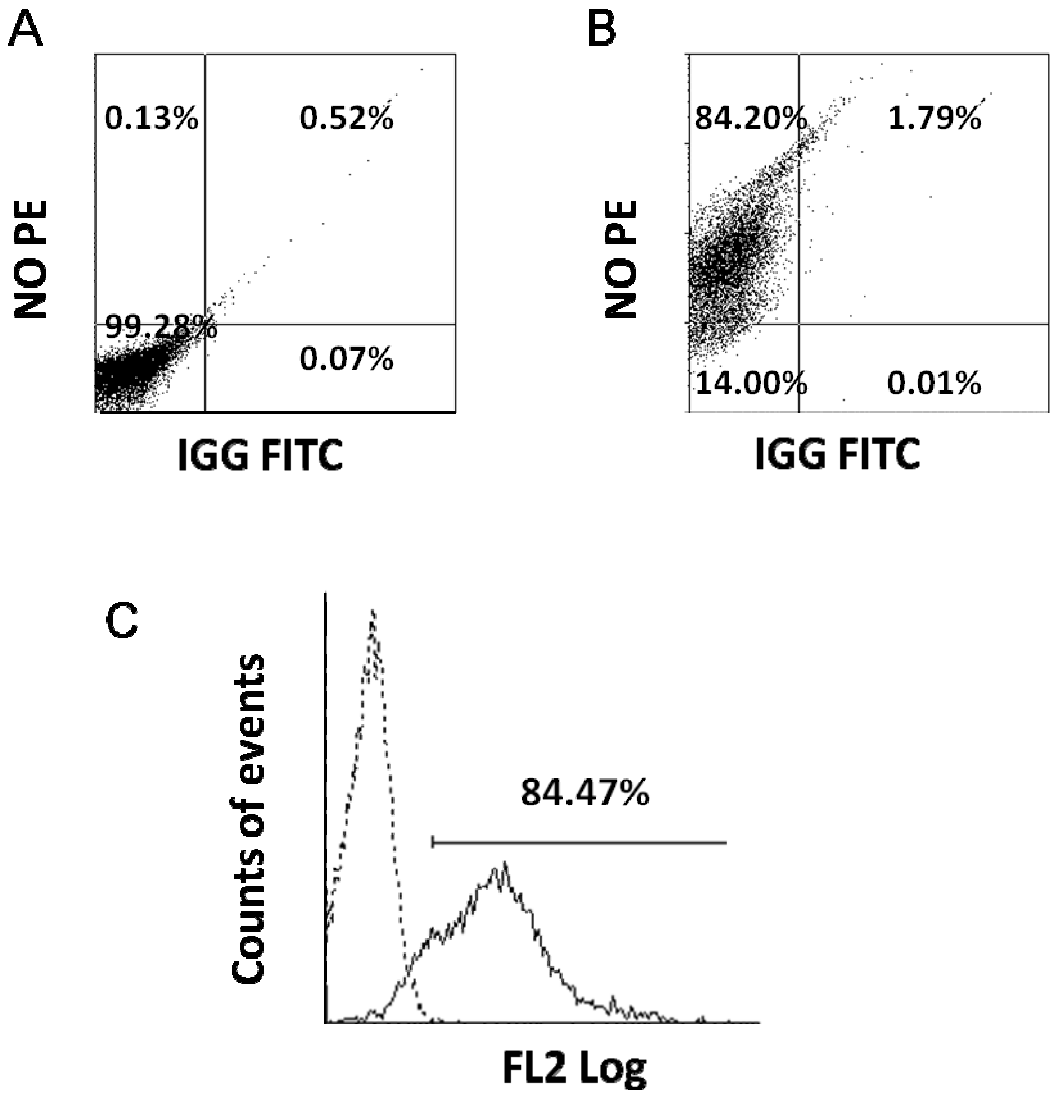


**Figure 5.1 Human gingival fibroblasts were successfully surface labelled with CyDye shown by flow cytometry**

Flow cytometric data displayed as dot plots of the unlabelled human gingival fibroblasts (A) and CyDye-labeled human gingival fibroblasts (B). Overlay histogram showed that 84.47% of human gingival fibroblasts were successfully labeled with CyDye (C).

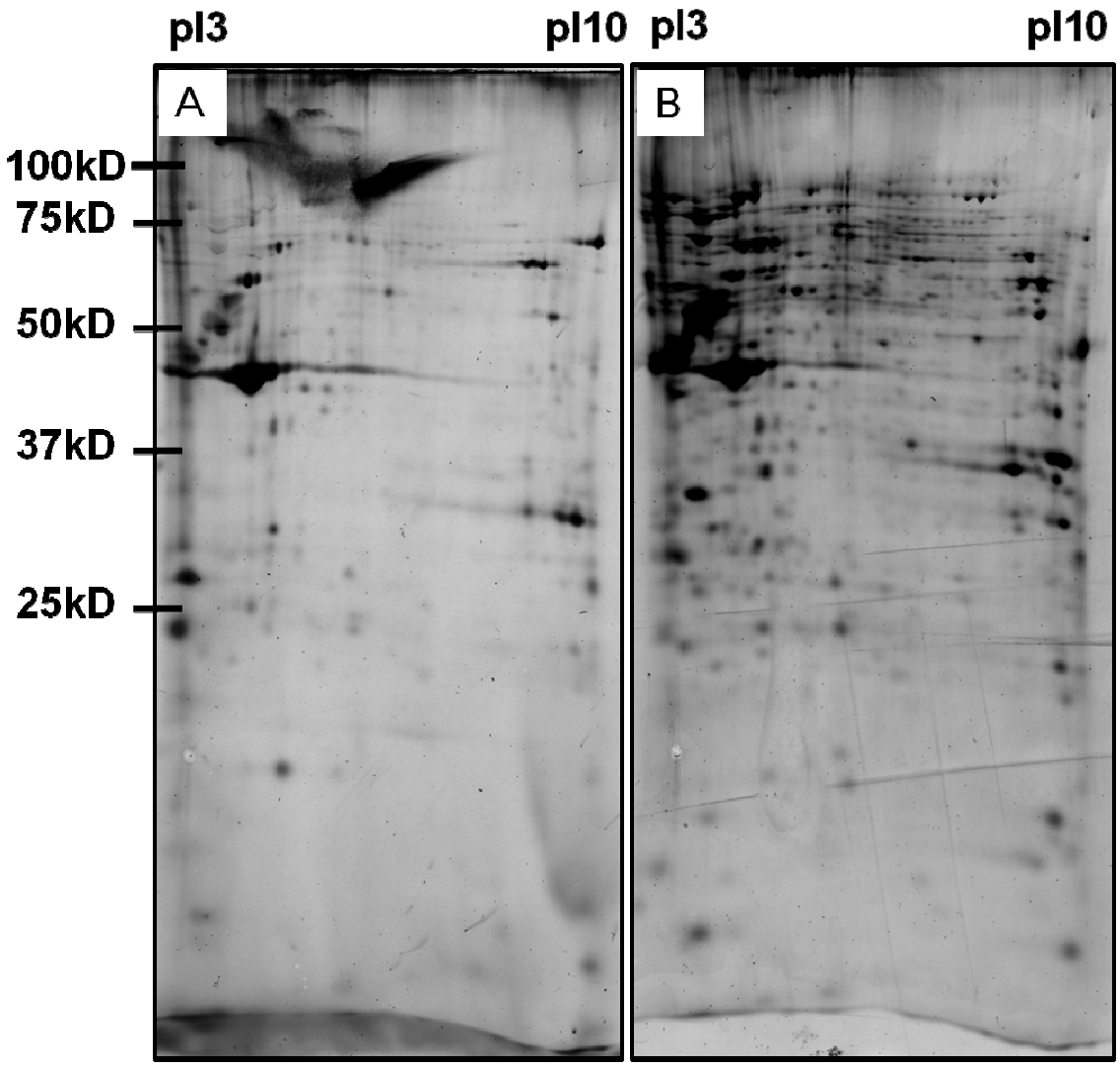


**Figure 5.2 Distinct 2-DE patterns of CyDye-labelled (A) and flamingo-stained (B) hydrophobic proteins of cell surface-labelled human gingival fibroblasts**

Prior to 2-DE, hydrophobic proteins of CyDye-labelled human gingival fibroblasts were enriched before being separated by 2-DE. Gels were scanned at the wavelength for CyDye (A) and then stained with Flamingo fluorescent dye (B). All CyDye-labelled protein spots were displayed by flamingo staining on the same gel.

To assess the labelling specificity of the cell surface exposed membrane proteome, hydrophilic protein preparations were analysed for the presence of CyDye labelled spots. Figure 5.3 shows, in the same gel, the 2-DE patterns of CyDye-labelled (A) and flamingo fluorescent dye stained (B) hydrophilic proteins of GF. Some CyDye-positive protein spots were detected in the aqueous layer (Figure 5.3A). The same gel was stained with flamingo fluorescent dye to show the presence of CyDye unlabelled proteins in the gel. As expected, large numbers of hydrophilic proteins were labelled with flamingo fluorescent dye and

resolved on 2-DE gels (Figure 5.3B). This indicated that the low level of CyDye-stained proteins was not due to the poor recovery of proteins during separation. The comparison of 2-DE patterns of CyDye-labelled and flamingo fluorescent dye spots showed that the majority of hydrophilic proteins in the gel were not labelled with CyDye (Figure 5.3). However, low levels of CyDye labelling were not exclusive to surface exposed membrane proteins.

### 5.2.3 Membrane protein enrichment step in surface protein sample preparation

To determine whether membrane protein enrichment was necessary prior to 2-DE, a comparison was made between the 2-DE profiles of CyDye labelled proteins with and without membrane protein enrichment. 2-DE patterns of CyDye-labelled proteins following membrane fractionation (A) and the total cellular lysate (B) are shown in Figure 5.4. Compared to the 2-DE pattern of the total cellular lysate, the membrane fractionation displayed protein spots which were well defined with reduced streaking (Figure 5.4). Although Mayrhofer *et al* believed that there were only minor differences in the spot patterns between samples with or without the membrane enrichment step [213], in the present study, comparison of CyDye fluorescent maps of the two samples showed that the membrane fractionation step was necessary, as it significantly improved the protein separation and should allow a greater representation of membrane proteins in the sample loaded onto 2-DE gels. Based on these results, a membrane protein enrichment step was performed prior to performing the 2-DE.

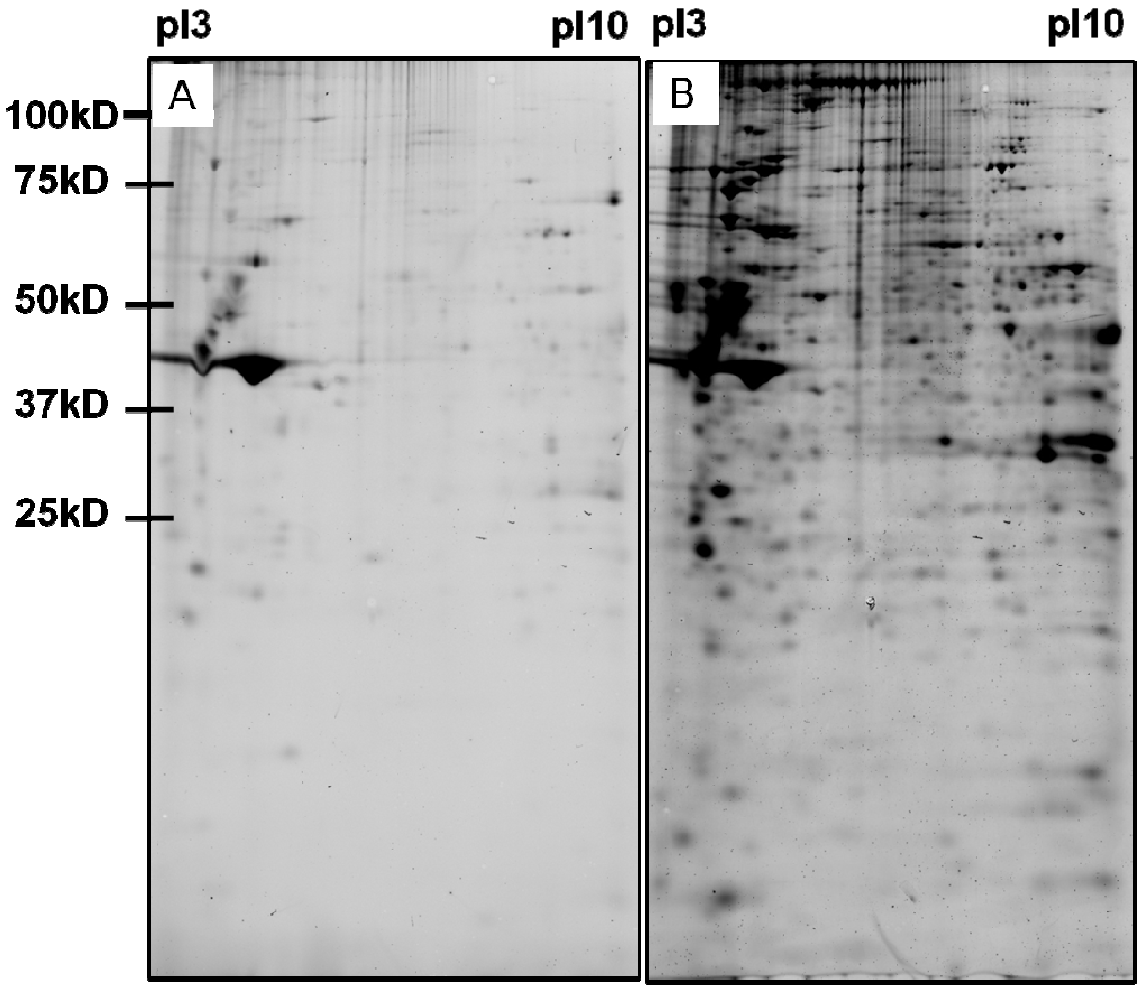


**Figure 5.3 Distinct 2-DE patterns of CyDye-labelled (A) and flamingo-stained (B) hydrophilic proteins of surface-labelled human gingival fibroblasts**

Prior to 2-DE, hydrophilic proteins of CyDye-labelled human gingival fibroblasts were enriched before being separated by 2-DE. Gels were scanned at the wavelength for CyDye (A) and then stained with Flamingo fluorescent dye (B).

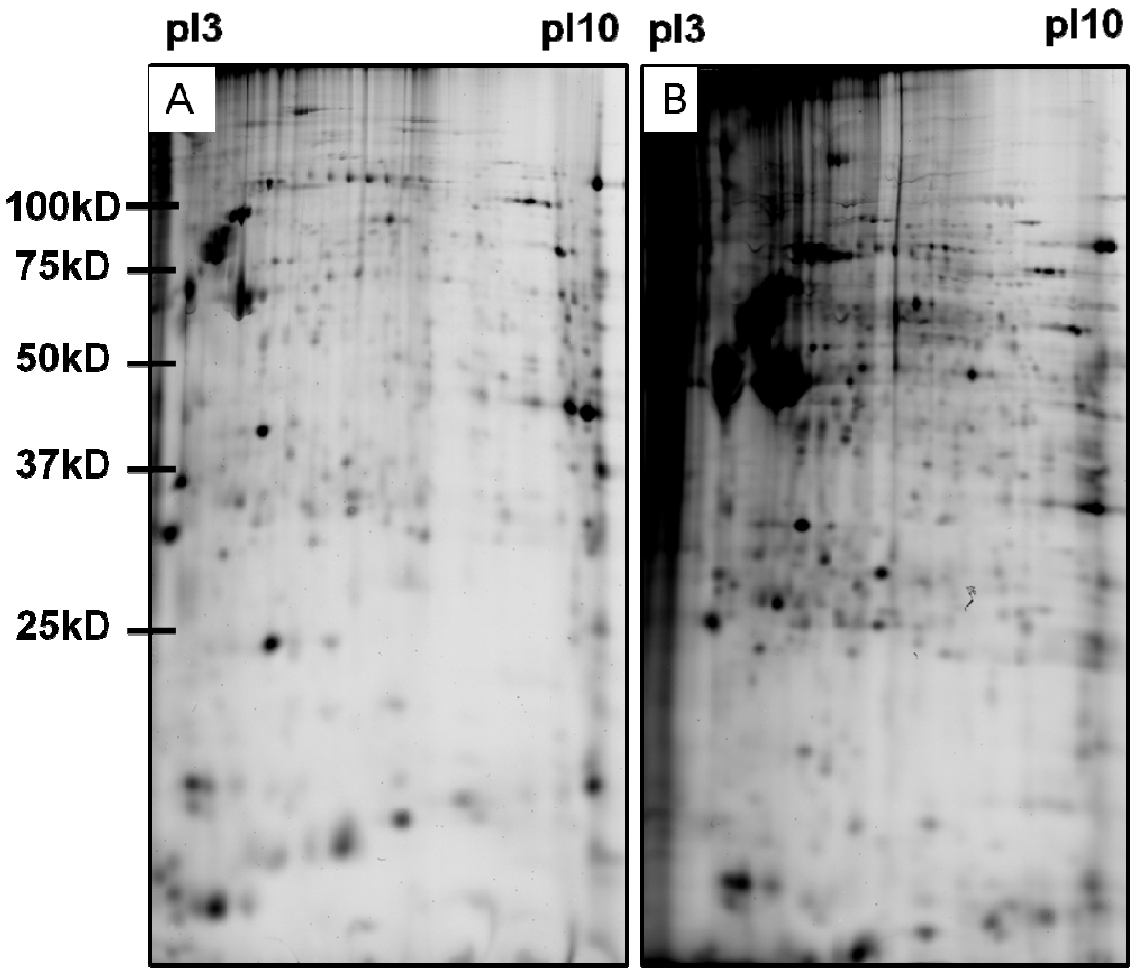


**Figure 5.4 Membrane protein enrichment step was necessary for surface protein sample preparation**

Comparison of the 2-DE profiles of human gingival fibroblasts showed that, compared to the total cellular lysate (B), the membrane fractionation (A) displayed a "cleaner" gel with defined spots and less streaking.

### 5.2.4 Protein identification of five randomly picked protein spots demonstrated cytosolic protein contamination in the membrane protein samples.

To determine whether CyDye labelling was exclusive to cell surface exposed proteins, five protein spots were randomly chosen from the CyDye-labelled proteins in 2-DE gels and were identified by MS (Figure 5.5). These proteins were identified by MS analysis; chaperone protein (heat shock protein 70), β-actin, elongation factor-1-γ, and two spots were identified as glyceraldehyde 3-phosphate dehydrogenase (G-3-PDH). The association of chaperone (heat shock protein family) [213, 355, 356] and cytoskeletal proteins (such as β-actin, tubulin and profilin) with the plasma membrane has been well-documented in

several studies [352, 357-360]. However, G-3-PDH and elongation factor-1-γ are believed to be cytosolic proteins, although G-3-PDH might assemble with other glycolytic enzymes on the inside of the plasma membrane [361]. Based on the cytoplasmic location of some of these identified proteins, we concluded that membrane protein preparations were contaminated with cytosolic proteins. To reduce cytosolic protein contamination and therefore improve membrane protein resolution, we then used multiple membrane protein enrichment steps.

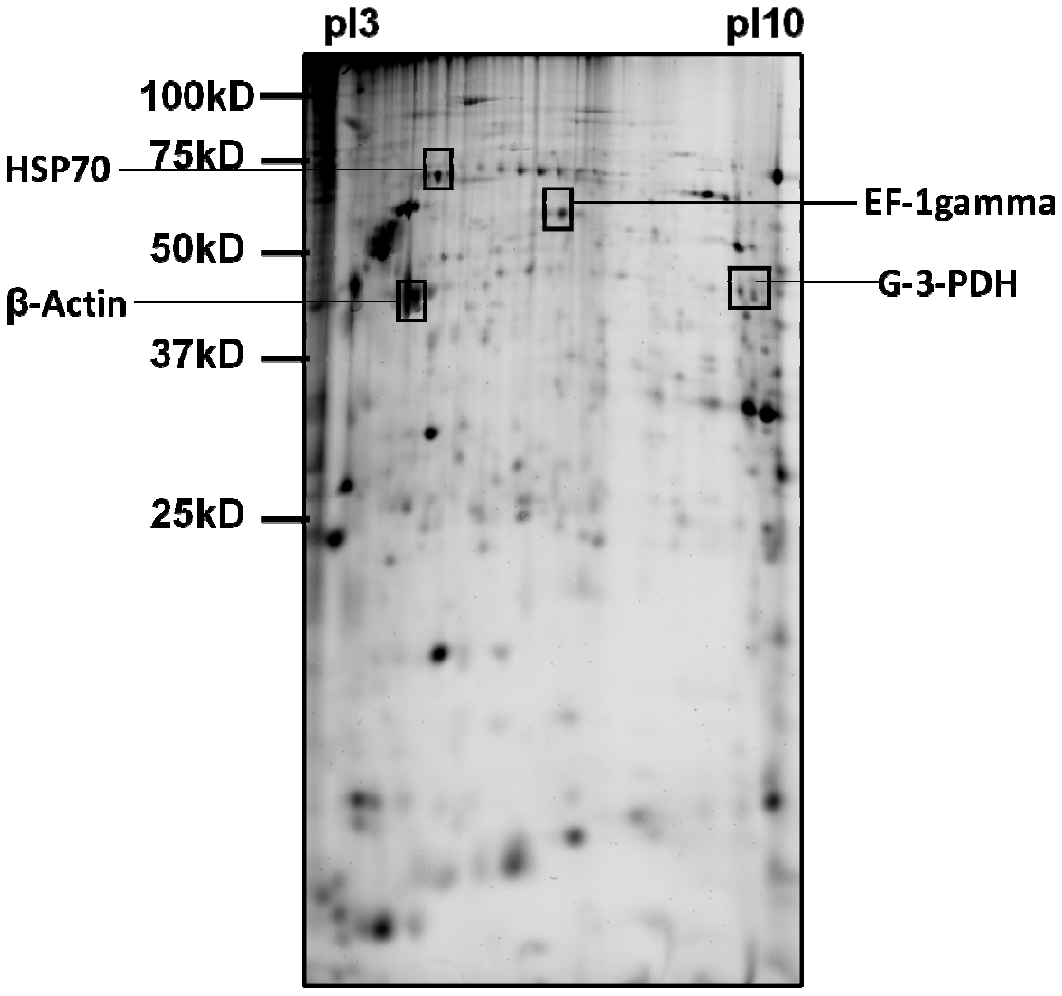


**Figure 5.5 Protein identification of five random spots demonstrated cytosolic protein contamination in the membrane protein samples**

Five protein spots were randomly picked from the CyDye-tagged proteins in the membrane protein preparations of human gingival fibroblasts for MS identification. These proteins were identified as one chaperone protein, heat shock protein 70 (HSP70), β-actin, elongation factor-1-γ (EF-1gamma), and two spots of glyceraldehyde 3-phosphate dehydrogenase (G-3-PDH), showing cytosolic protein contamination in the membrane protein samples.

### 5.2.5 Preparation of membrane proteins using multiple membrane protein enrichment steps

To test whether multiple membrane protein enrichment steps improved the resolution of membrane proteins in samples, GF were surface-labelled with CyDye and subjected to multiple sequential membrane protein enrichment steps (designated as membrane protein 1, membrane protein 2 and membrane protein 3). The flow chart for the multiple membrane protein enrichment protocol is shown in Figure 2.2 in Chapter 2. Following multiple enrichment steps, membrane protein samples were analysed by 2-DE, and both membrane protein and cytosolic protein preparations were assessed using western immunoblotting to monitor the enrichment of CD29 and CD44 (membrane proteins) and loss of tubulin and β-actin (cytosolic proteins).

#### *5.2.5.1 Multiple membrane protein enrichment steps gave rise to similar 2-DE profiles*

Membrane protein 1, membrane protein 2 and membrane protein 3 were analysed by 2-DE as shown in Figure 5.6A, B and C, respectively. The 2-DE patterns of the three samples were similar, as illustrated by no changes in the spot density of β-actin (red rectangles). Western immunoblotting was then used for further analysis to determine the enrichment levels of membrane proteins, CD29 and CD44.

#### *5.2.5.2 Multiple membrane protein enrichment steps diminished but did not eliminate cytosolic protein contamination*

The abundance of proteins in the sample was compared using western immunoblotting, with tubulin and β-actin representative of cytosolic proteins, and CD29 and CD44 indicative of membrane proteins. As shown in Figure 5.7, the band density of total cellular lysate (Lane 1), compared with that of membrane protein 1 (Lane 2) and membrane protein 2 (Lane 4) suggested that multiple membrane protein enrichment steps decreased the expression of tubulin and β-actin, and gave improved enrichment of the expression of CD29 and CD44. However, the multiple membrane protein enrichment steps could not

completely eliminate cytosolic protein contamination in membrane protein preparations. This would be expected, as cytosolic proteins which were relatively hydrophobic would associate with the detergent phase of the membrane extraction kit used. Alternatively, another possibility was that the detachment of cells from the flask may have produced a significant number of damaged or leaky cells. If significant cell death was occurring, CyDye would enter these cells and lead to staining of cytoplasmic proteins.

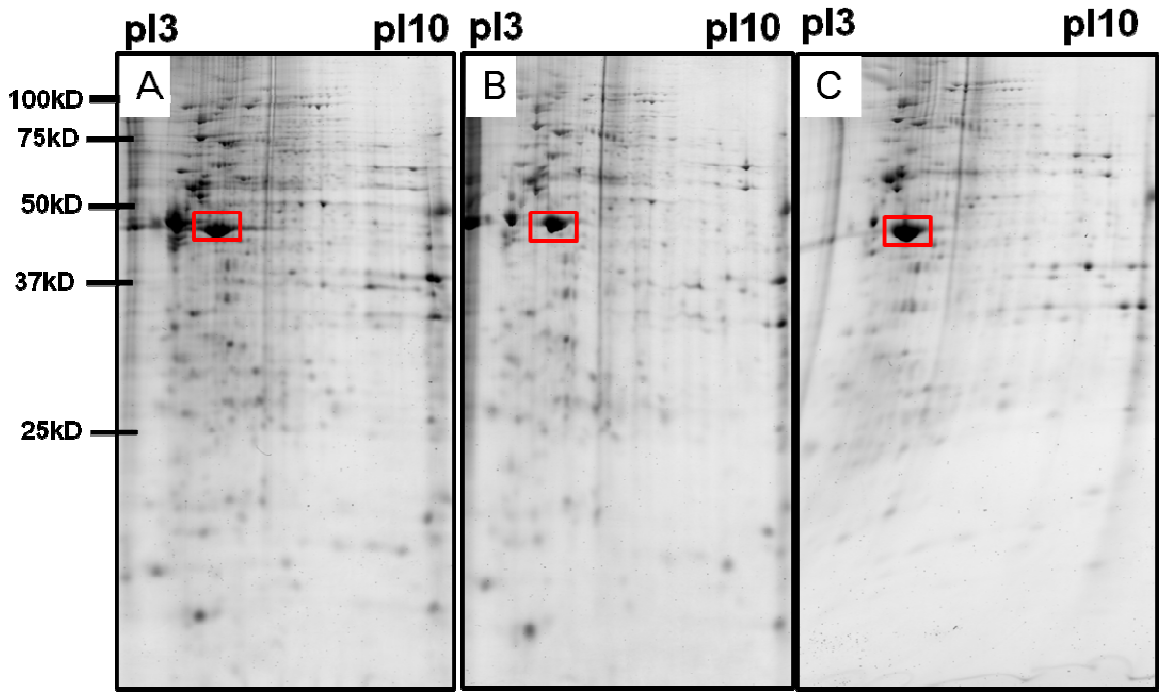


**Figure 5.6 Multiple membrane protein enrichment steps gave rise to similar 2-DE profiles**

Human gingival fibroblasts were surface-labelled with CyDye and subjected to up to three membrane protein enrichment steps. The 2-DE patterns of three membrane protein preparations, designated as membrane protein 1, membrane protein 2 and membrane protein 3, were shown in Figure 5.6A, B and C, respectively.

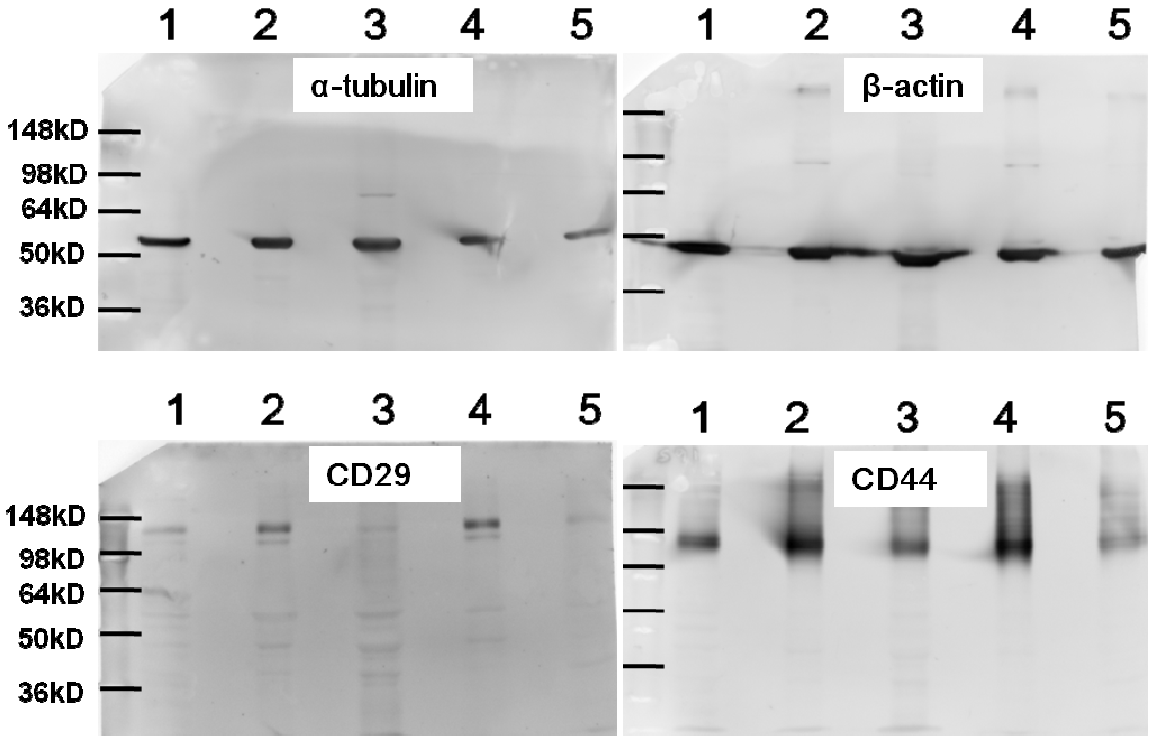


**Figure 5.7 Multiple membrane protein enrichment steps diminished but did not eliminate cytosolic protein contamination**

Human gingival fibroblasts were surface-labelled with CyDye and subjected to up to three membrane protein enrichment steps (designated as membrane protein 1, membrane protein 2 and membrane protein 3, respectively). The abundance of proteins in the sample was compared using western immunoblotting, with tubulin and β-actin representative of cytosolic proteins, and CD29 and CD44 indicative of membrane proteins. The comparison between the band density of total cellular lysate, membrane protein 1 and membrane protein 2 suggested that multiple membrane protein enrichment steps decreased the expression of tubulin and β-actin, and gave improved enrichment of CD29 and CD44. However, the multiple membrane protein enrichment steps could not eliminate cytosolic protein contamination in membrane protein preparations. (Lane 1= whole cell lysate; Lane 2= membrane protein 1; Lane 3= cytosolic protein 1; Lane 4= membrane protein 2; Lane 5= cytosolic protein 2; Molecular weight ladders from the top to the bottom: 148KD, 98KD, 64KD, 50KD and 36KD.)

### 5.2.6 Collagenase detachment gave rise to better cell viability compared to EDTA detachment

To investigate this possibility, alternative approaches of detachment were investigated. EDTA is thought to preserve the structural and functional integrity of cell surface proteins in contrast to the use of general proteases such as Trypsin and Dispase, and thus EDTA was used to detach cells in the previous experiments. However, EDTA treatment was found to give rise to approximately 20% of non-viable cells in cultured PDLSC and GF, as

shown by trypan blue dye exclusion. Therefore, the permeability of the plasma membrane in the high proportion of dead cells could explain the CyDye uptake and labelling of cytosolic proteins. In an attempt to lower the death rate of cells during detachment, collagen specific protease collagenase was used as an alternate method to detach culture expanded cells. The comparison of cell viability following EDTA and collagenase treatment demonstrated that collagenase treatment gave rise to minimal cell death (around 2%) compared to EDTA treatment (Table 5.1).

### 5.2.7 Collagenase detachment minimised cytosolic protein contamination in the membrane protein preparations

As collagenase detachment largely preserved cell viability, cell surface labelling and 2-DE were performed on samples detached with collagenase. The side-by-side comparison of 2-DE profiles in Figure 5.8 demonstrates that samples with collagenase detachment (A) led to less CyDye-tagged spots compared with those with EDTA treatment (B). More importantly, β-actin CyDye labelling was reduced significantly following collagenase detachment (red rectangles). All total proteins in the gel were resolved using flamingo fluorescent dye (Figure 5.8C).

**Table 5.1 Collagenase detachment gave rise to better cell viability compared to EDTA detachment.**

The comparison of cell viability following EDTA and collagenase treatment demonstrated that the collagenase treatment gave rise to minimal cell death in human PDLSC and HGF compared to EDTA treatment. The data represent the mean values ± standard deviations of replicate experiments. PDLSC, periodontal ligament stem cells; HGF, human gingival fibroblasts.

| | **Cell type** | **Dead cells (%) by trypan blue** |
|---|---|---|
| **EDTA treatment** | PDLSC (n=5) | 24.35±7.62 |
| | HGF (n=10) | 21.45±5.86 |
| **Collageanase treatment** | PDLSC (n=3) | 2.35±1.28 |
| | HGF (n=4) | 2.07±1.59 |

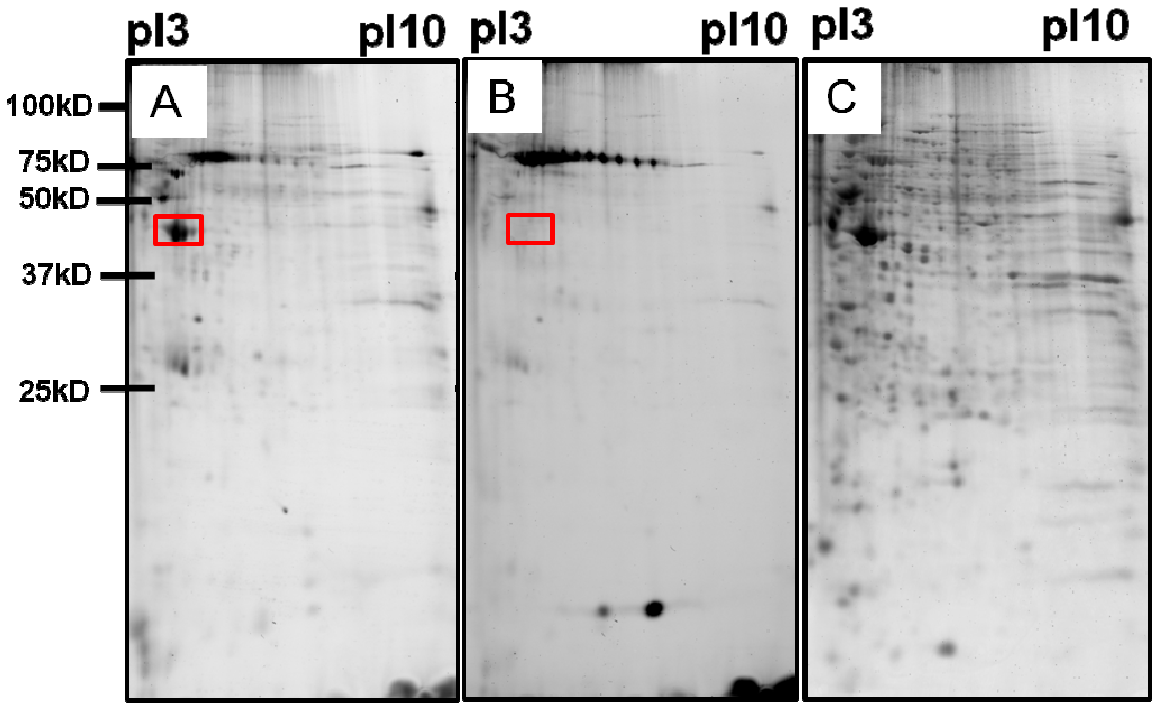


**Figure 5.8 Collagenase detachment minimised cytosolic protein contamination in the membrane protein preparations**

As collagenase detachment gave rise to satisfactory cell viability, we performed cell surface labelling and 2-DE on human gingival fibroblast samples detached by collagenase. Samples with collagenase detachment (A) led to less CyDye-tagged spots compared with those with EDTA treatment (B). β-actin (red rectangles) was not visibly stained with CyDye following collagenase detachment (B). All total proteins in the gel were resolved with Flamingo fluorescent dye (C).

## 5.3 Discussion

The cell membrane is the interface between the cell contents and the external environment. Membrane proteins have been classified into three categories: integral, anchored and peripheral membrane proteins, according to their localisation and interactions with the lipid layer [362]. Integral proteins contain hydrophobic regions that allow them to traverse the plasma membrane once or multiple times, termed as single-pass and multi-pass membrane proteins, respectively [363]. They may also contain a hydrophilic region that protrudes into the cytoplasm or the extracellular environment. The hydrophobicity of these proteins is proportional to the increased number of trans-membrane domains [363]. Membrane anchored proteins attach to one side of the membrane by anchoring to the lipid layer, while peripheral proteins do not span the membrane but adhere temporarily to the membrane by

interacting with integral membrane proteins [362]. As anchored and peripheral proteins do not cross the hydrophobic lipid layer, they are not as hydrophobic as integral membrane proteins [362]. It is believed that the majority of proteins presented on the external surface of mammalian cells are glycoproteins [364], and several studies have documented cohorts of stem cell associated glycoproteins [365-368].

### 5.3.1 Studies using CyDye cell surface labelling

The difference in gel electrophoresis (DIGE) methods provide a powerful technique for quantitative proteomics, where three similar cyanine dyes (Cy2, Cy3 or Cy5) allow the separation of up to three samples on the same gel, thus avoiding gel-to-gel variation. In standard DIGE experiments, cells lysates are labelled with different fluorescent dyes, mixed and separated on the same gel. Conversely, in the cell surface labelling protocol by Mayrhofer *et al*, intact cells are labelled with CyDye, followed by cell lysis and protein separation in 2-DE [213]. The authors believed that CyDye cell surface labelling proved to be efficient *in vitro* and *in vivo*. To our knowledge, there have been a few publications using CyDye cell surface labelling technology since Mayrhofer's protocol was published in 2006.

A recent study compared the proteome of adult smooth muscle cells with ESC-derived smooth muscle cells using a combination of cell surface fluorescent CyDye labelling (slightly modified from Mayrhofer's protocol [213]) and biotin/avidin labelling [354]. DIGE/biotin labelling was performed when the cells were attached to the substratum, whereas the study by Mayrhofer *et al* labelled cells in suspension with CyDye. The DIGE fluor tags allowed membrane-associated proteins to be easily distinguished from contaminant proteins, and subsequently biotin/avidin affinity columns were used for the enrichment of membrane-associated proteins to reduce sample complexity [354]. The

addition of CyDye labelling with biotin membrane enrichment showed a significant enrichment for membrane or membrane associated proteins from 5% to 32% with a corresponding reduction of intracellular proteins [354]. They reported that ESC-derived smooth muscle cells maintained properties indicative of their ESC origin including the cell expression profiles and the positive expression to pluripotent markers [354]. A second study used CyDye cell surface labelling to investigate the effect of HIV-1 on the monocyte plasma membrane proteome and reported the translocation of traditionally cytosolic redox and cell activating proteins to the cell membrane when exposed to HIV-1 [352]. A third study used both gel and non-gel based MS to investigate the membrane proteome of human BMSC under adipogenic induction [353]. Although CyDye cell surface labelling coupled with gel based proteomic analysis demonstrated some changes of spot densities during adipogenesis, both whole cellular proteome and cell surface subproteome were somewhat inert to adipogenic differentiation [353]. Collectively, the lack of publications using CyDye cell surface labelling techniques might indicate that this technique is technically challenging.

### 5.3.2 Challenges in membrane protein investigation

#### *5.3.2.1 Inconsistency of stem cell membrane proteome data*

Although a wealth of data has been derived from proteomic studies of MSC, it is apparent that it is difficult to compare data from different studies because few common proteins have been consistently reported. This is partly due to a lack of standardized protocols used in these studies. Some of the hurdles for standardization include the differening quantitative methods used to analyse similar cell populations and the use of different separation methods to reduce sample complexity. As a result, the sensitivity, accuracy and relevance of the data generated can be highly variable. Another contributor to the inconsistency in proteomic data was the lack of uniformity of *in vitro* culture conditions of MSC, particularly differences in expansion and differentiation induction media as well as

the density and passage number of cultured cells. For example, fetal calf serum-based media or serum-free media have a significant influence on the patterns of surface protein expression. This highlights the need to establish standard stem cell culture conditions as well as protein separation and analysis techniques [369]. Moreover, cell surface protein expression undergoes constant changes in response to stress in the environment, and therefore, the cell surface proteome can only reveal “snapshots” of the cell surface at the moment that samples are collected [338]. For example, cells under constant stress, such as during trypsin detachment, demonstrate the up-regulation of apoptosis-related proteins [370]. Another study has also highlighted that the formation of microbial biofilms causes major changes in the bacterial proteome expression [371].

While 20-30% of the whole genome is thought to encode membrane proteins [372], only some of these proteins have been investigated [373]. As such, extensive efforts have been directed into optimizing membrane proteomic approaches. The investigation of the cell membrane proteome remains an extremely difficult task compared to that of the cytosolic proteome [213]. Firstly, the high hydrophobicity of membrane proteins makes them extremely difficult to dissolve in an aqueous sample preparation [338], particularly membrane proteins containing multiple trans-membrane domains [362]. The separation efficiency in 2-DE decreases with the increase of protein hydrophobicity [363], which is mainly due to their insolubility during iso-electric focussing [373]. Given the strategic roles of membrane proteins in regulating cell functions and properties, researchers have attempted to develop and modify novel methods to optimise sample preparation for better separation using 2-DE. The introduction of detergents, chaotropes and solvents in the sample preparations, such as thiourea and CHAPS, has improved solubilisation by covering the hydrophobic parts of the protein, thus making the resolution of membrane proteins possible using 2-DE [374]. As such, conventional 2-DE could efficiently identify

membrane proteins with minor hydrophobicity (one or two transmembrane domains), but has strong bias over the separation of proteins with more than three transmembrane domains [363]. Secondly, some drawbacks of MS analysis on membrane proteins have been reported. Integral proteins are not easily accessible for proteolytic enzymes such as trypsin [362]. In addition, their hydrophilic terminus may be too short to be identified in routine MS techniques [362]. The current approaches in membrane proteomics during sample preparation and MS identification steps have been reviewed [362] and it was concluded that there is no approach that could meet the needs of all membrane protein studies, as a broad variation existed between cell functions and their membrane compositions [362]. Thirdly, other than abundant plasma membrane proteins such as integrins, membrane proteins are largely under-represented and poorly resolved against the background of highly abundant cytosolic proteins due to a low abundance [373]. To acquire sufficient amounts of low abundant membrane proteins, it is important to start with a large cell number, such as 20 million mammalian cells. Even starting with large cell numbers, the low abundance makes detection difficult in proteomic approaches without additional fractionation or enrichment steps. Pre-fractionation steps are often required to reduce sample diversity and complexity, leaving the sample enriched for a desired subset of proteins [375].

#### *5.3.2.2 Fractionation and enrichment of membrane proteins*

Subcellular fractionation targeting membrane proteins is utilised to reduce sample complexity and access less abundant proteins by removing highly abundant ones. With regards to the enrichment of membrane proteins, commonly used strategies include physical sub-fractionation using density gradient centrifugation [376], detergent-based fractionation based on hydrophobicity [377] and chemical-tagging approaches such as biotin/avidin labelling [378], which are often utilised in conjunction with physical

separation techniques [338]. Cell surface biotinylation, which covalently attaches biotin to the extracellular domain of a plasma membrane protein in conjunction with affinity capture by avidin chromatography, has been widely used to label cell surface proteins as biotin does not penetrate plasma membrane [379-382]. The high affinity of avidin to biotin makes the avidin-biotin affinity chromatography an efficient method of cell surface protein purification. In an earlier study, biotin labelling was found to minimise cytoplasmic protein contamination as well as increase the solubility of the compounds it was associated with [375]. However, a number of limitations in this technique for labelling cell surface proteins have been recognised. Essentially, necrotic and apoptotic cells need to be avoided in sample preparation as intact plasma membranes are vitally important to avoid labelling of unwanted intracellular proteins [338]. When coupled with one-dimensional electrophoresis, the co-migration of proteins separated in the same band with compromised resolution has been noticed [383, 384]. Additionally, this technique falls short of detecting quantitative changes and comparing the expression levels across multiple samples [376, 385]. In the present study, impermeable CyDye cell surface protein labelling and a detergent-based membrane fractionation were used for the enrichment of membrane proteins. While it has been demonstrated that membrane protein fractionation is unnecessary for CyDye cell surface labelling [213], our results showed that membrane fractionation (based on protein hydrophobicity) significantly reduced sample complexity. Although multiple membrane fractionations gave rise to the enrichment of membrane proteins, we have found that the fractionation technique in the present study was not able to exclude contamination by cytosolic proteins and other compartmental membrane proteins. This has also been recognised by other studies [338, 362]. Collectively, current fractionation techniques result in an enrichment of membrane proteins, rather than the complete elimination of other proteins. In the present study, a solution containing multiple chaotropes (dithiothreitol or DTT and thiourea) and sulfabetaine detergents was used to

improve the solubility. Additionally, optimized IEF running conditions were used in the first dimension to enhance the separation during IEF as previously described [214], due to the poor solubility and low abundance of hydrophobic membrane proteins.

#### *5.2.2.3 CyDye cell surface labelling does not exclude intracellular protein labelling.*

Another challenge associated with the study of the membrane proteome has been to eliminate cytosolic protein contamination from the membrane protein sample. Several strategies were performed in Mayrhofer's protocol to minimise unwanted intracellular labelling [213]. To assure the specificity of the CyDye labelling to surface proteins, cells were kept on ice prior to and during the labelling step, which minimised the possibility of dye transport across the plasma membrane [213]. The authors suggested that, even if the dye passed the membrane, the pH inside the cells (<7.4) was not suitable for the efficient labelling reaction as the pH value of the labelling buffer must be 8.5 for efficient labelling [213]. Furthermore, cells were exposed to the dye in a relatively short period of time (20 minutes) before the reaction was quenched with lysine which binds unreacted CyDye [386]. Despite these efforts, β-actin was identified from the MS analysis of Mayrhofer *et al* [213]. The incomplete removal of intracellular proteins from cell membrane protein preparations has been a consistent finding [213, 354]. Although the combination of DIGE/biotin labelling had substantially increased the percentage of membrane and membrane-associated proteins from 5 to 32%, significant amounts of other proteins were identified such as proteins related to mitochondrial (18%), cytoplasm (15%), nucleus (15%) and cytoskeleton (8%) [354]. In the present study, preliminary analysis of five randomly selected spots identified them as intracellular proteins. Multiple membrane protein enrichment steps failed to eliminate cytosolic proteins from the membrane protein preparations, as mildly hydrophobic cytosolic proteins remained in the detergent phase. Nonetheless this process gave rise to the enrichment of membrane proteins. It should be

noted that the impermeability of the plasma membrane is a prerequisite for the selective labelling of cell surface-exposed proteins [213]. However, EDTA detachment in the present study led to significant amount of non-viable dead cells (approximately 20% and similar to that seen using mechanical scrapping of adherent cells, data not shown). Not surprisingly, the leaking cell membrane of these cells led to non-specific CyDye labelling of abundant cytosolic proteins. Accordingly, alternative cell dissociation approaches were performed to minimise dead cell numbers and cytosolic protein contamination.

#### *5.2.2.4 Cell dissociation approaches*

To establish an overall profile of cell surface proteins, one of the technical challenges is to preserve the integrity of cell surface proteins without cleaving their structure when detaching adherent cells from the substratum. Proteolytic enzymes, such as trypsin, should be avoided as trypsin dissociation leads to the down-regulation of growth- and metabolism-related proteins and the up-regulation of apoptosis-related proteins [370]. Therefore, alternative cell dissociation reagents are used, such as EDTA and Accutase (a mild commercially available collagenase-based cell detachment solution). Clearly, in the protocol of Mayrhofer *et al* [213], the intact cell membrane is indispensible to avoid contaminating CyDye labelling of cytosolic proteins. Therefore, the cell viability after detachment is an important factor to consider. EDTA was used in our preliminary experiments following the protocol of Mayrhofer *et al*. EDTA is thought to preserve the cell surface protein structure, and is therefore suitable to investigate enzyme-sensitive cell surface proteins in studies using flow cytometry. However, due to its limited detachment potency, EDTA has trouble detaching tightly adherent cell types and cells cultured on the substratum for more than two days. Moreover, in studies using large cell numbers, the high proportion of necrotic or apoptotic cells after EDTA treatment (more than 20% trypan blue positive cells) made this cell detachment approach unsuitable for the present study.

Another alternative is temperature sensitive dishes, named as UpCell Surface (Nunc). UpCell Surface is coated with polymer poly (N-isopropylacrylamide), or PIPAAm, which is slightly hydrophobic at 37°C, assisting cell adherance to dishes, and becomes very hydrophilic below 32°C, leading to the release of adherent cells [387, 388]. This product allows cells to be harvested with high viability and intact surface proteins. However, in addition to the high cost of these dishes, one needs to consider that cells on UpCell Surface detach as a sheet or cluster, which would challenge the downstream applications requiring single cell suspension, such as flow cytometry and CyDye cell surface labelling. Similarly, there are technical and cost issues concerning the use of *in situ* CyDye labelling of cell populations directly in large culture preparations prior to cell detachment and the preparation of single cell suspensions thereafter for flow cytometric analysis.

In the present study, the 2-DE patterns of human GF after EDTA and collagenase treatment were studied. Following unwinding of the triple helical structures of collagen molecules, human collagenase is believed to cleave native collagens at a specific Gly-Leu or Gly-Ile bond, which is located at a locus 3/4 the distance from the N-terminus [389-392]. The lack of CyDye labelling of β-actin following collagenase treatment indicated that collagenase treatment gave satisfactory results for selective cell surface labelling. This was mainly due to the significant improvement in cell viability using collagenase versus EDTA (around 2% versus 20% trypan blue positive cells). Therefore, collagenase detachment was used in the present study (Chapter 6). In conclusion, the protocol for cell surface labelling on adherent cell populations such as GF favoured using collagenase as a dissociation reagent, followed by the enrichment of hydrophobic proteins using detergent-based phase separation. These techniques were used to investigate the surface protein profile of PDLSC.

# Chapter 6. Investigation of the cell surface proteome of periodontal ligament stem cells (PDLSC) using cell surface labelling

## 6.1 Introduction

Despite the encouraging outcomes for the therapeutic use of stem cells, their clinical application is still uncertain due to a lack of understanding of their properties and developmental status following *ex vivo* expansion. Of these, the heterogeneity present within stem cell populations hinders the clinical progress within the stem cell and regenerative medicine fields. The heterogeneity of morphology, proliferation and functions of stem cells indicates potential hierarchies of cellular differentiation [180], that is, different stages of cell immaturity [181]. In terms of the biological significance of this heterogeneity, it seems that subpopulations with distinct phenotypes demonstrate different biological functions [177]. Currently there is no single marker or set of markers that can distinguish different MSC-like populations of different origins from more differentiated fibroblastic cells in any tissue.

Periodontal diseases are highly prevalent among all human populations and if untreated cause the destruction of periodontal supporting tissues and can potentially result in tooth loss. The treatment of advanced periodontal diseases is beyond current technologies and therefore, alternative strategies are being investigated. Recently, the discovery of PDLSC has offered a novel therapeutic avenue for treating damaged periodontal tissues. PDLSC reside in the periodontium within various cell types including fibroblasts, endothelial cells, ERM cells, osteoblasts and cementoblasts [82]. The presence of multiple cell types within the periodontium requires the use of specific markers for the proper isolation and characterisation of each population. Studies have shown that PDLSC share a similar expression profile with BMSC, such as the positive expression of CD29, CD44, CD90 and

CD105 [153]. Importantly, PDLSC also express the early BMSC and perivascular cell surface markers STRO-1 and CD146/MUC18 [126]. In addition, a subset of PDLSC has been shown to express other antigens associated with perivascular tissues (alpha-smooth muscle actin and periocyte-associated antigen, 3G5) [5]. Taken together, these findings indicate a possible perivascular origin of PDLSC, in accord with the earlier findings by McCulloch and colleagues [143, 145]. However, comparative analyses showed that PDLSC exhibit higher expression levels of scleraxis (a tendon-specific transcription factor) [126] and periodontal ligament associated protein-1 (PLAP-1, which is a member of the class I small leucine-rich repeat proteoglycan family, also known as asporin) compared to bone marrow and dental pulp counterparts [202], suggesting unique features of PDLSC compared to BMSC and DPSC. A panel of markers has been proposed for the identification of PDLSC which include alkaline phosphatase, type I collagen, periostin, runt-related transcription factor-2 (Runx2) and epithelial growth factor receptor, which are also expressed by BMSC which is not surprising since both cell populations form a similar mineralised matrix in the form of cementum and bone, respectively [203]. As surface markers such as CD29, CD44, CD90, CD73, CD105, CD146 and others are ubiquitously expressed by MSC-like populations derived from all dental tissues, specific cell surface markers have yet to be identified capable of distinguishing between individual dental stem cell population subsets [133]. Therefore, our understanding of the cell surface phenotype of PDLSC falls short when considering the need to isolate and purify stem/progenitor cell subsets from the heterogeneous PDL populations. This has driven the use of technologies investigating global protein expression (proteomics) to characterise the cell surface phenotype of PDLSC.

Studies investigating dental tissues using proteomic techniques have been summarized by McCulloch [350]. In comparison to the publications on protein expression by periodontal

microbiota [393-395], only limited numbers of papers have been published examining the protein expression by periodontal ligament cells and tissues [350]. The first proteomic reference map of undifferentiated periodontal ligament fibroblasts identified 117 proteins consistently expressed across three clones, which included a variety of expected cytoskeleton- and metabolism-related proteins [396]. A number of novel proteins were also identified, however the significance of their expression was not discussed. A comparative proteome analysis revealed that the percentage of total proteins identified as cytoskeleton-related was higher in periodontal ligament fibroblasts (26.5%) compared with dermal fibroblasts (15%). This difference may relate to the mechanical loading and remodelling of periodontal ligament. Another study using difference in gel electrophoresis (DIGE) reported that a total of 29 proteins were differentially expressed during early cementoblastic/osteogenic differentiation of PDLSC [397]. Reduced expression of cytoskeletal proteins vimentin, caldesmon and tropomyosin was thought to relate to cytoskeletal rearrangements during differentiation processes, while the regulation of binding partners caldesmon and tropomyosin also plays a role in cytokenesis. This study also detected the decreased expression of heterogeneous nuclear ribonucleoprotein C (hnRNPC) (approximately two-fold) during osteogenic differentiation, however, this was in contrast to previous findings in BMSC [398]. Interestingly, higher expression of the calcium-binding protein Annexin A4 was noted following osteogenic differentiation. Annexins are thought to play an important role in osteogenic development, including Annexin A2 and A5 which are highly expressed in skeletal tissues and up-regulated in osteogenic cultures of MSC [399, 400]. In the third study, a direct comparison of protein expression profiles between ovine PDLSC, DPSC and BMSC identified 58 differentially expressed proteins between at least two MSC populations, with six proteins upregulated in PDLSC relative to both DPSC and BMSC, five proteins upregulated in DPSC relative to both PDLSC and BMSC, and one protein upregulated in BMSC relative to both PDLSC

and DPSC [346]. More importantly, all three cell populations were derived from individual donors, thus eliminating the possibility that differentially expressed proteins were a consequence of inter-donor variability. Higher PDLSC expression of heat shock protein beta 1, Annexin A3 and Annexin A4 compared to DPSC and BMSC was thought to relate to high turnover of periodontal tissues due to mastication loads and the remodelling of these tissues. While these PDLSC proteomic studies present some interesting findings, more extensive investigation of the expression of less abundant membrane, nuclear or signalling-related proteins has yet to be attempted.

In this chapter, based on the experimental conditions optimised in Chapter 5, we aim to provide an insight into the cell surface proteome of PDLSC to identify potential markers that could discriminate PDLSC from other periodontal derived populations such as ERM. Briefly, PDLSC were detached from the substratum using collagenase before cell surface labelling with CyDye. Following cell lysis, hydrophobic proteins, predominantly membrane proteins, were enriched using a detergent-based phase separation kit. Following this, the membrane protein preparations were separated using 2-DE and selected protein "spots" were identified using MS. To confirm the expression of selected proteins, flow cytometric and immunocytochemical analyses were performed to investigate their expression in human PDLSC, GF and keratinocytes derived from three donors, and ovine PDLSC and ERM derived from three individual sheep.

## 6.2 Results

### *6.2.1 Membrane protein expression of ex-vivo expanded human PDLSC*

Immobilized pH gradient (IPG) strips with a pI range of pH 3-10 were used to separate CyDye-labelled membrane associated proteins derived from human PDLSC following *ex vivo* expansion. The use of broad-range strips (pH 3–10) allows the display of most

proteins in a single gel. Proteins with a molecular weight range of 10-110 kDa were separated in the second dimension using 8% polyacrylamide gels (8% T, 3.3% C, 0.1% SDS and 375 mM Tris/HCl pH 8.8). Proteins were detected using a fluorescent imager (Typhoon Trio Variable Mode Imager with a pixel resolution of 100 µm) and analysed using PD-Quest v8.0 software and DyCyder v6.5 software. A total of four replicate gels were used for analysis. Representative raw 2-DE gels are shown in Figure 6.1. Based on the CyDye imaging, a total of 80 well-resolved protein spots were detected after automatic exclusion of pseudospots. The location of identified protein spots on the raw image is shown in Figure 6.2.

### 6.2.2 Protein identification

Following spot excision using automated spot picking (section 2.5.8) and in-gel digestion (section 2.5.9), all 80 well-resolved protein spots were identified by liquid chromatography-electrospray ionisation ion-trap (LC-ESI-IT) mass spectrometry (MS) and database searching. A total of 32 protein spots were identified as membrane-associated proteins. Table 6.1 shows details of these membrane-associated proteins, including the protein name, spot number, predicted molecular weight and pI values, ID/total queries, combined ion scores and coverage. Some proteins were identified in two or several spots (e.g. 5'-nucleotidase, Annexin A2 and sphingosine kinase 1), suggesting the presence of isoforms, possibly as a result of post-translational modifications. Differences in the observed molecular weight/pI and the expected values were observed in some proteins (e.g. sphingosine kinase 1), possibly due to post-translational modifications, proteolysis or protein aggregation. Importantly, this approach was validated by the identification of well known MSC associated stem cell surface proteins such as 5'-nucleotidase (also known as CD73) and Thy-1 membrane glycoprotein (also known as CD90), previously shown to be expressed by PDLSC [153]. Furthermore, MS identification showed the presence of other

membrane associated markers such as Annexin A2 and sphingosine kinase 1, which had not been reported previously as surface proteins expressed by human PDLSC. All four proteins were chosen for further confirmatory analyses.

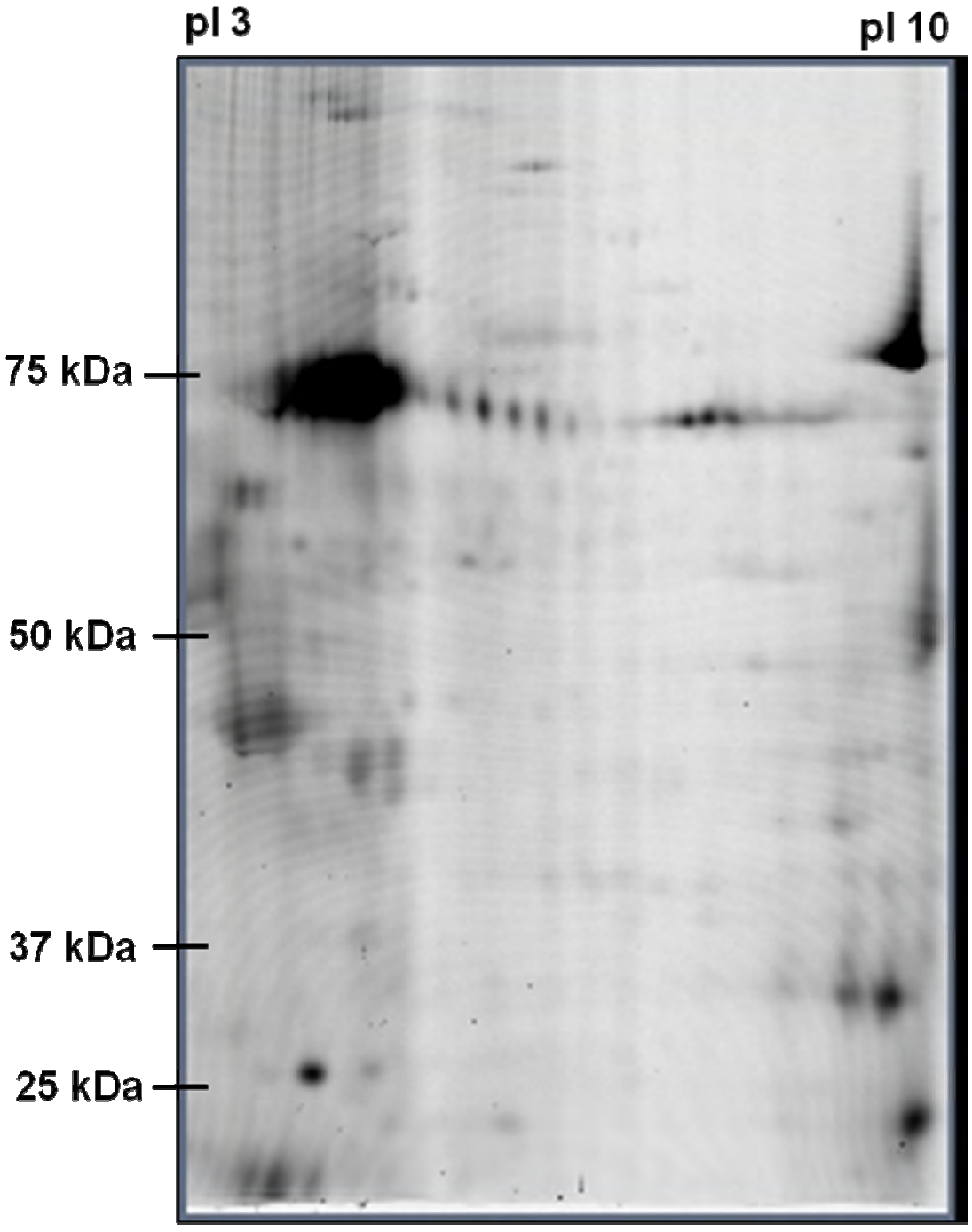


**Figure 6.1 Representative raw 2-DE gels of CyDye labelled proteins of *ex vivo* expanded human periodontal ligament stem cells (PDLSC)**

Following cell surface labelling with CyDye and membrane protein enrichment, proteins were separated by 2-DE using a pI range of pH 3-10 and a molecular weight range of 10-110 kDa. Following image analysis, 80 well-resolved protein spots were detected.

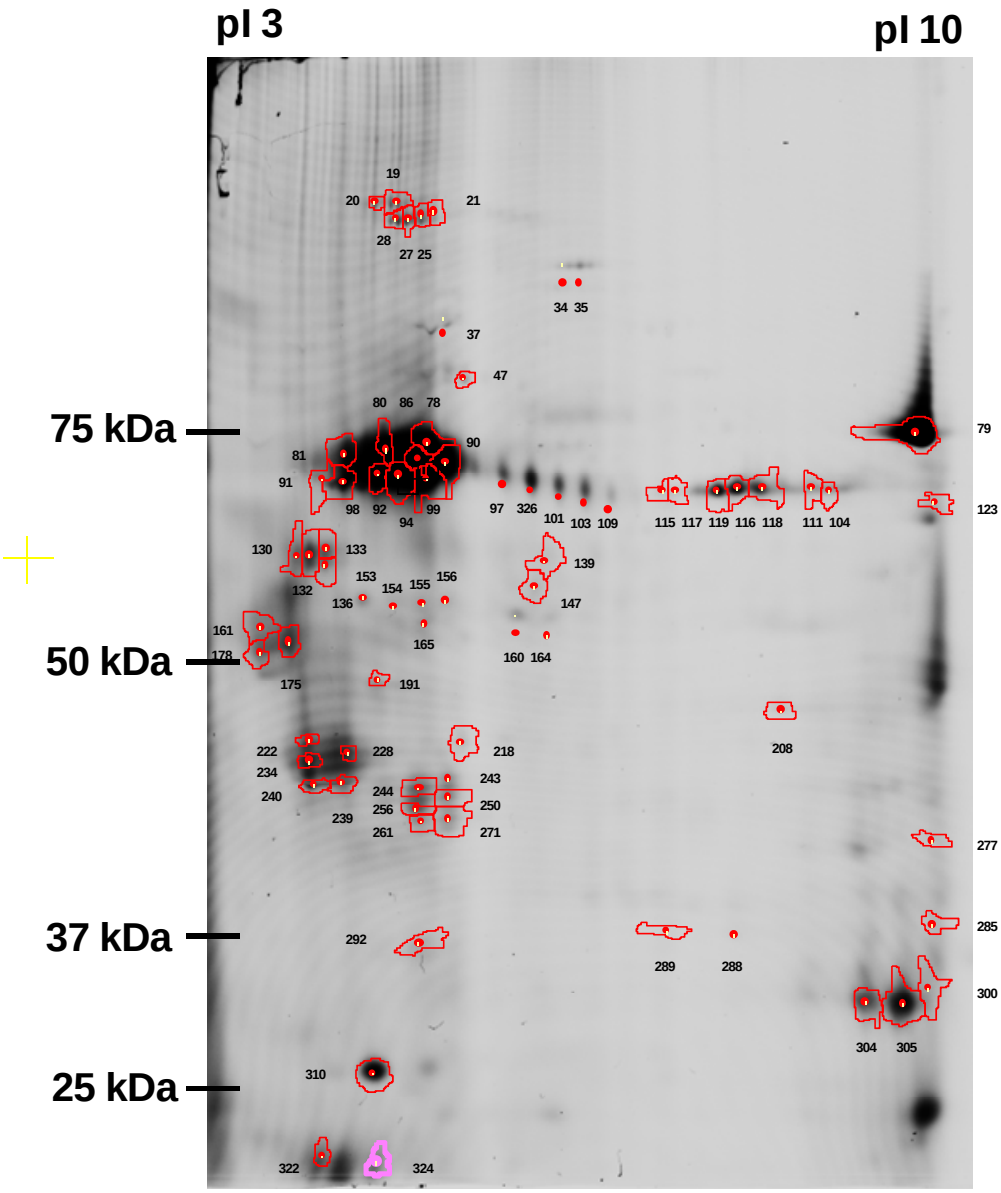


**Figure 6.2 The location of protein spots identified on the raw 2-DE image**

A total of 32 membrane associated protein spots were consistently identified on replicate gels.

**Table 6.1 Membrane-associated proteins on human PDLSC**

| SwissProt 57.7 Accession No. | Protein name | Spot No. | Predicted MW(kDa)/pI | ID/Total queries | Combined ion scores | Coverage (%) |
|---|---|---|---|---|---|---|
| 1A01_HUMAN | HLA class I histocompatibility antigen, A-1 alpha chain | 243 | 41.1/6.1 | 2/612 | 66 | 10 |
| 1C06_HUMAN | HLA class I histocompatibility antigen, Cw-6 alpha chain | 239 | 41.4/5.7 | 4/638 | 175 | 18 |
| 5NTD_HUMAN | 5'-nucleotidase | 78 | 63.9/6.6 | 13/518 | 287 | 17 |
| | | 80 | 63.9/6.6 | 8/513 | 206 | 11 |
| | | 90 | 63.9/6.6 | 41/546 | 872 | 32 |
| | | 99 | 63.9/6.6 | 13/535 | 191 | 15 |
| | | 101 | 63.9/6.6 | 39/517 | 945 | 38 |
| | | 103 | 63.9/6.6 | 42/539 | 933 | 33 |
| | | 109 | 63.9/6.6 | 25/536 | 606 | 22 |
| | | 111 | 63.9/6.6 | 2/558 | 34 | 6 |
| | | 326 | 63.9/6.6 | 53/544 | 961 | 35 |
| | | 86 | 63.9/6.6 | 25/356 | 521 | 31 |
| | | 97 | 63.9/6.6 | 45/414 | 1044 | 39 |
| AMPB_HUMAN | Aminopeptidase B | 94 | 73.2/5.5 | 5/559 | 172 | 10 |
| ANXA2_HUMAN | Annexin A2 | 285 | 38.8/7.6 | 36/581 | 489 | 47 |
| | | 288 | 38.8 /7.6 | 87/585 | 1907 | 67 |
| | | 289 | 38.8/7.6 | 56/600 | 950 | 55 |
| | | 292 | 38.8/7.6 | 3/594 | 76 | 11 |
| | | 304 | 38.8/7.6 | 14/536 | 241 | 28 |
| CAP2_HUMAN | Adenylyl cyclase-associated protein 2 | 154 | 53.1/6.0 | 2/576 | 67 | 6 |
| | | 156 | 53.1/6.0 | 4/557 | 102 | 8 |
| | | 165 | 53.1/6.0 | 3/619 | 102 | 11 |
| CO1A1_HUMAN | Collagen alpha-1(I) chain | 292 | 139.9/5.6 | 7/594 | 103 | 4 |
| CO6A3_HUMAN | Collagen alpha-3(VI) chain | 20 | 345.2/6.3 | 9/568 | 159 | 3 |

| | | | | | | |
|---|---|---|---|---|---|---|
| DNJA1_HUMAN | DnaJ homolog subfamily A member 1 | 208 | 45.6/6.6 | 4/521 | 95 | 12 |
| EHD3_HUMAN | EH domain-containing protein 3 | 139 | 62.0/6.1 | 4/600 | 71 | 8 |
| EZRI_HUMAN | Ezrin | 65 | 69.5/5.9 | 28/558 | 455 | 26 |
| FLNC_HUMAN | Filamin-C | 29 | 293.4/5.6 | 4/492 | 49 | 2 |
| | | 78 | 293.4/5.6 | 3/518 | 65 | 1 |
| | | 139 | 293.4/5.6 | 14/600 | 363 | 6 |
| | | 147 | 293.4/5.6 | 13/525 | 237 | 4 |
| | | 191 | 293.4/5.6 | 4/586 | 147 | 2 |
| GELS_HUMAN | Gelsolin | 46 | 86.0/5.9 | 46/636 | 1011 | 35 |
| K2C1_HUMAN | Keratin, type II cytoskeletal 1 | 25 | 66.2/8.2 | 5/578 | 128 | 9 |
| | | 46 | 66.2/8.2 | 11/636 | 456 | 17 |
| | | 47 | 66.2/8.2 | 7/491 | 170 | 7 |
| | | 80 | 66.2/8.2 | 11/513 | 227 | 13 |
| | | 91 | 66.2/8.2 | 3/666 | 94 | 12 |
| | | 94 | 66.2/8.2 | 4/559 | 146 | 8 |
| | | 98 | 66.2/8.2 | 2/639 | 57 | 7 |
| | | 104 | 66.2/8.2 | 2/520 | 80 | 3 |
| | | 111 | 66.2/8.2 | 5/558 | 79 | 10 |
| | | 130 | 66.2/8.2 | 3/614 | 60 | 8 |
| | | 147 | 66.2/8.2 | 20/525 | 256 | 13 |
| | | 153 | 66.2/8.2 | 2/615 | 126 | 7 |
| | | 154 | 66.2/8.2 | 3/576 | 107 | 8 |
| | | 228 | 66.2/8.2 | 10/664 | 466 | 22 |
| | | 289 | 66.2/8.2 | 14/600 | 386 | 15 |
| | | 292 | 66.2/8.2 | 2/594 | 55 | 3 |
| | | 324 | 66.2/8.2 | 5/570 | 127 | 10 |
| KAP2_HUMAN | cAMP-dependent protein kinase type II-alpha regulatory subunit | 178 | 45.8/5.0 | 13/621 | 360 | 22 |
| NOMO2_HUMAN | Nodal modulator 2 | 19 | 140.4/5.5 | 9/599 | 244 | 8 |

| | | | | | | |
|---|---|---|---|---|---|---|
| | | 20 | 140.4/5.5 | 10/568 | 189 | 12 |
| | | 25 | 140.4/5.5 | 10/578 | 226 | 8 |
| | | 27 | 140.4/5.5 | 11/583 | 224 | 10 |
| | | 28 | 140.4/5.5 | 11/436 | 244 | 12 |
| NUCB2_HUMAN | Nucleobindin-2 | 178 | 50.3/5.0 | 3/621 | 100 | 5 |
| PDIA6_HUMAN | Protein disulfide-isomerase A6 | 175 | 48.5/5.0 | 6/592 | 209 | 12 |
| | | 178 | 48.5/5.0 | 7/621 | 278 | 10 |
| RUVB2_HUMAN | RuvB-like 2 | 191 | 51.3/5.5 | 25/586 | 614 | 34 |
| SBP1_HUMAN | Selenium-binding protein 1 | 165 | 52.9/5.9 | 7/619 | 126 | 8 |
| SNX4_HUMAN | Sorting nexin-4 | 155 | 52.2/5.7 | 5/637 | 157 | 14 |
| SPHK1_HUMAN | Sphingosine kinase 1 | 19 | 42.9/6.6 | 12/599 | 253 | 18 |
| | | 20 | 42.9/6.6 | 5/568 | 188 | 16 |
| | | 21 | 42.9/6.6 | 4/518 | 138 | 11 |
| | | 34 | 42.9/6.6 | 3/517 | 200 | 11 |
| STML2_HUMAN | Stomatin-like protein 2 | 239 | 38.6/6.9 | 13/638 | 584 | 37 |
| | | 240 | 38.6/6.9 | 6/656 | 266 | 27 |
| STXB3_HUMAN | Syntaxin-binding protein 3 | 111 | 68.6/8.0 | 5/558 | 97 | 7 |
| | | 118 | 68.6/8.0 | 6/479 | 103 | 7 |
| SWP70_HUMAN | Switch-associated protein 70 | 94 | 69.4/5.7 | 3/559 | 80 | 5 |
| | | 99 | 69.4/5.7 | 6/535 | 136 | 7 |
| THY1_HUMAN | Thy-1 membrane glycoprotein | 304 | 18.2/9.0 | 3/536 | 55 | 16 |
| UBP14_HUMAN | Ubiquitin carboxyl-terminal hydrolase 14 | 130 | 56.5/5.2 | 6/614 | 176 | 15 |
| | | 132 | 56.5/5.2 | 8/611 | 184 | 18 |
| | | 133 | 56.5/5.2 | 3/635 | 100 | 5 |
| | | 136 | 56.5/5.2 | 15/642 | 372 | 24 |
| ULA1_HUMAN | NEDD8-activating enzyme E1 regulatory subunit | 133 | 60.7/5.2 | 6/635 | 127 | 8 |

| | | | | | | |
|---|---|---|---|---|---|---|
| VATB2_HUMAN | V-type proton ATPase subunit B, brain isoform | 153 | 56.8/5.6 | 4/615 | 191 | 12 |
| | | 154 | 56.8/5.6 | 9/576 | 252 | 14 |
| | | 155 | 56.8/5.6 | 7/637 | 300 | 16 |
| VDAC1_HUMAN | Voltage-dependent anion-selective channel protein 1 | 300 | 30.9/8.6 | 7/601 | 128 | 18 |
| | | 304 | 30.9/8.6 | 34/536 | 902 | 59 |
| | | 305 | 30.9/8.6 | 19/524 | 319 | 38 |
| VIME_HUMAN | Vimentin | 130 | 53.7/5.1 | 2/614 | 68 | 6 |
| | | 161 | 53.7/5.1 | 28/626 | 710 | 46 |
| | | 175 | 53.7/5.1 | 44/592 | 1026 | 63 |
| | | 178 | 53.7/5.1 | 46/621 | 1306 | 58 |
| | | 222 | 53.7/5.1 | 3/630 | 87 | 6 |
| | | 228 | 53.7/5.1 | 5/664 | 139 | 9 |
| | | 239 | 53.7/5.1 | 4/638 | 139 | 9 |
| | | 240 | 53.7/5.1 | 5/656 | 169 | 12 |
| VINC_HUMAN | Vinculin | 25 | 124.3/5.5 | 14/578 | 226 | 16 |
| | | 27 | 124.3/5.5 | 30/583 | 643 | 25 |

### 6.2.3 Validation of the expression of 5'-nucleotidase, Thy-1 membrane glycoprotein, Annexin A2 and sphingosine kinase 1

To confirm the expression of selected proteins, including CD73, CD90, Annexin A2 and Sphingosine Kinase 1 (SPK1), additional studies were performed to investigate their expression in human PDLSC, GF and keratinocytes (epithelial cell population) derived from three different donors, and ovine PDLSC and ERM derived from three individual sheep.

Following cell dissociation using Type I collagenase (section 2.5.1), flow cytometric analysis was used to demonstrate the surface expression of the selected proteins. Human PDLSC from three donors showed high surface expression for CD73 and CD90, where they showed low cell surface levels of Annexin A2 expression (Figure 6.3). The phenotypic profiles of human GF were similar to those of human PDLSC, as shown in Figure 6.4. In contrast, human keratinocytes showed a lack of cell surface expression for CD73, CD90 and Annexin A2 (Figure 6.5). No reactivity was observed with anti-CD73 and anti-CD90 antibodies to ovine PDLSC which appeared to only be reactive against human epitopes (Figure 6.6). However, ovine PDLSC showed low level expression for Annexin A2 (Figure 6.6). Ovine ERM cells demonstrated a similar phenotype as ovine PDLSC in the expression of Annexin A2 and no reaction was detected for anti-CD73 and anti-CD90 antibodies (Figure 6.7). Table 6.2 summarises the surface expression of these four antigens on various cell types. In summary, CD73 and CD90 were found to be expressed by human PDLSC and GF, but not by human keratinocytes, confirming that they are MSC-associated markers. The reaction of CD73 and CD90 was not detected in ovine PDLSC or ERM cells, as these two antibodies may not react with ovine epitopes. Annexin A2 was demonstrated to be expressed at low levels by human PDLSC (1.92-7.83%), human GF (2.41-4.66%), ovine PDLSC (8.05-12.45%) and ovine ERM cells (1.25-10.60%), while human keratinocytes were largely negative for Annexin A2 expression

(0.88-1.64%). Previous studies have shown that SPK1 can translocate to the plasma membrane upon cell stimulation by cytokines [401-407]. No positive expression with the anti-SPK1 antibody was detected in either human or ovine cells by flow cytometric analysis (data not shown), most likely because the available antibody reagent did not react with the extracellular domain of SPK1.

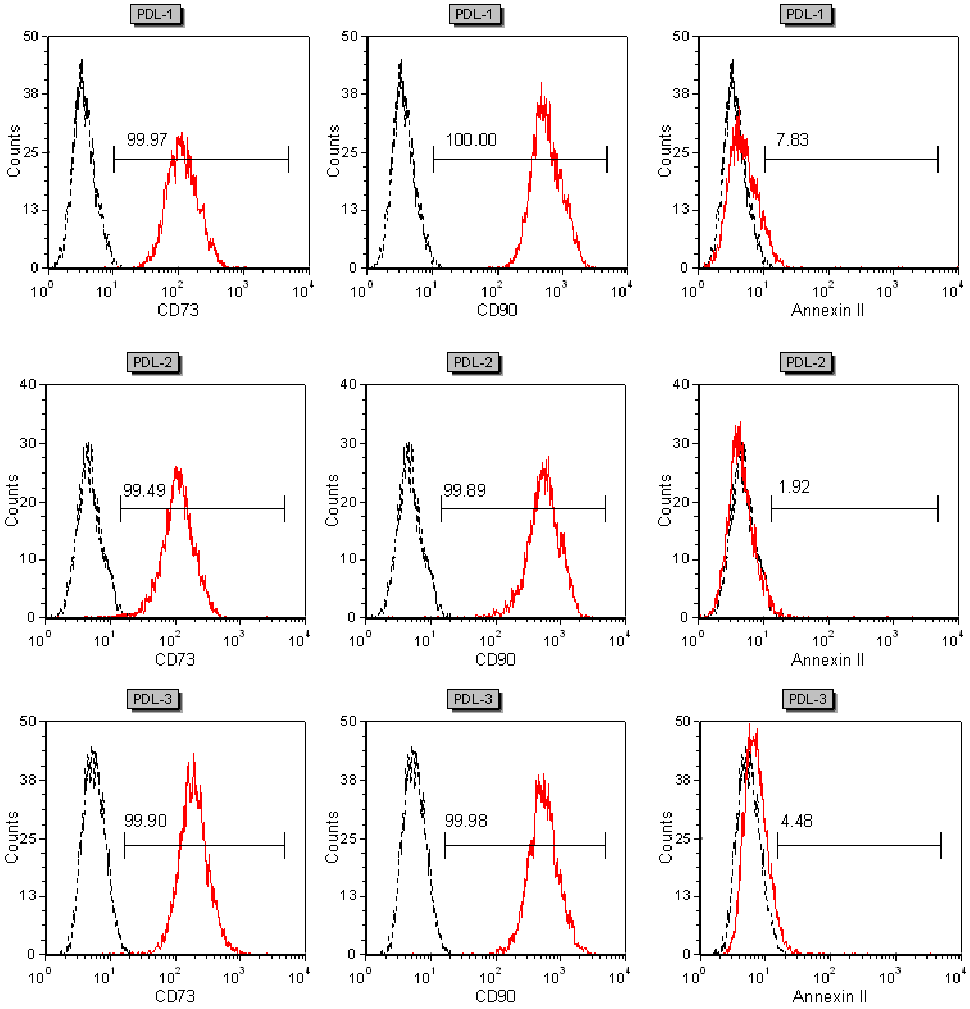


**Figure 6.3 Validation of cell surface expression of CD73, CD90 and Annexin A2 using flow cytometric analysis in human periodontal ligament stem cells (PDLSC)**

Human PDLSC from three donors showed highly positive expression for CD73 and CD90 and low level expression for Annexin A2 (Annexin II). Three human donors were used (PDL 1-3).

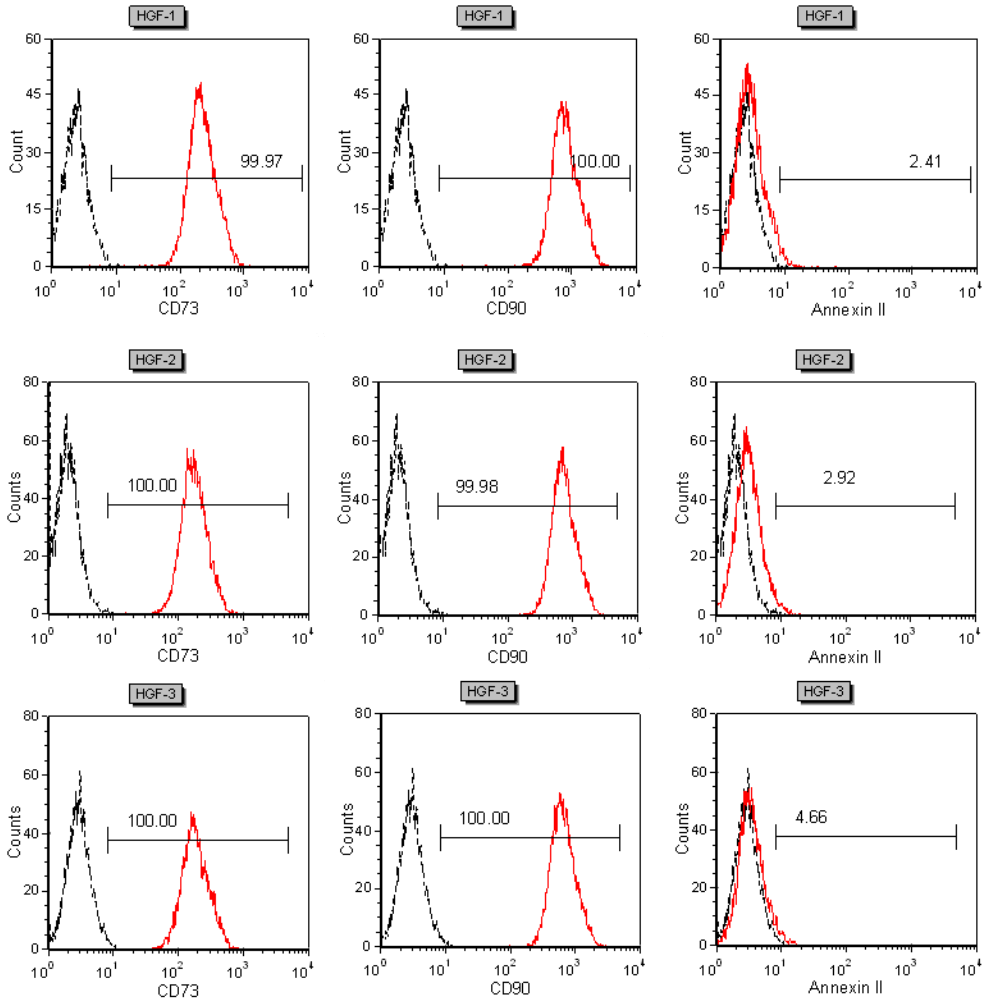


**Figure 6.4 Validation of cell surface expression of CD73, CD90 and Annexin A2 using flow cytometric analysis in human gingival fibroblasts (HGF)**

Human GF from three donors showed highly positive expression for CD73 and CD90, and low level expression for Annexin A2 (Annexin II). Three human donors were used (HGF 1-3).

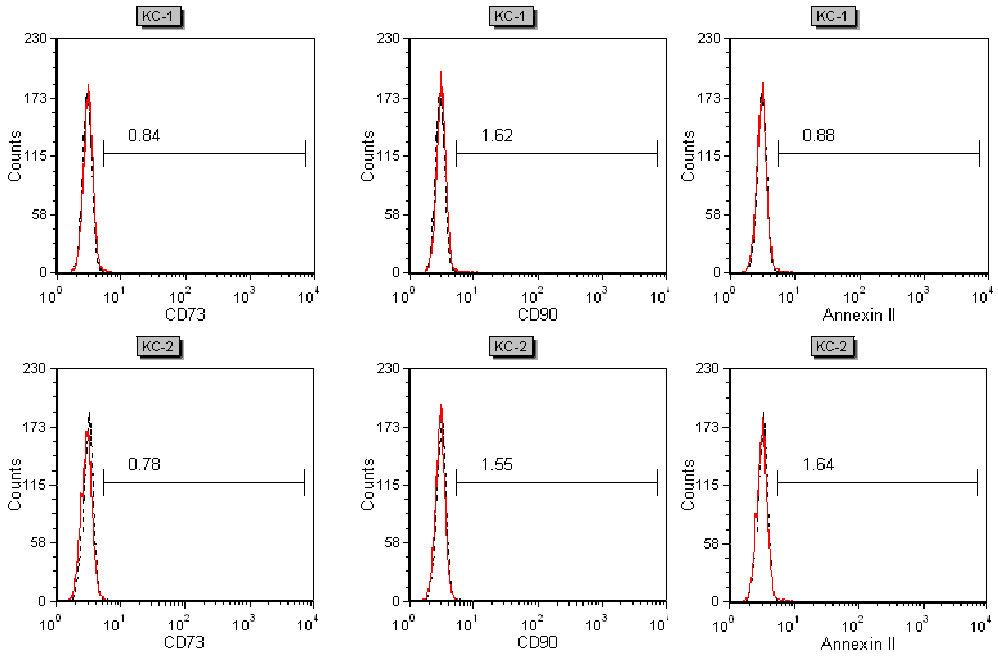


**Figure 6.5 Validation of cell surface expression of CD73, CD90 and Annexin A2 using flow cytometric analysis in human keratinocytes**

Human keratinocytes from two donors (KC 1-2) showed negative expression for CD73, CD90 and Annexin A2 (Annexin II).

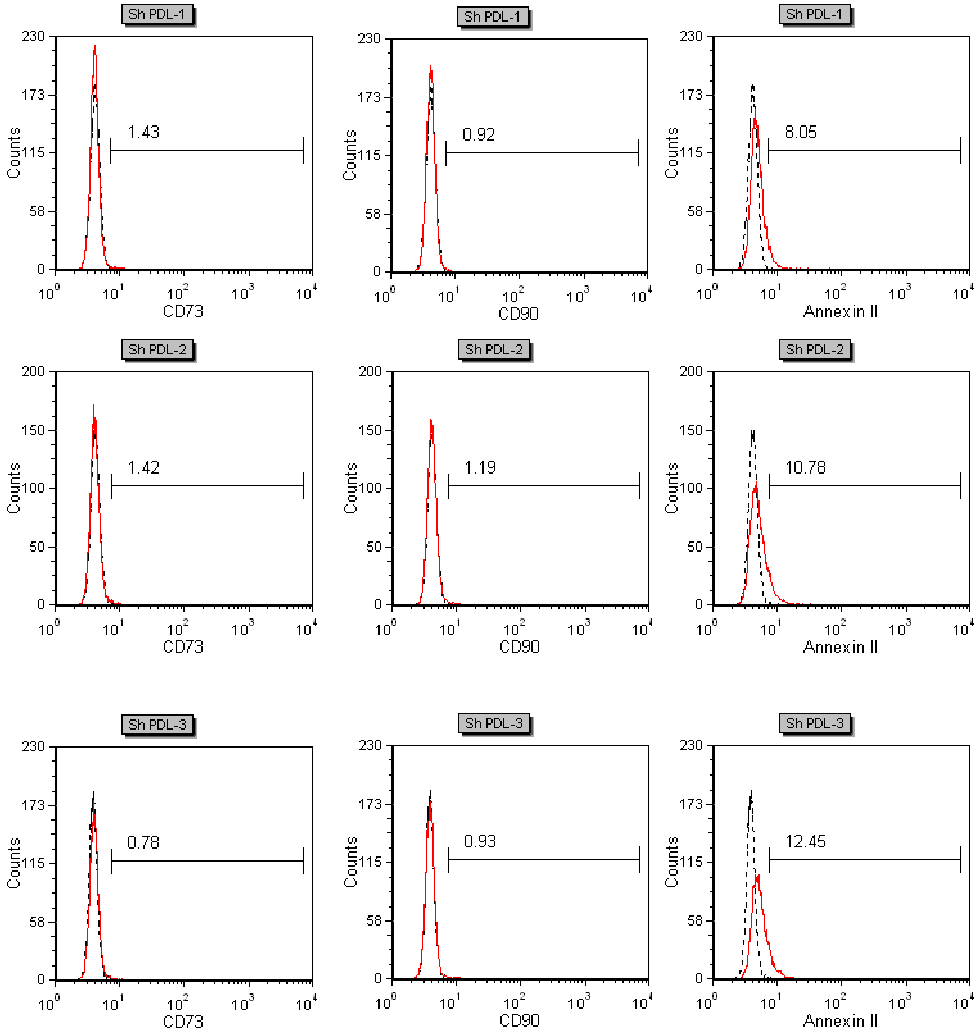


**Figure 6.6 Validation of cell surface expression of CD73, CD90 and Annexin A2 using flow cytometric analysis in ovine periodontal ligament stem cells (PDLSC)**

No reactivity was observed with the anti-CD73 and anti-CD90 antibodies to ovine PDLSC, which showed low level expression for Annexin A2 (Annexin II). Three ovine donors were used (Sh PDL 1-3).

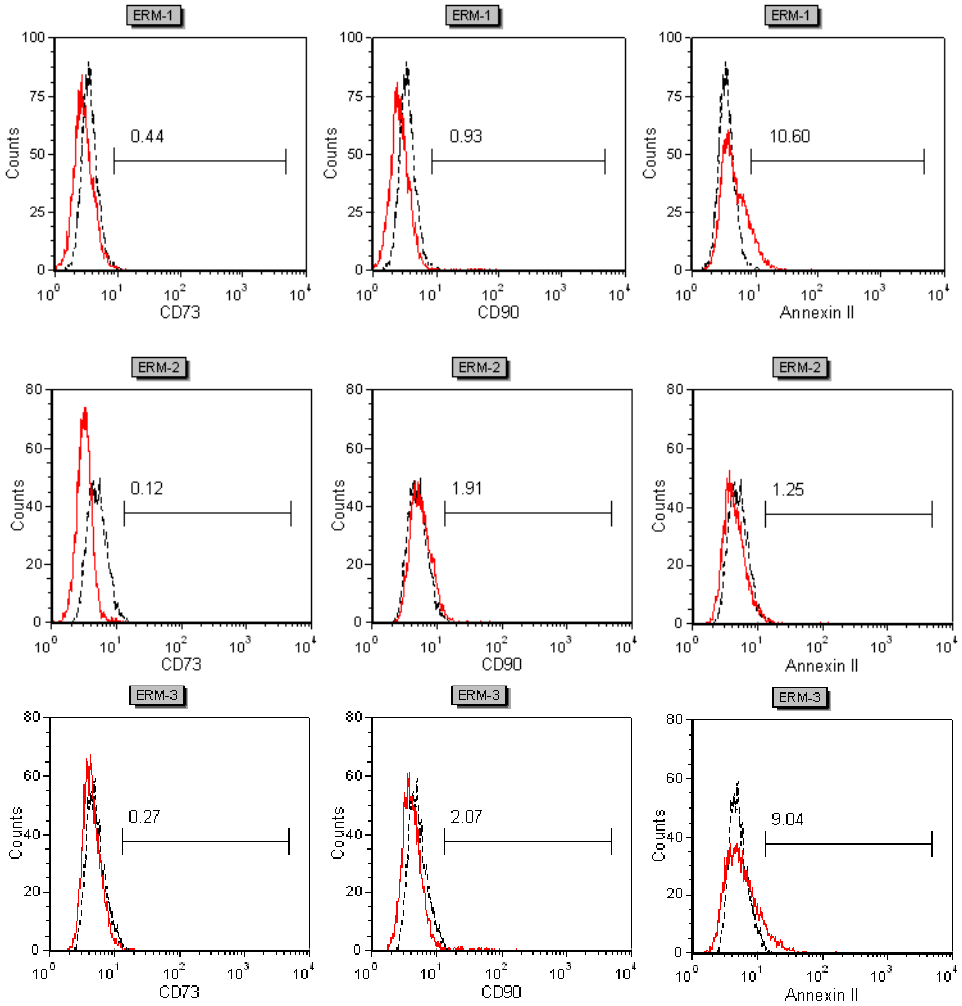


**Figure 6.7 Validation of cell surface expression of CD73, CD90 and Annexin A2 using flow cytometric analysis in ovine Epithelial cell Rests of Malassez (ERM)**

No reactivity was observed with the anti-CD73 and anti-CD90 antibodies to ovine ERM, which showed low level expression for Annexin A2 (Annexin II). Three ovine donors were used (ERM 1-3).

**Table 6.2 Cell surface expression of CD73, CD90 and Annexin A2 by flow cytometric analysis. Data represent median %(range).**

| | Human PDLSC | Human GF | Human Keratinocyte | Ovine PDLSC | Ovine ERM |
|---|---|---|---|---|---|
| CD73 | 99.90 (99.49-99.97) | 99.97 (99.97-100.00) | (0.78-0.84) | 1.42 (0.78-1.43) | 0.27 (0.12-0.44) |
| CD90 | 99.98 (99.89-100.00) | 99.98 (99.98-100.00) | (1.55-1.62) | 0.93 (0.92-1.19) | 1.91 (0.93-2.07) |
| Annexin A2 | 4.48 (1.92-7.83) | 2.92 (2.41-4.66) | (0.88-1.64) | 10.78 (8.05-12.45) | 9.04 (1.25-10.60) |

Additional studies were performed to investigate the expression of Annexin A2 and SPK1 in human PDLSC, GF and keratinocytes, ovine PDLSC and ERM using immunocytochemical analysis following permeabilization of the cellular membrane using Triton X-100 (0.25%). All cell types studied were shown to be positive to anti-Annexin A2 and anti-SPK1 antibodies (Figure 6.8). Of note, no reactivity was observed with the anti-CD73 or anti-CD90 antibodies to the five cell types examined (data not shown), indicating that the specific epitopes identified by these antibodies were compromised following processing for immunocytochemical analysis.

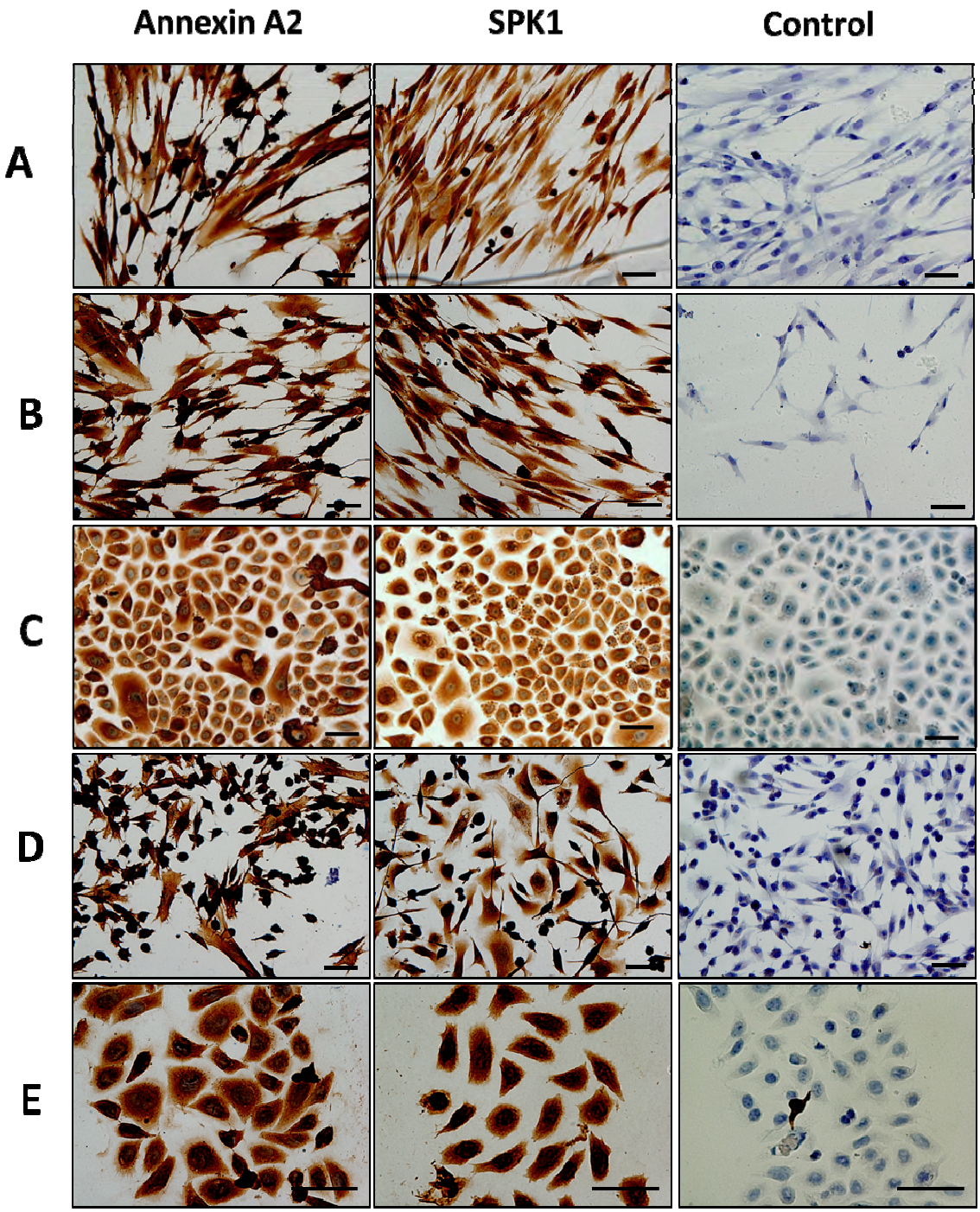


**Figure 6.8 The expression of Annexin A2 and Sphingosine Kinase 1 (SPK1) in various human and ovine cell populations using immunocytochemical analysis**

All cell types studied were shown to be positive to anti-Annexin A2 and anti-SPK1 antibodies. (A) human periodontal ligament stem cells (PDLSC), (B) human gingival fibroblasts (GF), (C) human keratinocytes, (D) ovine PDLSC, (E) ovine Epithelial cell Rest of Malassez (ERM). Scale bar=50 µm

## 6.3 Discussion

The aim of the present study was to demonstrate the cell surface expression profiles of human PDLSC and to compare the expression of prospective cell surface markers in human GF, human keratinocytes (as a source of epithelial cells), ovine PDLSC and ovine ERM. Unfortunately we were unable to analyse the cell surface proteome of human or ovine ERM due to technical challenges in this type of analysis. These included the low proliferation rate of ERM cells which made it difficult to obtain sufficient amounts of membrane enriched protein for 2-DE analysis. ERM cells were also tightly adhered to the surface of the flask precluding cell dissociation using collagenase. Four proteins were selected for validation; CD73, CD90, Annexin A2 and SPK1. CD73 and CD90 were further characterised as they are well known MSC-associated markers. Annexin A2 was selected as it is calcium dependent [408-414] and has been reported to be associated with the stem cell niche [415-421]. SPK1 has recently been demonstrated to be associated with the progenitor phenotype of endothelial cells [422]. CD73 and CD90 were highly expressed by human PDLSC and GF but not by human keratinocytes, indicating that these antigens could be used as potential markers for distinguishing between mesenchymal cells and epithelial cell populations. Whether their ovine equivalents (PDLSC and GF) display similar expression of CD73 and CD90 awaits investigation using antibodies manufactured to be reactive against ovine epitopes. Annexin A2 was demonstrated to be expressed on the cell surface at low copy number by human PDLSC, human GF, ovine PDLSC and ovine ERM cells using flow cytometric analysis, while human keratinocytes lacked any cell surface expression of Annexin A2. The positive reaction using anti-SPK1 antibody was detected in all the cell types studied using immunocytochemical analysis.

### 6.3.1 CD73

CD73, also known as ecto-5'-nucleotidase (ecto-5'-NT, EC 3.1.3.5), consists of a dimer of two identical 70kD subunits linked by glycosyl phosphatidylinositol (GPI). It is originally defined as a lymphocyte differentiation antigen that functions as a co-signaling molecule on T lymphocytes and is required for lymphocyte binding to endothelium [423]. CD73 has been shown to be expressed on various cell types, including lymphocytes, endothelial cells, and MSC. It is thought to play a physiological role in epithelial ion and fluid transport, maintaining barrier functions, mediating endothelial permeability, adapting to hypoxia and contributing to microbial responses [424]. CD73 is a cell surface enzyme that converts adenosine 5'-monophosphate (AMP) to its bioactive intermediate, adenosine, which in turn activates adenosine receptors when released into the extracellular space and regulates various physiologic functions [424]. As shown in Figure 6.9, ATP is catalysed by CD39 to form the intermediates ADP and AMP, which is subsequently converted to immunosuppressive adenosine by CD73 [425]. In other words, the balance between adenosine and ATP in immune homeostasis may be regulated by CD39 and CD73 as a result of the conversion of immunostimulatory ATP to immunosuppressive and anti-inflammatory adenosine [425].

As the generation of immunosuppressive adenosine is catalysed by CD73, the expression of CD73 might be correlated with the immunomodulatory properties of MSC. In addition to well-documented immunosuppressive factors such as tryptophan catabolizing enzyme indoleamine 2,3-dioxygenase (IDO), TGF-β1, hepatocyte growth factor and Prostaglandin $E_2$ ($PGE_2$) [115], adenosine signalling modulated by CD39 and CD73 expression has been highlighted as a novel modulator in the immunosuppression of T-cell proliferation by MSC [426, 427]. As adenosine has been shown to modulate activated T-cell proliferation through the adenosine A2A receptor [426], the blockage of the adenosine pathway

diminishes MSC-mediated immunosuppression of T cell proliferation [426]. A recent study demonstrated the immunomodulatory properties of PDLSC and suggested that PDLSC can be used as a potential allogeneic stem cell source for periodontal tissue engineering [153]. Can these properties be regulated through the up or down-regulation of CD73 expression? Moreover, CD73 expression on human GF has been shown to inhibit interleukin-1α-induced granulocyte-macrophage colony stimulating factor (GM-CSF) production and thus exhibits an anti-inflammatory effect in periodontal disease [428]. Promising data warrant further analysis of the therapeutic potential of adenosine signalling by CD39 and CD73 expression in MSC and its potential in the treatment of inflammatory diseases. Taken together, CD73 is an extracellular enzyme that catalyzes the formation of immunosuppressive adenosine. This mechanism may also contribute to the immunomodulatory properties of PDLSC [153], and may offer an avenue for anti-inflammatory therapy in periodontal disease.

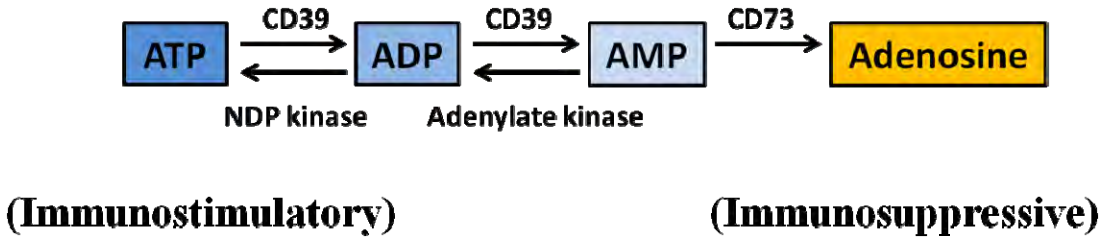


**Figure 6.9 CD73 is involved in the generation of adenosine**

Immunostimulatory ATP is catalysed by CD39 to form the intermediates ADP and AMP, which is subsequently converted to immunosuppressive adenosine by CD73. The conversion of ATP to AMP can be reversed by adenylate kinase and NDP kinase.

### 6.3.2 CD90

The expression of CD90 on PDLSC has been well documented [153, 429-431], however, the role of CD90 expression in PDLSC remains largely unknown. CD90, also known as Thy-1 (Thymocyte differentiation antigen-1), is a 25-37kD glycosyl phosphatidylinositol (GPI)-anchored glycoprotein first identified in the thymus as a T-cell maturation and

differentiation marker. It is a highly glycosylated membrane protein with 30% of its molecular mass consisting of carbohydrate [432]. CD90 is highly conserved throughout evolution [433] existing in both membrane-bound and soluble forms [433]. CD90 (Thy-1) is found to be expressed in various cell types such as hematopoietic stem/progenitor cells [434], hepatic stem cells in human fetal liver [435], liver cancer stem cells [436], neurons, fibroblasts, vascular pericytes and MSC [433]. The expression of CD90 differs by species [432]; for example it is present in mice peripheral T cells but not in human T cells [433]. While Thy-1 is present on mouse keratinocytes [432], it is not expressed by human keratinocytes as shown in the present study. Mice Thy-1 has two alleles known as Thy-1.1 and Thy-1.2, distinguished by the amino acid at the position 89, with Thy-1.1 occupied by arginine and Thy-1.2 by glutamine [433]. Human Thy-1 is present in a pro form of 161 amino acids, which then undergoes several post translational modifications [433]. In addition, the expression of CD90 is developmentally regulated. It has been shown to be lowly expressed by developing neurons but highly expressed in mature neurons [432]. As a marker for stemness [433], positive CD90 expression remains one of the minimal criteria for defining human MSC proposed by the Committee for the International Society for Cellular Therapy (ISCT) [123]. CD90 expression is associated with undifferentiated hematopoietic stem cells and stromal stem cells [433] and CD90 positive cells may also reside within the endothelial niche to initiate self renewal [437].

While the biological roles of CD90 are unclear, a number of immunological and non-immunological functions have been discussed [432]. In addition to its involvement in T cell activation [432], it is believed to be associated with many cellular processes and pathologic conditions in a context-dependent manner [433], including cell-cell, cell-matrix interactions, cell motility, thymocyte adhesion to epithelium [432]. It has been shown to modulate neurite outgrowth through the interaction between Thy-1 on neurons and integrin

β3 on astrocytes [432]. Moreover, CD90 expression is also associated with fibroblast phenotypes relevant to wound healing and fibrosis. Differential CD90 expression is correlated with distinct cellular morphology [432]. While CD90 positive murine fibroblasts display a more spindle-shaped morphology, CD90 negative sub-populations demonstrate a more polygonal morphology [432]. This is attributed to CD90 expression being associated with cell-extracellular matrix interactions and cell migration [432]. Whilst the immunological and non-immunological functions of CD90 have been investigated, the contribution of CD90 expression in PDLSC or periodontal tissues remains largely unknown.

### 6.3.3 Annexin A2

Our proteomic data identified Annexin A2 as one of the cell surface proteins expressed by human PDLSC. Further flow cytometric analysis showed cell surface expression of Annexin A2 at low copy numbers by human GF, ovine PDLSC and ovine ERM cells. This resemblance of the surface expression of Annexin A2 in PDLSC and ERM cells is consistent with our previous findings in Chapter 3 that ovine ERM cells demonstrated a similar immunophenotype with ovine dental MSC. As a member of the Annexin family which plays important roles in the mineralization process [408-414], the low expression of Annexin A2 in human GF may be correlated with the fact that human GF demonstrated limited osteogenic potential when cultured in osteogenic conditions (data not shown). The higher Annexin A2 expression in ovine PDLSC than in the human counterparts most likely indicates species differences in the expression levels of different antigens.

Structurally, Annexins contain four or eight 70-80 amino acid repeats, which form the conserved core region, and a highly variable N-terminus, which endows specific functions of various Annexins [438]. Annexin A2, also known as Annexin II, Annexin II heavy

chain, P36, lipocortin II, calpactin I heavy chain, placental anticoagulant protein IV and chromobindin 8, can exist as a monomer or a heterotetramer by binding to its natural ligand, S100-A10 (or P11, calpactin I light chain, Annexin II light chain) *via* its N-terminus [439-441]. Although first identified as an intracellular protein, it has been found extracellularly both in a secreted and membrane bound form [442]. While Annexin A2 monomer is largely in the cytoplasm, the formation of the heterotetramer allows it to bind to the plasma membrane [443]. The binding to the cell surface is calcium dependent and therefore it could be stripped from the cell surface by EGTA [442]. As Annexin A2 lacks a signal peptide, the translocation to the cell surface is thought to be through an unconventional pathway, which is independent of the classical endoplasmic reticulum (ER)-Golgi secretion pathway [444]. Surface translocation of Annexin A2 can be regulated by thrombin [445] and interferon-γ [444]. Potential roles of extracellular Annexin A2 include plasminogen activation, cell-cell adhesion and immunoglobulin transport [442].

As calcium-dependent phospholipid-binding proteins, ever increasing evidence has highlighted the roles of the Annexin family in the mineralization process [408-414]. Three members of the Annexin family, A2, A5 and A6 have been reported to be highly expressed in calcifying cartilage and bone, and serve to initiate mineralization of extracellular matrix [446]. Among these three Annexins, Annexin A2 and A5 seem to function in a similar fashion [446]. Interestingly, Annexin A5 knockout mice demonstrated normal skeletal development, suggesting a compensatory effect of other Annexin members [447]. In a study investigating the intracellular process during mineralization, the overexpression of Annexin A2 has been shown to increase ALP activity as well as cartilage and bone formation, whilst diminished Annexin A2 expression resulted in decreased mineralization [410]. Annexin A6 is believed to be a marker of late chondrogenic differentiation as it is predominantly expressed on terminally differentiated chondrocytes [413].

Current understanding of the roles of Annexin family in dental tissues has been obtained mainly from studies using proteomic techniques and mass spectrometry. Two members of Annexin family, Annexin A3 and A4, have been shown to be more highly expressed in ovine PDLSC compared to BMSC and DPSC derived from the individual donor [346]. An up-regulation of Annexin A4 was identified in the proteome of PDLSC [397] and BMSC [399] during osteogenic induction compared with undifferentiated equivalents. A study of BMP-7 on cementoblast proteome and genome reported that Annexin A1, A2, A3, A5 and A6 were identified in both treated and untreated cementoblast cell lysate, while Annexin A4 was only identified in treated cells [448]. Another study comparing the PDLSC cell lysate treated with P15, a commercial cell-binding peptide to coat anorganic bovine mineral, with that of untreated cells, identified Annexin A2 as one of the main contributors for enhanced osteogenesis of P15 treated bovine hydroxyapatite [449]. Collectively, these studies on stem cells from dental tissues are consistent with previous reports that Annexins play important roles in contributing to the capacity of MSC-like populations derived from different tissues to form mineralized tissues.

A recent study highlighted the role of Annexin A2 in regulating the adhesion of hematopoietic stem cells to osteoblasts and endothelial cells, as well as stem cell homing and engraftment [450], thus Annexin A2 may be involved in different BMSC niche including endosteal [415-419] and vascular [420, 421] sites. Due to the important roles of adhesion molecules in the maintenance of the hematopoietic stem cell niche, the effect of Annexin A2 on presenting stromal cell-derived factor–1/CXCL12 to hematopoietic stem cells has been investigated [451]. Annexin A2 has been shown to bind to CXCL12 directly and therefore enhance the localization of hematopoietic stem cells to their endosteal niche [451]. Therefore, it has been suggested that CXCL12/Annexin A2 might be used as

markers for stem cell niche [451]. Taken together, these findings suggest that Annexin A2 may be a potential marker of the PDLSC niche in periodontal tissues.

### 6.3.4 SPK1

Initially identified in human PDLSC by proteomic data, sphingosine kinase 1 (SPK1) has been shown to be highly expressed in all five cell types examined by immunochemical analysis in the present study. However it remains to be determined why the observed molecular weight of SPK1 following 2-DE is higher than its predicted molecular weight. One possibility could be attributed to SPK1 binding to other proteins or the alternate isoform of SPK, SPK2, or due to the formation of protein aggregates.

SPK is a highly conserved lipid kinase that catalyzes the phosphorylation of sphingosine to form sphingosine-1-phosphate (S1P), which can be irreversibly degraded by S1P lyase and reversibly dephosphorylated by S1P phosphatases (Figure 6.10) [452]. Two SPK isoforms have been identified so far (SPK1 and SPK2) generated from separate genes with distinct biological functions, where SPK2 remains less characterized than SPK1. While SPK2 induces apoptosis, SPK1 enhances cell growth and proliferation [453]. S1P is a lipid mediator responsible for activating cell surface S1P receptors to mediate various intra- and extracellular processes. S1P binds to five different cognate G protein-coupled receptors, which are transmembrane receptors that receive extracellular signals that activate intracellular responses (designated as S1P receptor 1-5), which also acts as an intracellular second messenger with an unidentified intracellular target.

S1P, sphingosine and ceramide (*N*-acyl sphingosine) are three key sphingolipid metabolites that regulate various physiological and pathological processes such as cell proliferation, differentiation, apoptosis, migration, invasion and angiogenesis [454].

Among them, the involvement of SPK in cell growth, immune regulation and tumourgenesis is well established. While sphingosine and ceramide are believed to be associated with cell cycle arrest, apoptosis, and inhibition of proliferation, S1P promotes cell growth, proliferation and suppresses apoptosis (Figure 6.10) [455]. In other words, the balance between these pro- and anti-apoptotic sphingolipids, is an important cell fate determinant [454], where SPK plays a central role in the conversion of pro-apoptotic sphingosine to anti-apoptotic S1P [455]. In addition to their roles in regulating cell proliferation and apoptosis, SPK-S1P-S1P receptors have been shown to be involved in immune regulation such as immune cell trafficking, activation and T cell differentiation [452]. Moreover, the oncogenic potential of SPK1 has been demonstrated by the observation that the overexpression of human SPK1 in fibroblasts was able to give rise to tumours in NOD/SCID mice [456]. The overexpression of SPK1 has been identified in various types of cancer such as breast, colon, kidney and ovarian cancer and thus it is suggested as a marker for cancer prognosis [457]. The correlation between SPK1 expression and tumour progression might be attributed to the fact that the elevated expression of SPK1 leads to the upregulation of S1P, which has proliferation enhancing characteristics to increase the proliferation and suppress the apoptosis of cancer cells [457].

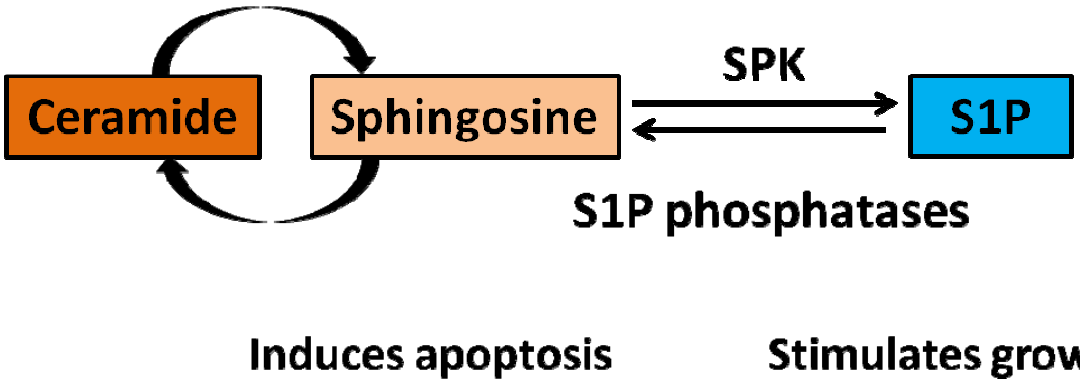


**Figure 6.10 Sphingosine kinase (SPK) plays important roles in regulating cell proliferation and apoptosis**

SPK catalyses the phosphorylation of sphingosine to form sphingosine-1-phosphate (S1P), which can be reversibly dephosphorylated by S1P phosphatases. Ceramide, sphingosine and S1P are three key sphingolipid metabolites regulating cell proliferation and apoptosis. Ceramide and sphingosine are associated with cell apoptosis and inhibition of proliferation, and S1P promotes cell growth, proliferation and suppresses apoptosis.

Recently, the role of SPK in progenitor/stem cells has received considerable attention [453]. The high expression level of SPK in endothelial progenitor cells decreases when they undergo maturation, suggesting SPK regulates the rate of endothelial progenitor cell differentiation [458]. It has been reported that the overexpression of SPK1 promoted the de-differentiation of human endothelial cells to a progenitor cell phenotype both phenotypically and functionally [422, 459]. The depletion of SPK1 led to fewer neurons and progenitor cells through a decrease in cell proliferation as well as an increase in apoptosis, highlighting the central roles of SPK1/S1P during sensory ganglia formation [460]. S1P, which is catalysed by SPK, seems to have major effects on the maintenance of human embryonic stem cells [453]. S1P has been shown to increase haematopoietic stem cell motility to leave the stem cell niche and migrate to other sites [453]. Combinations of extracellular S1P and platelet-derived growth factor (PDGF) in a serum free culture media maintained human embryonic stem cells in an undifferentiated state [461] and increased the proliferation of mesangial cells [462]. S1P was able to induce quiescent muscle satellite cells to a proliferative state and in turn initiate muscle regeneration [463]. Conversely, the

blockage of SPK1 was shown to impair muscle cell regeneration [463]. These observations support the notion that SPK and S1P play important roles in the maintenance of stem cells.

While SPK2 is localized in the cellular organelles such as endoplasmic reticulum and nucleus, SPK1 is predominantly a cytosolic enzyme which lacks an obvious membrane anchoring sequence. However, considerable evidence has suggested that SPK1 can be translocated to the plasma membrane upon cell stimulation by growth factors and cytokines [401-407]. This is also suggested by the slightly positive grand average of hydropathicity (GRAVY) values of SPK1 (0.054) (http://www.expasy.org/tools/protparam.html). In general, proteins with positive GRAVY values are considered as hydrophobic proteins, while negative GRAVY values are associated with hydrophilic proteins. SPK1 has been shown to be released outside of cells and contribute to the production of S1P in the extracellular environment [401]. This translocation allows SPK1 to exert on its substrate sphingosine and subsequently promotes the production of extracellular S1P [406] [457]. In addition, translocation to the plasma membrane is essential for the pro-oncogenic properties of SPK1 [404]. Although the mechanisms for the translocation of SPK1 to the plasma membrane remains unclear, there is evidence that it is a result of the phosphorylation at serine 225 by Erk1/2 or a related kinase [404], which increases the affinity of SPK1 with anionic lipids [406].Conversely, other contributors are involved in translocation, such as carbochol stimulation of the M3 muscarinic receptor, which is independent of serine 225 phosphorylation [406]. Recently, calcium and integrin binding protein-1 has been shown to play an important role in this translocation [403]. The present study demonstrated the SPK1 expression using immunocytochemical analysis, however, was unable to demonstrate the cell surface expression of this enzyme, which is attributed to the availability of a SPK1 antibody suitable for flow cytometry.

## 6.4 Conclusion

Various techniques are widely used to validate proteomic data, such as western immunoblotting, flow cytometry, immunocytochemistry/immunohistochemistry and real time PCR. However, the discrepancy has been noted between data from proteomics and other transcriptome technologies. Post translational modifications are not detected by real time PCR and the transcript levels do not frequently correlate with translated protein expression at the functional level [349]. Discrepancies between comparative analyses using proteomic techniques and western immunoblotting have also been reported, where western immunoblotting is a semiquantitative technique [464]. The use of antibody-based technologies to validate proteomic data largely relies on the antibody availability, affinity and accessibility. Further confirmative studies of the remaining candidate cell surface proteins identified by proteomics in the present study were not carried out due to the lack of available reagents suitable for flow cytometry.

In summary, to our knowledge this study is the first to investigate the cell surface proteome of *ex vivo* expanded human PDLSC. In addition to the expression of well known MSC associated cell surface antigens such as CD73 and CD90, PDLSC were also found to express two novel cell surface proteins; Annexin A2 and sphingosine kinase 1. Interestingly, previous studies have implicated the expression of CD73, CD90, Annexin A2 and sphingosine kinase 1 in the maintenance of various stem cell populations. Importantly, this study found that human skin epithelial cells lacked any cell surface expression for CD73, CD90 and Annexin A2. Further investigations are required to determine the functional significance of these proteins for PDLSC maintenance, growth and differentiation. These proteonomic studies form the foundation to further define the cell surface protein expression profile of PDLSC in order to better characterise this cell population and help develop novel strategies for their purification.

# Chapter 7. Discussion and concluding remarks

## 7.1 Result summary and discussion

Tooth development is a complex process which involves a cascade of events coordinated in both a spatial and temporal manner, where epithelial and mesenchymal interactions play an important role. In light of this, we propose that successful periodontal tissue regeneration calls for the coordination of epithelial and mesenchymal populations. This study characterised these two cellular components in the periodontium, ERM cells and PDLSC that are thought to interact during formation of the PDL and during the tissue repair process. As human ERM cells were found to be refractory to standard cell culture and exhibited limited proliferative capacity, ovine ERM cells were used in this study.

The present study provides evidence to support the notion that ovine ERM contain a subpopulation of stem cells that can undergo epithelial mesenchymal transition. Rather than being “cell rests” as indicated by their name, functional analysis demonstrated their developmental potential to differentiate into cells from two embryonic germ layers, including three major mesodermal lineages (bone, fat and cartilage) and one ectodermal lineage (neuron-like cells) (Figure 7.1) when cultured in conditions previously described for BMSC, PDLSC and DPSC. Collectively, the *in vitro* findings support the idea that ectoderm-derived ERM cells share similar functional attributes with other MSC-like populations. The present study also lends support to the notion that ERM cells are able to undergo epithelial mesenchymal transition (EMT), shown by a decline of the expression of epithelial markers, an up-regulation in gene expression of mesenchymal-associated markers and the high expression of various transcription factors known to regulate EMT. In addition, these studies showed that ERM cells were able to generate bone, cementum-like and periodontal ligament-like tissues in an ectopic transplantation model (Figure 7.1).

This work lays the foundation for further studies investigating ERM cells as a potential candidate for mediating periodontal tissue regeneration.

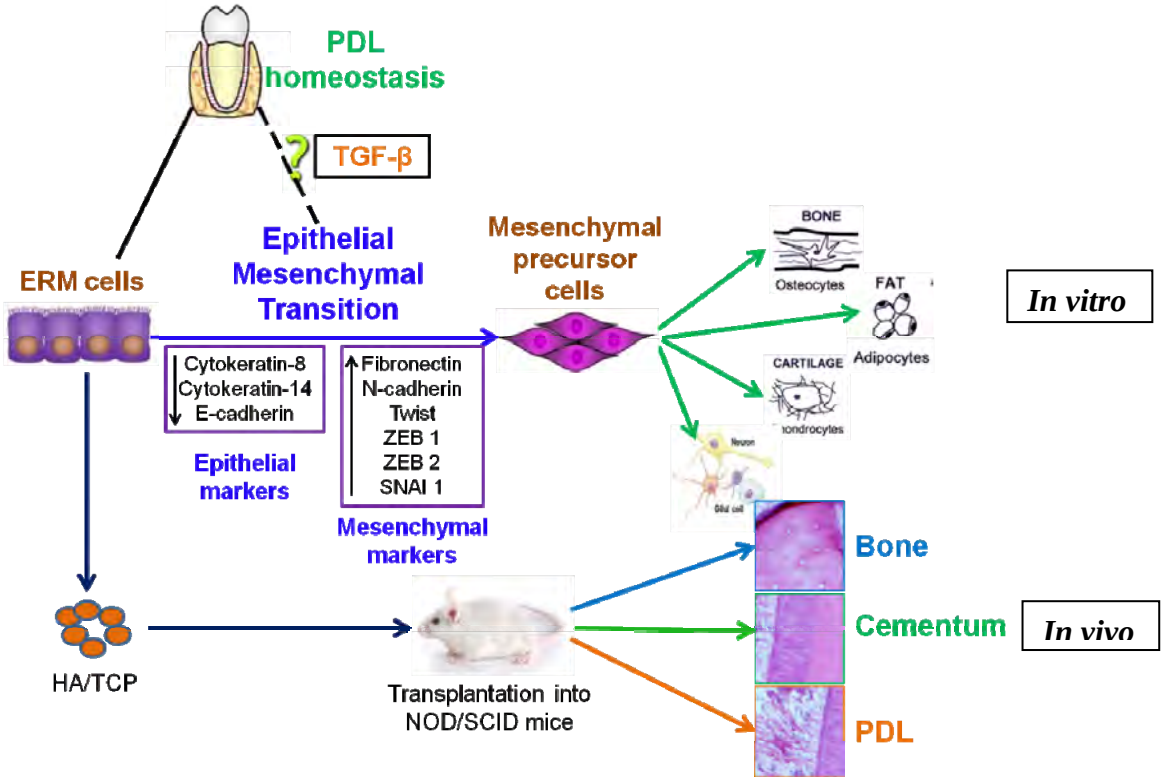


**Figure 7.1 Schematic representations of the stem cell-like properties of ovine ERM cells and putative association of epithelial mesenchymal transition with the maintenance of periodontal ligament homeostasis**

Epithelial mesenchymal transition may be induced by TGF-β [64], and is associated with a downregulation in the expression of cytokeratin-8, cytokeratin-14 and E cadherin together with increased expression of fibronectin, N-cadherin, Twist, ZEB1, ZEB2 and SNAI 1 [465]. Abbreviations: ERM, Epithelial cell Rests of Malassez; PDL, Periodontal ligament; HA/TCP, Hydroxyapatite/tricalcium phosphate; TGF-β, Transforming Growth Factor-beta, NOD/SCID mice, Non-obese diabetic–severe combined immunodeficient mice.

Despite their epithelial characteristics, ERM cells exhibit comparable protein expression profiles with PDLSC, including the expression of several MSC associated markers, CD29, CD44 and HSP90β, as well as two novel proteins identified in the present study, Annexin A2 and SPK1, lending support to the notion that ERM display a cell surface phenotypic profile overlapping with PDLSC. In addition to this, ERM demonstrate similar immunophenotypic features with other epithelial cells, such as the expression of E-

cadherin, cytokeratin-8, EMP-1 and integrin α6. To optimize the selection techniques for ERM cells, the present study successfully identified integrin α6/CD49f as a selective cell surface marker of ERM cells within a heterogeneous periodontal ligament cell population which is absent or lowly expressed in other PDL populations, such as PDLSC.

The second aspect of this thesis focused on the cell surface proteome of human PDLSC using 2-DE. This was achieved by the assessment of the proteomic profile using selective cell surface labelling with CyDye and collagenase as a cell dissociation reagent. The cell surface proteome of ERM cells was not characterized using 2-DE, mainly due to the limited proliferative capacity of ERM cells to obtain sufficient cell numbers for proteomic analyses. Specifically, CD73, CD90, Annexin A2 and SPK1 have been found to be expressed as surface proteins by human PDLSC. The expression of these four proteins has been validated using flow cytometric and immunocytochemical analysis on human PDLSC, human GF, human keratinocytes, ovine PDLSC and ovine ERM cells. As summarised in Table 7.1, human PDLSC and GF shared similar immunophenotypic profile in terms of the expression of CD73, CD90, Annexin A2 and SPK1, which is consistent with previous studies [153]. This similarity indicates the common properties and origin of periodontal ligament and gingival tissues. The expression of CD73 and CD90 was not detected in ovine cells as both antibodies were manufactured to be reactive against human epitopes. The positive expression of Annexin A2 and SPK1 has been demonstrated by ovine PDLSC and ERM cells. These data indicate that ovine PDLSC and ERM cells showed comparable phenotypic profile with human PDLSC. This also provides evidence for the notion that ERM cells are unique cell population that exhibit a similar phenotypic profile to PDLSC.

**Table 7.1 The expression of CD73, CD90, Annexin A2 and sphingosine kinase 1**

| | CD73 | CD90 | Annexin A2 | Sphingosine kinase 1 |
|---|---|---|---|---|
| Human PDLSC | + | + | + | + |
| Human GF | + | + | + | + |
| Human keratinocyte | - | - | + | + |
| Ovine PDLSC | NA | NA | + | + |
| Ovine ERM | NA | NA | + | + |

Abbreviations: PDLSC, periodontal ligament stem cells; GF, gingival fibroblasts; ERM, epithelial cell rests of Malassez.

## 7.2 Future directions

### 7.2.1 What is the binding subunit of integrin α6 in ERM cells?

In the present study, integrin α6 has been shown to be a surface marker for the enrichment of ERM cells from heterogeneous PDL cell populations. Integrin α6 subunit may either combine with beta 4 subunit to form tumour-associated antigen (TSP) 180 (in epithelial cells), or with beta 1 subunit as VLA-6 (in many cell types). Immunoprecipitation experiments would help to investigate the binding subunit of α6 in ERM cells (either β1 or β4) to identify different potential binding ligands. This could help optimize future *in vitro* culture conditions by pre-coating the culture flasks with the corresponding ligand for selective attachment of ERM cell populations.

### 7.2.2 What keeps ERM cells in mesenchymal surroundings in adulthood?

To our knowledge, ERM cells are the only epithelial cell population that is able to reside within a mesenchymal matrix during postnatal life, while epithelial cells in other tissues exist as a layer separated from the underlying connective tissues by a basal lamina. The factors endowing ERM cells with this unique property are yet to be understood. Future studies would provide insight into the underlying mechanisms which maintain ERM cells

in the mesenchymal surroundings and whether these molecular signals change during times of tissue regeneration. Understanding these factors is paramount to elucidating the roles of ERM in adult periodontium.

Epithelial cells derived from different tissues need to be enforced through viral transduction techniques to overexpress transcription factors such as Twist or Snail in order to elicit MSC-like properties [337]. In contrast, ERM cells have been shown in the present study to be able to readily exhibit MSC-like multipotency without ectopic expression of epithelial mesenchymal transition-associated genes. Therefore, it seems that ERM cells demonstrate higher plasticity compared to epithelial cells from other tissues. Further assessment would involve examining the factors endowing ERM cells with the higher plasticity and higher adaptive capacity to the foreign environment.

### 7.2.3 Further functional characterisation of ERM cells

#### *7.2.3.1 Does epithelial mesenchymal transition regulate periodontal ligament homeostasis?*

It has been shown that HERS/ERM are able to undergo epithelial mesenchymal transition [64, 465]. However, it remains to be proven if this property is correlated to the roles of ERM in periodontal ligament homeostasis. Epithelial mesenchymal transition involves a phenotypic shift from epithelial cells to mesenchymal cells and allows epithelial cells to migrate to other locations of the body during development and in postnatal tissues [307]. It can be induced by a variety of contextual signals including the exposure to certain cytokines and chemokines such as TGF-β1 [64], and exogenous expression of transcription factors such as Twist or Snail families [307]. Epithelial mesenchymal transition and the reverse process, mesenchymal epithelial transition, allow mesenchymal or epithelial cells to lose their own traits and to transform to the other lineages. They are thought to play important roles in embryonic development for most tissues and organs [304]. Moreover,

epithelial mesenchymal transition is believed to be involved in the regulation of cellular plasticity in normal adult tissues and therefore contribute to tissue repair [304]. Studies on induced pluripotent stem cells have implicated epithelial mesenchymal transition and mesenchymal epithelial transition as crucial procedures in regulating stem cell plasticity [306, 327]. However, emerging data suggest that, if dysregulated, epithelial mesenchymal transition can disturb normal epithelial homeostasis and contribute to pathologic conditions, such as cancer progression and organ fibrosis [304, 305, 307-312]. Epithelial mesenchymal transition endows tumour cells with increased migratory capacity to invade into the extracellular matrix and subsequently metastasize throughout the body [312, 337]. Interstitial fibrosis is characterised by the accumulation of fibroblasts, excessive deposition of collagen and other matrix components [310], and changes in cytokine milieu such as TGF-β [466], which is a well-documented epithelial mesenchymal transition inducer. Although the implication of epithelial mesenchymal transition in tissue fibrosis remains a topic of intense debate, increasing evidence has shown that epithelial mesenchymal transition is involved in the fibrosis of the kidney, heart and lung [467-472]. Cell tracing studies have revealed that the increased number of fibroblasts during renal fibrosis largely arise from tubular epithelial cells undergoing epithelial mesenchymal transition [473]. The recruitment of matrix-producing fibroblast thereby results in the abnormal accumulation of extracellular matrix such as collagen type I and II, which arises from the imbalance between the production and degradation of extracellular matrix and subsequently leads to interstitial fibrosis [471, 472].

The present study has highlighted that ERM cells are capable of undergoing epithelial mesenchymal transition *in vitro* and *in vivo* [465]. As epithelial mesenchymal transition has been shown to contribute to tissue fibrosis, an intriguing question remains whether epithelial mesenchymal transition is associated with the homeostasis of the periodontal

ligament, possibly by regulating the fibrosis and calcification of periodontal ligament (Figure 7.1). Further studies addressing this issue will help identify the mechanisms of the functions of ERM cells in the periodontium, such as the prevention of ankylosis and tooth root resorption.

#### *7.2.3.2 ERM and neuronal regulation in the periodontium*

It has been previously demonstrated that ERM cells in human periodontium exhibit a close association with Ruffini-like and free nerve endings [87]. Further evidence comes from report that ERM cells are immunoreactive to neuropeptides calcitonin gene-related peptide, substance P and vasoactive intestinal peptide [91]. Together with the neurogenic phenotype of ERM cells shown in the present study, it is likely that ERM cells may contribute to periodontium innervations and neuronal regulations. However, this has not been shown conclusively. Further studies would aid to assess the association of ERM cells and periodontium innervation, and whether ERM cells could differentiate into functional active neurons *in vitro* that can produce action potentials using patch clamping techniques [141].

#### *7.2.3.3 Further investigation of mineral formation of ERM cells in a xenogeneic ectopic transplantation model*

In this study, ERM cells demonstrated the potential to generate three tissues of periodontium, including bone, cementum-like and Sharpey's fibre-like structures in a xenogeneic ectopic transplantation model (Figure 7.1). Further characterization is required to identify the nature of the newly formed mineralized tissues in terms of calcium/phosphate ratio and crystal composition, using Electron Probe Micro-Analysis (EPMA) or Energy Dispersive X-ray Analysis (EDX) [332-335]. Intriguingly, transplanted ERM cells maintained CK-8 expression following differentiation into bone lining cells, but lost CK-8 expression when they had terminally differentiated into osteocytes. Further studies would help elucidate the underlining mechanisms regulating the loss of epithelial

nature of ERM cells, and whether this is mediated by the process of epithelial mesenchymal transition.

#### *7.2.3.4 Are ERM cells able to contribute to tissue regeneration in periodontal defects?*

As the present work has shown that ERM cells exhibit mineral forming capacity *in vitro* and *in vivo*, the question arises as to whether they are able to contribute to periodontal tissue regeneration. Consequently, a more direct demonstration of this point will depend on transplantation of these cells into a rodent or ovine periodontal defect model to investigate whether they are able to form tooth supporting tissues by themselves, enhance the regenerative capacity of surrounding mesenchymal cells such as PDLSC, osteoblasts and cementoblasts, or provide biological signals to the microenvironment to recruit more stem cells to the periodontal defect sites? Similar pre-clinical studies would also help determine whether periodontal regeneration is optimised following the implantation of combinations of ERM and PDLSC into defect sites. It is worth noting that further investigatin of ERM cells might be hindered by their limited proliferative capacity. This could be overcome by the isolation and expansion of long-lived ERM clones with multipotential or the generation of immortalised multipotential ERM lines with no chromosomal abnormalities or tumour forming potential.

#### *7.2.3.5 Do ERM cells have immunomodulatory properties?*

The immunomodulatory properties of MSC are an important aspect for their potential use in allogeneic transplantation for cell-based tissue engineering. Studies have shown that PDLSC are able to inhibit peripheral blood mononuclear cell proliferation induced by mitogen or an allogeneic mixed lymphocyte reaction [153]. Considering that ERM cells exhibit comparable multilineage differentiation characteristics with PDLSC, an analysis of the potential immunomodulatory properties of ERM would be a prerequisite for assessing the periodontal regeneration capacity of allogeneic ERM preparations. Studies on the

underlining mechanisms of immunomodulatory properties have demonstrated that, in addition to the well-documented immunosuppressive factors such as the tryptophan catabolizing enzyme indoleamine 2,3-dioxygenase (IDO), TGF-β1, hepatocyte growth factor and Prostaglandin $E_2$ ($PGE_2$) [115], adenosine signalling modulated by CD39 and CD73 expression has been highlighted as a novel modulator in the immunosuppression of T-cell proliferation by MSC [426, 427]. In particular, the expression of CD73 on ERM cells, which is a cell surface enzyme that catalyses the formation of immunosuppressive adenosine, would be an important aspect for future investigations.

### 7.2.4 Functional studies of CD73, CD90, Annexin A2 and SPK1

Whether ovine PDLSC and ERM cells exhibit cell surface expression of CD73 and CD90 remains to be determined, which is dependent on the generation of antibodies reactive with the respective ovine epitopes. The findings in the present study implicated CD73, CD90, Annexin A2 and SPK1 as cell surface proteins in human PDLSC. However, functional analysis is required for the further investigation of their roles on PDLSC. *In vitro* functional studies can be carried out using FACS sorted periodontal ligament cells using one of these four proteins, or using cells being forced to overexpress or knockdown one of these four proteins. Loss-of-function studies could also be performed using knockout mice of each of the four genes. These functional studies would lead to a more in-depth understanding of the role of each gene in PDLSC growth, differentiation and during tooth development and periodontal tissue regeneration following insult.

As discussed in Chapter 6, CD73 is able to catalyse the formation of immunosuppressive adenosine and thus is thought to be associated with the immunomodulatory properties of MSC, which exhibit an anti-inflammatory effect in periodontal disease. These findings suggest directions for further study such as whether the manipulation of CD73 expression

by PDLSC affects their immunomodulatory properties or changes the progression of periodontitis. It would be of interest to determine if there is any change in the level of CD73 expression in the periodontium between chronic and aggressive periodontitis. In addition, it would be worthwhile assessing the correlation between the levels of CD73 expression and oromaxillofacial tumour progression, or whether target inhibition of CD73 would open up new opportunities for cancer therapy based on adenosine signalling.

Although the positive expression of CD90 is one of the minimal criteria for defining MSC, the roles of CD90 in PDLSC and periodontal tissues remain largely unknown. Gene manipulation studies would confirm whether altered CD90 expression leads to changes in the proliferative rate of PDLSC, where CD90 has been associated with changes in fibroblast morphology from spindle shaped CD90 positive cells to polygonal shaped CD90 negative cells. Furthermore, if ERM cells are found to express CD90, it would be interesting to determine if CD90 expression is regulated during epithelial mesenchymal transition and whether this gene plays a role during this process.

Annexin A2 has previously been shown to be closely related to the mineralisation process. It would be interesting to investigate whether the overexpression or depletion of Annexin A2 in PDLSC would affect the *in vitro* and *in vivo* mineral forming capacity. It would be worthwhile to determine whether Annexin A2 knockout mice have impaired alveolar bone/cementum formation during development and impaired bone/cementum repair in surgically created periodontal defects.

SPK1 catalyses the production of sphingosine-1-phosphate (S1P) which enhances cell proliferation and inhibits apoptosis. It is speculated that enforced increase and/or reduction of the expression levels of SPK1 in PDLSC may affect their proliferation rate and/or life

span. Moreover, as SPK1 has been associated with the de-differentiation and the immature stage of stem cells, further studies would reveal whether cells with enforced increase of the expression levels of SPK1 would give rise to higher incidences of CFU-F (colony forming unit-fibroblasts) that may exhibit enhanced multi-differentiation potentials.

### 7.2.5 Further assessment of the proteomic data

Due to the time limit and availability of antibodies, only four proteins were selected for validation in the present study. Additional examination of other prospective cell surface proteins on PDLSC might reveal other potential candidates to be used as stem cell surface markers or to distinguish between PDLSC and ERM cells. Further studies on other proteins identified in the present study might improve our understanding of biology of the periodontium. For example, Filamin C has been identified in the proteomic data, which is believed to play a central role in myogenesis and structural integrity of muscle fibers [474-476]. What are the functional roles of this muscle-specific isform of filamins in the periodontium?

### 7.2.6 Cell surface proteome by non gel-based proteomic technologies

Considering the limitation associated with 2-DE based technologies in the investigation of very hydrophobic membrane proteins, non gel-based methods, such as isotope coded affinity tag (ICAT) [477], which show better representation of membrane proteins could be performed to analyse cell surface proteome of PDLSC. In ICAT, cysteine residues in different samples are labelled with either light ($^{12}C$) or heavy ($^{13}C$) stable isotopes of the same chemical reagent before samples are combined, digested and subjected to avidin affinity chromatography to isolate peptides labelled with isotope-coded tagging reagents. These peptides are then analyzed by MS, where protein expression is quantified by identifying the light- and heavy-labelled peptides with the ratio of ion signal intensities or peak areas being directly related to peptide abundance.

## 7.3 Concluding remarks

Our understanding of many of the basic processes underlying periodontal tissue development and regeneration is still very limited. Results from the present study indicate that ERM cells, rather than being “cell rests” in adult periodontium, contain a subpopulation of stem cells that can undergo epithelial mesenchymal transition with comparable properties with PDLSC. An intriguing question which remains to be answered is whether epithelial mesenchymal transition of ERM cells is associated with the homeostasis of the periodontal ligament, possibly by regulating the fibrosis and calcification of periodontal ligament. This line of investigation will facilitate future treatment modalities for periodontal regeneration. In addition, proteomic technologies provide important information on the cell surface proteome of PDLSC. In conclusion, this work lays foundation for using the combination of two cell populations, PDLSC and ERM cells in regenerative periodontal tissue therapy.

# 8. References


1. Beertsen, W., C.A. McCulloch, and J. Sodek, *The periodontal ligament: a unique, multifunctional connective tissue.* Periodontol 2000, 1997. **13**: p. 20-40.
2. Burt, B., *Position paper: epidemiology of periodontal diseases.* J Periodontol, 2005. **76**(8): p. 1406-19.
3. Ten Cate, A.R., *The role of epithelium in the development, structure and function of the tissues of tooth support.* Oral Dis, 1996. **2**(1): p. 55-62.
4. Greenwell, H., *Position paper: Guidelines for periodontal therapy.* J Periodontol, 2001. **72**(11): p. 1624-8.
5. Bartold, P.M., S. Shi, and S. Gronthos, *Stem cells and periodontal regeneration.* Periodontol 2000, 2006. **40**: p. 164-72.
6. Lin, N.H., S. Gronthos, and P.M. Bartold, *Stem cells and periodontal regeneration.* Aust Dent J, 2008. **53**(2): p. 108-21.
7. Tomazela-Herndl, S.A. and V.E. Arana-Chavez, *Ultrastructure of early mineral deposition during hyaline layer formation in rat molars.* Arch Oral Biol, 2001. **46**(4): p. 305-11.
8. Ten Cate, A.R., *The development of the periodontium--a largely ectomesenchymally derived unit.* Periodontol 2000, 1997. **13**: p. 9-19.
9. Bosshardt, D.D. and A. Nanci, *Hertwig's epithelial root sheath, enamel matrix proteins, and initiation of cementogenesis in porcine teeth.* J Clin Periodontol, 2004. **31**(3): p. 184-92.
10. Bosshardt, D.D. and H.E. Schroeder, *Cementogenesis reviewed: a comparison between human premolars and rodent molars.* Anat Rec, 1996. **245**(2): p. 267-92.
11. Thomas, H.F., *Root formation.* Int J Dev Biol, 1995. **39**(1): p. 231-7.
12. Zeichner-David, M., et al., *Role of Hertwig's epithelial root sheath cells in tooth root development.* Dev Dyn, 2003. **228**(4): p. 651-63.
13. Huang, X., et al., *Smad4-Shh-Nfic signaling cascade-mediated epithelial-mesenchymal interaction is crucial in regulating tooth root development.* J Bone Miner Res, 2010. **25**(5): p. 1167-78.
14. Fleischmannova, J., et al., *Formation of the tooth-bone interface.* J Dent Res, 2010. **89**(2): p. 108-15.
15. Tummers, M. and I. Thesleff, *Root or crown: a developmental choice orchestrated by the differential regulation of the epithelial stem cell niche in the tooth of two rodent species.* Development, 2003. **130**(6): p. 1049-57.

16. Von, B.A., *Uber die Ausdehnung des Schmelzorganes and seine Bedeutung fur die Zahnbildung.* Arch. mikrosk. Anat. EntwMech, 1887. **29**: p. 367-395.
17. Kim, M.Y., et al., *Role of the transcription factor NFIC in odontoblast gene expression.* J Calif Dent Assoc, 2009. **37**(12): p. 875-81.
18. Lee, D.S., et al., *Nuclear factor I-C is essential for odontogenic cell proliferation and odontoblast differentiation during tooth root development.* J Biol Chem, 2009. **284**(25): p. 17293-303.
19. Lee, T.Y., et al., *Disruption of Nfic causes dissociation of odontoblasts by interfering with the formation of intercellular junctions and aberrant odontoblast differentiation.* J Histochem Cytochem, 2009. **57**(5): p. 469-76.
20. Park, J.C., et al., *Nfic gene disruption inhibits differentiation of odontoblasts responsible for root formation and results in formation of short and abnormal roots in mice.* J Periodontol, 2007. **78**(9): p. 1795-802.
21. Steele-Perkins, G., et al., *Essential role for NFI-C/CTF transcription-replication factor in tooth root development.* Mol Cell Biol, 2003. **23**(3): p. 1075-84.
22. Bartold, P.M. and A.S. Narayanan, *Composition of the Extracellular Matrix,* in *Biology of periodontal connective tissues*, P.M. Bartold and A.S. Narayanan, Editors. 1998, Quintessence Publications, Inc.: Carol Stream, Illinois. p. 151-172.
23. Bosshardt, D.D., *Are cementoblasts a subpopulation of osteoblasts or a unique phenotype?* J Dent Res, 2005. **84**(5): p. 390-406.
24. Hammarstrom, L., I. Alatli, and C.D. Fong, *Origins of cementum.* Oral Dis, 1996. **2**(1): p. 63-9.
25. Schroeder, H.E., *Development, structure and function of periodontal tissues* in *Handbook of microscopic anatomy,* A. Oksche and L. Vollrath, Editors. 1985, Springer-Verlag: Berlin. p. 23-228.
26. Bosshardt, D.D. and K.A. Selvig, *Dental cementum: the dynamic tissue covering of the root.* Periodontol 2000, 1997. **13**: p. 41-75.
27. Saygin, N.E., W.V. Giannobile, and M.J. Somerman, *Molecular and cell biology of cementum.* Periodontol 2000, 2000. **24**: p. 73-98.
28. Schroeder, H.E., *Biological problems of regenerative cementogenesis: synthesis and attachment of collagenous matrices on growing and established root surfaces.* Int Rev Cytol, 1992. **142**: p. 1-59.
29. Bartold PM, N.A., *Composition of the Extracellular Matrix,* in *Biology of the Periodontal Connective Tissues*. 1998, Quintessence Publishing Co, Inc: Carol Stream, Illinois.

30. Cortellini, P. and M.S. Tonetti, *Clinical and radiographic outcomes of the modified minimally invasive surgical technique with and without regenerative materials: a randomized-controlled trial in intra-bony defects.* J Clin Periodontol, 2011. **38**(4): p. 365-73.
31. Heijl, L., *Periodontal regeneration with enamel matrix derivative in one human experimental defect. A case report.* J Clin Periodontol, 1997. **24**(9 Pt 2): p. 693-6.
32. Listl, S., Y.K. Tu, and C.M. Faggion, Jr., *A cost-effectiveness evaluation of enamel matrix derivatives alone or in conjunction with regenerative devices in the treatment of periodontal intra-osseous defects.* J Clin Periodontol, 2010. **37**(10): p. 920-7.
33. Meyle, J., et al., *A multi-centre randomized controlled clinical trial on the treatment of intra-bony defects with enamel matrix derivatives/synthetic bone graft or enamel matrix derivatives alone: results after 12 months.* J Clin Periodontol, 2011. **38**(7): p. 652-60.
34. Nokhbehsaim, M., et al., *Effects of enamel matrix derivative on periodontal wound healing in an inflammatory environment in vitro.* J Clin Periodontol, 2011. **38**(5): p. 479-90.
35. Yukna, R.A. and J.T. Mellonig, *Histologic evaluation of periodontal healing in humans following regenerative therapy with enamel matrix derivative. A 10-case series.* J Periodontol, 2000. **71**(5): p. 752-9.
36. Paynter, K.J. and G. Pudy, *A study of the structure, chemical nature, and development of cementum in the rat.* Anat Rec, 1958. **131**(2): p. 233-51.
37. Lindskog, S. and L. Hammarstrom, *Formation of intermediate cementum. III: 3H-tryptophan and 3H-proline uptake into the epithelial root sheath of Hertwig in vitro.* J Craniofac Genet Dev Biol, 1982. **2**(2): p. 171-7.
38. Lindskog, S., *Formation of intermediate cementum. II: a scanning electron microscopic study of the epithelial root sheath of Hertwig in monkey.* J Craniofac Genet Dev Biol, 1982. **2**(2): p. 161-9.
39. Mahmoud Torabinejad, R.E.W., *Endodontics: Principles and Practice 4th Ed.* 2008: p. 3-4.
40. Bosshardt, D.D., *Biological mediators and periodontal regeneration: a review of enamel matrix proteins at the cellular and molecular levels.* J Clin Periodontol, 2008. **35**(8 Suppl): p. 87-105.
41. Brookes, S.J., et al., *Biochemistry and molecular biology of amelogenin proteins of developing dental enamel.* Arch Oral Biol, 1995. **40**(1): p. 1-14.

42. Hammarstrom, L., *The role of enamel matrix proteins in the development of cementum and periodontal tissues.* Ciba Found Symp, 1997. **205**: p. 246-55; discussion 255-60.
43. Hammarstrom, L., *Enamel matrix, cementum development and regeneration.* J Clin Periodontol, 1997. **24**(9 Pt 2): p. 658-68.
44. Hammarstrom, L., L. Heijl, and S. Gestrelius, *Periodontal regeneration in a buccal dehiscence model in monkeys after application of enamel matrix proteins.* J Clin Periodontol, 1997. **24**(9 Pt 2): p. 669-77.
45. Slavkin, H.C., et al., *Hertwig's epithelial root sheath differentiation and initial cementum and bone formation during long-term organ culture of mouse mandibular first molars using serumless, chemically-defined medium.* J Periodontal Res, 1989. **24**(1): p. 28-40.
46. Fong, C.D. and L. Hammarstrom, *Expression of amelin and amelogenin in epithelial root sheath remnants of fully formed rat molars.* Oral Surg Oral Med Oral Pathol Oral Radiol Endod, 2000. **90**(2): p. 218-23.
47. Bosshardt, D.D., et al., *Developmental appearance and distribution of bone sialoprotein and osteopontin in human and rat cementum.* Anat Rec, 1998. **250**(1): p. 13-33.
48. Bosshardt, D.D. and A. Nanci, *Immunolocalization of epithelial and mesenchymal matrix constituents in association with inner enamel epithelial cells.* J Histochem Cytochem, 1998. **46**(2): p. 135-42.
49. Lindskog, S., *Formation of intermediate cementum. I: early mineralization of aprismatic enamel and intermediate cementum in monkey.* J Craniofac Genet Dev Biol, 1982. **2**(2): p. 147-60.
50. Slavkin, H.C., et al., *Human and mouse cementum proteins immunologically related to enamel proteins.* Biochim Biophys Acta, 1989. **991**(1): p. 12-8.
51. Hamamoto, Y., et al., *Production of amelogenin by enamel epithelium of Hertwig's root sheath.* Oral Surg Oral Med Oral Pathol Oral Radiol Endod, 1996. **81**(6): p. 703-9.
52. Rincon, J.C., et al., *Enhanced proliferation, attachment and osteopontin expression by porcine periodontal cells exposed to Emdogain.* Arch Oral Biol, 2005. **50**(12): p. 1047-54.
53. Tenorio, D., A. Cruchley, and F.J. Hughes, *Immunocytochemical investigation of the rat cementoblast phenotype.* J Periodontal Res, 1993. **28**(6 Pt 1): p. 411-9.
54. Cho, M.I., W.L. Lin, and P.R. Garant, *Occurrence of epidermal growth factor-*

*binding sites during differentiation of cementoblasts and periodontal ligament fibroblasts of the young rat: a light and electron microscopic radioautographic study.* Anat Rec, 1991. **231**(1): p. 14-24.

55. Lezot, F., et al., *Epithelial Dlx-2 homeogene expression and cementogenesis.* J Histochem Cytochem, 2000. **48**(2): p. 277-84.
56. Webb, P.P., et al., *Changing expression of intermediate filaments in fibroblasts and cementoblasts of the developing periodontal ligament of the rat molar tooth.* J Anat, 1996. **188 ( Pt 3)**: p. 529-39.
57. Thomas HF, K.E., *Tissue interactions in normal murine root development*, in *The Biological Mechanisms of Tooth Eruption and Root Resorption.* , D. Z, Editor. 1988, EBSCO Medi: Birmingham, AL. p. 145-151.
58. Heritier, M., *Experimental induction of cementogenesis on the enamel of transplanted mouse tooth germs.* Arch Oral Biol, 1982. **27**(2): p. 87-97.
59. Slavkin, H.C., *Towards a cellular and molecular understanding of periodontics. Cementogenesis revisited.* J Periodontol, 1976. **47**(5): p. 249-55.
60. Cho, M.I. and P.R. Garant, *Ultrastructural evidence of directed cell migration during initial cementoblast differentiation in root formation.* J Periodontal Res, 1988. **23**(4): p. 268-76.
61. Cho, M.I. and P.R. Garant, *Radioautographic study of [3H]mannose utilization during cementoblast differentiation, formation of acellular cementum, and development of periodontal ligament principal fibers.* Anat Rec, 1989. **223**(2): p. 209-22.
62. Luan, X., Y. Ito, and T.G. Diekwisch, *Evolution and development of Hertwig's epithelial root sheath.* Dev Dyn, 2006. **235**(5): p. 1167-80.
63. Yamamoto, T. and S. Takahashi, *Hertwig's epithelial root sheath cells do not transform into cementoblasts in rat molar cementogenesis.* Ann Anat, 2009. **191**(6): p. 547-55.
64. Sonoyama, W., et al., *Human Hertwig's epithelial root sheath cells play crucial roles in cementum formation.* J Dent Res, 2007. **86**(7): p. 594-9.
65. Terling, C., et al., *Dynamic expression of E-cadherin in ameloblasts and cementoblasts in mice.* Eur J Oral Sci, 1998. **106 Suppl 1**: p. 137-42.
66. Alatli, I., C. Lundmark, and L. Hammarstrom, *The localization of epithelial root sheath cells during cementum formation in rat molars.* J Periodontal Res, 1996. **31**(6): p. 433-40.
67. Moxham, B.J., et al., *Changes in the cytoskeleton of cells within the periodontal*

*ligament and dental pulp of the rat first molar tooth during ageing.* Eur J Oral Sci, 1998. **106 Suppl 1**: p. 376-83.

68. Shore, R.C., B.K. Berkovitz, and B.J. Moxham, *Intercellular contacts between fibroblasts in the periodontal connective tissues of the rat.* J Anat, 1981. **133**(Pt 1): p. 67-76.
69. Yamaoka, Y., et al., *Desmosomal proteins in cultured and intact human periodontal ligament fibroblasts.* Tissue Cell, 1999. **31**(6): p. 605-9.
70. Owens, P.D., *The root surface in human teeth: a microradiographic study.* J Anat, 1976. **122**(Pt 2): p. 389-401.
71. Owens, P.D., *Ultrastructure of Hertwig's epithelial root sheath during early root development in premolar teeth in dogs.* Arch Oral Biol, 1978. **23**(2): p. 91-104.
72. Huang, X., et al., *Fate of HERS during tooth root development.* Dev Biol, 2009. **334**(1): p. 22-30.
73. Cerri, P.S., E. Freymuller, and E. Katchburian, *Apoptosis in the early developing periodontium of rat molars.* Anat Rec, 2000. **258**(2): p. 136-44.
74. Cerri, P.S. and E. Katchburian, *Apoptosis in the epithelial cells of the rests of Malassez of the periodontium of rat molars.* J Periodontal Res, 2005. **40**(5): p. 365-72.
75. Kaneko, H., et al., *Cell proliferation and death of Hertwig's epithelial root sheath in the rat.* Cell Tissue Res, 1999. **298**(1): p. 95-103.
76. Loe, H. and J. Waerhaug, *Experimental replantation of teeth in dogs and monkeys.* Arch Oral Biol, 1961. **3**: p. 176-84.
77. Shimono, M., et al., *Regulatory mechanisms of periodontal regeneration.* Microsc Res Tech, 2003. **60**(5): p. 491-502.
78. Fujiyama, K., et al., *Denervation resulting in dento-alveolar ankylosis associated with decreased Malassez epithelium.* J Dent Res, 2004. **83**(8): p. 625-9.
79. Lindskog, S., L. Blomlof, and L. Hammarstrom, *Evidence for a role of odontogenic epithelium in maintaining the periodontal space.* J Clin Periodontol, 1988. **15**(6): p. 371-3.
80. Reitan, K., *Behavior of Malassez' epithelial rests during orthodontic tooth movement.* Acta Odontol Scand, 1961. **19**: p. 443-68.
81. Wesselink, P.R. and W. Beertsen, *The prevalence and distribution of rests of Malassez in the mouse molar and their possible role in repair and maintenance of the periodontal ligament.* Arch Oral Biol, 1993. **38**(5): p. 399-403.
82. Rincon, J.C., W.G. Young, and P.M. Bartold, *The epithelial cell rests of Malassez--*

*a role in periodontal regeneration?* J Periodontal Res, 2006. **41**(4): p. 245-52.

83. Wallace, J.A. and K. Vergona, *Epithelial rests' function in replantation: is splinting necessary in replantation?* Oral Surg Oral Med Oral Pathol, 1990. **70**(5): p. 644-9.
84. Brice, G.L., W.J. Sampson, and M.R. Sims, *An ultrastructural evaluation of the relationship between epithelial rests of Malassez and orthodontic root resorption and repair in man.* Aust Orthod J, 1991. **12**(2): p. 90-4.
85. Kat, P.S., et al., *Distribution of the epithelial rests of Malassez and their relationship to blood vessels of the periodontal ligament during rat tooth development.* Aust Orthod J, 2003. **19**(2): p. 77-86.
86. Talic, N.F., et al., *Proliferation of epithelial rests of Malassez during experimental tooth movement.* Am J Orthod Dentofacial Orthop, 2003. **123**(5): p. 527-33.
87. Lambrichts, I., J. Creemers, and D. Van Steenberghe, *Periodontal neural endings intimately relate to epithelial rests of Malassez in humans. A light and electron microscope study.* J Anat, 1993. **182 ( Pt 2)**: p. 153-62.
88. Tadokoro, O., et al., *Merkel-like cells in Malassez epithelium in the periodontal ligament of cats: an immunohistochemical, confocal-laser scanning and immuno electron-microscopic investigation.* J Periodontal Res, 2002. **37**(6): p. 456-63.
89. Beck, F., et al., *The expression of the gene coding for parathyroid hormone-related protein (PTHrP) during tooth development in the rat.* Cell Tissue Res, 1995. **280**(2): p. 283-90.
90. Heyeraas, K.J., et al., *Nerve fibers immunoreactive to protein gene product 9.5, calcitonin gene-related peptide, substance P, and neuropeptide Y in the dental pulp, periodontal ligament, and gingiva in cats.* Acta Odontol Scand, 1993. **51**(4): p. 207-21.
91. Kvinnsland, I.H., et al., *Neuroendocrine cells in Malassez epithelium and gingiva of the cat.* Acta Odontol Scand, 2000. **58**(3): p. 107-12.
92. Tadokoro, O., V. Vandevska-Randunovic, and K. Inoue, *Epithelial cell rests of Malassez and OX6-immunopositive cells in the periodontal ligament of rat molars: a light and transmission electron microscope study.* Anat Rec (Hoboken), 2008. **291**(3): p. 242-53.
93. Yamashiro, T., et al., *Epithelial rests of Malassez express immunoreactivity of TrkA and its distribution is regulated by sensory nerve innervation.* J Histochem Cytochem, 2000. **48**(7): p. 979-84.
94. Hasegawa, N., et al., *Immunohistochemical characteristics of epithelial cell rests of Malassez during cementum repair.* J Periodontal Res, 2003. **38**(1): p. 51-6.

95. Mizuno, N., et al., *Characterization of epithelial cells derived from periodontal ligament by gene expression patterns of bone-related and enamel proteins.* Cell Biol Int, 2005. **29**(2): p. 111-7.
96. Mouri, Y., et al., *Differential gene expression of bone-related proteins in epithelial and fibroblastic cells derived from human periodontal ligament.* Cell Biol Int, 2003. **27**(7): p. 519-24.
97. Rincon, J.C., et al., *Production of osteopontin by cultured porcine epithelial cell rests of Malassez.* J Periodontal Res, 2005. **40**(5): p. 417-26.
98. Bronckers, A.L., et al., *Immunolocalization of osteopontin, osteocalcin, and dentin sialoprotein during dental root formation and early cementogenesis in the rat.* J Bone Miner Res, 1994. **9**(6): p. 833-41.
99. Macneil, R.L., et al., *Bone sialoprotein is localized to the root surface during cementogenesis.* J Bone Miner Res, 1994. **9**(10): p. 1597-606.
100. Huang, G.T., S. Gronthos, and S. Shi, *Mesenchymal stem cells derived from dental tissues vs. those from other sources: their biology and role in regenerative medicine.* J Dent Res, 2009. **88**(9): p. 792-806.
101. Selvig, K.A., et al., *Bone repair following recombinant human bone morphogenetic protein-2 stimulated periodontal regeneration.* J Periodontol, 2002. **73**(9): p. 1020-9.
102. Pittenger, M.F., et al., *Multilineage potential of adult human mesenchymal stem cells.* Science, 1999. **284**(5411): p. 143-7.
103. Evans, M.J. and M.H. Kaufman, *Establishment in culture of pluripotential cells from mouse embryos.* Nature, 1981. **292**(5819): p. 154-6.
104. Martin, G.R., *Isolation of a pluripotent cell line from early mouse embryos cultured in medium conditioned by teratocarcinoma stem cells.* Proc Natl Acad Sci U S A, 1981. **78**(12): p. 7634-8.
105. Thomson, J.A., et al., *Embryonic stem cell lines derived from human blastocysts.* Science, 1998. **282**(5391): p. 1145-7.
106. Takahashi, K., et al., *Induction of pluripotent stem cells from adult human fibroblasts by defined factors.* Cell, 2007. **131**(5): p. 861-72.
107. Takahashi, K. and S. Yamanaka, *Induction of pluripotent stem cells from mouse embryonic and adult fibroblast cultures by defined factors.* Cell, 2006. **126**(4): p. 663-76.
108. Yamanaka, S. and H.M. Blau, *Nuclear reprogramming to a pluripotent state by three approaches.* Nature, 2010. **465**(7299): p. 704-12.

109. Young, F.E., *A time for restraint.* Science, 2000. **287**(5457): p. 1424.
110. Lenoir, N., *Europe confronts the embryonic stem cell research challenge.* Science, 2000. **287**(5457): p. 1425-7.
111. Bongso, A., C.Y. Fong, and K. Gauthaman, *Taking stem cells to the clinic: Major challenges.* J Cell Biochem, 2008. **105**(6): p. 1352-60.
112. Lee, H., et al., *Induced pluripotent stem cells in regenerative medicine: an argument for continued research on human embryonic stem cells.* Regen Med, 2009. **4**(5): p. 759-69.
113. Leblond, C.P., *classification of cell populations on the basis of their proliferative behavior.* Natl Cancer Inst Monogr, 1964. **14**: p. 119-50.
114. Aggarwal, S. and M.F. Pittenger, *Human mesenchymal stem cells modulate allogeneic immune cell responses.* Blood, 2005. **105**(4): p. 1815-22.
115. Nauta, A.J. and W.E. Fibbe, *Immunomodulatory properties of mesenchymal stromal cells.* Blood, 2007. **110**(10): p. 3499-506.
116. Friedenstein, A.J., et al., *Stromal cells responsible for transferring the microenvironment of the hemopoietic tissues. Cloning in vitro and retransplantation in vivo.* Transplantation, 1974. **17**(4): p. 331-40.
117. Friedenstein, A.J., J.F. Gorskaja, and N.N. Kulagina, *Fibroblast precursors in normal and irradiated mouse hematopoietic organs.* Exp Hematol, 1976. **4**(5): p. 267-74.
118. Friedenstein, A.J., S. Piatetzky, II, and K.V. Petrakova, *Osteogenesis in transplants of bone marrow cells.* J Embryol Exp Morphol, 1966. **16**(3): p. 381-90.
119. Owen, M., *Marrow stromal stem cells.* J Cell Sci Suppl, 1988. **10**: p. 63-76.
120. Sale, G.E. and R. Storb, *Bilateral diffuse pulmonary ectopic ossification after marrow allograft in a dog. Evidence for allotransplantation of hemopoietic and mesenchymal stem cells.* Exp Hematol, 1983. **11**(10): p. 961-6.
121. Caplan, A.I., *Mesenchymal stem cells.* J Orthop Res, 1991. **9**(5): p. 641-50.
122. Horwitz, E.M., et al., *Clarification of the nomenclature for MSC: The International Society for Cellular Therapy position statement.* Cytotherapy, 2005. **7**(5): p. 393-5.
123. Dominici, M., et al., *Minimal criteria for defining multipotent mesenchymal stromal cells. The International Society for Cellular Therapy position statement.* Cytotherapy, 2006. **8**(4): p. 315-7.
124. Park, D., et al., *Endogenous bone marrow MSCs are dynamic, fate-restricted participants in bone maintenance and regeneration.* Cell Stem Cell, 2012. **10**(3): p. 259-72.

125. Sacchetti, B., et al., *Self-renewing osteoprogenitors in bone marrow sinusoids can organize a hematopoietic microenvironment.* Cell, 2007. **131**(2): p. 324-36.
126. Seo, B.M., et al., *Investigation of multipotent postnatal stem cells from human periodontal ligament.* Lancet, 2004. **364**(9429): p. 149-55.
127. Gronthos, S., et al., *Postnatal human dental pulp stem cells (DPSCs) in vitro and in vivo.* Proc Natl Acad Sci U S A, 2000. **97**(25): p. 13625-30.
128. Sonoyama, W., et al., *Characterization of the apical papilla and its residing stem cells from human immature permanent teeth: a pilot study.* J Endod, 2008. **34**(2): p. 166-71.
129. Sonoyama, W., et al., *Mesenchymal stem cell-mediated functional tooth regeneration in swine.* PLoS One, 2006. **1**: p. e79.
130. Sonoyama, W., et al., *Mesenchymal stem cell-mediated functional tooth regeneration in swine.* PLoS ONE, 2006. **1**: p. e79.
131. Miura, M., et al., *SHED: stem cells from human exfoliated deciduous teeth.* Proc Natl Acad Sci U S A, 2003. **100**(10): p. 5807-12.
132. Morsczeck, C., et al., *Isolation of precursor cells (PCs) from human dental follicle of wisdom teeth.* Matrix Biol, 2005. **24**(2): p. 155-65.
133. Morsczeck, C., et al., *Somatic stem cells for regenerative dentistry.* Clin Oral Investig, 2008. **12**(2): p. 113-8.
134. Zhang, Q., et al., *Mesenchymal stem cells derived from human gingiva are capable of immunomodulatory functions and ameliorate inflammation-related tissue destruction in experimental colitis.* J Immunol, 2009. **183**(12): p. 7787-98.
135. Liao, J., et al., *Cells isolated from inflamed periapical tissue express mesenchymal stem cell markers and are highly osteogenic.* J Endod, 2011. **37**(9): p. 1217-24.
136. Jiang, H.W., J.Q. Ling, and Q.M. Gong, *The expression of stromal cell-derived factor 1 (SDF-1) in inflamed human dental pulp.* J Endod, 2008. **34**(11): p. 1351-4.
137. Alongi, D.J., et al., *Stem/progenitor cells from inflamed human dental pulp retain tissue regeneration potential.* Regen Med, 2010. **5**(4): p. 617-31.
138. Park, J.C., et al., *Isolation and characterization of human periodontal ligament (PDL) stem cells (PDLSCs) from the inflamed PDL tissue: in vitro and in vivo evaluations.* J Clin Periodontol, 2011. **38**(8): p. 721-31.
139. Gronthos, S., et al., *Ovine periodontal ligament stem cells: isolation, characterization, and differentiation potential.* Calcif Tissue Int, 2006. **79**(5): p. 310-7.
140. Giordano, G., et al., *Stem cells from oral niches: a review.* Ann Stomatol (Roma),

2011. **2**(1-2): p. 3-8.

141. Arthur, A., et al., *Adult human dental pulp stem cells differentiate toward functionally active neurons under appropriate environmental cues.* Stem Cells, 2008. **26**(7): p. 1787-95.
142. Widera, D., et al., *Highly efficient neural differentiation of human somatic stem cells, isolated by minimally invasive periodontal surgery.* Stem Cells Dev, 2007. **16**(3): p. 447-60.
143. McCulloch, C.A., et al., *Paravascular cells in endosteal spaces of alveolar bone contribute to periodontal ligament cell populations.* Anat Rec, 1987. **219**(3): p. 233-42.
144. Chen, S.C., et al., *Location of putative stem cells in human periodontal ligament.* J Periodontal Res, 2006. **41**(6): p. 547-53.
145. McCulloch, C.A., *Progenitor cell populations in the periodontal ligament of mice.* Anat Rec, 1985. **211**(3): p. 258-62.
146. Bianco, P., et al., *Bone marrow stromal stem cells: nature, biology, and potential applications.* Stem Cells, 2001. **19**(3): p. 180-92.
147. Liu, Y., et al., *Periodontal ligament stem cell-mediated treatment for periodontitis in miniature swine.* Stem Cells, 2008. **26**(4): p. 1065-73.
148. Xie, H. and H. Liu, *A Novel Mixed Type Stem Cell Pellet for Cementum/Periodontal Ligament-Like Complex.* J Periodontol, 2011.
149. Lang, H., et al., *Formation of differentiated tissues in vivo by periodontal cell populations cultured in vitro.* J Dent Res, 1995. **74**(5): p. 1219-25.
150. Ma, Z., et al., *The biological effect of dentin noncollagenous proteins (DNCPs) on the human periodontal ligament stem cells (HPDLSCs) in vitro and in vivo.* Tissue Eng Part A, 2008. **14**(12): p. 2059-68.
151. Yang, Z., et al., *Tissue engineering of cementum/periodontal-ligament complex using a novel three-dimensional pellet cultivation system for human periodontal ligament stem cells.* Tissue Eng Part C Methods, 2009. **15**(4): p. 571-81.
152. Li, S., et al., *NASA-approved rotary bioreactor enhances proliferation and osteogenesis of human periodontal ligament stem cells.* Stem Cells Dev, 2009.
153. Wada, N., et al., *Immunomodulatory properties of human periodontal ligament stem cells.* J Cell Physiol, 2009. **219**(3): p. 667-76.
154. Ding, G., et al., *Allogeneic periodontal ligament stem cell therapy for periodontitis in swine.* Stem Cells, 2010. **28**(10): p. 1829-38.
155. Feng, F., et al., *Utility of PDL progenitors for in vivo tissue regeneration: a report*

*of 3 cases.* Oral Dis, 2010. **16**(1): p. 20-8.

156. Diekwisch, T.G., *The developmental biology of cementum.* Int J Dev Biol, 2001. **45**(5-6): p. 695-706.
157. Ikeda, E., et al., *Fully functional bioengineered tooth replacement as an organ replacement therapy.* Proc Natl Acad Sci U S A, 2009. **106**(32): p. 13475-80.
158. Nakao, K., et al., *The development of a bioengineered organ germ method.* Nat Methods, 2007. **4**(3): p. 227-30.
159. Oshima, M., et al., *Functional tooth regeneration using a bioengineered tooth unit as a mature organ replacement regenerative therapy.* PLoS One, 2011. **6**(7): p. e21531.
160. Bai, Y., et al., *Cementum- and periodontal ligament-like tissue formation by dental follicle cell sheets co-cultured with Hertwig's epithelial root sheath cells.* Bone, 2011. **48**(6): p. 1417-26.
161. Jung, H.S., et al., *Directing the differentiation of human dental follicle cells into cementoblasts and/or osteoblasts by a combination of HERS and pulp cells.* J Mol Histol, 2011. **42**(3): p. 227-35.
162. Shinmura, Y., et al., *Quiescent epithelial cell rests of Malassez can differentiate into ameloblast-like cells.* J Cell Physiol, 2008. **217**(3): p. 728-38.
163. Maria, O.M., et al., *Cells from bone marrow that evolve into oral tissues and their clinical applications.* Oral Dis, 2007. **13**(1): p. 11-6.
164. Murray, P.E., F. Garcia-Godoy, and K.M. Hargreaves, *Regenerative endodontics: a review of current status and a call for action.* J Endod, 2007. **33**(4): p. 377-90.
165. Ohazama, A., et al., *Stem-cell-based tissue engineering of murine teeth.* J Dent Res, 2004. **83**(7): p. 518-22.
166. Sloan, A.J. and A.J. Smith, *Stem cells and the dental pulp: potential roles in dentine regeneration and repair.* Oral Dis, 2007. **13**(2): p. 151-7.
167. Hu, B., et al., *Bone marrow cells can give rise to ameloblast-like cells.* J Dent Res, 2006. **85**(5): p. 416-21.
168. Song, A.M., et al., *A study of enamel matrix proteins on differentiation of porcine bone marrow stromal cells into cementoblasts.* Cell Prolif, 2007. **40**(3): p. 381-96.
169. Yang, Y., F.M. Rossi, and E.E. Putnins, *Periodontal regeneration using engineered bone marrow mesenchymal stromal cells.* Biomaterials, 2010. **31**(33): p. 8574-82.
170. Kim, S.H., et al., *Alveolar bone regeneration by transplantation of periodontal ligament stem cells and bone marrow stem cells in a canine peri-implant defect model: a pilot study.* J Periodontol, 2009. **80**(11): p. 1815-23.

171. Yamada, Y., et al., *A novel approach to periodontal tissue regeneration with mesenchymal stem cells and platelet-rich plasma using tissue engineering technology: A clinical case report.* Int J Periodontics Restorative Dent, 2006. **26**(4): p. 363-9.
172. Lang, H., N. Schuler, and R. Nolden, *Attachment formation following replantation of cultured cells into periodontal defects--a study in minipigs.* J Dent Res, 1998. **77**(2): p. 393-405.
173. Tobita, M., et al., *Periodontal tissue regeneration with adipose-derived stem cells.* Tissue Eng Part A, 2008. **14**(6): p. 945-53.
174. Lin, N.H., S. Gronthos, and P. Mark Bartold, *Stem cells and future periodontal regeneration.* Periodontol 2000, 2009. **51**: p. 239-51.
175. Wang, J., et al., *Stem cells from human-exfoliated deciduous teeth can differentiate into dopaminergic neuron-like cells.* Stem Cells Dev, 2010. **19**(9): p. 1375-83.
176. Arthur, A., et al., *Implanted adult human dental pulp stem cells induce endogenous axon guidance.* Stem Cells, 2009. **27**(9): p. 2229-37.
177. Graf, T. and M. Stadtfeld, *Heterogeneity of embryonic and adult stem cells.* Cell Stem Cell, 2008. **3**(5): p. 480-3.
178. Ho, A.D., W. Wagner, and W. Franke, *Heterogeneity of mesenchymal stromal cell preparations.* Cytotherapy, 2008. **10**(4): p. 320-30.
179. Gronthos, S., et al., *Stem cell properties of human dental pulp stem cells.* J Dent Res, 2002. **81**(8): p. 531-5.
180. Owen, M. and A.J. Friedenstein, *Stromal stem cells: marrow-derived osteogenic precursors.* Ciba Found Symp, 1988. **136**: p. 42-60.
181. Gronthos, S., et al., *Differential cell surface expression of the STRO-1 and alkaline phosphatase antigens on discrete developmental stages in primary cultures of human bone cells.* J Bone Miner Res, 1999. **14**(1): p. 47-56.
182. Chambers, I., et al., *Nanog safeguards pluripotency and mediates germline development.* Nature, 2007. **450**(7173): p. 1230-4.
183. Hayashi, K., et al., *Dynamic equilibrium and heterogeneity of mouse pluripotent stem cells with distinct functional and epigenetic states.* Cell Stem Cell, 2008. **3**(4): p. 391-401.
184. Haug, J.S., et al., *N-cadherin expression level distinguishes reserved versus primed states of hematopoietic stem cells.* Cell Stem Cell, 2008. **2**(4): p. 367-79.
185. Jones, P.H. and F.M. Watt, *Separation of human epidermal stem cells from transit amplifying cells on the basis of differences in integrin function and expression.*

Cell, 1993. **73**(4): p. 713-24.

186. Jones, P.H., S. Harper, and F.M. Watt, *Stem cell patterning and fate in human epidermis.* Cell, 1995. **80**(1): p. 83-93.

187. Li, A., P.J. Simmons, and P. Kaur, *Identification and isolation of candidate human keratinocyte stem cells based on cell surface phenotype.* Proc Natl Acad Sci U S A, 1998. **95**(7): p. 3902-7.

188. Kaur, P., et al., *Keratinocyte stem cell assays: an evolving science.* J Investig Dermatol Symp Proc, 2004. **9**(3): p. 238-47.

189. Li, A. and P. Kaur, *FACS enrichment of human keratinocyte stem cells.* Methods Mol Biol, 2005. **289**: p. 87-96.

190. Greco, S.J., K. Liu, and P. Rameshwar, *Functional similarities among genes regulated by OCT4 in human mesenchymal and embryonic stem cells.* Stem Cells, 2007. **25**(12): p. 3143-54.

191. Gronthos, S., et al., *Molecular and cellular characterisation of highly purified stromal stem cells derived from human bone marrow.* J Cell Sci, 2003. **116**(Pt 9): p. 1827-35.

192. Miura, Y., et al., *Defective osteogenesis of the stromal stem cells predisposes CD18-null mice to osteoporosis.* Proc Natl Acad Sci U S A, 2005. **102**(39): p. 14022-7.

193. Shi, S. and S. Gronthos, *Perivascular niche of postnatal mesenchymal stem cells in human bone marrow and dental pulp.* J Bone Miner Res, 2003. **18**(4): p. 696-704.

194. Simmons, P.J. and B. Torok-Storb, *Identification of stromal cell precursors in human bone marrow by a novel monoclonal antibody, STRO-1.* Blood, 1991. **78**(1): p. 55-62.

195. Gronthos, S., et al., *The STRO-1+ fraction of adult human bone marrow contains the osteogenic precursors.* Blood, 1994. **84**(12): p. 4164-73.

196. Dennis, J.E. and P. Charbord, *Origin and differentiation of human and murine stroma.* Stem Cells, 2002. **20**(3): p. 205-14.

197. Tamayo, E., et al., *A quantitative assay that evaluates the capacity of human stromal cells to support granulomonopoiesis in situ.* Stem Cells, 1994. **12**(3): p. 304-15.

198. Stewart, K., et al., *Further characterization of cells expressing STRO-1 in cultures of adult human bone marrow stromal cells.* J Bone Miner Res, 1999. **14**(8): p. 1345-56.

199. Tanaka-Douzono, M., et al., *Detection of murine adult bone marrow stroma-*

*initiating cells in Lin(-)c-fms(+)c-kit(low)VCAM-1(+) cells.* J Cell Physiol, 2001. **189**(1): p. 45-53.

200. Gronthos, S., et al., *A novel monoclonal antibody (STRO-3) identifies an isoform of tissue nonspecific alkaline phosphatase expressed by multipotent bone marrow stromal stem cells.* Stem Cells Dev, 2007. **16**(6): p. 953-63.
201. Gronthos, S., et al., *Heat shock protein-90 beta is expressed at the surface of multipotential mesenchymal precursor cells: generation of a novel monoclonal antibody, STRO-4, with specificity for mesenchymal precursor cells from human and ovine tissues.* Stem Cells Dev, 2009. **18**(9): p. 1253-62.
202. Yamada, S., et al., *Expression profile of active genes in human periodontal ligament and isolation of PLAP-1, a novel SLRP family gene.* Gene, 2001. **275**(2): p. 279-86.
203. Saito, Y., et al., *A cell line with characteristics of the periodontal ligament fibroblasts is negatively regulated for mineralization and Runx2/Cbfa1/Osf2 activity, part of which can be overcome by bone morphogenetic protein-2.* J Cell Sci, 2002. **115**(Pt 21): p. 4191-200.
204. Takatalo, M.S., et al., *Novel Golgi protein, GoPro49, is a specific dental follicle marker.* J Dent Res, 2009. **88**(6): p. 534-8.
205. Kaur, P. and A. Li, *Adhesive properties of human basal epidermal cells: an analysis of keratinocyte stem cells, transit amplifying cells, and postmitotic differentiating cells.* J Invest Dermatol, 2000. **114**(3): p. 413-20.
206. Calenic, B., et al., *Magnetic separation and characterization of keratinocyte stem cells from human gingiva.* J Periodontal Res, 2010. **45**(6): p. 703-8.
207. Izumi, K., T. Tobita, and S.E. Feinberg, *Isolation of human oral keratinocyte progenitor/stem cells.* J Dent Res, 2007. **86**(4): p. 341-6.
208. Somerman, M.J., et al., *A comparative study of human periodontal ligament cells and gingival fibroblasts in vitro.* J Dent Res, 1988. **67**(1): p. 66-70.
209. Owens, R.B., et al., *Epithelial cell cultures from normal and cancerous human tissues.* J Natl Cancer Inst, 1976. **56**(4): p. 843-9.
210. Mohammadpour, H.A., *Isolation and culture of human colon epithelial cells using a modified explant technique employing a noninjurious approach.* Methods Mol Med, 2005. **107**: p. 237-47.
211. Kuznetsov, S.A., et al., *Single-colony derived strains of human marrow stromal fibroblasts form bone after transplantation in vivo.* J Bone Miner Res, 1997. **12**(9): p. 1335-47.

212. Menicanin, D., et al., *Identification of a common gene expression signature associated with immature clonal mesenchymal cell populations derived from bone marrow and dental tissues.* Stem Cells Dev, 2010. **19**(10): p. 1501-10.
213. Mayrhofer, C., et al., *DIGE compatible labelling of surface proteins on vital cells in vitro and in vivo.* Proteomics, 2006. **6**(2): p. 579-85.
214. Zilm, P.S., et al., *Effect of alkaline growth pH on the expression of cell envelope proteins in Fusobacterium nucleatum.* Microbiology, 2010. **156**(Pt 6): p. 1783-94.
215. Gorg, A., et al., *Two-dimensional electrophoresis of proteins in an immobilized pH 4-12 gradient.* Electrophoresis, 1998. **19**(8-9): p. 1516-9.
216. Gade, D., et al., *Evaluation of two-dimensional difference gel electrophoresis for protein profiling. Soluble proteins of the marine bacterium Pirellula sp. strain 1.* J Mol Microbiol Biotechnol, 2003. **5**(4): p. 240-51.
217. Gimble, J.M., *Marrow stromal adipocytes,* in *Marrow stromal cell culture,* J.N.a.O. Beresford, M., Editor. 1998, Cambridge: Cambridge University Press. p. 67-87.
218. Isenmann, S., et al., *TWIST family of basic helix-loop-helix transcription factors mediate human mesenchymal stem cell growth and commitment.* Stem Cells, 2009. **27**(10): p. 2457-68.
219. Brunette, D.M., A.H. Melcher, and H.K. Moe, *Culture and origin of epithelium-like and fibroblast-like cells from porcine periodontal ligament explants and cell suspensions.* Arch Oral Biol, 1976. **21**(7): p. 393-400.
220. Brunette, D.M., *Mechanical stretching increases the number of epithelial cells synthesizing DNA in culture.* J Cell Sci, 1984. **69**: p. 35-45.
221. Brunette, D.M., *Cholera toxin and dibutyryl cyclic-AMP stimulate the growth of epithelial cells derived from epithelial rests from porcine periodontal ligament.* Arch Oral Biol, 1984. **29**(4): p. 303-9.
222. Brunette, D.M., et al., *In-vitro cultural parameters and protein and prostaglandin secretion of epithelial cells derived from porcine rests of Malassez.* Arch Oral Biol, 1979. **24**(3): p. 199-203.
223. Firth, J.D., et al., *Bacterial phospholipase C upregulates matrix metalloproteinase expression by cultured epithelial cells.* Infect Immun, 1997. **65**(12): p. 4931-6.
224. Firth, J.D., et al., *Chymotrypsin-like enzyme secretion is stimulated in cultured epithelial cells during proliferation and in response to Actinobacillus actinomycetemcomitans.* J Periodontal Res, 1996. **31**(5): p. 345-54.
225. Kurashige, Y., et al., *Profiling of differentially expressed genes in porcine epithelial cells derived from periodontal ligament and gingiva by DNA microarray.*

Arch Oral Biol, 2008. **53**(5): p. 437-42.

226. Merrilees, M.J., J. Sodek, and J.E. Aubin, *Effects of cells of epithelial rests of Malassez and endothelial cells on synthesis of glycosaminoglycans by periodontal ligament fibroblasts in vitro.* Dev Biol, 1983. **97**(1): p. 146-53.
227. Nip, L.H., V.J. Uitto, and L.M. Golub, *Inhibition of epithelial cell matrix metalloproteinases by tetracyclines.* J Periodontal Res, 1993. **28**(5): p. 379-85.
228. Rao, L.G., H.K. Moe, and J.N. Heersche, *In-vitro culture of porcine periodontal ligament cells: response of fibroblast-like and epithelial-like cells to prostaglandin E1, parathyroid hormone and calcitonin and separation of a pure population of fibroblast-like cells.* Arch Oral Biol, 1978. **23**(11): p. 957-64.
229. Salonen, J., et al., *Proliferating oral epithelial cells in culture are capable of both extracellular and intracellular degradation of interstitial collagen.* Matrix, 1991. **11**(1): p. 43-55.
230. Uitto, V.J., et al., *Collagenase-3 (matrix metalloproteinase-13) expression is induced in oral mucosal epithelium during chronic inflammation.* Am J Pathol, 1998. **152**(6): p. 1489-99.
231. Uitto, V.J., et al., *Expression of fibronectin and integrins in cultured periodontal ligament epithelial cells.* J Dent Res, 1992. **71**(5): p. 1203-11.
232. Yamawaki, K., et al., *Effects of epidermal growth factor and/or nerve growth factor on Malassez's epithelial rest cells in vitro: expression of mRNA for osteopontin, bone morphogenetic protein 2 and vascular endothelial growth factor.* J Periodontal Res, 2010. **45**(3): p. 421-7.
233. Akimoto, T., et al., *Establishment of Hertwig's epithelial root sheath cell line from cells involved in epithelial-mesenchymal transition.* Biochem Biophys Res Commun, 2010. **404**(1): p. 308-12.
234. Blomlof, L. and P. Otteskog, *Composition of human periodontal ligament cells in tissue culture.* Scand J Dent Res, 1981. **89**(1): p. 43-7.
235. Ragnarsson, B., G. Carr, and J.C. Daniel, *Isolation and growth of human periodontal ligament cells in vitro.* J Dent Res, 1985. **64**(8): p. 1026-30.
236. Jung, H.S., et al., *Directing the differentiation of human dental follicle cells into cementoblasts and/or osteoblasts by a combination of HERS and pulp cells.* J Mol Histol, 2011.
237. Nam, H., et al., *Expression profile of the stem cell markers in human Hertwig's epithelial root sheath/Epithelial rests of Malassez cells.* Mol Cells, 2011. **31**(4): p. 355-60.

238. Shimonishi, M., et al., *In vitro differentiation of epithelial cells cultured from human periodontal ligament.* J Periodontal Res, 2007. **42**(5): p. 456-65.
239. Shimonishi, M., et al., *Expression of type IV collagen and laminin at the interface between epithelial cells and fibroblasts from human periodontal ligament.* Eur J Oral Sci, 2005. **113**(1): p. 34-40.
240. Yamanaka, T., et al., *Isolation and serum-free culture of epithelial cells derived from epithelial rests of Malassez in human periodontal ligament.* In Vitro Cell Dev Biol Anim, 2000. **36**(8): p. 548-53.
241. Rincon, J.C., *Expression of non-collagenous proteins by the epithelial rest cells of Malassez* in *School of Dentistry*2004, The University of Queensland: Brisbane. p. 172.
242. Jiang, X.Y., et al., *Methods for isolating highly-enriched embryonic spinal cord neurons: a comparison between enzymatic and mechanical dissociations.* J Neurosci Methods, 2006. **158**(1): p. 13-8.
243. Varani, J., et al., *Retinoic acid stimulation of human dermal fibroblast proliferation is dependent on suboptimal extracellular Ca2+ concentration.* Am J Pathol, 1990. **136**(6): p. 1275-81.
244. Tsao, M.C., B.J. Walthall, and R.G. Ham, *Clonal growth of normal human epidermal keratinocytes in a defined medium.* J Cell Physiol, 1982. **110**(2): p. 219-29.
245. Mercurio, A.M., I. Rabinovitz, and L.M. Shaw, *The alpha 6 beta 4 integrin and epithelial cell migration.* Curr Opin Cell Biol, 2001. **13**(5): p. 541-5.
246. Mizutani, K., et al., *Interaction of nectin-like molecule 2 with integrin alpha6beta4 and inhibition of disassembly of integrin alpha6beta4 from hemidesmosomes.* J Biol Chem, 2011. **286**(42): p. 36667-76.
247. Sun, H., S.A. Santoro, and M.M. Zutter, *Downstream events in mammary gland morphogenesis mediated by reexpression of the alpha2beta1 integrin: the role of the alpha6 and beta4 integrin subunits.* Cancer Res, 1998. **58**(10): p. 2224-33.
248. Nishimura, M., et al., *Effect of cell plating density and extracellular matrix protein on cell growth of epithelial rests of Malassez in vitro.* Med Electron Microsc, 1999. **32**(2): p. 127-132.
249. Berkovitz, B.K., et al., *The structure of bovine periodontal ligament with special reference to the epithelial cell rests.* J Periodontol, 1997. **68**(9): p. 905-13.
250. Peters, B.H., et al., *Maintenance of cell-type-specific cytoskeletal character in epithelial cells out of epithelial context: cytokeratins and other cytoskeletal*

*proteins in the rests of Malassez of the periodontal ligament.* Differentiation, 1995. **59**(2): p. 113-26.

251. Sculean, A., et al., *Patterns of cytokeratin expression in monkey and human periodontium following regenerative and conventional periodontal surgery.* J Periodontal Res, 2001. **36**(4): p. 260-8.
252. Cavey, M., et al., *A two-tiered mechanism for stabilization and immobilization of E-cadherin.* Nature, 2008. **453**(7196): p. 751-6.
253. Knust, E. and O. Bossinger, *Composition and formation of intercellular junctions in epithelial cells.* Science, 2002. **298**(5600): p. 1955-9.
254. Nelson, W.J., *Adaptation of core mechanisms to generate cell polarity.* Nature, 2003. **422**(6933): p. 766-74.
255. Hirohashi, S., *Inactivation of the E-cadherin-mediated cell adhesion system in human cancers.* Am J Pathol, 1998. **153**(2): p. 333-9.
256. Taylor, V., et al., *Epithelial membrane protein-1, peripheral myelin protein 22, and lens membrane protein 20 define a novel gene family.* J Biol Chem, 1995. **270**(48): p. 28824-33.
257. Lee, H.S., et al., *EMP-1 is a junctional protein in a liver stem cell line and in the liver.* Biochem Biophys Res Commun, 2005. **334**(4): p. 996-1003.
258. Zhang, J., et al., *The expression of EMP1 is downregulated in oral squamous cell carcinoma and possibly associated with tumour metastasis.* J Clin Pathol, 2010. **64**(1): p. 25-9.
259. Jain, A., et al., *Epithelial membrane protein-1 is a biomarker of gefitinib resistance.* Proc Natl Acad Sci U S A, 2005. **102**(33): p. 11858-63.
260. Gronthos, S., et al., *Integrin expression and function on human osteoblast-like cells.* J Bone Miner Res, 1997. **12**(8): p. 1189-97.
261. Aldridge, V., et al., *Human mesenchymal stem cells are recruited to injured liver in a beta1 integrin and CD44 dependent manner.* Hepatology, 2012.
262. Zoller, M., *CD44: can a cancer-initiating cell profit from an abundantly expressed molecule?* Nat Rev Cancer, 2011. **11**(4): p. 254-67.
263. Bajorath, J., *Molecular organization, structural features, and ligand binding characteristics of CD44, a highly variable cell surface glycoprotein with multiple functions.* Proteins, 2000. **39**(2): p. 103-11.
264. Goodison, S., V. Urquidi, and D. Tarin, *CD44 cell adhesion molecules.* Mol Pathol, 1999. **52**(4): p. 189-96.
265. Wang, S.J. and L.Y. Bourguignon, *Role of hyaluronan-mediated CD44 signaling in*

*head and neck squamous cell carcinoma progression and chemoresistance.* Am J Pathol, 2011. **178**(3): p. 956-63.

266. Pure, E. and C.A. Cuff, *A crucial role for CD44 in inflammation.* Trends Mol Med, 2001. **7**(5): p. 213-21.
267. Gunthert, U., et al., *A new variant of glycoprotein CD44 confers metastatic potential to rat carcinoma cells.* Cell, 1991. **65**(1): p. 13-24.
268. Takaishi, S., et al., *Identification of gastric cancer stem cells using the cell surface marker CD44.* Stem Cells, 2009. **27**(5): p. 1006-20.
269. Marhaba, R., et al., *CD44 and EpCAM: cancer-initiating cell markers.* Curr Mol Med, 2008. **8**(8): p. 784-804.
270. Leonardi, R., et al., *Immunolocalization of CD44 adhesion molecules in human periradicular lesions.* Oral Surg Oral Med Oral Pathol Oral Radiol Endod, 2000. **89**(4): p. 480-5.
271. Messaoudi, S., et al., *Heat-shock protein 90 inhibitors as antitumor agents: a survey of the literature from 2005 to 2010.* Expert Opin Ther Pat, 2011. **21**(10): p. 1501-42.
272. Ruckova, E., P. Muller, and B. Vojtesek, *[Hsp90--a target for anticancer therapy]*. Klin Onkol, 2011. **24**(5): p. 329-37.
273. Beck, R., et al., *Molecular chaperone Hsp90 as a target for oxidant-based anticancer therapies.* Curr Med Chem, 2011. **18**(18): p. 2816-25.
274. Wang, R.E., *Targeting heat shock proteins 70/90 and proteasome for cancer therapy.* Curr Med Chem, 2011. **18**(27): p. 4250-64.
275. Andersen, D.C., et al., *Development of novel monoclonal antibodies that define differentiation stages of human stromal (mesenchymal) stem cells.* Mol Cells, 2011.
276. Prowse, A.B., et al., *Stem cell integrins: implications for ex-vivo culture and cellular therapies.* Stem Cell Res, 2011. **6**(1): p. 1-12.
277. Hynes, R.O., *Integrins: bidirectional, allosteric signaling machines.* Cell, 2002. **110**(6): p. 673-87.
278. Stephens, L.E., et al., *Deletion of beta 1 integrins in mice results in inner cell mass failure and peri-implantation lethality.* Genes Dev, 1995. **9**(15): p. 1883-95.
279. Cheresh, D.A., et al., *A novel vitronectin receptor integrin (alpha v beta x) is responsible for distinct adhesive properties of carcinoma cells.* Cell, 1989. **57**(1): p. 59-69.
280. Kennel, S.J., et al., *Analysis of the tumor-associated antigen TSP-180. Identity with alpha 6-beta 4 in the integrin superfamily.* J Biol Chem, 1989. **264**(26): p. 15515-

21.

281. Van der Neut, R., et al., *Epithelial detachment due to absence of hemidesmosomes in integrin beta 4 null mice.* Nat Genet, 1996. **13**(3): p. 366-9.

282. Dowling, J., Q.C. Yu, and E. Fuchs, *Beta4 integrin is required for hemidesmosome formation, cell adhesion and cell survival.* J Cell Biol, 1996. **134**(2): p. 559-72.

283. Goldfinger, L.E., M.S. Stack, and J.C. Jones, *Processing of laminin-5 and its functional consequences: role of plasmin and tissue-type plasminogen activator.* J Cell Biol, 1998. **141**(1): p. 255-65.

284. Lotz, M.M., I. Rabinovitz, and A.M. Mercurio, *Intestinal restitution: progression of actin cytoskeleton rearrangements and integrin function in a model of epithelial wound healing.* Am J Pathol, 2000. **156**(3): p. 985-96.

285. Mercurio, A.M. and I. Rabinovitz, *Towards a mechanistic understanding of tumor invasion--lessons from the alpha6beta 4 integrin.* Semin Cancer Biol, 2001. **11**(2): p. 129-41.

286. Rabinovitz, I. and A.M. Mercurio, *The integrin alpha6beta4 functions in carcinoma cell migration on laminin-1 by mediating the formation and stabilization of actin-containing motility structures.* J Cell Biol, 1997. **139**(7): p. 1873-84.

287. Georges-Labouesse, E., et al., *Essential role of alpha 6 integrins in cortical and retinal lamination.* Curr Biol, 1998. **8**(17): p. 983-6.

288. Xu, C., et al., *Feeder-free growth of undifferentiated human embryonic stem cells.* Nat Biotechnol, 2001. **19**(10): p. 971-4.

289. Gu, Y.C., et al., *Laminin isoform-specific promotion of adhesion and migration of human bone marrow progenitor cells.* Blood, 2003. **101**(3): p. 877-85.

290. Brooke, G., et al., *Molecular trafficking mechanisms of multipotent mesenchymal stem cells derived from human bone marrow and placenta.* Stem Cells Dev, 2008. **17**(5): p. 929-40.

291. Flanagan, L.A., et al., *Regulation of human neural precursor cells by laminin and integrins.* J Neurosci Res, 2006. **83**(5): p. 845-56.

292. Gronthos, S., et al., *Integrin-mediated interactions between human bone marrow stromal precursor cells and the extracellular matrix.* Bone, 2001. **28**(2): p. 174-81.

293. Saito, T., S.M. Albelda, and C.T. Brighton, *Identification of integrin receptors on cultured human bone cells.* J Orthop Res, 1994. **12**(3): p. 384-94.

294. Clover, J., R.A. Dodds, and M. Gowen, *Integrin subunit expression by human osteoblasts and osteoclasts in situ and in culture.* J Cell Sci, 1992. **103 ( Pt 1)**: p. 267-71.

295. Wong, J.C., et al., *Definitive endoderm derived from human embryonic stem cells highly express the integrin receptors alphaV and beta5.* Cell Adh Migr, 2010. **4**(1): p. 39-45.
296. van Laake, L.W., et al., *Extracellular matrix formation after transplantation of human embryonic stem cell-derived cardiomyocytes.* Cell Mol Life Sci, 2010. **67**(2): p. 277-90.
297. Colter, D.C., et al., *Rapid expansion of recycling stem cells in cultures of plastic-adherent cells from human bone marrow.* Proc Natl Acad Sci U S A, 2000. **97**(7): p. 3213-8.
298. Colter, D.C., I. Sekiya, and D.J. Prockop, *Identification of a subpopulation of rapidly self-renewing and multipotential adult stem cells in colonies of human marrow stromal cells.* Proc Natl Acad Sci U S A, 2001. **98**(14): p. 7841-5.
299. Smith, J.R., et al., *Isolation of a highly clonogenic and multipotential subfraction of adult stem cells from bone marrow stroma.* Stem Cells, 2004. **22**(5): p. 823-31.
300. Caplan, A.I. and S.P. Bruder, *Mesenchymal stem cells: building blocks for molecular medicine in the 21st century.* Trends Mol Med, 2001. **7**(6): p. 259-64.
301. Haynesworth, S.E., M.A. Baber, and A.I. Caplan, *Cytokine expression by human marrow-derived mesenchymal progenitor cells in vitro: effects of dexamethasone and IL-1 alpha.* J Cell Physiol, 1996. **166**(3): p. 585-92.
302. Lennon, D.P. and A.I. Caplan, *Isolation of human marrow-derived mesenchymal stem cells.* Exp Hematol, 2006. **34**(11): p. 1604-5.
303. Meirelles Lda, S., et al., *Mechanisms involved in the therapeutic properties of mesenchymal stem cells.* Cytokine Growth Factor Rev, 2009. **20**(5-6): p. 419-27.
304. Thiery, J.P., et al., *Epithelial-mesenchymal transitions in development and disease.* Cell, 2009. **139**(5): p. 871-90.
305. Blick, T., et al., *Epithelial mesenchymal transition traits in human breast cancer cell lines parallel the CD44(hi/)CD24 (lo/-) stem cell phenotype in human breast cancer.* J Mammary Gland Biol Neoplasia, 2010. **15**(2): p. 235-52.
306. Ocana, O.H. and M.A. Nieto, *Epithelial plasticity, stemness and pluripotency.* Cell Res, 2010. **20**(10): p. 1086-8.
307. Radisky, D.C. and M.A. LaBarge, *Epithelial-mesenchymal transition and the stem cell phenotype.* Cell Stem Cell, 2008. **2**(6): p. 511-2.
308. Peinado, H., D. Olmeda, and A. Cano, *Snail, Zeb and bHLH factors in tumour progression: an alliance against the epithelial phenotype?* Nat Rev Cancer, 2007. **7**(6): p. 415-28.

309. Mani, S.A., et al., *The epithelial-mesenchymal transition generates cells with properties of stem cells.* Cell, 2008. **133**(4): p. 704-15.
310. Lee, J.M., et al., *The epithelial-mesenchymal transition: new insights in signaling, development, and disease.* J Cell Biol, 2006. **172**(7): p. 973-81.
311. Baum, B., J. Settleman, and M.P. Quinlan, *Transitions between epithelial and mesenchymal states in development and disease.* Semin Cell Dev Biol, 2008. **19**(3): p. 294-308.
312. Polyak, K. and R.A. Weinberg, *Transitions between epithelial and mesenchymal states: acquisition of malignant and stem cell traits.* Nat Rev Cancer, 2009. **9**(4): p. 265-73.
313. Zavadil, J., et al., *Genetic programs of epithelial cell plasticity directed by transforming growth factor-beta.* Proc Natl Acad Sci U S A, 2001. **98**(12): p. 6686-91.
314. Peinado, H., M. Quintanilla, and A. Cano, *Transforming growth factor beta-1 induces snail transcription factor in epithelial cell lines: mechanisms for epithelial mesenchymal transitions.* J Biol Chem, 2003. **278**(23): p. 21113-23.
315. Burdsal, C.A., C.H. Damsky, and R.A. Pedersen, *The role of E-cadherin and integrins in mesoderm differentiation and migration at the mammalian primitive streak.* Development, 1993. **118**(3): p. 829-44.
316. Huber, M.A., N. Kraut, and H. Beug, *Molecular requirements for epithelial-mesenchymal transition during tumor progression.* Curr Opin Cell Biol, 2005. **17**(5): p. 548-58.
317. Techawattanawisal, W., et al., *Isolation of multipotent stem cells from adult rat periodontal ligament by neurosphere-forming culture system.* Biochem Biophys Res Commun, 2007. **357**(4): p. 917-23.
318. Azizi, S.A., et al., *Engraftment and migration of human bone marrow stromal cells implanted in the brains of albino rats--similarities to astrocyte grafts.* Proc Natl Acad Sci U S A, 1998. **95**(7): p. 3908-13.
319. Ferrari, G., et al., *Muscle regeneration by bone marrow-derived myogenic progenitors.* Science, 1998. **279**(5356): p. 1528-30.
320. Kopen, G.C., D.J. Prockop, and D.G. Phinney, *Marrow stromal cells migrate throughout forebrain and cerebellum, and they differentiate into astrocytes after injection into neonatal mouse brains.* Proc Natl Acad Sci U S A, 1999. **96**(19): p. 10711-6.
321. Oswald, J., et al., *Mesenchymal stem cells can be differentiated into endothelial*

*cells in vitro.* Stem Cells, 2004. **22**(3): p. 377-84.

322. Reyes, M., et al., *Origin of endothelial progenitors in human postnatal bone marrow.* J Clin Invest, 2002. **109**(3): p. 337-46.
323. Brzoska, M., et al., *Epithelial differentiation of human adipose tissue-derived adult stem cells.* Biochem Biophys Res Commun, 2005. **330**(1): p. 142-50.
324. Clarke, D.L., et al., *Generalized potential of adult neural stem cells.* Science, 2000. **288**(5471): p. 1660-3.
325. Kucia, M., et al., *A population of very small embryonic-like (VSEL) CXCR4(+)SSEA-1(+)Oct-4+ stem cells identified in adult bone marrow.* Leukemia, 2006. **20**(5): p. 857-69.
326. Krause, D.S., et al., *Multi-organ, multi-lineage engraftment by a single bone marrow-derived stem cell.* Cell, 2001. **105**(3): p. 369-77.
327. Li, R., et al., *A mesenchymal-to-epithelial transition initiates and is required for the nuclear reprogramming of mouse fibroblasts.* Cell Stem Cell, 2010. **7**(1): p. 51-63.
328. Samavarchi-Tehrani, P., et al., *Functional genomics reveals a BMP-driven mesenchymal-to-epithelial transition in the initiation of somatic cell reprogramming.* Cell Stem Cell, 2010. **7**(1): p. 64-77.
329. Aasen, T., et al., *Efficient and rapid generation of induced pluripotent stem cells from human keratinocytes.* Nat Biotechnol, 2008. **26**(11): p. 1276-84.
330. Bonewald, L.F., et al., *von Kossa staining alone is not sufficient to confirm that mineralization in vitro represents bone formation.* Calcif Tissue Int, 2003. **72**(5): p. 537-47.
331. McDermott, S.P., et al., *Comparison of human cord blood engraftment between immunocompromised mouse strains.* Blood, 2010. **116**(2): p. 193-200.
332. Bayuseno, A.P. and W.W. Schmahl, *Understanding the chemical and mineralogical properties of the inorganic portion of MSWI bottom ash.* Waste Manag, 2010. **30**(8-9): p. 1509-20.
333. Hegde, M.N. and A. Moany, *Remineralization of enamel subsurface lesions with casein phosphopeptide-amorphous calcium phosphate: A quantitative energy dispersive X-ray analysis using scanning electron microscopy: An in vitro study.* J Conserv Dent, 2012. **15**(1): p. 61-7.
334. Piantone, P., Bodenan, F., Chatelet-Snidaro, L, *Mineralogical study of secondary mineral phases from weathered MSWI bottom ash: implications for the modelling and trapping of heavy metals.* Applied Geochemistry, 2004. **19**(12): p. 1891-1904.
335. Pownceby, M.I., MacRae, C.M., Wilson, N.C, *Mineral characterisation by EPMA*

*mapping.* Minerals Engineering 2007. **20**(5): p. 444-51.

336. Lian, N., et al., *Vimentin inhibits ATF4-mediated osteocalcin transcription and osteoblast differentiation.* J Biol Chem, 2009. **284**(44): p. 30518-25.
337. Battula, V.L., et al., *Epithelial-mesenchymal transition-derived cells exhibit multilineage differentiation potential similar to mesenchymal stem cells.* Stem Cells, 2010. **28**(8): p. 1435-45.
338. Gundry, R.L., et al., *A novel role for proteomics in the discovery of cell-surface markers on stem cells: Scratching the surface.* Proteomics Clin Appl, 2008. **2**(6): p. 892-903.
339. Naylor, S., *Biomarkers: current perspectives and future prospects.* Expert Rev Mol Diagn, 2003. **3**(5): p. 525-9.
340. Hopkins, A.L. and C.R. Groom, *The druggable genome.* Nat Rev Drug Discov, 2002. **1**(9): p. 727-30.
341. Celebi, B., A.E. Elcin, and Y.M. Elcin, *Proteome analysis of rat bone marrow mesenchymal stem cell differentiation.* J Proteome Res, 2010. **9**(10): p. 5217-27.
342. Choi, Y.A., et al., *Secretome analysis of human BMSCs and identification of SMOC1 as an important ECM protein in osteoblast differentiation.* J Proteome Res, 2010. **9**(6): p. 2946-56.
343. Giusta, M.S., et al., *Proteomic analysis of human mesenchymal stromal cells derived from adipose tissue undergoing osteoblast differentiation.* Cytotherapy, 2010. **12**(4): p. 478-90.
344. Maurer, M.H., *Proteomic definitions of mesenchymal stem cells.* Stem Cells Int, 2011. **2011**(2011): p. 704256.
345. Menicanin, D., et al., *Genomic Profiling of Mesenchymal Stem Cells.* Stem Cell Rev, 2009.
346. Mrozik, K.M., et al., *Proteomic characterization of mesenchymal stem cell-like populations derived from ovine periodontal ligament, dental pulp, and bone marrow: analysis of differentially expressed proteins.* Stem Cells Dev, 2010. **19**(10): p. 1485-99.
347. Pivoriuunas, A., et al., *Proteomic analysis of stromal cells derived from the dental pulp of human exfoliated deciduous teeth.* Stem Cells Dev, 2009. **19**(7): p. 1081-93.
348. Yang, J.Y., et al., *Chloride intracellular channel 1 regulates osteoblast differentiation.* Bone, 2009. **45**(6): p. 1175-85.
349. Gygi, S.P., et al., *Correlation between protein and mRNA abundance in yeast.* Mol Cell Biol, 1999. **19**(3): p. 1720-30.

350. McCulloch, C.A., *Proteomics for the periodontium: current strategies and future promise.* Periodontol 2000, 2006. **40**: p. 173-83.
351. Unwin, R.D., et al., *The potential for proteomic definition of stem cell populations.* Exp Hematol, 2003. **31**(12): p. 1147-59.
352. Kadiu, I., et al., *HIV-1 transforms the monocyte plasma membrane proteome.* Cell Immunol, 2009. **258**(1): p. 44-58.
353. Jeong, J.A., et al., *Membrane proteomic analysis of human mesenchymal stromal cells during adipogenesis.* Proteomics, 2007. **7**(22): p. 4181-91.
354. Sidibe, A., et al., *Integrated membrane protein analysis of mature and embryonic stem cell-derived smooth muscle cells using a novel combination of CyDye/biotin labeling.* Mol Cell Proteomics, 2007. **6**(10): p. 1788-97.
355. Shin, B.K., et al., *Global profiling of the cell surface proteome of cancer cells uncovers an abundance of proteins with chaperone function.* J Biol Chem, 2003. **278**(9): p. 7607-16.
356. Jang, J.H. and S. Hanash, *Profiling of the cell surface proteome.* Proteomics, 2003. **3**(10): p. 1947-54.
357. Gastpar, R., et al., *Heat shock protein 70 surface-positive tumor exosomes stimulate migratory and cytolytic activity of natural killer cells.* Cancer Res, 2005. **65**(12): p. 5238-47.
358. Hunter-Lavin, C., et al., *Hsp70 release from peripheral blood mononuclear cells.* Biochem Biophys Res Commun, 2004. **324**(2): p. 511-7.
359. Jolly, C., I. Mitar, and Q.J. Sattentau, *Requirement for an intact T-cell actin and tubulin cytoskeleton for efficient assembly and spread of human immunodeficiency virus type 1.* J Virol, 2007. **81**(11): p. 5547-60.
360. Kadiu, I., et al., *Cytoskeletal protein transformation in HIV-1-infected macrophage giant cells.* J Immunol, 2007. **178**(10): p. 6404-15.
361. Campanella, M.E., H. Chu, and P.S. Low, *Assembly and regulation of a glycolytic enzyme complex on the human erythrocyte membrane.* Proc Natl Acad Sci U S A, 2005. **102**(7): p. 2402-7.
362. Dormeyer, W., et al., *A practical guide for the identification of membrane and plasma membrane proteins in human embryonic stem cells and human embryonal carcinoma cells.* Proteomics, 2008. **8**(19): p. 4036-53.
363. Braun, R.J., et al., *Two-dimensional electrophoresis of membrane proteins.* Anal Bioanal Chem, 2007. **389**(4): p. 1033-45.
364. Gahmberg, C.G. and M. Tolvanen, *Why mammalian cell surface proteins are*

*glycoproteins.* Trends Biochem Sci, 1996. **21**(8): p. 308-11.

365. He, J., et al., *Identification of cell surface glycoprotein markers for glioblastoma-derived stem-like cells using a lectin microarray and LC-MS/MS approach.* J Proteome Res, 2010. **9**(5): p. 2565-72.
366. Hemmoranta, H., et al., *N-glycan structures and associated gene expression reflect the characteristic N-glycosylation pattern of human hematopoietic stem and progenitor cells.* Exp Hematol, 2007. **35**(8): p. 1279-92.
367. Wearne, K.A., H.C. Winter, and I.J. Goldstein, *Temporal changes in the carbohydrates expressed on BG01 human embryonic stem cells during differentiation as embryoid bodies.* Glycoconj J, 2008. **25**(2): p. 121-36.
368. Wearne, K.A., et al., *Use of lectins for probing differentiated human embryonic stem cells for carbohydrates.* Glycobiology, 2006. **16**(10): p. 981-90.
369. Baharvand, H., et al., *Concise review: trends in stem cell proteomics.* Stem Cells, 2007. **25**(8): p. 1888-903.
370. Huang, H.L., et al., *Trypsin-induced proteome alteration during cell subculture in mammalian cells.* J Biomed Sci, 2010. **17**: p. 36.
371. Cabral, M.P., et al., *Proteomic and functional analyses reveal a unique lifestyle for Acinetobacter baumannii biofilms and a key role for histidine metabolism.* J Proteome Res, 2011. **10**(8): p. 3399-417.
372. Wallin, E. and G. von Heijne, *Genome-wide analysis of integral membrane proteins from eubacterial, archaean, and eukaryotic organisms.* Protein Sci, 1998. **7**(4): p. 1029-38.
373. Ahn, S.M., R.J. Goode, and R.J. Simpson, *Stem cell markers: insights from membrane proteomics?* Proteomics, 2008. **8**(23-24): p. 4946-57.
374. Rabilloud, T., *Membrane proteins and proteomics: love is possible, but so difficult.* Electrophoresis, 2009. **30 Suppl 1**: p. S174-80.
375. Busch, G., et al., *Selective isolation of individual cell surface proteins from tissue culture cells by a cleavable biotin label.* Eur J Cell Biol, 1989. **50**(2): p. 257-62.
376. Adam, P.J., et al., *Comprehensive proteomic analysis of breast cancer cell membranes reveals unique proteins with potential roles in clinical cancer.* J Biol Chem, 2003. **278**(8): p. 6482-9.
377. Bordier, C., *Phase separation of integral membrane proteins in Triton X-114 solution.* J Biol Chem, 1981. **256**(4): p. 1604-7.
378. Hastie, C., et al., *Combined affinity labelling and mass spectrometry analysis of differential cell surface protein expression in normal and prostate cancer cells.*

Oncogene, 2005. **24**(38): p. 5905-13.

379. Aggelis, V., et al., *Proteomic identification of differentially expressed plasma membrane proteins in renal cell carcinoma by stable isotope labelling of a von Hippel-Lindau transfectant cell line model.* Proteomics, 2009. **9**(8): p. 2118-30.
380. Gu, B., et al., *Global expression of cell surface proteins in embryonic stem cells.* PLoS One, 2011. **5**(12): p. e15795.
381. Gu, B., et al., *Proteomic analyses reveal common promiscuous patterns of cell surface proteins on human embryonic stem cells and sperms.* PLoS One, 2011. **6**(5): p. e19386.
382. Larkin, S. and C. Aukim-Hastie, *Proteomic evaluation of cancer cells: identification of cell surface proteins.* Methods Mol Biol, 2011. **731**: p. 395-405.
383. Sabarth, N., et al., *Identification of surface proteins of Helicobacter pylori by selective biotinylation, affinity purification, and two-dimensional gel electrophoresis.* J Biol Chem, 2002. **277**(31): p. 27896-902.
384. Hurley, W.L., E. Finkelstein, and B.D. Holst, *Identification of surface proteins on bovine leukocytes by a biotin-avidin protein blotting technique.* J Immunol Methods, 1985. **85**(1): p. 195-202.
385. Simpson, R.J., et al., *Proteomic analysis of the human colon carcinoma cell line (LIM 1215): development of a membrane protein database.* Electrophoresis, 2000. **21**(9): p. 1707-32.
386. Hagner-McWhirter, A., et al., *Selective labelling of cell-surface proteins using CyDye DIGE Fluor minimal dyes.* J Vis Exp, 2008(21).
387. Kumashiro, Y., M. Yamato, and T. Okano, *Cell attachment-detachment control on temperature-responsive thin surfaces for novel tissue engineering.* Ann Biomed Eng, 2010. **38**(6): p. 1977-88.
388. Kushida, A., et al., *Decrease in culture temperature releases monolayer endothelial cell sheets together with deposited fibronectin matrix from temperature-responsive culture surfaces.* J Biomed Mater Res, 1999. **45**(4): p. 355-62.
389. Yu, Z., et al., *Defining the requirements for collagenase cleavage in collagen type III using a bacterial collagen system.* J Biol Chem, 2012.
390. Weingarten, H., R. Martin, and J. Feder, *Synthetic substrates of vertebrate collagenase.* Biochemistry, 1985. **24**(23): p. 6730-4.
391. Weingarten, H. and J. Feder, *Cleavage site specificity of vertebrate collagenases.* Biochem Biophys Res Commun, 1986. **139**(3): p. 1184-7.
392. Harris, E.D., Jr. and S.M. Krane, *Collagenases (first of three parts).* N Engl J Med,

1974. **291**(11): p. 557-63.

393. Zhang, Y., et al., *Differential protein expression by Porphyromonas gingivalis in response to secreted epithelial cell components.* Proteomics, 2005. **5**(1): p. 198-211.

394. Xia, Q., et al., *Quantitative proteomics of intracellular Porphyromonas gingivalis.* Proteomics, 2007. **7**(23): p. 4323-37.

395. Veith, P.D., et al., *Identification of a novel heterodimeric outer membrane protein of Porphyromonas gingivalis by two-dimensional gel electrophoresis and peptide mass fingerprinting.* Eur J Biochem, 2001. **268**(17): p. 4748-57.

396. Reichenberg, E., et al., *Proteomic analysis of protein components in periodontal ligament fibroblasts.* J Periodontol, 2005. **76**(10): p. 1645-53.

397. Wu, L., et al., *Early osteogenic differential protein profile detected by proteomic analysis in human periodontal ligament cells.* J Periodontal Res, 2009. **44**(5): p. 645-56.

398. Foster, L.J., et al., *Differential expression profiling of membrane proteins by quantitative proteomics in a human mesenchymal stem cell line undergoing osteoblast differentiation.* Stem Cells, 2005. **23**(9): p. 1367-77.

399. Zhang, A.X., et al., *Proteomic identification of differently expressed proteins responsible for osteoblast differentiation from human mesenchymal stem cells.* Mol Cell Biochem, 2007. **304**(1-2): p. 167-79.

400. Sun, H.J., et al., *A proteomic analysis during serial subculture and osteogenic differentiation of human mesenchymal stem cell.* J Orthop Res, 2006. **24**(11): p. 2059-71.

401. Ancellin, N., et al., *Extracellular export of sphingosine kinase-1 enzyme. Sphingosine 1-phosphate generation and the induction of angiogenic vascular maturation.* J Biol Chem, 2002. **277**(8): p. 6667-75.

402. Hengst, J.A., et al., *Sphingosine kinase 1 localized to the plasma membrane lipid raft microdomain overcomes serum deprivation induced growth inhibition.* Arch Biochem Biophys, 2009. **492**(1-2): p. 62-73.

403. Jarman, K.E., et al., *Translocation of sphingosine kinase 1 to the plasma membrane is mediated by calcium- and integrin-binding protein 1.* J Biol Chem, 2010. **285**(1): p. 483-92.

404. Pitson, S.M., et al., *Phosphorylation-dependent translocation of sphingosine kinase to the plasma membrane drives its oncogenic signalling.* J Exp Med, 2005. **201**(1): p. 49-54.

405. Stahelin, R.V., et al., *The mechanism of membrane targeting of human sphingosine kinase 1.* J Biol Chem, 2005. **280**(52): p. 43030-8.
406. Wattenberg, B.W., *Role of sphingosine kinase localization in sphingolipid signaling.* World J Biol Chem, 2010. **1**(12): p. 362-8.
407. Young, K.W., et al., *Ca2+/calmodulin-dependent translocation of sphingosine kinase: role in plasma membrane relocation but not activation.* Cell Calcium, 2003. **33**(2): p. 119-28.
408. Balcerzak, M., et al., *The roles of annexins and alkaline phosphatase in mineralization process.* Acta Biochim Pol, 2003. **50**(4): p. 1019-38.
409. Genetos, D.C., et al., *Hypoxia increases Annexin A2 expression in osteoblastic cells via VEGF and ERK.* Bone, 2010. **47**(6): p. 1013-9.
410. Gillette, J.M. and S.M. Nielsen-Preiss, *The role of annexin 2 in osteoblastic mineralization.* J Cell Sci, 2004. **117**(Pt 3): p. 441-9.
411. Haut Donahue, T.L., et al., *Annexin V disruption impairs mechanically induced calcium signaling in osteoblastic cells.* Bone, 2004. **35**(3): p. 656-63.
412. Kirsch, T., B. Swoboda, and H. Nah, *Activation of annexin II and V expression, terminal differentiation, mineralization and apoptosis in human osteoarthritic cartilage.* Osteoarthritis Cartilage, 2000. **8**(4): p. 294-302.
413. Pfander, D., B. Swoboda, and T. Kirsch, *Expression of early and late differentiation markers (proliferating cell nuclear antigen, syndecan-3, annexin VI, and alkaline phosphatase) by human osteoarthritic chondrocytes.* Am J Pathol, 2001. **159**(5): p. 1777-83.
414. Wang, W. and T. Kirsch, *Retinoic acid stimulates annexin-mediated growth plate chondrocyte mineralization.* J Cell Biol, 2002. **157**(6): p. 1061-9.
415. Zhang, J., et al., *Identification of the haematopoietic stem cell niche and control of the niche size.* Nature, 2003. **425**(6960): p. 836-41.
416. Stier, S., et al., *Osteopontin is a hematopoietic stem cell niche component that negatively regulates stem cell pool size.* J Exp Med, 2005. **201**(11): p. 1781-91.
417. Nilsson, S.K., et al., *Osteopontin, a key component of the hematopoietic stem cell niche and regulator of primitive hematopoietic progenitor cells.* Blood, 2005. **106**(4): p. 1232-9.
418. Calvi, L.M., et al., *Osteoblastic cells regulate the haematopoietic stem cell niche.* Nature, 2003. **425**(6960): p. 841-6.
419. Arai, F., et al., *Tie2/angiopoietin-1 signaling regulates hematopoietic stem cell quiescence in the bone marrow niche.* Cell, 2004. **118**(2): p. 149-61.

420. Avecilla, S.T., et al., *Chemokine-mediated interaction of hematopoietic progenitors with the bone marrow vascular niche is required for thrombopoiesis.* Nat Med, 2004. **10**(1): p. 64-71.
421. Kiel, M.J., et al., *SLAM family receptors distinguish hematopoietic stem and progenitor cells and reveal endothelial niches for stem cells.* Cell, 2005. **121**(7): p. 1109-21.
422. Barrett, J.M., et al., *Over-expression of sphingosine kinase-1 enhances a progenitor phenotype in human endothelial cells.* Microcirculation, 2011. **18**(7): p. 583-97.
423. Zhang, B., *CD73: a novel target for cancer immunotherapy.* Cancer Res, 2010. **70**(16): p. 6407-11.
424. Colgan, S.P., et al., *Physiological roles for ecto-5'-nucleotidase (CD73).* Purinergic Signal, 2006. **2**(2): p. 351-60.
425. Beavis, P.A., et al., *CD73: a potent suppressor of antitumor immune responses.* Trends Immunol, 2012.
426. Sattler, C., et al., *Inhibition of T-cell proliferation by murine multipotent mesenchymal stromal cells is mediated by CD39 expression and adenosine generation.* Cell Transplant, 2011. **20**(8): p. 1221-30.
427. Saldanha-Araujo, F., et al., *Mesenchymal stromal cells up-regulate CD39 and increase adenosine production to suppress activated T-lymphocytes.* Stem Cell Res, 2011. **7**(1): p. 66-74.
428. Nemoto, E., et al., *Expression of CD73/ecto-5'-nucleotidase on human gingival fibroblasts and contribution to the inhibition of interleukin-1alpha-induced granulocyte-macrophage colony stimulating factor production.* J Periodontal Res, 2004. **39**(1): p. 10-9.
429. Kato, T., et al., *Osteogenic potential of rat stromal cells derived from periodontal ligament.* J Tissue Eng Regen Med, 2011. **5**(10): p. 798-805.
430. Tomokiyo, A., et al., *A multipotent clonal human periodontal ligament cell line with neural crest cell phenotypes promotes neurocytic differentiation, migration, and survival.* J Cell Physiol, 2012. **227**(5): p. 2040-50.
431. Trubiani, O., et al., *Expression profile of the embryonic markers nanog, OCT-4, SSEA-1, SSEA-4, and frizzled-9 receptor in human periodontal ligament mesenchymal stem cells.* J Cell Physiol, 2010. **225**(1): p. 123-31.
432. Haeryfar, S.M. and D.W. Hoskin, *Thy-1: more than a mouse pan-T cell marker.* J Immunol, 2004. **173**(6): p. 3581-8.
433. Bradley, J.E., G. Ramirez, and J.S. Hagood, *Roles and regulation of Thy-1, a*

*context-dependent modulator of cell phenotype.* Biofactors, 2009. **35**(3): p. 258-65.

434. Baum, C.M., et al., *Isolation of a candidate human hematopoietic stem-cell population.* Proc Natl Acad Sci U S A, 1992. **89**(7): p. 2804-8.
435. Masson, N.M., et al., *Hepatic progenitor cells in human fetal liver express the oval cell marker Thy-1.* Am J Physiol Gastrointest Liver Physiol, 2006. **291**(1): p. G45-54.
436. Yang, Z.F., et al., *Significance of CD90+ cancer stem cells in human liver cancer.* Cancer Cell, 2008. **13**(2): p. 153-66.
437. He, J., et al., *CD90 is identified as a marker for cancer stem cells in primary high-grade gliomas using tissue microarrays.* Mol Cell Proteomics, 2011.
438. Crompton, M.R., S.E. Moss, and M.J. Crumpton, *Diversity in the lipocortin/calpactin family.* Cell, 1988. **55**(1): p. 1-3.
439. Zobiack, N., V. Gerke, and U. Rescher, *Complex formation and submembranous localization of annexin 2 and S100A10 in live HepG2 cells.* FEBS Lett, 2001. **500**(3): p. 137-40.
440. Glenney, J.R., Jr., *Co-precipitation of intestinal p36 with a 73-K protein and a high molecular weight factor.* Exp Cell Res, 1986. **162**(1): p. 183-90.
441. Gerke, V. and K. Weber, *Identity of p36K phosphorylated upon Rous sarcoma virus transformation with a protein purified from brush borders; calcium-dependent binding to non-erythroid spectrin and F-actin.* EMBO J, 1984. **3**(1): p. 227-33.
442. Siever, D.A. and H.P. Erickson, *Extracellular annexin II.* Int J Biochem Cell Biol, 1997. **29**(11): p. 1219-23.
443. Thiel, C., M. Osborn, and V. Gerke, *The tight association of the tyrosine kinase substrate annexin II with the submembranous cytoskeleton depends on intact p11- and Ca(2+)-binding sites.* J Cell Sci, 1992. **103 ( Pt 3)**: p. 733-42.
444. Fang, Y.T., et al., *Interferon-gamma stimulates p11-dependent surface expression of annexin A2 in lung epithelial cells to enhance phagocytosis.* J Cell Physiol, 2011.
445. Peterson, E.A., et al., *Thrombin induces endothelial cell-surface exposure of the plasminogen receptor annexin 2.* J Cell Sci, 2003. **116**(Pt 12): p. 2399-408.
446. Anderson, H.C., *Molecular biology of matrix vesicles.* Clin Orthop Relat Res, 1995(314): p. 266-80.
447. Brachvogel, B., et al., *Annexin A5 is not essential for skeletal development.* Mol Cell Biol, 2003. **23**(8): p. 2907-13.
448. Bozic, D., et al., *The proteome and gene expression profile of cementoblastic cells*

*treated by bone morphogenetic protein-7 in vitro.* J Clin Periodontol, 2011.

449. Yuan, K., et al., *A mineralization-associated membrane protein plays a role in the biological functions of the peptide-coated bovine hydroxyapatite.* J Periodontal Res, 2007. **42**(5): p. 420-8.
450. Jung, Y., et al., *Annexin II expressed by osteoblasts and endothelial cells regulates stem cell adhesion, homing, and engraftment following transplantation.* Blood, 2007. **110**(1): p. 82-90.
451. Jung, Y., et al., *Annexin-2 is a regulator of stromal cell-derived factor-1/CXCL12 function in the hematopoietic stem cell endosteal niche.* Exp Hematol, 2010. **39**(2): p. 151-166 e1.
452. Chi, H., *Sphingosine-1-phosphate and immune regulation: trafficking and beyond.* Trends Pharmacol Sci, 2011. **32**(1): p. 16-24.
453. Pebay, A., C.S. Bonder, and S.M. Pitson, *Stem cell regulation by lysophospholipids.* Prostaglandins Other Lipid Mediat, 2007. **84**(3-4): p. 83-97.
454. Olivera, A. and S. Spiegel, *Sphingosine kinase: a mediator of vital cellular functions.* Prostaglandins Other Lipid Mediat, 2001. **64**(1-4): p. 123-34.
455. Spiegel, S., et al., *Sphingosine-1-phosphate in cell growth and cell death.* Ann N Y Acad Sci, 1998. **845**: p. 11-8.
456. Xia, P., et al., *An oncogenic role of sphingosine kinase.* Curr Biol, 2000. **10**(23): p. 1527-30.
457. Shida, D., et al., *Targeting SphK1 as a new strategy against cancer.* Curr Drug Targets, 2008. **9**(8): p. 662-73.
458. Bonder, C.S., et al., *Sphingosine kinase regulates the rate of endothelial progenitor cell differentiation.* Blood, 2009. **113**(9): p. 2108-17.
459. Limaye, V., et al., *Sphingosine kinase-1 enhances endothelial cell survival through a PECAM-1-dependent activation of PI-3K/Akt and regulation of Bcl-2 family members.* Blood, 2005. **105**(8): p. 3169-77.
460. Meng, H., Y. Yuan, and V.M. Lee, *Loss of Sphingosine kinase 1/S1P signaling impairs cell growth and survival of neurons and progenitor cells in the developing sensory ganglia.* PLoS One, 2011. **6**(11): p. e27150.
461. Pebay, A., et al., *Essential roles of sphingosine-1-phosphate and platelet-derived growth factor in the maintenance of human embryonic stem cells.* Stem Cells, 2005. **23**(10): p. 1541-8.
462. Katsuma, S., et al., *Signalling mechanisms in sphingosine 1-phosphate-promoted mesangial cell proliferation.* Genes Cells, 2002. **7**(12): p. 1217-30.

463. Nagata, Y., et al., *Entry of muscle satellite cells into the cell cycle requires sphingolipid signaling.* J Cell Biol, 2006. **174**(2): p. 245-53.
464. Leth-Larsen, R., et al., *Metastasis-related plasma membrane proteins of human breast cancer cells identified by comparative quantitative mass spectrometry.* Mol Cell Proteomics, 2009. **8**(6): p. 1436-49.
465. Xiong, J., et al., *Epithelial Cell Rests of Malassez contain unique stem cell populations capable of undergoing epithelial-mesenchymal transition.* Stem Cells Dev, 2012.
466. Stahl, P.J. and D. Felsen, *Transforming growth factor-beta, basement membrane, and epithelial-mesenchymal transdifferentiation: implications for fibrosis in kidney disease.* Am J Pathol, 2001. **159**(4): p. 1187-92.
467. Chapman, H.A., *Epithelial-mesenchymal interactions in pulmonary fibrosis.* Annu Rev Physiol, 2011. **73**: p. 413-35.
468. Fragiadaki, M. and R.M. Mason, *Epithelial-mesenchymal transition in renal fibrosis - evidence for and against.* Int J Exp Pathol, 2011. **92**(3): p. 143-50.
469. King, T.E., Jr., A. Pardo, and M. Selman, *Idiopathic pulmonary fibrosis.* Lancet, 2011. **378**(9807): p. 1949-61.
470. Kriz, W., B. Kaissling, and M. Le Hir, *Epithelial-mesenchymal transition (EMT) in kidney fibrosis: fact or fantasy?* J Clin Invest, 2011. **121**(2): p. 468-74.
471. Carew, R.M., B. Wang, and P. Kantharidis, *The role of EMT in renal fibrosis.* Cell Tissue Res, 2012. **347**(1): p. 103-16.
472. Lekkerkerker, A.N., et al., *Cellular players in lung fibrosis.* Curr Pharm Des, 2012.
473. Iwano, M., et al., *Evidence that fibroblasts derive from epithelium during tissue fibrosis.* J Clin Invest, 2002. **110**(3): p. 341-50.
474. Dalkilic, I., et al., *Loss of FilaminC (FLNc) results in severe defects in myogenesis and myotube structure.* Mol Cell Biol, 2006. **26**(17): p. 6522-34.
475. Guergueltcheva, V., et al., *Distal myopathy with upper limb predominance caused by filamin C haploinsufficiency.* Neurology, 2011. **77**(24): p. 2105-14.
476. Zhou, X., J. Boren, and L.M. Akyurek, *Filamins in cardiovascular development.* Trends Cardiovasc Med, 2007. **17**(7): p. 222-9.
477. Ramus, C., et al., *An optimized strategy for ICAT quantification of membrane proteins.* Mol Cell Proteomics, 2006. **5**(1): p. 68-78.